Cover Page

Universiteit Leiden

Author: Coomans, Claudia Pascalle
Title: Insulin sensitivity : modulation by the brain
Date: 2012-06-14

INSULIN SENSITIVITY MODULATION BY THE BRAIN

Claudia P. Coomans

INSULIN SENSITIVITY MODULATION BY THE BRAIN

Proefschrift

ter verkrijging van

de graad van Doctor aan de Universiteit Leiden,

op gezag van Rector Magnificus prof.mr. P.F. van der Heijden,

volgens besluit van het College voor Promoties

te verdedigen op donderdag 14 juni 2012

klokke 13:45 uur

door

Claudia Pascalle Coomans

geboren op 22 juni 1980

te Rotterdam

PROMOTIECOMMISSIE

Promotores: Prof. dr. J.A. Romijn
                   Prof. dr. ir. L.M. Havekes
                   Prof. dr. P.C.N. Rensen

Overige leden: Prof. dr. E. Fliers (AMC, Amsterdam)
                   Prof. dr. A. Kalsbeek (NIH, Amsterdam)
                   Prof. dr. J.H. Meijer
                   Prof. dr. H. Pijl
                   Prof. dr. K. Willems van Dijk
                   Dr. N.R. Biermasz

Sic Parvis Magna

TABLE OF CONTENTS

GENERAL INTRODUCTION

1

As a consequence of the growing obesity prevalence, type 2 diabetes mellitus (T2DM) has become a global epidemic. Currently, this disease affects 171 million individuals globally, with an estimated mortality of about 4 million deaths each year (1). The development of T2DM is the result of insulin resistance of target organs (i.e. liver, adipose tissue, skeletal muscle) and impaired insulin secretion *by* pancreatic β-cells, ultimately leading to hyperglycemia. In addition to glucose metabolism, lipid metabolism is disturbed in T2DM patients, resulting in concomitant dyslipidemia.
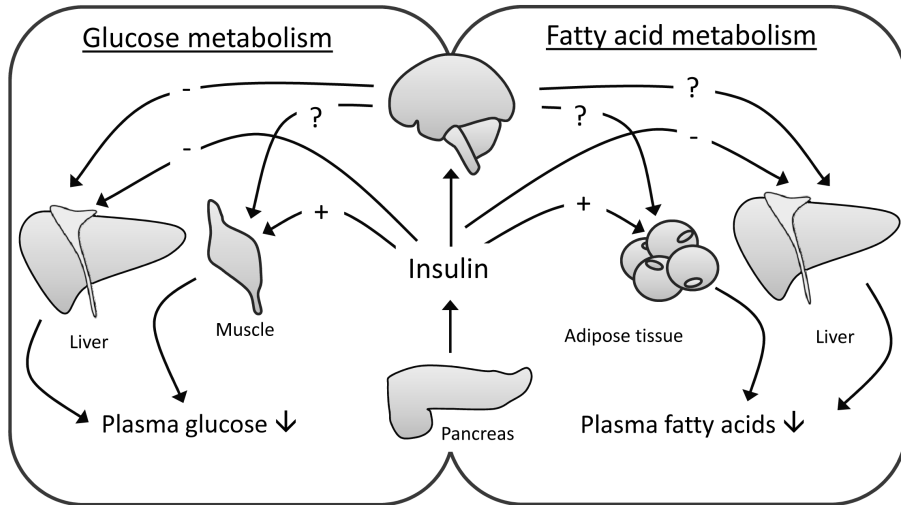
GLUCOSE METABOLISM

Dietary carbohydrates enter the body in complex forms, such as disaccharides and polymers (starch). In the gut, these complex carbohydrates are digested into glucose and other simple carbohydrates that can be transported across the intestinal wall to the hepatic portal vein and delivered to liver parenchymal cells (i.e. hepatocytes) and other tissues. The maintenance of narrow-controlled blood glucose concentrations (glucose homeostasis) is essential for a constant provision of glucose to the brain.

Glucose homeostasis is regulated by the balance between endogenous production of glucose, mainly by the liver, and uptake and utilization of glucose by peripheral tissues. To prevent hypoglycemia in the fasted state, glucose is released from the liver (and in small amounts from the kidneys (2)) by two pathways: glycogenolysis and gluconeogenesis. Glycogenolysis is the biochemical breakdown of stored glycogen to glucose, while gluconeogenesis is the process of generating new glucose molecules from non-carbohydrate sources, such as amino acids and the glycerol portion of triglycerides. Glucose disposal takes place in peripheral tissues like skeletal muscle, adipose tissue and heart. Once glucose is transported into the cell, it can undergo glycolysis (catabolism of glucose) to render energy in the form of ATP, e.g. required for muscle contraction, or can be stored either as glycogen in liver or muscle or as the glycerol moiety of TG in adipose tissue.

Glucose homeostasis is controlled primarily by the anabolic hormone insulin. Several catabolic hormones (glucagon, catecholamines, cortisol, and growth hormone) oppose the actions of insulin. After a meal containing carbohydrates, plasma glucose levels rise and as a result, insulin is secreted by pancreatic β-cells (Fig. 1). Insulin inhibits glycogenolysis and gluconeogenesis, and as a result inhibits endogenous glucose production. In addition, insulin stimulates glucose disposal in peripheral tissues. The net result of these actions of insulin is a normalization of plasma glucose levels after a meal.

Insulin initiates its effects on target tissues by binding to the insulin receptor (IR), which results in the tyrosine phosphorylation of insulin receptor substrates (IRS) by the insulin receptor tyrosine kinase. This allows association of IRS with the regulatory subunit of phosphoinositide 3-kinase (PI3K). PI3K activates 3-phosphoinositide-dependent protein kinase-1 (PDK), which activates protein kinase B (PKB)/Akt, a serine kinase. PKB/Akt in turn deactivates glycogen synthase kinase 3 (GSK-3), leading to activation of glycogen synthase and thus glycogen synthesis. Activation of PKB/Akt also results in the translocation of GLUT4 vesicles from their intracellular pool to the plasma membrane, where they allow uptake of glucose into the cell.

Fig. 1. Schematic representation of insulin's effect in glucose and fatty acid metabolism. Insulin reduces glucose levels by stimulating glucose uptake by peripheral tissues (e.g. muscle) and inhibiting glucose production by the liver. The latter involves insulin action in the brain. Insulin reduces fatty acid levels by stimulating fatty acid uptake by white adipose tissue and by inhibiting triglyceride secretion by the liver.

Furthermore, activated PKB/Akt phosphorylates the nuclear protein Proline-rich Akt substrate of 40 kDa (PRAS40), of which the precise function is still under debate.

The golden standard for investigating and quantifying insulin sensitivity in a clinical setting, but also in experimental setting in rodents, is the hyperinsulinemic-euglycemic clamp. During the hyperinsulinemic-euglycemic clamp, a constant concentration of insulin is infused intravenously. In order to prevent hypoglycemia induced by the insulin rise, glucose is infused to maintain plasma glucose levels at euglycemic levels. The rate of glucose infusion necessary to maintain euglycemia, as determined by checking plasma glucose levels every 5-10 minutes, is a measure for insulin sensitivity. A high glucose infusion rate indicates sensitivity to insulin action, whereas a low glucose infusion rate indicates that the body is resistant to insulin action. The information obtained by the hyperinsulinemic-euglycemic clamp can be extended by the use of glucose tracers. Glucose can be labeled with either stable or radioactive atoms, including [1-^{14}C]glucose or [3-^{3}H]glucose (3;4). Prior to beginning the hyperinsulinemic period, a tracer infusion enables quantification of the basal rate of glucose production. During the clamp, the plasma tracer concentrations enable the calculation of whole-body insulin-stimulated glucose disposal, as well as the endogenous glucose production (5). The hyperinsulinemic-euglycemic clamp can be further extended using radioactive-labeled 2-deoxyglucose. This tracer is administered during the clamp as a bolus when steady-state euglycemia is reached to determine organ-specific glucose uptake in organs that are unable to glycolyse 2-deoxyglucose (all organs except liver and kidney) (6).

In addition to insulin, other hormones affect glucose metabolism. For example, the thyroid hormones (TH) thyroxine (T$_4$) and triiodothyronine (T$_3$), are tyrosine-based hormones produced by the thyroid gland. TH production by thyroid gland is regulated by thyroid-stimulating

hormone (TSH) produced by the anterior pituitary, which itself is regulated by thyrotropin-releasing hormone (TRH) produced by the hypothalamus. TH are crucial regulators of metabolism, as illustrated by the profound alterations in metabolism during hyper- and hypothyroidism (7). Hyperthyroid animals develop elevated plasma glucose and insulin levels, due to increased endogenous glucose production, including increased gluconeogenesis and glycogenolysis, and decreased glucose clearance and disposal (8;9). Conversely, in hypothyroid animals, basal endogenous glucose production is reduced (10;11), whereas glucose utilization and turnover in skeletal muscle and adipose tissue is decreased (12).

FATTY ACID METABOLISM

The most common lipids in our diet are cholesterol and triglycerides (TG). Since lipids are hydrophobic, they are transported in the circulation in water-soluble spherical particles called lipoproteins. These lipoproteins carry TG and esterified cholesterol in their core, surrounded by a shell of phospholipids, free cholesterol and proteins termed apolipoproteins. Based on their composition and origin, lipoproteins can be divided into five major classes i.e. chylomicrons, very low lipoproteins (VLDL), intermediate density lipoproteins (IDL), low density lipoproteins (LDL) and high density lipoproteins (HDL) (13).

In the intestine, dietary lipid is emulsified by the action of bile and TG are hydrolyzed into monoacylglycerol and fatty acids (FA) by pancreatic lipase. Cholesterol, monoacylglycerol and FA are absorbed by the intestinal cells where FA are re-esterified to TG. The TG and cholesterol are packaged in chylomicrons. Upon entering the circulation, chylomicrons are processed by lipoprotein lipase (LPL) (14). LPL hydrolyzes TG, thereby delivering FA to peripheral tissues, where it can be used as energy source (skeletal muscle and heart) or can be stored in adipose tissue. The resulting TG-depleted remnant chylomicrons are taken up by the liver. The liver can secrete cholesterol and TG, packaged in VLDL particles for transport to peripheral tissues. After VLDL enters the circulation, the TG content of VLDL can be hydrolyzed into FA by LPL and used as energy source. The processing of VLDL by LPL results in the formation of IDL (or VLDL-remnant), which can be further processed to become cholesterol-rich LDL. IDL and LDL can be cleared by the liver. High levels of chylomicrons, VLDL, IDL and LDL can lead to accumulation of lipids in the vascular wall and the development of atherosclerosis. HDL, as formed by the liver and intestine, can remove excess cholesterol from peripheral tissues. Next, HDL-derived cholesterol can be taken up by the liver. In the liver, excess cholesterol is secreted in the bile, thereby maintaining cholesterol homeostasis (15).

FA are important metabolic substrates. The uptake, transport and storage of FA is intensively regulated and plasma FA levels show little variation. TG in TG-rich lipoproteins are hydrolyzed into FA by the action of LPL, located at the capillary endothelium. The released FA are taken up by the underlying tissue via passive diffusion across cell membrane or via active transport, which is facilitated by FA transporters, such as the FA translocase CD36 (16). In WAT, these FA can be re-esterified and stored as TG in intracellular lipid droplets. In heart and skeletal muscle, these FA are metabolized to produce ATP. Excess FA are complexed to serum albumin and transported back to the liver.

In brown adipose tissue (BAT), FA is metabolized by uncoupling FA oxidation from ATP generation, thereby resulting in dissipation of energy as heat. Only recently, it was shown that BAT is also present and functional in human adults (17). At birth, human newborns have considerable amount of BAT, mostly surrounding the vasculature and organs, to defend the body from cold exposure. In adults, BAT is mainly present in the supraclavicular and neck region (18;19). BAT burns FA stored as TG in lipid droplets as a response to sympathetic innervation. BAT comprises only a small percentage of total body weight and lipids stored in BAT can sustain thermogenesis for only a short time. A recent study revealed that TG-rich lipoproteins are an important substrate for heat production by BAT (20). Cold exposure accelerates clearance of plasma TG as a result of increased uptake into BAT, a process dependent on LPL activity and CD36 (20).

Insulin exerts direct effects on VLDL production, by accelerating the degradation of apoB (the principal apolipoprotein of VLDL), thereby acutely decreasing VLDL secretion by the liver (21;22) (Fig. 1). In adipose tissue, insulin stimulates TG storage in adipose tissue in three ways. First, insulin activates LPL in the capillary walls of adipose tissue, thereby stimulating lipolysis (breakdown of TG into FA and glycerol), enabling FA uptake by adipocytes. Second, insulin stimulates glucose transport into adipocytes, providing substrate for the glycerol portion of TG. Third, insulin inhibits hormone-sensitive lipase (HSL), thereby inhibiting hydrolysis (breakdown of TG into FA and glycerol) in adipocytes. The inhibition of lipolysis in adipose tissue by insulin decreases the flux of FFA towards the liver, contributing to decreased hepatic VLDL secretion.

The role of TH in the regulation of lipid metabolism has been extensively studied ever since the link between thyroid function and body weight has been recognized. Plasma concentrations of cholesterol and TG are inversely correlated with TH levels. TH stimulate hepatic LDL receptors, thereby promoting uptake of (V)LDL. Therefore, hypothyroidism results in decreased LDL receptors and increased plasma cholesterol and TG levels. Hypermetabolism is one of the hallmarks of hyperthyroidism, reflected in an increase of resting energy expenditure (REE). It is unknown whether this increase in REE coincides with an increase in spontaneous physical activity. FA are important substrates fuelling the increase in REE during hyperthyroidism (23). The FA are provided by several mechanisms. First, lipolysis (breakdown of TG into FA and glycerol) is stimulated by TH (24). Second, hepatic *de novo* lipogenesis is promoted by T3 via induction of lipogenic enzymes (25). Third, TH increase the amount of available nutrients, including FA, by increasing food intake. Although TH stimulate lipolysis, it is still unknown how FA fluxes are modulated by TH status in metabolically relevant tissues *in vivo*.

ROLE OF THE BRAIN IN GLUCOSE AND FATTY ACID METABOLISM

The first evidence that the brain is involved in control of peripheral glucose homeostasis already dates back from 1855, when the French physiologist Claude Bernard showed in rabbits that punctures in the floor of the fourth ventricle resulted in hyperglycemia. Several brain regions from cortex to brainstem are involved in the regulation of homeostasis, but the hypothalamus is considered the main integrator and processor of peripheral metabolic information. The hypothalamus consists of several nuclei (collection of neuronal cells) involved in metabolism,

including the arcuate nucleus (ARC), the paraventricular nucleus (PVN), the lateral hypothalamic area (LHA), the ventromedial nucleus (VMH), and the dorsomedial nucleus (DMH).

One of the critical neuronal structures involved in the regulation of metabolism is the ARC, situated around the base of the third ventricle in the hypothalamus. The ARC contains neurons that exert potent effects on food intake, energy expenditure and glucose and FA metabolism. Both hormonal and nutrient-related signals regulate these neurons. One group of neurons co-express neuropeptide Y (NPY) and agouti-related peptide (AgRP), peptides that potently stimulate food intake and reduce energy expenditure, thereby promoting weight gain. Another group of neurons co-express pro-opiomelanocortin (POMC) and cocaine- and amphetamine-regulated transcript (CART), peptides that decrease food intake and increase energy expenditure, thereby promoting weight loss. The expression of these orexigenic and anorexigenic neuropeptides is dependent on the fed status and a balance between the neuropeptides is essential for maintaining energy homeostasis.

Studies have shown that the brain is an insulin-sensitive organ and insulin receptors are widely distributed in the brain (26). Insulin crosses the blood-brain barrier through insulin-receptor mediated active transport (27;28). The origin of insulin in the brain is mostly peripheral and only a modest amount is synthesized locally (29). By activating its receptors, insulin decreases the expression of NPY and stimulates expression of POMC, both contributing to a decrease in food intake and increase in energy expenditure. Activation of insulin signaling in the brain plays an important role in the regulation of glucose metabolism (Fig. 1). Central administration of insulin, resulting in activation of insulin signaling in the brain without elevating plasma insulin levels, is sufficient to decrease plasma glucose levels by inhibiting endogenous glucose production (30). Conversely, blockade of central insulin action results in decreased ability of circulating insulin to suppress endogenous glucose production (30;31). Insulin may obtain its effects on endogenous glucose production by decreasing NPY neuronal activity, as it has been shown that central NPY administration impairs the ability of circulating insulin to suppress endogenous glucose production (32). The effect of central insulin action on endogenous glucose production is dependent on ATP-dependent potassium (K_{ATP}) channel activation in the brain. Central administration of sulfonylureas (K_{ATP} channel blockers) abolishes the central effects of insulin on endogenous glucose production and prevents in part the suppression of endogenous glucose production by circulating insulin (30). Moreover, K_{ATP} channel activation *per se* is sufficient to lower plasma glucose levels via inhibition of glycogenolysis and gluconeogenesis (33). Although it is established that insulin signaling in the brain is required for inhibitory effect of circulating insulin on endogenous glucose production, it is unknown whether the central effects of insulin are involved in the stimulation of disposal of glucose by circulating insulin.

Recently, it was shown that central insulin action is not only involved in peripheral glucose metabolism, but also in FA metabolism. Insulin administration in the brain promotes lipogenesis and suppresses intracellular lipolysis in white adipose tissue (WAT), which results in increased fat mass and adipocyte cell size upon chronic insulin administration (34;35). Furthermore, suppression of VLDL secretion by circulating insulin can in part be prevented by central administration of NPY (32). However, it is unknown whether the central effects of insulin are also involved in the stimulation of uptake of (F)FA and TG by adipose tissue from plasma.

In addition to insulin, the effects of TH on glucose metabolism are partly mediated via a central mechanism. Comparable to peripheral administration, TH administration directly into the PVN of the brain increases endogenous glucose production and induces hepatic insulin resistance (36;37). Furthermore, both the peripheral as well as the central effects of TH on glucose production depend on sympathetic projections to the liver (37;38).

METABOLIC DISTURBANCES IN TYPE 2 DIABETES MELLITUS

T2DM is a multifactorial, chronic disease characterized by hyperglycemia and often accompanied by dyslipidemia. T2DM is no immediate life threatening disease, but it does increase the risk for developing complications such as cardiovascular disease, retinopathy, neuropathy, and nephropathy. The diagnosis of diabetes mellitus is based on WHO recommendations in 2006. Criteria include fasting plasma glucose level ≥ 7.0 mmol/l or a 2 h-plasma glucose level of ≥ 11.1 mmol/l following a glucose load.

The development of T2DM is the result of both a deficient insulin secretion by pancreatic ß-cells and insulin resistance. In the insulin resistant state, skeletal muscle, liver and adipose tissue display a decreased responsiveness to insulin mediated glucose disposal. Furthermore, hepatic insulin resistance results in decreased insulin-mediated suppression of endogenous glucose production. In the early stage of the development of T2DM, insulin resistance leads to an increase in insulin secretion by the β-cells to overcome the reduced sensitivity of peripheral organs, thereby maintaining normal glucose levels. In a later stage, β-cells fail to compensate, leading to progressive hyperglycemia and ultimately T2DM.

FA metabolism is also disturbed in T2DM patients. Insulin resistance is associated with increased intracellular lipolysis of TG in adipose tissue by HSL, resulting in an increased FA flux from adipose tissue to liver, skeletal muscle and heart where it is stored as TG, contributing to the development of insulin resistance in these tissues (39). The increased storage of TG in liver in combination with hepatic insulin resistance results in increased secretion of VLDL (40;41). The increased plasma levels of TG in VLDL are a hallmark of the dyslipidemia associated with insulin resistance and T2DM.

As mentioned before, central insulin actions are critical for the maintenance of glucose and energy homeostasis. Obesity has been shown to result in elevated insulin levels in cerebrospinal fluid (42). Recently it was shown that high-fat feeding induces central insulin resistance already following short exposure to the diet, as demonstrated by reduced insulin signaling in the brain (43). A high-fat diet induces central insulin resistance independently of adiposity as the development of central insulin resistance occurs within days of exposure to the high-fat diet. The attenuated insulin signaling in neurons occurs through three mechanisms: first, the inactivation of IRS-1 by serine phosphorylation, second, the proteasomal degradation of IRS-1, and third, the lysosomal degradation of the IR (44). Since central insulin actions are critical in the regulation of glucose and FA metabolism, the central effects of insulin resistance require more attention.

CIRCADIAN RHYTHM AND INSULIN SENSITIVITY

A recently described environmental trigger associated with development of T2DM is disturbance of circadian rhythms, which can be due to environmental light pollution, reduction of sleep duration and/or quality, jet lags and shift work. Circadian rhythms are 24 h cycles generated by the suprachiasmatic nucleus (SCN) located in the anterior hypothalamus. The SCN induces daily rhythms in body temperature, heart rate, blood pressure, feeding behavior, glucose levels and many more. This circadian clock is synchronized to the environmental cycle by light-dark information perceived by the eyes. Many hormones involved in metabolism, such as insulin, glucagon, cortisol and leptin have been shown to exhibit circadian oscillation (45-49). In addition, the circadian clock has been reported to regulate metabolism and energy homeostasis, by mediating expression and/or activity of certain metabolic enzymes and transport systems involved in e.g. cholesterol metabolism and glycogen and glucose metabolism. Disruption of circadian rhythms due to shift work can result in hormone imbalance, psychological and sleep disorders, cancer proneness and reduced life span (50;51). Furthermore, shift work and reductions in sleep duration result in impaired glucose tolerance (52-55) and increased adiposity (56).

The rhythmic expression and activity of the metabolic pathways is mainly attributed to the coordinated circadian oscillation of clock genes (*Clock*, *Bmal1*, *Per1*, *Per2*, *Per3*, *Cry1* and *Cry2*) that are expressed in each organ and cell. By phenotyping clock gene mutant and knockout mice, a direct link was made between the circadian clock and metabolic disorders. Homozygous *Clock* mutant mice have greatly attenuated diurnal feeding rhythm, are hyperphagic and obese and develop a metabolic syndrome of hyperleptinemia, hyperlipidemia, hepatic steatosis and hyperglycemia (57). $Bmal^{-/-}$ mice exhibit suppressed diurnal variations in glucose and TG levels as well as abolished gluconeogenesis (58). Mice knockout for *Clock* and *Bmal1* in pancreatic β-cells show impaired glucose tolerance, hypoinsulinemia, and defects in size and proliferation of pancreatic islets, suggesting that the loss of the pancreatic clock inhibited the β-cells from secreting insulin (59).

The increased prevalence of obesity and T2DM in shift workers can be the result of discrepancy between behavior and endogenous phase, as shift workers consume energy at times of their cycles when intake is normally absent and energy expenditure levels are low (60-63). Studies in mice and rats have confirmed that food intake restricted to the resting phase results in abdominal obesity (64-67). However, a disturbed circadian rhythm can alter insulin sensitivity without affecting adiposity. For example, a single night of partial sleep deprivation is already sufficient to induce insulin resistance in patients with type 1 diabetes mellitus as well as in healthy subjects (68;69). Disruption of circadian rhythms accelerates the development of diabetes through pancreatic β-cell loss and function, as shown in a diabetes-prone rat model (70). In elderly, the SCN is decreased in volume and cell number, thereby losing rhythmicity (71-73). This may underlie the high prevalence of profound disturbances of sleep and hormonal circadian rhythms, common in the elderly (74-77), which may contribute to the development of T2DM. More insight into the role of SCN loss and the role of desynchronized central and peripheral clocks in the development of insulin resistance would lead to better understanding of the pathophysiology of T2DM in shift workers and elderly.

THERAPIES FOR TYPE 2 DIABETES MELLITUS

T2DM imposes a major health risk, due to increased morbidity and mortality. Lifestyle changes, such as restricted caloric intake and exercise, can often significantly improve the outcome of the disease. However, the need for pharmacological strategies remains. The major goal of therapeutic intervention in T2DM is to ameliorate hyperglycemia and insulin resistance, but also increased risk factors including dyslipidemia and hypertension should be taken into account. Sulfonylureas and biguanides are the most prescribed drugs used to treat hyperglycemia in T2DM. Insulin therapy is necessary when medication alone is unable to control glucose levels and when β-cells fail to produce sufficient insulin. There is much interest in drugs that not only improve glucose metabolism, but also have beneficial effects on body weight and dyslipidemia.

Biguanides are the first-line treatment drug of choice for the treatment of T2DM, in particular in overweight patients. Metformin is the sole agent clinically used in this class. The molecular mechanisms of action underlying its beneficial effects on glucose metabolism are not fully known, although activation of AMP-activated protein kinase (AMK) in the liver appears critically involved (78;79). Metformin decreases hepatic gluconeogenesis, inhibits glycogenolysis and improves insulin sensitivity especially in skeletal muscle. As it does not affect insulin secretion, it is not associated with hypoglycemia when used as monotherapy. Metformin has modest improving effects on LDL cholesterol and TG levels, the underlying mechanism(s) not being understood. It does not reduce body weight, but is also not associated with body weight gain.

Sulfonylureas act mainly by stimulating insulin release from the β-cells of the pancreas. They bind to K_{ATP} channels on the cell membrane of β-cells. This inhibits a tonic, hyperpolarizing efflux of potassium, thus causing the electric potential over the membrane to become more positive. This depolarization opens voltage-gated calcium channels. The rise in intracellular calcium leads to increased fusion of insulin granules with the cell membrane, and therefore increased secretion of insulin. There is some evidence that sulfonylureas also sensitize β-cells to glucose, limit endogenous glucose production, decrease lipolysis (breakdown and release of FA by adipose tissue) and decrease clearance of insulin by the liver. Hypoglycemia is unfortunately a common side-effect as a result of increased insulin release and decreased insulin clearance. Since sulfonylureas increase appetite and weight gain, they are not the first choice for the management of T2DM in obese patients.

Glucagon-like peptide-1 (GLP1) is a cleavage product of the proglucagon molecule which is secreted by the intestinal L-cells and in the brain (80;81). It is released in response to food intake in proportion to caloric content to inhibit endogenous glucose production and to stimulate glucose-dependent insulin secretion (80;82). In addition, GLP-1 exerts multiple other effects, including inhibition of food intake, slowing of gastric emptying and inhibition of glucagon secretion (83;84). GLP-1 is known to beneficially affect glucose metabolism in T2DM patients (84;85). However, GLP-1 is easily degraded by the enzyme dipeptidyl-peptidase IV (DPP-IV), limiting its therapeutic efficacy (86). Therefore, pharmaceutical companies are developing GLP-1 analogues resistant to inactivation by DPP-IV. Clinical studies have shown that these analogues are very effective in reducing body weight, improving glucose metabolism and reducing plasma lipids in patients with T2DM. The anorexic effect and the hepatic insulin sensitizing effect of GLP-1 are in part mediated via GLP-1 receptors in the brain (83;87;88).

Topiramate, a sulfamate-substituted derivative of the monosaccharide D-fructose (89), is a broad-spectrum antiepileptic drug with potentially additional neurotherapeutic applications such as bipolar disorder and migraine (90;91). Its precise mechanism of action is unknown, although topiramate is considered to produce its antiepileptic effects through at least six mechanisms of action in the central nervous system: enhancement of GABA-ergic activity (92;93), inhibition of kainite/AMPA receptors (94), inhibition of voltage-dependent sodium channels (95), inhibition of high-voltage-activated calcium channels (96), increase in potassium conductance (97) and inhibition of carbonic anhydrase (98). Besides its antiepileptic action, topiramate is associated with a decrease in body weight. The reduction in body weight upon topiramate treatment has been shown in epileptic patients as well as in obese persons (99-101). Although loss of appetite resulting in reduced caloric intake can account for initial reductions in body weight, other mechanisms might be involved in the long-term effects of topiramate on weight, as weight loss continued after caloric intake returned to baseline levels (102). Several studies in lean as well as in obese mouse and rat models have confirmed that topiramate also reduces food intake and body weight (103;104). Interestingly, studies in obese, diabetic rats demonstrate that topiramate treatment reduces plasma glucose levels and improved insulin sensitivity independent of weight loss (105;106). It is not known whether the enhancement in insulin sensitivity is the result of improved hepatic insulin sensitivity or improved peripheral insulin sensitivity. It is also unknown if topiramate improves insulin sensitivity via actions in the brain. These observations are of interest for target discovery of new antidiabetic drugs.

OUTLINE OF THIS THESIS

The aim of the present thesis was to gain more insight into the role of the brain in the regulation of insulin sensitivity. Increasing evidence suggests a link between circadian rhythms and insulin sensitivity. Shift workers display a higher incidence of T2DM and already one night of partial sleep deprivation leads to reduced insulin sensitivity. Mice mutant for circadian clock genes, that as a consequence have a disturbed circadian rhythmicity, develop obesity affected glucose homeostasis. Since the causal relation between disturbed circadian rhythm and insulin resistance is not known, we determined the effect of a disturbance in circadian rhythm on energy metabolism and insulin sensitivity. The circadian rhythm was disturbed in mice either by exposure to constant light as this is known to suppress rhythmicity as well as lengthen circadian rhythm (**chapter 2**), or by removal of the SCN by thermic ablation (**chapter 3**). Glucose homeostasis is determined by the balance between endogenous production of glucose and by uptake of glucose by peripheral tissues, which is primarily controlled by insulin. Central effects of insulin are involved in the inhibition of endogenous glucose production by circulating insulin. It is unknown whether central effects of insulin are also involved in stimulation of glucose uptake by peripheral tissues. In addition, the effects of high-fat feeding in these central effects of circulating insulin are unknown. Therefore, we determined the role of central insulin signaling in mice on insulin-stimulated glucose uptake by peripheral tissues and the effect of high-fat feeding (**chapter 4**). The antiepileptic drug topiramate improves insulin sensitivity, but the underlying mechanisms are unclear. Therefore, we studied which organs are responsible

for this effect of topiramate on insulin sensitivity and whether the central nervous system is involved in this effect of topiramate treatment in high fat-fed mice (**chapter 5**). In addition to its role in glucose homeostasis, circulating insulin is involved in FA metabolism as it promotes lipogenesis and suppresses intracellular lipolysis in WAT resulting in increased fat storage. Since the relative contribution of the indirect effects though the brain are unknown, we determined the extent to which central effects of insulin contributed to both TG-derived and albumin-bound FA uptake by WAT. In addition, we determined the effect of high-fat feeding on these central effects of insulin (**chapter 6**). Thyroid hormones (TH) are crucial regulators of glucose and FA metabolism, in part via TH action in the brain. Therefore, we studied the direct effects of thyroid status on whole body energy metabolism and on TG-derived and albumin-bound FA uptake by muscle, liver, WAT and BAT (**chapter 7**). The results of the studies described in this thesis and the future perspectives are discussed in **chapter 8**.

REFERENCE LIST

1. Wild, S, Roglic, G, Green, A, Sicree, R, King, H: Global prevalence of diabetes: estimates for the year 2000 and projections for 2030. *Diabetes Care* 27:1047-1053, 2004

2. Ekberg, K, Landau, BR, Wajngot, A, Chandramouli, V, Efendic, S, Brunengraber, H, Wahren, J: Contributions by kidney and liver to glucose production in the postabsorptive state and after 60 h of fasting. *Diabetes* 48:292-298, 1999

3. Wolfe, RR: Tracers in metabolic research: radioisotope and stable isotope/mass spectrometry methods. *Lab Res Methods Biol Med* 9:1-287, 1984

4. Royle, GT, Wolfe, RR, Burke, JF: The measurement of glucose turnover and oxidation using radioactive and stable isotopes. *J Surg Res* 34:187-193, 1983

5. Steele, R: Influences of glucose loading and of injected insulin on hepatic glucose output. *Ann N Y Acad Sci* 82:420-430, 1959

6. Goudriaan, JR, den Boer, MA, Rensen, PC, Febbraio, M, Kuipers, F, Romijn, JA, Havekes, LM, Voshol, PJ: CD36 deficiency in mice impairs lipoprotein lipase-mediated triglyceride clearance. *J Lipid Res* 46:2175-2181, 2005

7. Franklyn, JA: Thyroid disease and its treatment: short- and long-term consequences. *J R Coll Physicians Lond* 33:564-567, 1999

8. Dimitriadis, GD, Raptis, SA: Thyroid hormone excess and glucose intolerance. *Exp Clin Endocrinol Diabetes* 109 Suppl 2:S225-S239, 2001

9. Raboudi, N, Arem, R, Jones, RH, Chap, Z, Pena, J, Chou, J, Field, JB: Fasting and postabsorptive hepatic glucose and insulin metabolism in hyperthyroidism. *Am J Physiol* 256:E159-E166, 1989

10. Okajima, F, Ui, M: Metabolism of glucose in hyper- and hypo-thyroid rats in vivo. Minor role of endogenous insulin in thyroid-dependent changes in glucose turnover. *Biochem J* 182:577-584, 1979

11. Okajima, F, Ui, M: Metabolism of glucose in hyper- and hypo-thyroid rats in vivo. Glucose-turnover values and futile-cycle activities obtained with ^{14}C- and ^{3}H-labelled glucose. *Biochem J* 182:565-575, 1979

12. Cettour-Rose, P, Theander-Carrillo, C, Asensio, C, Klein, M, Visser, TJ, Burger, AG, Meier, CA, Rohner-Jeanrenaud, F: Hypothyroidism in rats decreases peripheral glucose utilisation, a defect partially corrected by central leptin infusion. *Diabetologia* 48:624-633, 2005

13. Mahley, RW, Innerarity, TL, Rall, SC, Jr., Weisgraber, KH: Plasma lipoproteins: apolipoprotein structure and function. *J Lipid Res* 25:1277-1294, 1984

14. Hussain, MM, Kancha, RK, Zhou, Z, Luchoomun, J, Zu, H, Bakillah, A: Chylomicron assembly and catabolism: role of apolipoproteins and receptors. *Biochim Biophys Acta* 1300:151-170, 1996

15. Voshol, PJ, Rensen, PC, van Dijk, KW, Romijn, JA, Havekes, LM: Effect of plasma triglyceride metabolism on lipid storage in adipose tissue: studies using genetically engineered mouse models. *Biochim Biophys Acta* 1791:479-485, 2009

16. Su, X, Abumrad, NA: Cellular fatty acid uptake: a pathway under construction. *Trends Endocrinol Metab* 20:72-77, 2009

17. Cypess, AM, Lehman, S, Williams, G, Tal, I, Rodman, D, Goldfine, AB, Kuo, FC, Palmer, EL, Tseng, YH, Doria, A, Kolodny, GM, Kahn, CR: Identification and importance of brown adipose tissue in adult humans. *N Engl J Med* 360:1509-1517, 2009

18. van Marken Lichtenbelt, WD, Vanhommerig, JW, Smulders, NM, Drossaerts, JM, Kemerink, GJ, Bouvy, ND, Schrauwen, P, Teule, GJ: Cold-activated brown adipose tissue in healthy men. *N Engl J Med* 360:1500-1508, 2009

19. Hany, TF, Gharehpapagh, E, Kamel, EM, Buck, A, Himms-Hagen, J, von Schulthess, GK: Brown adipose tissue: a factor to consider in symmetrical tracer uptake in the neck and upper chest region. *Eur J Nucl Med Mol Imaging* 29:1393-1398, 2002

20. Bartelt, A, Bruns, OT, Reimer, R, Hohenberg, H, Ittrich, H, Peldschus, K, Kaul, MG, Tromsdorf, UI, Weller, H, Waurisch, C, Eychmuller, A, Gordts, PL, Rinninger, F, Bruegelmann, K, Freund, B, Nielsen, P, Merkel, M, Heeren, J: Brown adipose tissue activity controls triglyceride clearance. *Nat Med* 17:200-205, 2011

21. Sparks, JD, Sparks, CE: Insulin regulation of triacylglycerol-rich lipoprotein synthesis and secretion. *Biochim Biophys Acta* 1215:9-32, 1994

22. Ginsberg, HN, Zhang, YL, Hernandez-Ono, A: Metabolic syndrome: focus on dyslipidemia. *Obesity (Silver Spring)* 14 Suppl 1:41S-49S, 2006

23. Bech, K, Damsbo, P, Eldrup, E, Beck-Nielsen, H, Roder, ME, Hartling, SG, Volund, A, Madsbad, S: beta-cell function and glucose and lipid oxidation in Graves' disease. *Clin Endocrinol (Oxf)* 44:59-66, 1996

24. Oppenheimer, JH, Schwartz, HL, Lane, JT, Thompson, MP: Functional relationship of thyroid hormone-induced lipogenesis, lipolysis, and thermogenesis in the rat. *J Clin Invest* 87:125-132, 1991

25. Radenne, A, Akpa, M, Martel, C, Sawadogo, S, Mauvoisin, D, Mounier, C: Hepatic regulation of fatty acid synthase by insulin and T3: evidence for T3 genomic and nongenomic actions. *Am J Physiol Endocrinol Metab* 295:E884-E894, 2008

26. Havrankova, J, Roth, J, Brownstein, M: Insulin receptors are widely distributed in the central nervous system of the rat. *Nature* 272:827-829, 1978

27. Banks, WA: The blood-brain barrier as a regulatory interface in the gut-brain axes. *Physiol Behav* 89:472-476, 2006

28. Gerozissis, K: Brain insulin: regulation, mechanisms of action and functions. *Cell Mol Neurobiol* 23:1-25, 2003

29. Banks, WA: The source of cerebral insulin. *Eur J Pharmacol* 490:5-12, 2004

30. Obici, S, Zhang, BB, Karkanias, G, Rossetti, L: Hypothalamic insulin signaling is required for inhibition of glucose production. *Nat Med* 8:1376-1382, 2002

31. Obici, S, Feng, Z, Karkanias, G, Baskin, DG, Rossetti, L: Decreasing hypothalamic insulin receptors causes hyperphagia and insulin resistance in rats. *Nat Neurosci* 5:566-572, 2002

32. van den Hoek, AM, Voshol, PJ, Karnekamp, BN, Buijs, RM, Romijn, JA, Havekes, LM, Pijl, H: Intracerebroventricular neuropeptide Y infusion precludes inhibition of glucose and VLDL production by insulin. *Diabetes* 53:2529-2534, 2004

33. Pocai, A, Lam, TK, Gutierrez-Juarez, R, Obici, S, Schwartz, GJ, Bryan, J, guilar-Bryan, L, Rossetti, L: Hypothalamic K(ATP) channels control hepatic glucose production. *Nature* 434:1026-1031, 2005

34. Koch, L, Wunderlich, FT, Seibler, J, Konner, AC, Hampel, B, Irlenbusch, S, Brabant, G, Kahn, CR, Schwenk, F, Bruning, JC: Central insulin action regulates peripheral glucose and fat metabolism in mice. *J Clin Invest* 118:2132-2147, 2008

35. Scherer, T, O'Hare, J, ggs-Andrews, K, Schweiger, M, Cheng, B, Lindtner, C, Zielinski, E, Vempati, P, Su, K, Dighe, S, Milsom, T, Puchowicz, M, Scheja, L, Zechner, R, Fisher, SJ, Previs, SF, Buettner, C: Brain insulin controls adipose tissue lipolysis and lipogenesis. *Cell Metab* 13:183-194, 2011

36. Klieverik, LP, Foppen, E, Ackermans, MT, Serlie, MJ, Sauerwein, HP, Scanlan, TS, Grandy, DK, Fliers, E, Kalsbeek, A: Central effects of thyronamines on glucose metabolism in rats. *J Endocrinol* 201:377-386, 2009

37. Klieverik, LP, Janssen, SF, van, RA, Foppen, E, Bisschop, PH, Serlie, MJ, Boelen, A, Ackermans, MT, Sauerwein, HP, Fliers, E, Kalsbeek, A: Thyroid hormone modulates glucose production via a sympathetic pathway from the hypothalamic paraventricular nucleus to the liver. *Proc Natl Acad Sci U S A* 106:5966-5971, 2009

38. Klieverik, LP, Sauerwein, HP, Ackermans, MT, Boelen, A, Kalsbeek, A, Fliers, E: Effects of thyrotoxicosis and selective hepatic autonomic denervation on hepatic glucose metabolism in rats. *Am J Physiol Endocrinol Metab* 294:E513-E520, 2008

39. Boden, G: Role of fatty acids in the pathogenesis of insulin resistance and NIDDM. *Diabetes* 46:3-10, 1997

40. den Boer, MA, Voshol, PJ, Kuipers, F, Romijn, JA, Havekes, LM: Hepatic glucose production is more sensitive to insulin-mediated inhibition than hepatic VLDL-triglyceride production. *Am J Physiol Endocrinol Metab* 291:E1360-E1364, 2006

41. den Boer, MA, Voshol, PJ, Kuipers, F, Havekes, LM, Romijn, JA: Hepatic steatosis: a mediator of the metabolic syndrome. Lessons from animal models. *Arterioscler Thromb Vasc Biol* 24:644-649, 2004

42. Owen, OE, Reichard, GA, Jr., Boden, G, Shuman, C: Comparative measurements of glucose, beta-hydroxybutyrate, acetoacetate, and insulin in blood and cerebrospinal fluid during starvation. *Metabolism* 23:7-14, 1974

43. Clegg, DJ, Gotoh, K, Kemp, C, Wortman, MD, Benoit, SC, Brown, LM, D'Alessio, D, Tso, P, Seeley, RJ, Woods, SC: Consumption of a high-fat diet induces central insulin resistance independent of adiposity. *Physiol Behav* 2011

44. Mayer, CM, Belsham, DD: Central insulin signaling is attenuated by long-term insulin exposure via insulin receptor substrate-1 serine phosphorylation, proteasomal degradation, and lysosomal insulin receptor degradation. *Endocrinology* 151:75-84, 2010

45. Kalsbeek, A, Ruiter, M, La Fleur, SE, Van, HC, Buijs, RM: The diurnal modulation of hormonal responses in the rat varies with different stimuli. *J Neuroendocrinol* 15:1144-1155, 2003

46. Ruiter, M, La Fleur, SE, Van, HC, van, d, V, Kalsbeek, A, Buijs, RM: The daily rhythm in plasma glucagon concentrations in the rat is modulated by the biological clock and by feeding behavior. *Diabetes* 52:1709-1715, 2003

47. Kalra, SP, Bagnasco, M, Otukonyong, EE, Dube, MG, Kalra, PS: Rhythmic, reciprocal ghrelin and leptin signaling: new insight in the development of obesity. *Regul Pept* 111:1-11, 2003

48. Kalsbeek, A, Fliers, E, Romijn, JA, La Fleur, SE, Wortel, J, Bakker, O, Endert, E, Buijs, RM: The suprachiasmatic nucleus generates the diurnal changes in plasma leptin levels. *Endocrinology* 142:2677-2685, 2001

49. Weibel, L, Follenius, M, Spiegel, K, Ehrhart, J, Brandenberger, G: Comparative effect of night and daytime sleep on the 24-hour cortisol secretory profile. *Sleep* 18:549-556, 1995

50. Vinogradova, IA, Anisimov, VN, Bukalev, AV, Semenchenko, AV, Zabezhinski, MA: Circadian disruption induced by light-at-night accelerates aging and promotes tumorigenesis in rats. *Aging (Albany NY)* 1:855-865, 2009

51. Scheer, FA, Hilton, MF, Mantzoros, CS, Shea, SA: Adverse metabolic and cardiovascular consequences of circadian misalignment. *Proc Natl Acad Sci U S A* 106:4453-4458, 2009

52. Spiegel, K, Leproult, R, Van, CE: Impact of sleep debt on metabolic and endocrine function. *Lancet* 354:1435-1439, 1999

53. Ayas, NT, White, DP, Al-Delaimy, WK, Manson, JE, Stampfer, MJ, Speizer, FE, Patel, S, Hu, FB: A prospective study of self-reported sleep duration and incident diabetes in women. *Diabetes Care* 26:380-384, 2003

54. Gottlieb, DJ, Punjabi, NM, Newman, AB, Resnick, HE, Redline, S, Baldwin, CM, Nieto, FJ: Association of sleep time with diabetes mellitus and impaired glucose tolerance. *Arch Intern Med* 165:863-867, 2005

55. Yaggi, HK, Araujo, AB, McKinlay, JB: Sleep duration as a risk factor for the development of type 2 diabetes. *Diabetes Care* 29:657-661, 2006

56. Karlsson, B, Knutsson, A, Lindahl, B: Is there an association between shift work and having a metabolic syndrome? Results from a population based study of 27, 485 people. *Occup Environ Med* 58:747-752, 2001

57. Turek, FW, Joshu, C, Kohsaka, A, Lin, E, Ivanova, G, McDearmon, E, Laposky, A, Losee-Olson, S, Easton, A, Jensen, DR, Eckel, RH, Takahashi, JS, Bass, J: Obesity and metabolic syndrome in circadian Clock mutant mice. *Science* 308:1043-1045, 2005

58. Rudic, RD, McNamara, P, Curtis, AM, Boston, RC, Panda, S, Hogenesch, JB, Fitzgerald, GA: BMAL1 and CLOCK, two essential components of the circadian clock, are involved in glucose homeostasis. *PLoS Biol* 2:e377, 2004

59. Marcheva, B, Ramsey, KM, Buhr, ED, Kobayashi, Y, Su, H, Ko, CH, Ivanova, G, Omura, C, Mo, S, Vitaterna, MH, Lopez, JP, Philipson, LH, Bradfield, CA, Crosby, SD, JeBailey, L, Wang, X, Takahashi, JS, Bass, J: Disruption of the clock components CLOCK and BMAL1 leads to hypoinsulinaemia and diabetes. *Nature* 466:627-631, 2010

60. Morikawa, Y, Nakagawa, H, Miura, K, Soyama, Y, Ishizaki, M, Kido, T, Naruse, Y, Suwazono, Y, Nogawa, K: Effect of shift work on body mass index and metabolic parameters. *Scand J Work Environ Health* 33:45-50, 2007

61. Boggild, H, Knutsson, A: Shift work, risk factors and cardiovascular disease. *Scand J Work Environ Health* 25:85-99, 1999

62. Kawachi, I, Colditz, GA, Stampfer, MJ, Willett, WC, Manson, JE, Speizer, FE, Hennekens, CH: Prospective study of shift work and risk of

coronary heart disease in women. *Circulation* 92:3178-3182, 1995

63. Niedhammer, I, Lert, F, Marne, MJ: Prevalence of overweight and weight gain in relation to night work in a nurses' cohort. *Int J Obes Relat Metab Disord* 20:625-633, 1996

64. Bray, MS, Tsai, JY, Villegas-Montoya, C, Boland, BB, Blasier, Z, Egbejimi, O, Kueht, M, Young, ME: Time-of-day-dependent dietary fat consumption influences multiple cardiometabolic syndrome parameters in mice. *Int J Obes (Lond)* 34:1589-1598, 2010

65. Bray, MS, Tsai, JY, Villegas-Montoya, C, Boland, BB, Blasier, Z, Egbejimi, O, Kueht, M, Young, ME: Time-of-day-dependent dietary fat consumption influences multiple cardiometabolic syndrome parameters in mice. *Int J Obes (Lond)* 34:1589-1598, 2010

66. Salgado-Delgado, R, ngeles-Castellanos, M, Saderi, N, Buijs, RM, Escobar, C: Food intake during the normal activity phase prevents obesity and circadian desynchrony in a rat model of night work. *Endocrinology* 151:1019-1029, 2010

67. Arble, DM, Bass, J, Laposky, AD, Vitaterna, MH, Turek, FW: Circadian timing of food intake contributes to weight gain. *Obesity (Silver Spring)* 17:2100-2102, 2009

68. Donga, E, van, DM, van Dijk, JG, Biermasz, NR, Lammers, GJ, van, KK, Hoogma, RP, Corssmit, EP, Romijn, JA: Partial sleep restriction decreases insulin sensitivity in type 1 diabetes. *Diabetes Care* 33:1573-1577, 2010

69. Donga, E, van, DM, van Dijk, JG, Biermasz, NR, Lammers, GJ, van Kralingen, KW, Corssmit, EP, Romijn, JA: A single night of partial sleep deprivation induces insulin resistance in multiple metabolic pathways in healthy subjects. *J Clin Endocrinol Metab* 95:2963-2968, 2010

70. Gale, JE, Cox, HI, Qian, J, Block, GD, Colwell, CS, Matveyenko, AV: Disruption of Circadian Rhythms Accelerates Development of Diabetes through Pancreatic Beta-Cell Loss and Dysfunction. *J Biol Rhythms* 26:423-433, 2011

71. Hofman, MA, Swaab, DF: Alterations in circadian rhythmicity of the vasopressin-producing neurons of the human suprachiasmatic nucleus (SCN) with aging. *Brain Res* 651:134-142, 1994

72. Hofman, MA, Swaab, DF: Living by the clock: the circadian pacemaker in older people. *Ageing Res Rev* 5:33-51, 2006

73. Swaab, DF, Fliers, E, Partiman, TS: The suprachiasmatic nucleus of the human brain in relation to sex, age and senile dementia. *Brain Res* 342:37-44, 1985

74. Aujard, F, Cayetanot, F, Bentivoglio, M, Perret, M: Age-related effects on the biological clock and its behavioral output in a primate. *Chronobiol Int* 23:451-460, 2006

75. Purnell, JQ, Brandon, DD, Isabelle, LM, Loriaux, DL, Samuels, MH: Association of 24-hour cortisol production rates, cortisol-binding globulin, and plasma-free cortisol levels with body composition, leptin levels, and aging in adult men and women. *J Clin Endocrinol Metab* 89:281-287, 2004

76. Van Someren, EJ: Circadian and sleep disturbances in the elderly. *Exp Gerontol* 35:1229-1237, 2000

77. van Cauter, E, Leproult, R, Kupfer, DJ: Effects of gender and age on the levels and circadian rhythmicity of plasma cortisol. *J Clin Endocrinol Metab* 81:2468-2473, 1996

78. Zhou, G, Myers, R, Li, Y, Chen, Y, Shen, X, Fenyk-Melody, J, Wu, M, Ventre, J, Doebber, T, Fujii, N, Musi, N, Hirshman, MF, Goodyear, LJ, Moller, DE: Role of AMP-activated protein kinase in mechanism of metformin action. *J Clin Invest* 108:1167-1174, 2001

79. Hawley, SA, Gadalla, AE, Olsen, GS, Hardie, DG: The antidiabetic drug metformin activates the AMP-activated protein kinase cascade via an adenine nucleotide-independent mechanism. *Diabetes* 51:2420-2425, 2002

80. Kreymann, B, Williams, G, Ghatei, MA, Bloom, SR: Glucagon-like peptide-1 7-36: a physiological incretin in man. *Lancet* 2:1300-1304, 1987

81. Larsen, PJ, Tang-Christensen, M, Holst, JJ, Orskov, C: Distribution of glucagon-like peptide-1 and other preproglucagon-derived peptides in the rat hypothalamus and brainstem. *Neuroscience* 77:257-270, 1997

82. Holst, JJ, Orskov, C, Nielsen, OV, Schwartz, TW: Truncated glucagon-like peptide I, an insulin-releasing hormone from the distal gut. *FEBS Lett* 211:169-174, 1987

83. Turton, MD, O'Shea, D, Gunn, I, Beak, SA, Edwards, CM, Meeran, K, Choi, SJ, Taylor, GM, Heath, MM, Lambert, PD, Wilding, JP, Smith, DM, Ghatei, MA, Herbert, J, Bloom, SR: A role for glucagon-like peptide-1 in the central regulation of feeding. *Nature* 379:69-72, 1996

84. Willms, B, Werner, J, Holst, JJ, Orskov, C, Creutzfeldt, W, Nauck, MA: Gastric emptying, glucose responses, and insulin secretion after a liquid test meal: effects of exogenous glucagon-like peptide-1 (GLP-1)-(7-36) amide in type 2 (noninsulin-dependent) diabetic

patients. *J Clin Endocrinol Metab* 81:327-332, 1996

85. Nauck, MA, Kleine, N, Orskov, C, Holst, JJ, Willms, B, Creutzfeldt, W: Normalization of fasting hyperglycaemia by exogenous glucagon-like peptide 1 (7-36 amide) in type 2 (non-insulin-dependent) diabetic patients. *Diabetologia* 36:741-744, 1993

86. Deacon, CF, Nauck, MA, Toft-Nielsen, M, Pridal, L, Willms, B, Holst, JJ: Both subcutaneously and intravenously administered glucagon-like peptide I are rapidly degraded from the NH2-terminus in type II diabetic patients and in healthy subjects. *Diabetes* 44:1126-1131, 1995

87. Parlevliet, ET, de Leeuw van Weenen JE, Romijn, JA, Pijl, H: GLP-1 treatment reduces endogenous insulin resistance via activation of central GLP-1 receptors in mice fed a high-fat diet. *Am J Physiol Endocrinol Metab* 299:E318-E324, 2010

88. Knauf, C, Cani, PD, Perrin, C, Iglesias, MA, Maury, JF, Bernard, E, Benhamed, F, Gremeaux, T, Drucker, DJ, Kahn, CR, Girard, J, Tanti, JF, Delzenne, NM, Postic, C, Burcelin, R: Brain glucagon-like peptide-1 increases insulin secretion and muscle insulin resistance to favor hepatic glycogen storage. *J Clin Invest* 115:3554-3563, 2005

89. Shank, RP, Gardocki, JF, Streeter, AJ, Maryanoff, BE: An overview of the preclinical aspects of topiramate: pharmacology, pharmacokinetics, and mechanism of action. *Epilepsia* 41 Suppl 1:S3-S9, 2000

90. Ferrari, A, Tiraferri, I, Neri, L, Sternieri, E: Clinical pharmacology of topiramate in migraine prevention. *Expert Opin Drug Metab Toxicol* 7:1169-1181, 2011

91. McIntyre, RS, Riccardelli, R, Binder, C, Kusumakar, V: Open-label adjunctive topiramate in the treatment of unstable bipolar disorder. *Can J Psychiatry* 50:415-422, 2005

92. White, HS, Brown, SD, Woodhead, JH, Skeen, GA, Wolf, HH: Topiramate modulates GABA-evoked currents in murine cortical neurons by a nonbenzodiazepine mechanism. *Epilepsia* 41 Suppl 1:S17-S20, 2000

93. White, HS, Brown, SD, Woodhead, JH, Skeen, GA, Wolf, HH: Topiramate enhances GABA-mediated chloride flux and GABA-evoked chloride currents in murine brain neurons and increases seizure threshold. *Epilepsy Res* 28:167-179, 1997

94. Gibbs, JW, III, Sombati, S, DeLorenzo, RJ, Coulter, DA: Cellular actions of topiramate: blockade of kainate-evoked inward currents in cultured hippocampal neurons. *Epilepsia* 41 Suppl 1:S10-S16, 2000

95. Zona, C, Ciotti, MT, Avoli, M: Topiramate attenuates voltage-gated sodium currents in rat cerebellar granule cells. *Neurosci Lett* 231:123-126, 1997

96. Zhang, X, Velumian, AA, Jones, OT, Carlen, PL: Modulation of high-voltage-activated calcium channels in dentate granule cells by topiramate. *Epilepsia* 41 Suppl 1:S52-S60, 2000

97. Herrero, AI, Del, ON, Gonzalez-Escalada, JR, Solis, JM: Two new actions of topiramate: inhibition of depolarizing GABA(A)-mediated responses and activation of a potassium conductance. *Neuropharmacology* 42:210-220, 2002

98. Dodgson, SJ, Shank, RP, Maryanoff, BE: Topiramate as an inhibitor of carbonic anhydrase isoenzymes. *Epilepsia* 41 Suppl 1:S35-S39, 2000

99. Ben-Menachem, E: Predictors of weight loss in adults with topiramate-treated epilepsy. 2003

100. Eliasson, B, Gudbjornsdottir, S, Cederholm, J, Liang, Y, Vercruysse, F, Smith, U: Weight loss and metabolic effects of topiramate in overweight and obese type 2 diabetic patients: randomized double-blind placebo-controlled trial. *Int J Obes (Lond)* 2007

101. Stenlof, K, Rossner, S, Vercruysse, F, Kumar, A, Fitchet, M, Sjostrom, L: Topiramate in the treatment of obese subjects with drug-naive type 2 diabetes. *Diabetes Obes Metab* 9:360-368, 2007

102. Ben-Menachem, E, Axelsen, M, Johanson, EH, Stagge, A, Smith, U: Predictors of weight loss in adults with topiramate-treated epilepsy. *Obes Res* 11:556-562, 2003

103. Wilkes, JJ, Nguyen, MT, Bandyopadhyay, GK, Nelson, E, Olefsky, JM: Topiramate treatment causes skeletal muscle insulin sensitization and increased Acrp30 secretion in high-fat-fed male Wistar rats. *Am J Physiol Endocrinol Metab* 289:E1015-E1022, 2005

104. Lalonde, J, Samson, P, Poulin, S, Deshaies, Y, Richard, D: Additive effects of leptin and topiramate in reducing fat deposition in lean and obese ob/ob mice. *Physiol Behav* 80:415-420, 2004

105. Picard, F, Deshaies, Y, Lalonde, J, Samson, P, Richard, D: Topiramate reduces energy and fat gains in lean (Fa/?) and obese (fa/fa) Zucker rats. *Obes Res* 8:656-663, 2000

106. Wilkes, JJ, Nelson, E, Osborne, M, Demarest, KT, Olefsky, JM: Topiramate is an insulin-sensitizing compound in vivo with direct effects on adipocytes in female ZDF rats. *Am J Physiol Endocrinol Metab* 288:E617-E624, 2005

ADDITIVE EFFECTS OF CONSTANT LIGHT EXPOSURE AND DIET ON CIRCADIAN RHYTHMS OF ENERGY METABOLISM AND INSULIN SENSITIVITY

Claudia P. Coomans*
Sjoerd A. A. van den Berg*
Thijs Houben
Jan-Bert van Klinken
Rosa van den Berg
Amanda C.M. Pronk
Louis M. Havekes
Johannes A. Romijn
Ko Willems van Dijk
Nienke R. Biermasz
Johanna H. Meijer

*Both authors contributed equally

2

ABSTRACT

Disturbances in circadian rhythms are associated with increased incidence of obesity and type 2 diabetes. We examined the effects of a disturbed circadian rhythm on energy metabolism and insulin sensitivity by exposing mice to constant light.

Mice were subjected to 12 h/12 h light/dark cycle (LD) or constant light (LL) for 5 weeks, and were fed chow or high-fat diet. Neuronal activity was measured by *in vivo* electrophysiological SCN recordings. During the last 4 days of the experiment, metabolic cage analysis was performed. Insulin sensitivity was assessed by hyperinsulinemic-euglycemic clamp in the middle of the resting (ZT 6) and active phases of the LD mice (ZT 18). Diet-independent contribution of the LL regimen to body weight gain was assessed by mixed model analysis.

Constant light exposure reduced the circadian amplitudes of the suprachiasmatic nucleus' (SCN) neuronal activity pattern by 55% and rhythm strength by 54% within three days. The first week in constant light, LL mice had increased total food intake over 24 h and decreased total energy expenditure over 24 h, which resulted in immediate body weight gain on both diets compared to LD mice. Mixed model analysis revealed that weight gain induced by constant light was apparent before high-fat diet resulted in weight gain. After four weeks in constant light, the circadian pattern in feeding and energy expenditure was completely lost. Total food intake and energy expenditure over 24 h was reduced compared to LD mice, which resulted in stabilization of weight gain caused by constant light. LL neutralized the normal circadian variation in insulin sensitivity of liver as well as peripheral tissues on both diets.

In conclusion, constant light exposure reduces SCN rhythm strength instantaneously and results in a complete absence of rhythm in energy metabolism and insulin sensitivity, exacerbating the effect of a high-fat diet. These data indicate that mild rhythm disorders can contribute to the pathophysiology of obesity and T2DM and may be of great relevance for people having reduced SCN rhythmicity such as, for instance, elderly and shift workers.

INTRODUCTION

The increasing prevalence of obesity and type 2 diabetes during the 20th century coincides with environmental light pollution, reduction of sleep duration and/or quality, jet lags and shift work, resulting in disruption of circadian rhythm. Circadian rhythms are 24 h cycles generated by the suprachiasmatic nuclei (SCN) located in the anterior hypothalamus. The SCN induces daily rhythms in hormone concentrations (1-3), body temperature (4), heart rate and blood pressure (5), feeding behavior and many other parameters, and adjusts these rhythms to local time, mainly by light-dark information received from the eyes (6-8). Disruption of circadian coordination may be manifested by endocrine imbalances, psychological and sleep disorders, cancer incidence and reduced life span (9). In contrast, the maintenance of robust circadian rhythms is associated with well-being and increased longevity (10;11).

Many hormones involved in metabolism, such as insulin, glucagon, corticosterone and leptin exhibit circadian oscillations (1-3). Furthermore, enzymes and transport systems involved in lipid and glucose metabolism, such as glucose-6-phosphate dehydrogenase and nuclear receptors are rhythmically expressed (12;13). Conversely, mice transgenic for clock genes show deficits in several aspects of glucose homeostasis (14;15). Disturbances in circadian rhythm due to shift work and sleep deprivation are associated with an increased incidence of obesity (16). Moreover, chronic disturbances in circadian rhythms have been proposed to be the underlying cause for the adverse metabolic and cardiovascular health effects of shift work (17-20). In part, this may be due to differences in the circadian pattern of energy intake (21).

Understanding of the causal relation between a disturbed circadian rhythm and features of the metabolic syndrome such as insulin resistance could lead to novel therapeutic strategies for patients, elderly and shift workers, who are prone to suffer from circadian rhythm disturbances. Importantly, circadian rhythms in these groups are reduced, rather than absent, whereas most animal studies have been performed in mouse models that are characterized by a total absence of circadian rhythmicity (15;22). Therefore, the aim of the present study was to determine the effect of reduced rather than total loss of circadian rhythm on energy metabolism and insulin sensitivity in mice. Furthermore, we studied the additive effects of high-fat feeding and constant light exposure. To this end, mice were subjected to constant light, which reduces the amplitude of circadian rhythms (23-25). *In vivo* recordings in freely moving mice indeed showed a reduction in SCN rhythm amplitude of ~50% in constant light. Remarkably, we found that the circadian variation in energy metabolism and insulin sensitivity was completely lost in animals housed in constant light, on chow and high-fat diet compared to mice on a light-dark cycle. The results indicate that a reduction in SCN rhythmicity strongly impairs glucose and energy homeostasis, thereby contributing to development of obesity and insulin resistance.

MATERIALS AND METHODS

Animals

Male C57Bl/6J mice (10 weeks old) were housed in a temperature-controlled room on a 12 h/12 h light/dark cycle (LD) or in constant light (LL, ≥ 180 lux) for 5 weeks. The mice had free access

to chow and water throughout the experiment. In the high-fat experiment, mice were fed *ad libitum* high-fat diet (45 energy% of fat derived from lard; D12451, Research Diet Services, Wijk bij Duurstede, The Netherlands). Body weight was monitored twice a week for all individual animals throughout the experiment. All animal experiments were performed in accordance with the regulations of Dutch law on animal welfare and the institutional ethics committee for animal procedures from the Leiden University Medical Center, Leiden, The Netherlands approved the protocol.

In vivo electrophysiological SCN recordings

For electrophysiological SCN recording, an electrode was implanted in the SCN of C57Bl/6J mice. For this, mice were anesthetized using a mixture of Ketamine (100 mg/kg, Aescoket, Boxtel, the Netherlands), Xylazine (10 mg/kg, Bayer AG, Leverkusen, Germany) and Atropine (0.1 mg/kg, Pharmachemie, Haarlem, The Netherlands) and mounted in a stereotactic device (Digital Just for Mouse Stereotaxic Instrument, Stoelting Co, Wood Dale, IL, USA). Tripolar stainless steel electrodes were used, with two of the electrodes twisted together and a third, uninsulated electrode for use as reference (125 μm, Plastics One, Roanoke, Virginia, USA). The reference electrode was placed in the cortex and the twisted electrode pair was implanted under a 5° angle in the coronal plane and aimed at the SCN, 0.46 mm posterior to bregma, 0.14 mm lateral to the midline, and 5.2 mm ventral to the surface of the cortex. At the end of the experiment, animals were sacrificed and the electrode placement was determined by histology. Recordings from animals in which the recording location was outside the SCN were excluded from the analysis.

Following a 7 day recovery period, mice were placed in a recording cage and the electrodes were connected to the recording hardware. The connection consisted of lightweight cables suspended from a counter-balanced rotating contact, allowing animals to move around freely. Water and food was available *ad libitum* during the recording. Neuronal signals from the electrodes were differentially amplified and band-pass filtered (0.5-5 KHz) before being fed into amplitude based spike triggers that converted action potentials into pulses that were counted every 10 sec and stored on a computer. During the first days of the recording, animals were kept in constant darkness (DD) to test for the presence of a circadian rhythm in the recorded action potential frequency. If a rhythm was detected, light were turned on and animals were exposed to constant light for a minimum duration of 7 days.

Action potential frequency was calculated for each 10 min interval of the recording. Peak and trough levels were quantified by averaging the firing rate over a 2 h interval. To compare changes in rhythm in constant light between animals, the amplitude values were normalized with respect to the amplitude in constant darkness.

Circadian rhythm analysis

Behavioral activity of the mice in LD and LL was recorded using passive infrared motion detection sensors (Hygrosens Instruments, Löffingen, Germany) that were mounted underneath the lid of the cage and connected to a ClockLab data collection system (Actimetrics Software, Illinois, U.S.) that recorded the amount of sensor activation in one min bins. The presence of circadian

rhythms was determined 25 days into the experiment for 10 consecutive days by F-periodogram analysis of activity based on the algorithm of Dörrscheidt and Beck (26).

Plasma corticosterone analysis

Three weeks after initiating the light intervention, blood samples were taken from mice on chow and high-fat diet via tail indentation at two different circadian times: one hour after the start of the subjective day (CT 1) and one hour before the start of the subjective night (CT 11), when corticosterone levels are at their lowest and highest, respectively (27). The activity (subjective night) period was determined for each mouse using passive infrared motion detection sensors (28). The samples were taken into capillaries, placed on ice and centrifuged at 4°C. Total plasma corticosterone concentrations were determined in an assay using a ^{125}I double-antibody kit (ICN Diagnostics). The high and low limits of detectability of the assay are 1,000 and 7.7 ng/ml, respectively.

Indirect calorimetry

To determine energy metabolism of mice in LD or LL, indirect calorimetry (Phenomaster, TSE Systems, Bad Homburg, Germany) was performed in individually housed animals on high-fat diet. Since exposure to constant light deteriorates circadian rhythm over time, these observations were obtained in two periods. The first period comprised the first 7 days of the continuous light, high-fat diet intervention, and the second period comprised 6 days of measurement, 4 weeks after initiation of the light/high-fat diet intervention.

Individual measurements of oxygen consumption and carbon dioxide production were performed every 9 min. In addition, food and water intake were measured. Furthermore, activity measurements were performed and pooled data were exported every 1 min. Before and after each experiment, animals were weighed to the nearest 100 mg. Since the LL regime lengthens the circadian period (29;30), activity patterns of individual animals were analyzed and corrected for the subjective day and subjective night periods. Total length of an individual day was determined as the time elapsed between two consecutive periods of high physical activity. Subjective day and night were set at 50% of that elapsed time.

Hyperinsulinemic-euglycemic clamp

Five weeks after initiating the light intervention, insulin sensitivity of mice on chow or high-fat diet was determined in a hyperinsulinemic-euglycemic clamp performed in the middle of the resting (ZT 6) and active phase of the LD mice (ZT 18). Since the LL regimen disrupts the circadian rhythm by elongating the circadian period, the exact circadian time at which a stable hyperinsulinemic-euglycemic infusion rate was established was subsequently calculated for each mouse in the LL group individually. Before the start of the experiment, mice fasted for 16 h were anesthetized with Acepromazine (6.25 mg/kg, Alfasan, Woerden, The Netherlands), Midazolam (6.25 mg/kg, Roche, Mijdrecht, The Netherlands), and Fentanyl (0.31 mg/kg, Janssen-Cilag, Tilburg, The Netherlands). Anaesthesia as well as body temperature was maintained throughout the procedure. At the end of the basal as well as the end of the hyperinsulinemic period, hematocrit values were determined to ensure that the animals were not anemic.

First, basal rates of glucose turnover were determined by primed (0.8 µCi), constant (0.02 µCi/min) intravenous (i.v.) infusion of 3-³H-glucose (Amersham, Little Chalfont, U.K.) for 60 minutes. Subsequently, insulin (Actrapid, Novo Nordisk, Denmark) was administered i.v. by primed (4.1 mU), constant (6.8 mU/h) infusion, with continuation of infusion of 3-³H-glucose for 90 min. A variable i.v. infusion of a 12.5% D-glucose solution was used to maintain euglycemia as determined at 10-min intervals via tail bleeding (<3 µl, Accu-chek, Sensor Comfort; Roche Diagnostics, Mannheim, Germany). In the last 20 min, blood samples were taken with intervals of 10 min. At the day of the hyperinsulinemic-euglycemic clamp, body composition was determined by dual-energy X-ray absorptiometry (DEXA) using the Norland pDEXA Sabre X-Ray Bone Densitometer (Norland Strateq, Hampshire, U.K.). Subsequently, the mice were sacrificed.

Plasma analysis

During the hyperinsulinemic-euglycemic clamp studies, blood samples were taken from the tail tip into chilled capillaries. The tubes were placed on ice and centrifuged at 4°C. Plasma glucose levels were determined using a commercially available kit and standard according to the instructions of the manufacturer (Instruchemie, Delfzijl, The Netherlands) in 96-wells plates (Greiner Bio-One, Alphen a/d Rijn, The Netherlands). Plasma insulin levels were measured using a mouse-specific insulin ELISA kit (Crystal Chem Inc., Downers Grove, U.S.). Total plasma 3-³H-glucose was determined in supernatant of 7.5 µl plasma, after protein precipitatation using 20% trichloroacetic acid and evaporation to eliminate tritiated water. Turnover rates of glucose (Rd, µmol/min/kg) were calculated in basal and hyperinsulinemic conditions as the rate of tracer infusion (dpm/min) divided by plasma specific activity of 3-³H-glucose (dpm/µmol) corrected for body mass. Endogenous glucose production (EGP) during the hyperinsulinemic period, was calculated as the difference between the tracer-derived rate of glucose turnover and the glucose infusion rate.

Statistical analysis

To assess the circadian variation of insulin sensitivity, clamp data from chow and high-fat fed mice was used for linear regression analysis. Data from mice in LD and LL was plotted against the calculated circadian time (CT; the time at which stable glucose infusion rates (GIR) were achieved) and linear regression analysis was performed with GIR as dependent and CT as independent variable using GraphPad Prism version 5.0 for Windows (GraphPad Software, La Jolla California U.S.). Slope deviation from 0 was assessed for the LD and LL group individually. Unpaired student T-Tests were performed to compare GIR, endogenous glucose production and glucose disposal rates obtained at ZT 6 and ZT 18 of the LD mice.

A mixed effects model was used to investigate the effect of the constant light and high-fat diet intervention on body weight gain. The model assumed body weight to increase linearly with time in the control group (LD mice on chow) and included subject specific random intercepts and slopes to model individual deviations from the group average. Additional effects of the light and high-fat diet intervention were modeled by time dependent covariates. The model allowed possible nonlinear time dependencies in weight gain and a possible interaction

between the high-fat diet and the light regimen. The within subject error was assumed to have an autoregressive covariance structure of order one.

RESULTS

### SCN recording and circadian rhythm analysis

The effect of constant light (LL) on the circadian rhythm in SCN neuronal activity was determined by *in vivo* electrophysiological recordings in the SCN of freely moving mice (Fig. 1). A circadian rhythm in neuronal activity was observed in seven mice, showing high activity during the day and low activity during the night. Upon exposure to LL, peak firing rate levels in the SCN decreased, whereas trough firing rate increased, causing a dampening of the amplitude of the rhythm (Fig. 1A, B). In LL, the amplitude was $73 \pm 5\%$ on day 1, $60 \pm 3\%$ on day 2, reaching a steady amplitude of $46 \pm 4\%$ from day 3 onwards (Fig. 1C, $P < 0.01$) compared to day 0. F-periodogram analysis over 10 days in LL revealed that the rhythm strength of locomotor activity under LL was $46 \pm 6\%$ of the rhythm strength in the LD control mice (n=12 per group, $P < 0.001$).

Body weight gain

Body weights of LD and LL mice on chow or high-fat diets measured during the course of the experiments are shown in Fig. 2A. LL mice were heavier compared to LD mice, both on chow and high-fat diet. To determine the isolated contribution of constant light to weight development as well as to assess its possible interaction with high-fat diet, a mixed effect
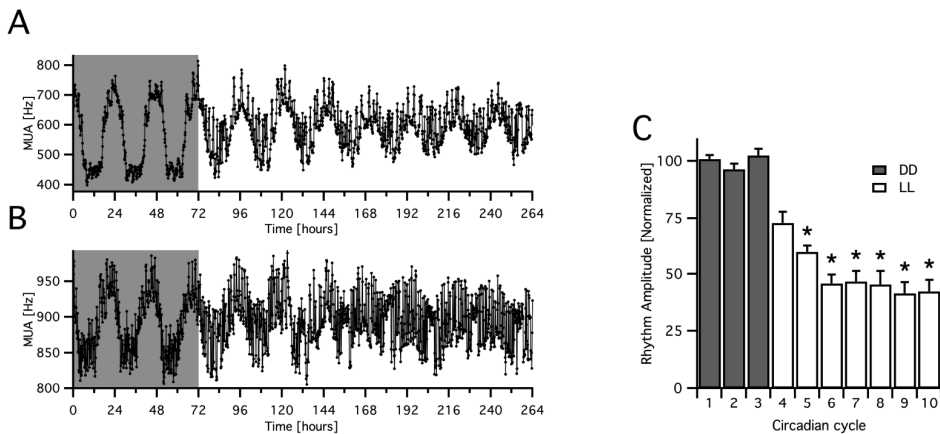
Fig. 1. Longterm *in vivo* multiunit activity recordings were performed in freely moving, awake mice (n=7) using implanted microelectrodes. Representative recordings under constant darkness (DD) followed by constant light (LL) (A, B). Action potential frequency (black trace) is indicated with a 10 min time resolution. Background represents light exposure, with grey representing lights off, and white representing lights on. After 3 cycles in DD, animals were exposed to LL. Analysis of the time course of the SCN rhythm deterioration and stabilization after 3 days of LL (C). Bars show the amplitude of the rhythm, normalized for each animal relative to the average amplitude during the last 3 cycles in DD (grey bars) and 7 cycles in LL (white bars). * $P < 0.01$.
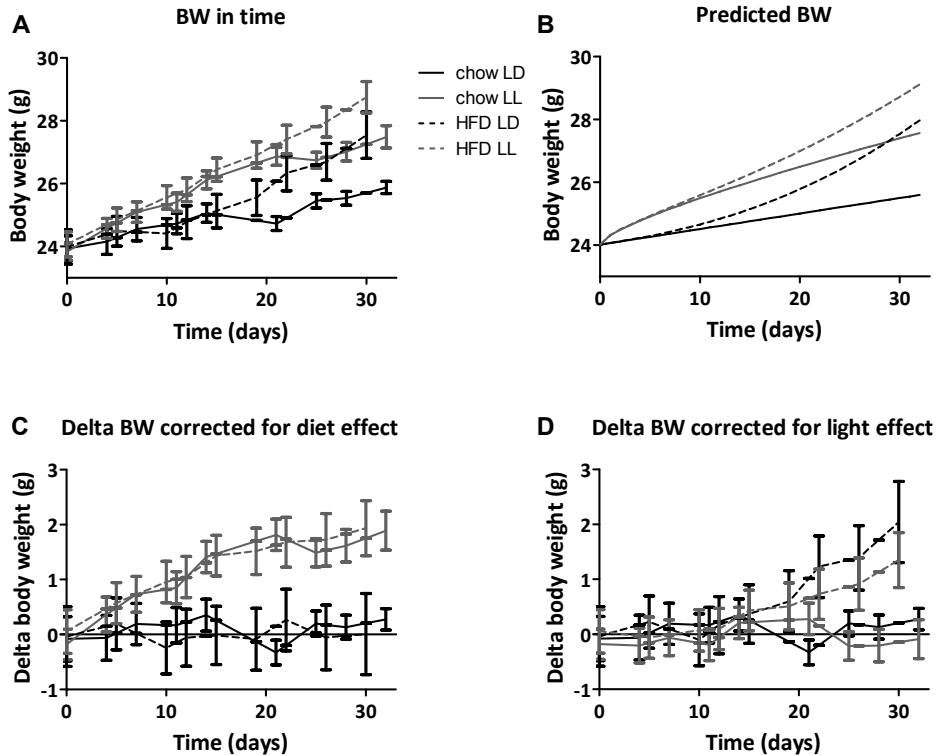
Fig. 2. A mixed effects model to investigate the effect of constant light (LL) and high-fat diet on body weight gain: average body weight (A), average body weight predicted by the mixed effect model (B), time dependent effect of the LL intervention on weight gain (C), the time dependent effect of the high-fat diet intervention on weight gain (D). Values represent means ± SEM for at least 7 mice per group.

model was developed, including light regimen and diet as covariates. The developed mixed effects model predicted group averages as shown in Fig. 2B.

Both the constant light intervention covariate and high-fat diet intervention covariate were found to be highly significant ($P < 0.00001$ for both covariates), showing that both interventions independently caused additional weight gain compared to the chow diet and light-dark regime. The interaction term did not reach statistical significance ($P = 0.081$). Interestingly, the time dependency in the LL and high-fat diet covariate was nonlinear, as the exponents of the fitted power functions were significantly different from one ($P < 0.00001$ for both covariates): the LL effect on weight gain was described by a power function with an exponent of 0.6 while the high-fat diet effect had an exponent of 2.4. This indicates that the onset and speed of weight gain is different for both interventions. Indeed, the constant light intervention immediately affected weight gain (Fig. 2C) and stabilized later on whereas the effect of high-fat diet became manifest at a later stage (Fig. 2D), indicating that exposure to constant light increases body weight faster than high-fat diet. These data clearly show that LL and high-fat diet have independent and additive effects during the development of weight gain.

Glucocorticoids

Corticosterone levels in plasma were determined at two different circadian times: one hour after the start of the subjective day (expected lowest corticosterone levels, CT 1) and one hour before the start of the subjective night (expected peak in corticosterone levels, CT 11) as determined for each mouse individually using passive infrared motion detection sensors. Indeed, LD mice on chow as well as on high-fat diet had lowest corticosterone levels one hour after the start of the subjective day, which increased dramatically one hour before the start of the subjective night: from 12 ± 2 to 90 ± 32 ng/ml on chow ($P < 0.01$) and from 19 ± 5 to 82 ± 24 ng/ml on high-fat diet ($P < 0.01$) (Fig. 3). In LL mice on a chow diet, corticosterone levels were similar to LD mice one hour before the start of the subjective day but significantly lower one hour before the start of the subjective night (28 ± 16 to 42 ± 34 ng/ml, ns). In addition, corticosterone levels did not differ within the LL group when the two sampling times were compared. On the high-fat diet, the differences between the LL and the LD group were similar, as corticosterone levels were similar one hour before the start of the subjective day but significantly lower in the LL group one hour before the start of the subjective night (high-fat diet from 16 ± 3 to 43 ± 21 ng/ml, $P < 0.01$). Interestingly, in contrast to the chow diet, levels did differ significantly within the LL group when the two sampling times were compared. These data show that the LL regimen did not result in a chronic stress response, and that corticosterone levels were lower compared to LD mice during the subjective night.
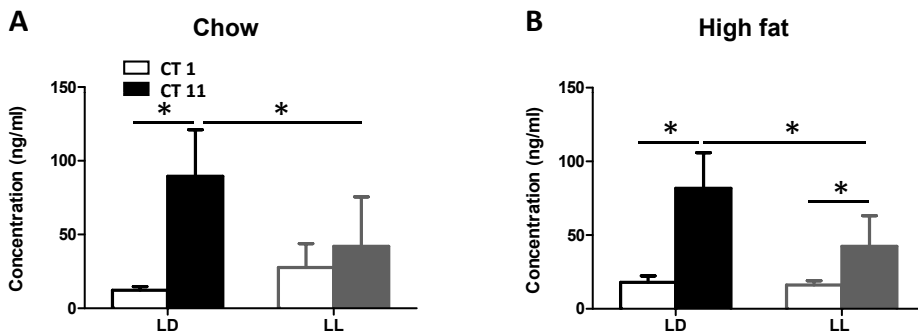
Fig. 3. Corticosterone plasma levels of chow (A) and high-fat (B) fed mice in LD or LL obtained at time of expected lowest (CT 1, open bars) and peak (CT 11, filled bars) corticosterone levels. Values represent means ± SD for 7-12 mice per group. * $P < 0.01$.

Indirect calorimetry

Short term

At the start of the light/high-fat intervention was started, body weight did not differ between the two groups of mice (LD, 25.5 ± 1.8 *vs*. LL, 25.6 ± 1.4 g, ns). LL mice had a higher energy intake measured over a circadian period compared to LD mice and consumed a larger fraction of the total circadian intake during the subjective day (44% *vs*. 36%, $P = 0.06$, Fig. 4A). Respiratory
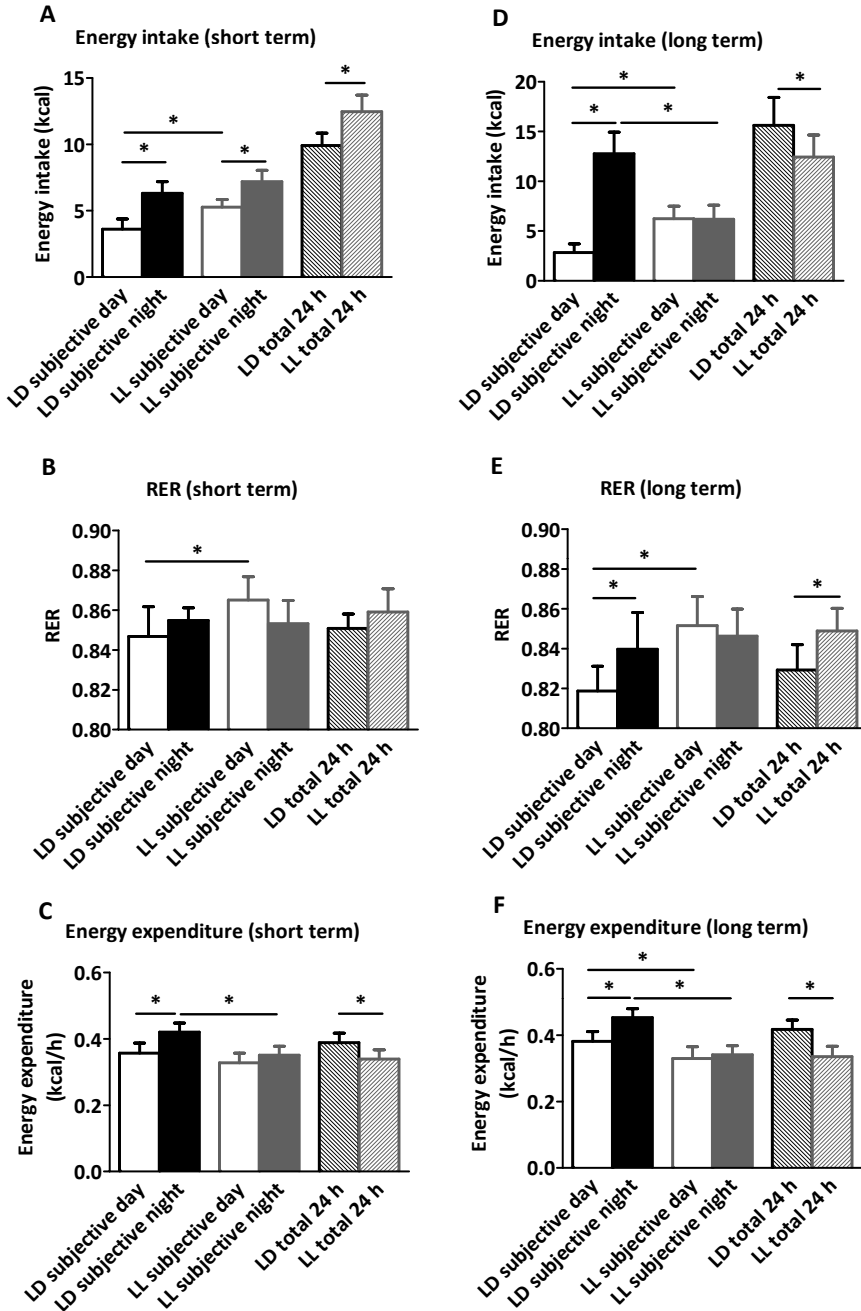
Fig. 4. Indirect calorimetric analysis of mice under light/dark (LD, n=8) and constant light (LL, n=8) conditions on high-fat diet analyzed for subjective day, subjective night and total 24 h levels. Energy intake (A), respiratory exchange rate (RER, B) and energy expenditure (C) during the first 6 days of the intervention. Panels D, E and F represent the same parameters measured in the same mice, for a period of 6 days, after 4 weeks of intervention. Values represent means ± SD. * $P < 0.05$.

exchange rate (RER) was significantly higher in the LL mice during the subjective day period indicating a higher relative carbohydrate to fat oxidation ratio (Fig. 4B). RER did not differ between groups during the night period. Total energy expenditure over a period of a circadian period was significantly lower in the LL mice (Fig. 4C), due to a significant reduction in energy expenditure during the subjective night period. Energy expenditure levels also tended to be lower during the subjective day period ($P = 0.06$).

Long term

As expected from the higher energy intake and lower energy expenditure rates measured during the short term period, body weights in the LL mice (33.8 ± 2.5 *vs*. 29.4 ± 1.8 g, *P* < 0.01) as well as body weight gain (8.1 ± 1.4 *vs*. 4.0 ± 1.6 g, *P* < 0.01) were significantly higher compared to LD mice. Interestingly, at the long term, total energy intake measured over a period of a circadian period was significantly lower in the LL mice, whereas energy intake during the subjective day was higher compared to LD mice (55 *vs*. 19%, *P* < 0.01, Fig. 4D). The circadian rhythm in energy intake present in LD mice, with higher energy intake during the night and lower energy intake during the day, was absent in LL mice. Reflecting the higher subjective day energy intake, RER was significantly higher in the LL mice (Fig. 4E). Interestingly, RER did not differ between groups during the night period, even though energy intake was higher in the LD group. Furthermore, RER strongly correlated to energy intake during both the subjective day and night period in the LD mice ($R^2 = 0.70$ and 0.63, *P* = 0.01 and *P* < 0.01, respectively), but not in the LL mice ($R^2 = 0.03$ and 0.03, ns for both periods). Total energy expenditure over a period of a circadian period was still significantly lower in the LL mice (Fig. 4F), due to a reduction during the subjective night period as well as subjective day period. Energy expenditure during the subjective night was strongly correlated to energy intake in the LD mice ($R^2 = 0.55$, *P* < 0.05). Interestingly, in the LL mice, the higher energy intake during the subjective day was not associated with an increase in energy expenditure.
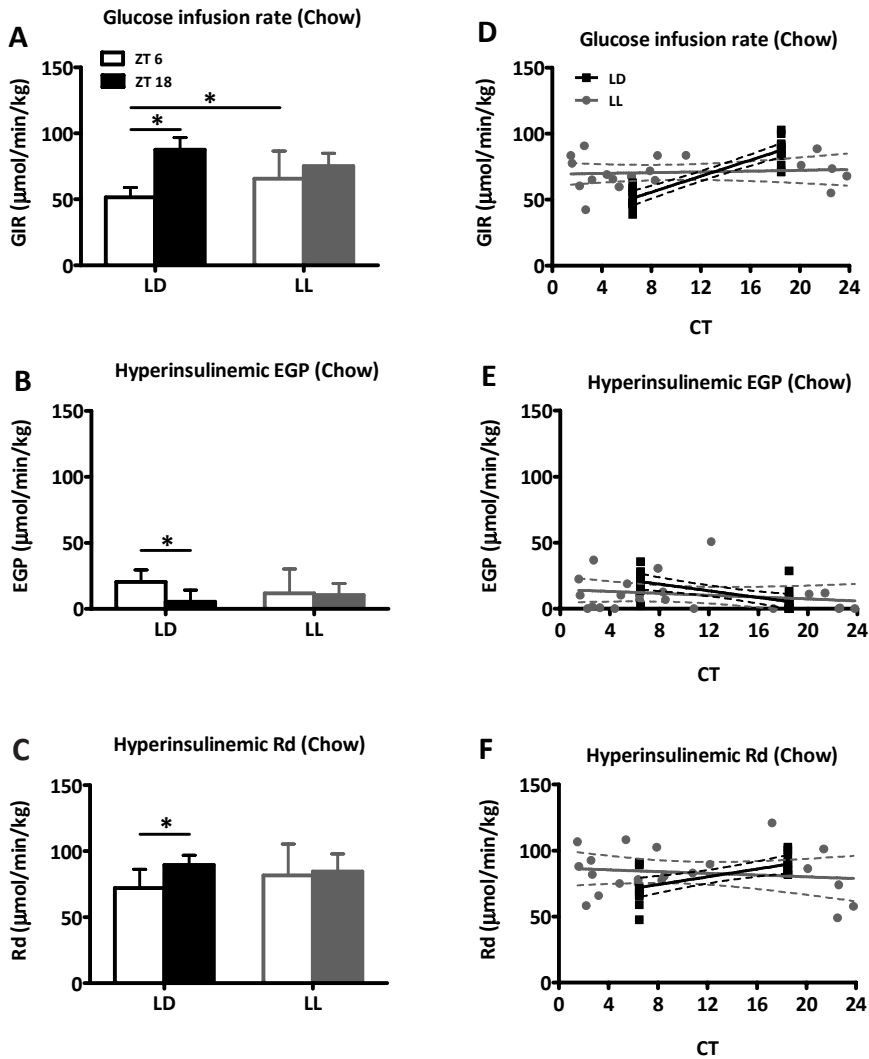
Hyperinsulinemic-euglycemic clamp analysis

Insulin sensitivity was determined in body-weight matched mice on chow and high-fat diet by hyperinsulinemic-euglycemic clamp analysis at two different circadian times: during the middle of the resting (ZT 6) and during the middle of the active phase (ZT 18) of the LD mice. Since the LL regimen disrupts the circadian rhythm by elongating the circadian period, the exact circadian time at which stable hyperinsulinemic-euglycemic infusion rate was achieved was subsequently determined for each individual mouse in LL.

Chow diet

Basal endogenous glucose production (EGP) did not differ at ZT 6 and ZT 18 between LD or LL mice (Table 1). In LD mice fed a chow diet, glucose infusion rates (GIR) depended on the clock times at which the clamp studies were performed. GIR was significantly higher at ZT 18 compared to ZT 6 (87.5 ± 9.2 *vs*. 51.6 ± 7.4 µmol/min/kg, *P* < 0.01, Fig. 5A). Furthermore, there was a strong correlation between GIR and circadian time (CT) in chow fed LD mice ($R^2 = 0.84$, *P* < 0.01, Fig. 5D). In chow fed LL mice, there was no difference in the GIR between ZT 6 and ZT 18 (65.7 ± 20.8 *vs*. 75.2 ± 9.7 µmol/min/kg, Fig. 5A). There was no relation found between GIR and CT in LL mice ($R^2 = 0.01$, ns, Fig. 5D). Interestingly, not only was the circadian rhythm of insulin sensitivity absent in LL mice, the GIR in LL mice was set at approximately 50% of the minimal

to maximal GIR seen in LD mice. This is in agreement with the similar reduction in SCN output (Fig. 1). In LD mice, EGP was significantly lower during the hyperinsulinemic-euglycemic clamp conditions at ZT 18 compared to ZT 6 (5.4 ± 8.8 *vs.* 20.5 ± 9.1 μmol/min/kg, respectively, *P* < 0.05, Fig. 5B). In addition, hyperinsulinemic-euglycemic glucose disposal rates (Rd) were higher at

Fig. 5. Glucose infusion rate (GIR, A, D), endogenous glucose production (EGP, B, E) and glucose disposal (Rd, C, F) in chow fed mice under light/dark (LD, black) and constant light (LL, grey) conditions as measured in hyperinsulinemic-euglycemic clamp. GIR (A), EGP (B) en Rd (C) as measured at ZT 6 (open bars) or ZT 18 (filled bars) as determined for LD mice. Linear regression analysis of the GIR (D), EGP (E) and Rd (F) against the circadian time (CT) for LD mice (n=21) and LL mice (n=20). Values represent means ± SD for at least 7 mice per group. * *P* < 0.05 *vs.* control.

Table 1. Results obtained from the hyperinsulinemic-euglycemic clamp performed in LD and LL mice on chow diet. Data is represented as mean ± SD, * $P < 0.05$ LL *vs.* LD, $ $P < 0.05$ ZT 6 *vs.* ZT 18.

	LD		LL	
	ZT 6	**ZT 18**	**ZT 6**	**ZT 18**
Body weight (g)	25.4 ± 1.2	22.7 ± 0.9 $	25.0 ± 2.5	23.9 ± 1.3
Basal hematocrit (%)	39.8 ± 1.7	42.4 ± 1.2	39.8 ± 0.9	41.1 ± 1.9
Clamp hematocrit (%)	36.9 ± 1.1	38.8 ± 1.0	37.0 ± 1.9	38.7 ± 1.1
Basal insulin (ng/ml)	0.4 ± 0.1	0.4 ± 0.2	0.6 ± 0.3 *	0.4 ± 0.1
Clamp insulin (ng/ml)	7.6 ± 1.4	6.7 ± 0.9	7.0 ± 1.4	5.2 ± 1.6 *
Basal glucose (mmol/l)	4.0 ± 0.3	5.0 ± 0.5	4.6 ± 0.6	5.0 ± 0.9
Clamp glucose (mmol/l)	4.3 ± 0.5	4.6 ± 0.5	4.7 ± 0.7	5.0 ± 0.6
Basal EGP (µmol/min/kg)	47.3 ± 20.5	43.3 ± 5.6	56.5 ± 20.3	43.9 ± 7.6

ZT 18 compared to ZT 6 (89.7 ± 7.2 *vs.* 72.1 ± 14.2 µmol/min/kg, respectively, $P < 0.05$, Fig. 5C). Both EGP and Rd correlated with CT in the LD group (R^2 = 0.44 and 0.41, respectively, $P < 0.01$ for both parameters, Fig. 5E, F). In LL mice, hyperinsulinemic-euglycemic EGP and Rd rates did not differ significantly between ZT 6 and ZT 18 (EGP, 11.8 ± 18.4 *vs.* 10.4 ± 8.8 and Rd, 81.7 ± 23.8 *vs.* 84.7 ± 13.2 µmol/min/kg, respectively, ns, Fig. 5B, C). Furthermore, EGP and Rd did not correlate with CT in chow fed LL mice (R^2 = 0.04 and 0.02, respectively, ns, Fig. 5E, F). These data show that the circadian variation in tissue-specific insulin sensitivity that is normally present in chow fed LD conditions was absent in mice subjected to constant light.

High-fat diet

LD mice fed a high-fat diet were more insulin resistant as GIR was lower at both time points compared to LD mice on chow diet (GIR -45% at ZT 6, $P < 0.01$ and -76% at ZT 18, $P < 0.01$). The lower insulin sensitivity was associated with diet-induced liver and peripheral insulin resistance, as hyperinsulinemic EGP was higher (EGP +48% at ZT 6, $P = 0.07$ and +117% at ZT18, $P = 0.09$) and hyperinsulinemic Rd was lower (Rd -7% at ZT 6, not significant and -35% at ZT 18, $P < 0.01$), when compared to chow fed LD mice. Basal EGP did not differ significantly at ZT 6 and ZT 18 between LD or LL mice (Table 2). GIR for LD mice on high-fat diet was significantly higher at ZT 18 compared to ZT 6 (49.7 ± 13.0 *vs.* 35.7 ± 7.4 µmol/min/kg, $P < 0.01$, Fig. 6A), but the magnitude of difference between ZT 6 and ZT 18 in LD mice on high-fat diet was less compared to LD mice on chow diet. Linear regression of GIR against CT still revealed a strong association with time in LD mice (R^2 = 0.31, $P < 0.01$, Fig. 6D). This dependency of GIR to time was absent in LL mice, as there was no difference in the GIR between ZT 6 and ZT 18 (31.1 ± 13.1 *vs.* 39.1 ± 8.4 µmol/min/kg, ns, Fig. 6A) and no correlation of GIR with CT (R^2 = 0.01, ns, Fig. 6D). In the LD mice, EGP during clamp conditions were significantly lower at ZT 18 compared to ZT 6 (11.7 ± 6.5 *vs.* 30.4 ± 12.9 µmol/min/kg, $P < 0.05$, Fig. 6B). Hyperinsulinemic Rd rates were not different between ZT 6 and ZT 18 (67.4 ± 18.8 *vs.* 58.2 ± 11.9 µmol/min/kg, ns, Fig. 6C). Linear regression analysis confirmed these data, as EGP was correlated with CT (R^2 = 0.50, $P < 0.01$, Fig. 6E), but Rd was not (R^2 = 0.09, ns, Fig. 6F). In LL mice, there was a small difference in EGP during the clamp studies at ZT 6 and ZT 18 (24.6 ± 4.9 *vs.* 17.0 ± 7.2 µmol/min/kg, respectively,

$P < 0.05$, Fig. 6B). However, there was no relation between EGP and CT ($R^2 = 0.05$, ns, Fig. 6E). Rd rates did not differ at ZT 6 and ZT 18 for LL mice (54.3 ± 11.1 *vs.* 50.2 ± 12.7 µmol/min/kg, respectively, ns, Fig. 6C) and Rd did not correlate with CT ($R^2 = 0.00$, ns, Fig. 6F). These data show that, even though high-fat feeding results in an obesity/insulin resistance phenotype, insulin sensitivity was still under circadian control. Furthermore, even in in obese, insulin resistant mice, LL resulted in a further deterioration of the circadian rhythm of insulin resistance.
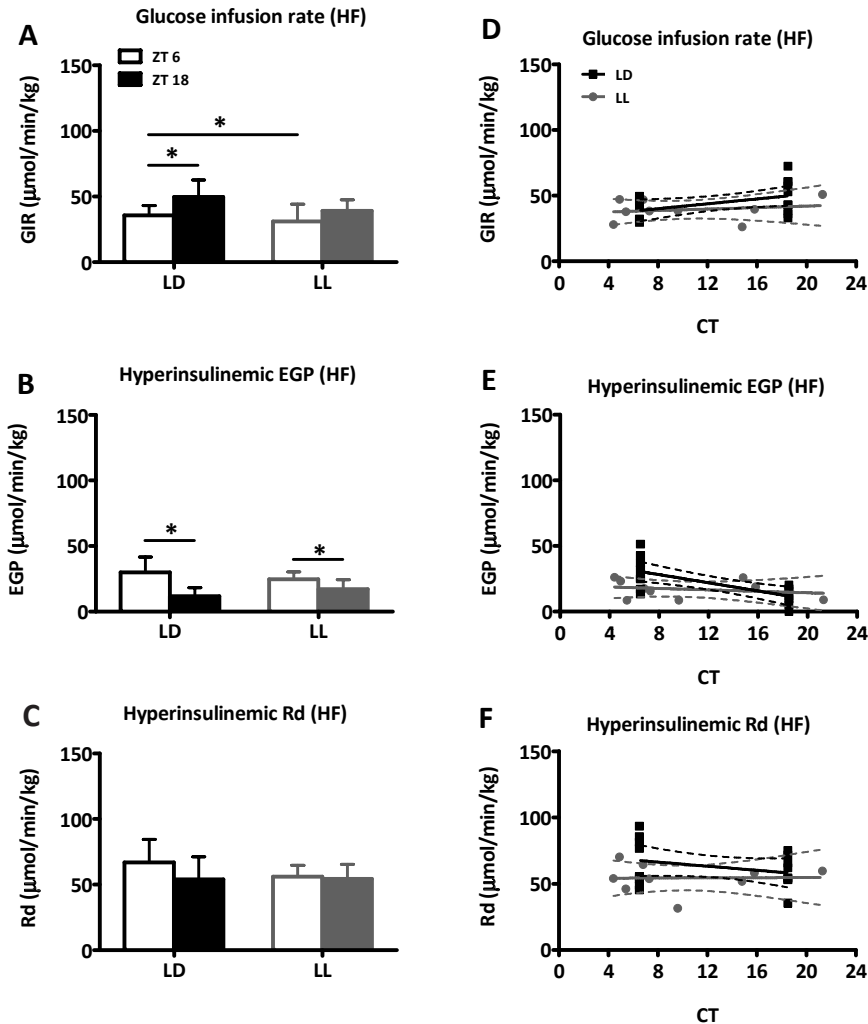
Fig. 6. Glucose infusion rate (GIR, A, D), endogenous glucose production (EGP, B, E) and glucose disposal (Rd, C, F) in high-fate fed mice under light/dark (LD, black) and constant light (LL, grey) conditions as measured in hyperinsulinemic-euglycemic clamp. GIR (A), EGP (B) en Rd (C) as measured at ZT 6 (open bars) or ZT 18 (filled bars) as determined for LD mice. Linear regression analysis of the GIR (D), EGP (E) and Rd (F) against the circadian time (CT) for LD mice (n=19) and LL mice (n=10). Values represent means ± SD for at least 7 mice per group. * *P < 0.05 vs.* control.

Table 2. Results obtained from the hyperinsulinemic-euglycemic clamp performed in LD and LL mice on high-fat diet. Data is represented as mean ± SD, * $P < 0.05$ LL *vs*. LD, $ $P < 0.05$ ZT 6 *vs*. ZT 18.

	LD		LL	
	ZT 6	**ZT 18**	**ZT 6**	**ZT 18**
Body weight (g)	32.4 ± 3.6	27.4 ± 2.5 $	32.5 ± 3.2	27.5 ± 1.8 $
Basal hematocrit (%)	n.a.	44.1 ± 1.8	n.a.	43.6 ± 1.1
Clamp hematocrit (%)	n.a.	40.6 ± 1.6	n.a.	40.5 ± 2.0
Basal insulin (ng/ml)	0.7 ± 0.3	0.8 ± 0.3	0.7 ± 0.7	0.9 ± 0.2
Clamp insulin (ng/ml)	5.9 ± 0.8	6.7 ± 0.9	5.4 ± 1.0	7.2 ± 1.2
Basal glucose (mmol/l)	5.0 ± 0.7	5.7 ± 0.7 $	5.8 ± 1.0	5.0 ± 0.5 $*
Clamp glucose (mmol/l)	5.6 ± 0.7	5.7 ± 1.1	6.2 ± 1.1	5.5 ± 0.6
Basal EGP (µmol/min/kg)	38.1 ± 12.9	41.5 ± 8.7	32.6 ± 15.3	38.1 ± 11.8

DISCUSSION

This study addressed the effect of a decline in rhythm amplitude on energy metabolism and insulin sensitivity. C57Bl/6J mice were exposed to constant light (LL) or a light-dark cycle (LD) as control. *In vivo* recordings showed that constant light resulted in an immediate decrease in SCN amplitude, which stabilized within 3 days at a level of 46%. Furthermore, constant light stimulated weight gain, even before high-fat diet resulted in weight gain. Finally, constant light exposure resulted in a complete loss of circadian rhythm in energy metabolism and hepatic and peripheral insulin sensitivity. Collectively, these data indicate that constant light exposure strongly reduces the circadian function of the central clock, as observed in aging and neurodegenerative diseases, associated with weight gain and insulin resistance.

The SCN generates a circadian rhythm in neuronal activity and neurotransmitter release that serves as a timing signal by downstream target nuclei. The SCN receives input on environmental light levels by a direct projection from a subset of ganglions in the retina (31). Under regular 12 h/12 h light/dark cycles, this input pathway keeps individual SCN neurons synchronized to each other and the environment with a majority of neurons that are active during the day and silent during the night. Exposing animals to constant light causes a desynchronization among neurons of the SCN, which results at the tissue level in a dampened circadian rhythm (32;33). Metabolic processes that manifest circadian fluctuations are regulated by a combination of excitatory and inhibitory inputs, with rhythmic SCN output regulating the balance between excitation and inhibition as a function of the time of day (34). To quantify the amplitude decrease and time course of the rhythm deterioration of the SCN output rhythm in our mice, we performed longitudinal behavioral activity recordings as well as a series of *in vivo* SCN electrophysiological recordings. These *in vivo* recordings are of great relevance as previous investigations on LL influence on SCN rhythm were exclusively performed in the isolated SCN *in vitro* (1;33), which did not allow for a quantitative estimation of the effect of constant light on the SCN rhythm *in vivo*. Our SCN recordings show that the desynchronizing effects of constant light occur

immediately, resulting in an amplitude reduction of 73% and 60% on days 1 and 2, and stabilizing at an amplitude of 54% of the original value from day 3 onwards. Importantly, this dampening of SCN function was caused by the combined effects of increased trough levels and decreased peak levels. This is consistent with the finding that dampening is caused by a desynchronization among SCN neurons (32;33). These effects lead to stronger output signals during the night and weaker signals during the day. In agreement with the effects within the SCN, home cage locomotor activity recordings show that the rhythm strength is reduced by 54% under constant light.

Alterations in light regime typically are considered stressful. In our study, constant light disturbed corticosterone rhythm, resulting in lower corticosterone peak levels, which is in line with previous studies showing that constant light exposure does not lead to increased corticosterone levels (35-37). As corticosterone release is mediated by hypothalamic nuclei that receive strong input from the SCN (38), the dampening of the corticosterone rhythm may be a direct result of the dampening of SCN neuronal activity.

Body weight development of all mice was measured twice a week. Disturbing circadian rhythm by constant light exposure resulted in higher body weights compared to mice on a normal light regime, independent of the diet. A mixed effects model was developed to determine the isolated contributions of constant light exposure and high-fat diet to weight gain as well as to assess the possible interaction between constant light exposure and high-fat feeding. Constant light exposure immediately affected weight gain, which stabilized later on, whereas the high-fat diet effect on body weight gain became manifest at a later stage. Our data are in line with a previous study showing that exposing chow fed Swiss-Webster mice to LL increases body weight compared to mice in LD only for the first two weeks. After this period, body weight gain in LL mice is equal to LD mice (35). The present study shows for the first time the independent effect of constant light exposure to weight gain in chow and high-fat fed mice and shows that the weight gain as a result of constant light exposure is evident before high-fat diet affects body weight gain. This immediate effect of constant light exposure on body weight coincides with the direct reduction in SCN output, suggesting that reduced SCN rhythmicity instantaneously affects energy homeostasis.

Disturbing circadian rhythm by constant light exposure aggravated diet-induced obesity and resulted in a shift of energy intake towards the period when energy intake is normally low. Furthermore, we show that constant light is associated with a reduction in energy expenditure. These disturbed circadian rhythms in energy metabolism deteriorated over time. Within the first days of the experiment, exposure to constant light led to lengthening of circadian rhythm in food intake, RER and energy expenditure. During the experiment, the circadian rhythm weakened further. This is in agreement with our findings that the amplitude of rhythmic SCN output dampened in constant light over time. Furthermore, LL mice showed an impaired oxidative response towards food intake, as was indicated by the absence of correlation between the respiratory exchange rate and energy intake. A blunted response of metabolism towards food intake, also known a metabolic inflexibility (39), has been shown to be associated with impaired insulin sensitivity and obesity (40). It is therefore likely that the reduced metabolic flexibility of the LL mice is a reflection of reduced insulin sensitivity.

We assessed the effect of disturbed circadian rhythm on insulin sensitivity in mice on chow as well as on high-fat diet. We determined insulin sensitivity by hyperinsulinemic-euglycemic clamp analysis at two different time points that corresponded to the middle of the resting phase (ZT 6) and middle of the active phase (ZT 18) for the LD mice. For the LL mice, the individual CT at the time of the clamp analysis was obtained afterwards on the basis of the activity period of each individual mouse. In line with studies form La Fleur *et al*. (41), LD mice on chow show a circadian variation in insulin sensitivity, with higher hepatic insulin sensitivity and higher insulin-stimulated glucose uptake by peripheral organs in the subjective night. Remarkably, the circadian variation of insulin sensitivity was lost in constant light. Moreover, the insulin sensitivity of LL mice was approximately 50% of the variation in insulin sensitivity of LD mice, which is in agreement with the ~50% reduction in SCN output.

In a previous study it was shown that disturbing circadian rhythm by light intervention results in deregultation of glucoregulatory genes in liver, such as phosphoenolpyruvate carboxykinase (PEPCK), glucose transporter 2 (GLUT2) and glucose-6-phosphatase (G6PC) (42). In muscle, glucoregulatory gene expression is dependent on circadian time (43) and glucose uptake in isolated muscle from rats show a circadian pattern (44). Deregulation in glucoregulatory genes in liver and muscle may underlie the disturbed insulin sensitivity we found in constant light exposed mice. Furthermore, disturbing circadian rhythm using constant light also accelerates loss of beta-cell mass and function (45). Together with the results obtained in our study, more insight is gained in how disturbances in circadian rhythm, for instance due to shift work, may lead to the development of obesity and T2DM.

Our studies provide more insight on the relation between disturbances in endogenous rhythms and the increase in the risk of obesity and T2DM. Specifically, we have shown that a decrease in SCN rhythm amplitude of about 50% is sufficient to completely abolish circadian rhythm in energy metabolism and insulin sensitivity. Furthermore, we have shown that the immediate reduction in SCN output by constant light coincides with an instantaneous increase in body weight. These findings indicate that a relatively mild decrease in rhythm amplitude, which is observed in sleeping disorders, degenerative diseases and aging, are a serious concern for health (46), as they may lead to secondary metabolic pathophysiology. SCN recordings in old and middle aged mice have in fact shown a reduction in SCN rhythm amplitude of about 50% (22). The data indicate that new avenues for prevention and treatment programs for patients with mild rhythm disturbances should include life style or light treatment programs to improve rhythm amplitude.

ACKNOWLEDGEMENTS

REFERENCE LIST

1. Kalsbeek, A, Fliers, E, Romijn, JA, La Fleur, SE, Wortel, J, Bakker, O, Endert, E, Buijs, RM: The suprachiasmatic nucleus generates the diurnal changes in plasma leptin levels. *Endocrinology* 142:2677-2685, 2001

2. Kalsbeek, A, Ruiter, M, La Fleur, SE, Van, HC, Buijs, RM: The diurnal modulation of hormonal responses in the rat varies with different stimuli. *J Neuroendocrinol* 15:1144-1155, 2003

3. Ruiter, M, La Fleur, SE, Van, HC, van, d, V, Kalsbeek, A, Buijs, RM: The daily rhythm in plasma glucagon concentrations in the rat is modulated by the biological clock and by feeding behavior. *Diabetes* 52:1709-1715, 2003

4. Scheer, FA, Kalsbeek, A, Buijs, RM: Cardiovascular control by the suprachiasmatic nucleus: neural and neuroendocrine mechanisms in human and rat. *Biol Chem* 384:697-709, 2003

5. Scheer, FA, Ter Horst, GJ, van, D, V, Buijs, RM: Physiological and anatomic evidence for regulation of the heart by suprachiasmatic nucleus in rats. *Am J Physiol Heart Circ Physiol* 280:H1391-H1399, 2001

6. Groos, GA, Meijer, JH: Effects of illumination on suprachiasmatic nucleus electrical discharge. *Ann N Y Acad Sci* 453:134-146, 1985

7. Freedman, MS, Lucas, RJ, Soni, B, von, SM, Munoz, M, vid-Gray, Z, Foster, R: Regulation of mammalian circadian behavior by non-rod, non-cone, ocular photoreceptors. *Science* 284:502-504, 1999

8. Meijer, JH, Watanabe, K, Detari, L, de Vries, MJ, Albus, H, Treep, JA, Schaap, J, Rietveld, WJ: Light entrainment of the mammalian biological clock. *Prog Brain Res* 111:175-190, 1996

9. Vinogradova, IA, Anisimov, VN, Bukalev, AV, Semenchenko, AV, Zabezhinski, MA: Circadian disruption induced by light-at-night accelerates aging and promotes tumorigenesis in rats. *Aging (Albany NY)* 1:855-865, 2009

10. Karasek, M: Melatonin, human aging, and age-related diseases. *Exp Gerontol* 39:1723-1729, 2004

11. Klarsfeld, A, Rouyer, F: Effects of circadian mutations and LD periodicity on the life span of Drosophila melanogaster. *J Biol Rhythms* 13:471-478, 1998

12. Fukuda, H, Iritani, N: Diurnal variations of lipogenic enzyme mRNA quantities in rat liver. *Biochim Biophys Acta* 1086:261-264, 1991

13. Yang, X, Downes, M, Yu, RT, Bookout, AL, He, W, Straume, M, Mangelsdorf, DJ, Evans, RM: Nuclear receptor expression links the circadian clock to metabolism. *Cell* 126:801-810, 2006

14. Rudic, RD, McNamara, P, Curtis, AM, Boston, RC, Panda, S, Hogenesch, JB, Fitzgerald, GA: BMAL1 and CLOCK, two essential components of the circadian clock, are involved in glucose homeostasis. *PLoS Biol* 2:e377, 2004

15. Turek, FW, Joshu, C, Kohsaka, A, Lin, E, Ivanova, G, McDearmon, E, Laposky, A, Losee-Olson, S, Easton, A, Jensen, DR, Eckel, RH, Takahashi, JS, Bass, J: Obesity and metabolic syndrome in circadian Clock mutant mice. *Science* 308:1043-1045, 2005

16. Ekmekcioglu, C, Touitou, Y: Chronobiological aspects of food intake and metabolism and their relevance on energy balance and weight regulation. *Obes Rev* 2010

17. Buijs, RM, Scheer, FA, Kreier, F, Yi, C, Bos, N, Goncharuk, VD, Kalsbeek, A: Organization of circadian functions: interaction with the body. *Prog Brain Res* 153:341-360, 2006

18. Karlsson, BH, Knutsson, AK, Lindahl, BO, Alfredsson, LS: Metabolic disturbances in male workers with rotating three-shift work. Results of the WOLF study. *Int Arch Occup Environ Health* 76:424-430, 2003

19. Kohsaka, A, Bass, J: A sense of time: how molecular clocks organize metabolism. *Trends Endocrinol Metab* 18:4-11, 2007

20. Copertaro, A, Barbaresi, M, Bracci, M: [Shift work and cardiometabolic risk]. *Recenti Prog Med* 100:502-507, 2009

21. Wong, H, Wong, MC, Wong, SY, Lee, A: The association between shift duty and abnormal eating behavior among nurses working in a major hospital: a cross-sectional study. *Int J Nurs Stud* 47:1021-1027, 2010

22. Nakamura, TJ, Nakamura, W, Yamazaki, S, Kudo, T, Cutler, T, Colwell, CS, Block, GD: Age-

related decline in circadian output. *J Neurosci* 31:10201-10205, 2011

23. Chen, R, Seo, DO, Bell, E, von, GC, Lee, C: Strong resetting of the mammalian clock by constant light followed by constant darkness. *J Neurosci* 28:11839-11847, 2008

24. Sudo, M, Sasahara, K, Moriya, T, Akiyama, M, Hamada, T, Shibata, S: Constant light housing attenuates circadian rhythms of mPer2 mRNA and mPER2 protein expression in the suprachiasmatic nucleus of mice. *Neuroscience* 121:493-499, 2003

25. Wideman, CH, Murphy, HM: Constant light induces alterations in melatonin levels, food intake, feed efficiency, visceral adiposity, and circadian rhythms in rats. *Nutr Neurosci* 12:233-240, 2009

26. Dörrscheidt, GJ, Beck, L: Advanced methods for evaluating characteristic parameters (T, 7, p) of Circadian Rhythms. *Journal of Mathematical Biology* 2:107-121, 1975

27. Dalm, S, Enthoven, L, Meijer, OC, van der Mark, MH, Karssen, AM, de Kloet, ER, Oitzl, MS: Age-related changes in hypothalamic-pituitary-adrenal axis activity of male C57BL/6J mice. *Neuroendocrinology* 81:372-380, 2005

28. Jud, C, Schmutz, I, Hampp, G, Oster, H, Albrecht, U: A guideline for analyzing circadian wheel-running behavior in rodents under different lighting conditions. *Biol Proced Online* 7:101-116, 2005

29. Aschoff, J: Exogenous and endogenous components in circadian rhythms. *Cold Spring Harb Symp Quant Biol* 25:11-28, 1960

30. Aschoff, J: Circadian rhythms: influences of internal and external factors on the period measured in constant conditions. *Z Tierpsychol* 49:225-249, 1979

31. Foster, RG, Hankins, MW: Circadian vision. *Curr Biol* 17:R746-R751, 2007

32. Ohta, H, Yamazaki, S, McMahon, DG: Constant light desynchronizes mammalian clock neurons. *Nat Neurosci* 8:267-269, 2005

33. Ohta, H, Mitchell, AC, McMahon, DG: Constant light disrupts the developing mouse biological clock. *Pediatr Res* 60:304-308, 2006

34. Kalsbeek, A, Scheer, FA, Perreau-Lenz, S, La Fleur, SE, Yi, CX, Fliers, E, Buijs, RM: Circadian disruption and SCN control of energy metabolism. *FEBS Lett* 585:1412-1426, 2011

35. Fonken, LK, Workman, JL, Walton, JC, Weil, ZM, Morris, JS, Haim, A, Nelson, RJ: Light at night increases body mass by shifting the time of food intake. *Proc Natl Acad Sci U S A* 107:18664-18669, 2010

36. Fonken, LK, Finy, MS, Walton, JC, Weil, ZM, Workman, JL, Ross, J, Nelson, RJ: Influence of light at night on murine anxiety- and depressive-like responses. *Behav Brain Res* 205:349-354, 2009

37. Claustrat, B, Valatx, JL, Harthe, C, Brun, J: Effect of constant light on prolactin and corticosterone rhythms evaluated using a noninvasive urine sampling protocol in the rat. *Horm Metab Res* 40:398-403, 2008

38. Kalsbeek, A, van der Spek, R, Lei, J, Endert, E, Buijs, RM, Fliers, E: Circadian rhythms in the hypothalamo-pituitary-adrenal (HPA) axis. *Mol Cell Endocrinol* 2011

39. Kelley, DE, He, J, Menshikova, EV, Ritov, VB: Dysfunction of mitochondria in human skeletal muscle in type 2 diabetes. *Diabetes* 51:2944-2950, 2002

40. Corpeleijn, E, Mensink, M, Kooi, ME, Roekaerts, PM, Saris, WH, Blaak, EE: Impaired skeletal muscle substrate oxidation in glucose-intolerant men improves after weight loss. *Obesity (Silver Spring)* 16:1025-1032, 2008

41. La Fleur, SE, Kalsbeek, A, Wortel, J, Fekkes, ML, Buijs, RM: A daily rhythm in glucose tolerance: a role for the suprachiasmatic nucleus. *Diabetes* 50:1237-1243, 2001

42. Cailotto, C, Lei, J, van, d, V, van, HC, van Eden, CG, Kalsbeek, A, Pevet, P, Buijs, RM: Effects of nocturnal light on (clock) gene expression in peripheral organs: a role for the autonomic innervation of the liver. *PLoS One* 4:e5650, 2009

43. Zambon, AC, McDearmon, EL, Salomonis, N, Vranizan, KM, Johansen, KL, Adey, D, Takahashi, JS, Schambelan, M, Conklin, BR: Time- and exercise-dependent gene regulation in human skeletal muscle. *Genome Biol* 4:R61, 2003

44. Leighton, B, Kowalchuk, JM, Challiss, RA, Newsholme, EA: Circadian rhythm in sensitivity of glucose metabolism to insulin in rat soleus muscle. *Am J Physiol* 255:E41-E45, 1988

45. Gale, JE, Cox, HI, Qian, J, Block, GD, Colwell, CS, Matveyenko, AV: Disruption of Circadian Rhythms Accelerates Development of Diabetes through Pancreatic Beta-Cell Loss and Dysfunction. *J Biol Rhythms* 26:423-433, 2011

46. Colwell, CS: Linking neural activity and molecular oscillations in the SCN. *Nat Rev Neurosci* 12: 553-569, 2011

THE SUPRACHIASMATIC NUCLEUS CONTROLS CIRCADIAN ENERGY METABOLISM AND HEPATIC INSULIN SENSITIVITY

Claudia P. Coomans*
Sjoerd A.A. van den Berg*
Eliane A. Lucassen
Thijs Houben
Amanda C. M. Pronk
Rianne D. C. van der Spek
Andries Kalsbeek
Nienke R. Biermasz
Ko Willems van Dijk
Johannes A. Romijn[$]
Johanna H. Meijer[$]

*, [$] *Both authors contributed equally*

3

ABSTRACT

The suprachiasmatic nucleus (SCN) functions as a central pacemaker in the circadian system. Disturbances in the circadian system are associated with the development of type 2 diabetes mellitus (T2DM). Here, we studied the direct contribution of the SCN in the development of insulin resistance. Bilateral microlesions of the SCN in male C57Bl/6J mice resulted in loss of circadian rhythm in locomotor activity. Histological verification by immunocytochemistry was performed to analyze the precision of the lesion. Exclusive SCN lesioned (SCNx) mice showed a small, but significant increase in body weight (+17%), which was accounted for by an increase in fat mass. In contrast, mice with collateral damage to the ventromedial hypothalamus (VMH) and paraventricular nucleus (PVN) showed severe obesity and insulin resistance. In mice with exclusive SCN ablation, indirect calorimetry/metabolic cage analysis four weeks after lesioning, revealed a loss of circadian rhythm in oxygen consumption and food intake. Hyperinsulinemic-euglycemic clamp analysis showed that the glucose infusion rate, required to maintain euglycemia, was significantly lower in SCNx mice compared to sham operated mice (-63%). While insulin potently inhibited endogenous glucose production (-84%), this was greatly reduced in SCNx mice (-7%), indicating severe hepatic insulin resistance. Our data indicate that malfunction of the SCN plays an important role in the development of insulin resistance, and underscore a direct role of the central pacemaker in the ontogeny of metabolic disorders.

INTRODUCTION

Obesity and type 2 diabetes mellitus (T2DM) have an increasing prevalence in modern society. In the past decade, a strong and potentially causal relationship between metabolic disorders and disturbances of the circadian system has been elucidated (1). The circadian system is responsible for 24 h rhythms in a wide variety of physiological and behavior functions (2;3). Generation of these rhythms occurs in the suprachiasmatic nuclei (SCN) of the anterior hypothalamus (2, 3) and is explained by a transcriptional-translational feedback loop, involving the clock genes CLOCK and BMAL1, Period (Per) and Cryptochrome (Cry) (1). The rhythms of the SCN are synchronized to the environmental 24 h cycle mainly by light-dark information perceived by the eyes. Rhythmic information is transferred from the SCN to the central nervous system and to peripheral organs of the body (4;5). This output is crucial for synchronization of many metabolic and endocrine factors such as glucose, insulin (6;7), cortisol (8), leptin, ghrelin (9;10) and neuropeptide Y (11).

Disturbances in circadian rhythms occur as a consequence of shift work and transitions in time zones, but also from irregular sleep-wake patterns (12), aging, or neurodegenerative disorders (13). Animal studies have indicated a link between clock gene mutations and metabolic disturbances. For instance, CLOCK$^{-/-}$ mutant mice have a greatly attenuated diurnal feeding rhythm, are hyperphagic and obese and develop a metabolic syndrome of hyperleptinemia, hyperlipidemia, hepatic steatosis and hyperglycemia (14). As clock gene mutants are not specific to the SCN, the detrimental effects of disturbed rhythms may have their origin in peripheral organs, other than the SCN. It is not clear, therefore, to what extent the SCN itself is involved in metabolic disorders. Given the accumulating evidence for disturbances of SCN cellular organization in aging (15), neurodegenerative disorders and dementia (13;16), this question is also clinically relevant, as it would explain comorbidity between various disorders.

To assess the role of disturbed function of the SCN *per se* in the development of obesity and T2DM, we performed bilateral microlesions of the SCN in male C57Bl/6J mice. Since the SCN is anatomically surrounded by areas regulating energy homeostasis, such as the ventromedial hypothalamus (VMH) and paraventricular nucleus (PVN), great care was taken to distinguish between exclusively SCN lesioned (SCNx) mice and mice with collateral damage to surrounding nuclei. We studied the effects of SCN ablation on energy expenditure, food intake and locomotor activity by analysis in metabolic cages employing indirect calorimetry. In addition, we assessed changes in body composition by dual energy x-ray absorptiometry (DEXA). Insulin sensitivity was assessed by hyperinsulinemic-euglycemic clamp analysis. We show that selective ablation of the SCN results in the development of severe hepatic insulin resistance.

MATERIALS AND METHODS

Animals

All animal experiments were approved by the Animal Ethic Committee from the Leiden University Medical Center (Leiden, the Netherlands) in accordance with the principles and guidelines established by the European Convention for the Protection of Laboratory Mice.

Male C57Bl/6J mice were obtained from Charles River Laboratories at an age of 9 weeks and acclimatized up to an age of 13 weeks at the Leiden University Medical Center animal facility. Mice were housed individually in a controlled environment (21°C, 40-50% humidity) under a 12 h/12 h light/dark cycle (07:00-19:00) unless otherwise mentioned. Food (chow, RM3, Special Diet Services, Sussex, UK) and tap water were available *ad libitum* during the whole experiment. Body weight was monitored weekly for all individual mice. Monitoring started 2 weeks prior to SCN lesions, and continued throughout the experiment.

SCN lesioning

At the age of 13 weeks, bilateral ablation of the SCN was performed as described before (17). Mice were anesthetized using a mixture of Ketamine (100 mg/kg, Aescoket, Boxtel, the Netherlands), Xylazine (10 mg/kg, Bayer AG, Leverkusen, Germany) and Atropine (0.1 mg/kg, Pharmachemie, Haarlem, The Netherlands) and mounted in a stereotactic device (Digital Just for Mouse Stereotaxic Instrument, Stoelting Co, Wood Dale, IL, USA). After identification of bregma, a hole was drilled through which the lesion electrode was inserted into the brain. Lesion needles were made by isolating a 0.3 mm stainless steel insect pin using isolating resin except for 0.2 mm at the tip. The electrode tip was aimed at the SCN, 0.46 mm posterior to bregma, 0.15 mm lateral to the midline, and 5.2 mm ventral to the surface of the cortex (Paxinos Mouse Brain Atlas, Franklin 2001). Bilateral SCN lesions were made by passing a 0.6 mA current through the electrode for duration of 10 s. The sham lesioned mice underwent the same operation, but no current was passed through the electrode.

Circadian rhythm analysis

Following SCN lesioning, all mice were housed in constant dark (DD) for 10 consecutive days to determine circadian rhythmicity in behavioral activity of each animal using passive infrared motion detection sensors (Hygrosens, Löffingen, Germany) that were mounted underneath the lid of the cage and connected to a ClockLab data collection system (Actimetrics, IL, USA) that recorded the amount of sensor activation in 1 min bins. The presence of circadian rhythms was determined by F-periodogram analysis based on the algorithm of Dörrscheidt and Beck (18). Mice were included in the lesion group when no significant rhythm was present.

Positional check of the SCN lesion

The SCN lesions were checked as described previously (10). To verify the position of the SCN lesions, brains were removed and fixed by immersion with 4% paraformaldehyde in 0.1 M phosphate buffer (pH 7.4) at 4°C. For cryoprotection, the brain tissue was equilibrated for 48 h with 30% sucrose in 0.1 M Tris-buffered saline (TBS) before sectioning. Thereafter, the brain tissue was cut into 30 μm sections and divided into two equal vials for immunocytochemical stainings. The two vials of brain sections were incubated overnight at 4°C with either rabbit anti-vasopressin or rabbit anti-VIP primary antibodies. Sections were then rinsed in 0.1 M TBS, incubated 1 h in biotinylated goat anti-rabbit IgG, and subsequently for 1 h in avidin-biotin complex (ABC, Vector Laboratories, Inc., Burlingame, CA, USA). The reaction product was visualized by incubation in 1% diaminobenzidine (DAB) with 0.01% hydrogen peroxide for

5-7 min. Nickel ammonium sulphate (0.05%) was added to the DAB solution to darken the reaction product (DAB/Ni). All sections were mounted on gelatine-coated glass slides, dried, run through ethanol and xylene and covered for observation by light microscopy. For every animal we blindly scored the amount of damage to the SCN and surrounding hypothalamic nuclei involved in metabolism (PVN and VMH).

Indirect calorimetry/metabolic cages

Individual measurements by indirect calorimetry were performed for a period of at least 4 consecutive days (Comprehensive Laboratory Animal Monitoring System, Columbus Instruments, Columbus Ohio, USA) (19-21). A period of 24 h was included at the start of the experiment to allow acclimatization of the mice to the cages. Experimental analysis started at 09:00. Analyzed parameters included real-time energy and water intake and locomotor activity. Oxygen consumption (energy expenditure) measurements were performed at intervals of 7 min throughout the whole period. Oxygen consumption, activity and energy intake were analyzed separately for day and night.

Hyperinsulinemic-euglycemic clamp analysis

Five weeks after SCN lesioning, hyperinsulinemic-euglycemic clamp experiments were performed as previously described (20;22-24) to determine insulin sensitivity. Clamp experiments were performed after an overnight fast. Mice were anesthetized by i.p. injection with a combination of Acepromazin (6.25 mg/kg, Sanofi Sant Nutrition Animale, Libourne Cedex, France), Midazolam (6.25 mg/kg, Roche, Mijdrecht, The Netherlands) and Fentanyl (0.31 mg/kg, Janssen-Cilag, Tilburg, The Netherlands). Anaesthesia as well as body temperature was maintained throughout the procedure. At the end of the basal and the hyperinsulinemic period, hematocrit values were determined to ensure that the mice were not anemic. During the basal period, 3-^{3}H-glucose was infused in the tail vein at a constant rate of 0.8 µCi/h (specific activity, 9.6 GBq/mmol; Amersham, Little Chalfont, UK). After 50 and 60 min of infusion, basal parameters of glucose and insulin were determined. Glucose rate of disposal (Rd, in µmol/min.kg) was determined as the rate of tracer infusion (dpm/min) divided by the plasma specific activity of 3-^{3}H-glucose (dpm/µmol) at both time points. The hyperinsulinemic period was started by a bolus of insulin (4.5 mU, Actrapid; Novo Nordisk, Chartres, France). Subsequently, insulin was infused at a constant rate (3.5 mU/min). Comparable to the basal period, 3-^{3}H-glucose was infused at a rate of 0.8 µCi/h. A variable infusion of 12.5% D-glucose (in PBS) was also started to maintain euglycemia, as measured by hand every 10 min (AccuCheck, Roche Diagnostics, The Netherlands). After reaching a steady state glucose infusion rate (GIR) for at least 30 min, blood samples were taken at 10 min intervals for 30 min to determine 3-^{3}H-glucose. Hyperinsulinemic Rd was determined similar to the basal period. The endogenous glucose production (EGP) was calculated as the difference between Rd and the GIR. Following the hyperinsulinemic-euglycemic clamp, body composition (lean *vs*. fat mass) was determined by DEXA using the Norland pDEXA Sabre X-Ray Bone Densitometer (Norland, Hampshire, U.K.). All data was analyzed according using the software and recommendations of the manufacturer. Subsequently, the mice were sacrificed.

Plasma analysis

Blood samples were taken from the tail tip into chilled capillaries coated with paraoxon to prevent *ex vivo* lipolysis. The tubes were placed on ice and centrifuged at 4°C. Plasma levels of free fatty acids (FFA) and glucose were determined using commercially available kits and standards according to the instructions of the manufacturer (Instruchemie, Delfzijl, The Netherlands) in 96-well plates (Greiner Bio-One, Alphen a/d Rijn, The Netherlands). Plasma insulin concentrations were measured by ELISA (Crystal Chem Inc., Downers Grove, USA). For measurement of plasma 3-^{3}H-glucose, trichloroacetic acid (final concentration 2%) was added to 10 µl plasma to precipitate proteins using centrifugation. The supernatant was dried to remove water and resuspended in milliQ. The samples were counted using scintillation counting (Packard Instruments, Downers Grove, USA).

Statistical analysis

Statistical analysis was performed using SPSS 17 for Windows (SPSS Inc, Chicago, IL, USA). Unpaired T-Tests were performed for all comparisons, with statistical significance threshold set at $P = 0.05$.

RESULTS

Behavioral and histological verification of SCN lesions

Periodogram analysis of locomotor activity showed that all sham operated mice retained a strong circadian rhythm (Fig. 1A), whereas SCN lesioned mice lost their circadian rhythm in activity after the lesion procedures (Fig. 1B). Histological analysis revealed SCN lesions without collateral damage in 6 mice (example shown in Fig. 2B). In addition to ablation of the SCN, 4 other mice had unilateral damage to the paraventricular nucleus (PVN), 10 other mice had bilateral damage to the PVN and 9 other mice had damage to both the PVN and the ventromedial hypothalamus (VMH). Sham operated controls (n=17) did not reveal damage to any of the aforementioned brain areas (example shown in Fig. 2A).

Selective SCN lesions

Body weight and composition

Five weeks after SCN lesioning, body mass of mice with an exclusive SCN lesion was 17% higher compared to the sham mice (24.9 ± 1.2 *vs.* 29.2 ± 1.9 g, $P < 0.01$, Fig. 3). Assessment of body composition by DEXA scan analysis revealed that fat mass was significantly higher in SCNx mice compared to sham (5.8 ± 2.6 *vs.* 1.9 ± 1.0 g, $P < 0.01$), whereas lean mass did not differ (17.7 ± 2.2 *vs.* 17.2 ± 1.7 g, ns). This indicates that SCN ablation results in only mild overweight compared to sham mice.

Indirect calorimetry

Metabolic cage data on oxidative metabolism, food intake and spontaneous physical activity data were obtained over a period of minimal 4 consecutive days and were analyzed separately for day and night. During the night, oxygen consumption rates were higher compared to the day in sham mice (3386 ± 174 *vs.* 2992 ± 155 ml/kg/h, $P < 0.01$, Fig. 4A). This circadian rhythm in
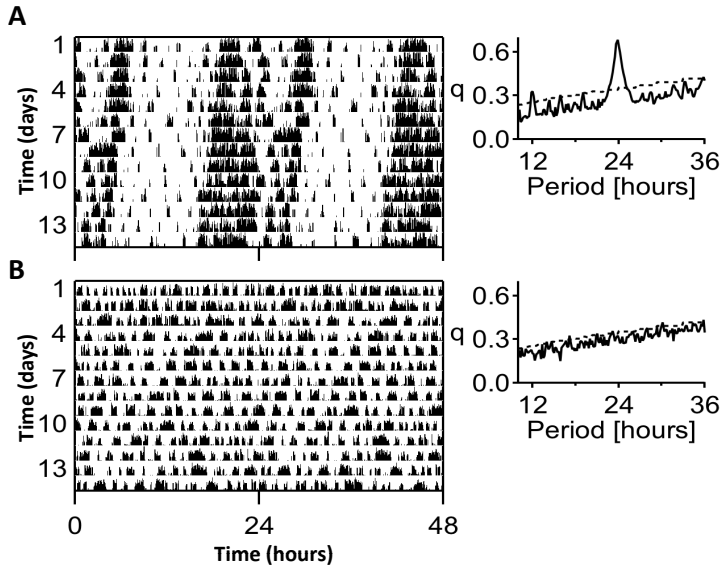
Fig. 1. Representative double-plotted actograms analyses of sham operated (A) and SCN lesioned (SCNx, B) mice under constant dark conditions. Each line of the double-plotted actograms represents 48 h.
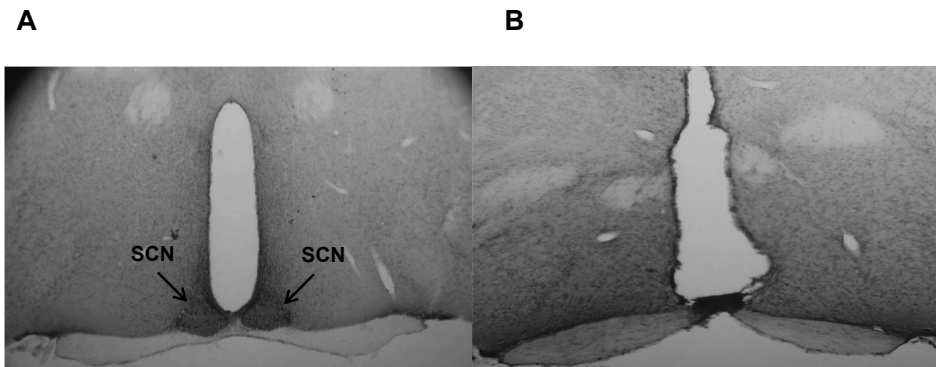
Fig. 2. Microphotographs of mouse brain sections at the level of the SCN. Middle region of the SCN is shown for sham operated (A) and SCN-lesioned (SCNx, B) mice. Note the relatively small size of the SCN lesion, leaving the paraventricular nuclei and ventromedial hypothalamus intact (B).

oxygen consumption was lost in SCNx mice, resulting in higher oxygen consumption during the day in SCNx mice compared to sham mice (3321 ± 252 *vs*. 2992 ± 155 ml/kg/h, $P < 0.01$). Total 24 h oxygen consumption was not different between sham and SCNx mice (76531 ± 3854 *vs*. 79518 ± 7595 ml/kg/day, ns). During the night, sham mice were more active compared to the day (195 ± 68 *vs*. 79 ± 33 beam breaks (bb), $P < 0.01$, Fig. 4B). In line with the oxygen consumption rates, circadian pattern in locomotor activity was lost in SCNx mice (123 ± 48 *vs*. 128 ± 38 bb, ns). This loss in activity

Body mass and composition
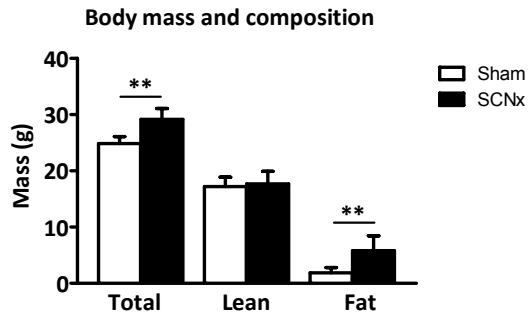
Fig. 3. Body mass and composition of sham (white bars) and SCN lesioned (SCNx, black bars) mice at the time of the hyperinsulinemic-euglycemic clamp. Total body mass, lean body mass and fat mass were determined. Data is represented as mean ± SD, ** $P < 0.01$.

A

Oxygen consumption

B

Activity

C
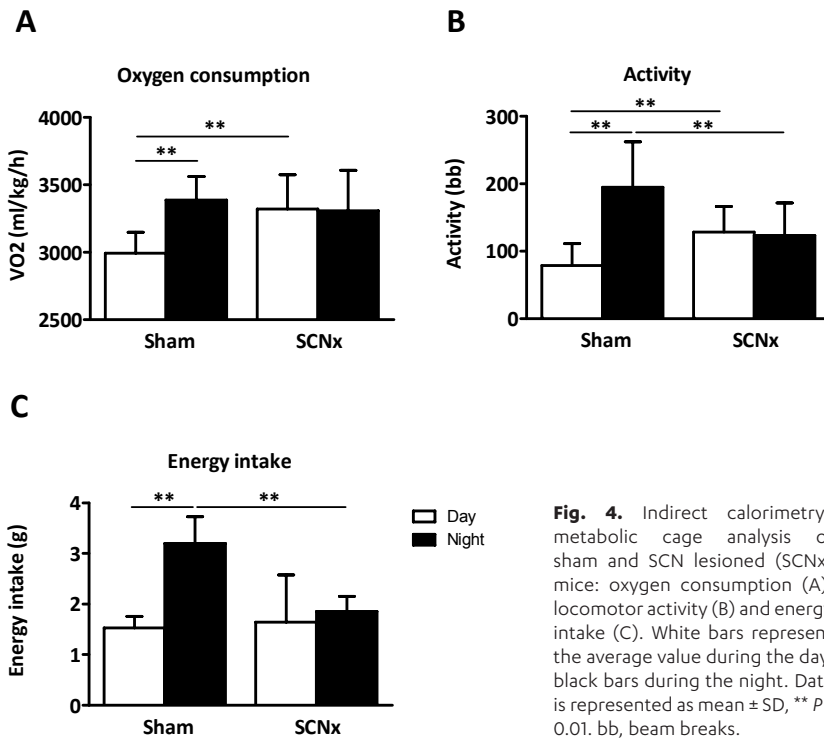
Energy intake

Fig. 4. Indirect calorimetry/metabolic cage analysis of sham and SCN lesioned (SCNx) mice: oxygen consumption (A), locomotor activity (B) and energy intake (C). White bars represent the average value during the day, black bars during the night. Data is represented as mean ± SD, ** $P < 0.01$. bb, beam breaks.

pattern in SCNx mice, resulted in increased activity levels during the day (128 ± 38 *vs*. 79 ± 33 bb, $P < 0.01$) and reduced activity levels during the night compared to sham mice (123 ± 48 *vs*. 195 ± 68 bb, $P < 0.01$). Total 24 h activity, however, was not different between sham and SCNx mice (273 ± 96 *vs*. 251 ± 81 bb, ns). Sham mice consumed 68% of their total food during the night (night *vs*.

day; 3.2 ± 0.5 *vs.* 1.5 ± 0.2 g, *P* < 0.01, Fig 4C), whereas SCNx mice consumed only 54% during the night (night *vs.* day; 1.9 ± 0.3 *vs.* 1.6 ± 0.9 g, ns). This resulted in reduced food intake during the night for SCNx mice compared to sham mice (1.9 ± 0.3 *vs.* 3.2 ± 0.5 g, *P* < 0.01). Furthermore, total 24 h food intake was also reduced for SCNx mice compared to sham mice (3.5 ± 1.2 *vs.* 4.7 ± 0.5 g, *P* < 0.01). Calculating the respiratory exchange rate (RER) showed that SCNx mice had a lower RER compared to sham mice during the day (0.86 ± 0.04 *vs.* 0.90 ± 0.01, *P* < 0.05) as well as during the night (0.87 ± 0.01 *vs.* 0.96 ± 0.02, *P* < 0.01). These data clearly show that ablation of the SCN results in a loss of circadian rhythm in respiratory metabolism and food intake.
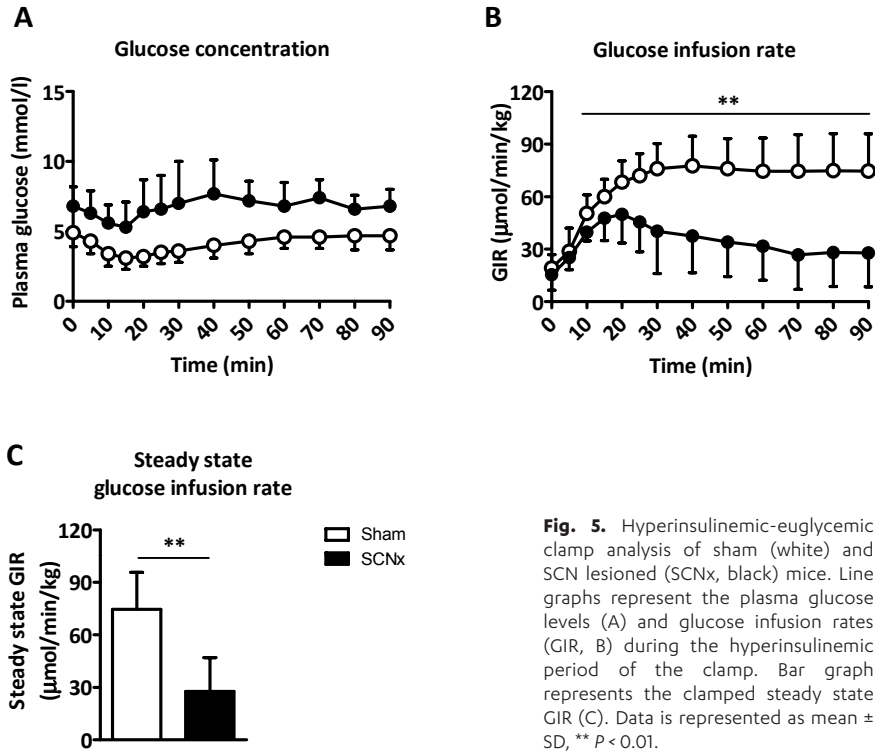
Hyperinsulinemic-euglycemic clamp studies

Insulin sensitivity was determined by hyperinsulinemic-euglycemic clamp analysis in overnight fasted mice. Hematocrit levels were similar at the basal and the hyperinsulinemic period for sham and SCNx mice, indicating that the mice were not anemic. At the start of the clamp, insulin, glucose and FFA plasma levels were significantly higher in SCNx mice compared to sham controls (table 1). During the hyperinsulinemic period, insulin levels were increased to a similar extent for both the sham and SCNx mice (table 1). All mice were clamped at their individual fasting plasma glucose level. At the end of the hyperinsulinemic period, circulating glucose levels were comparable to the fasting levels for sham as well as for SCNx mice, resulting in significantly higher glucose levels in the hyperinsulinemic period for SCNx mice compared to sham mice (table 1, Fig. 5A). At the end of the clamp, FFA levels were decreased compared to basal plasma levels in sham and SCNx mice, although this failed to reach statistical significance in SCNx mice (P = 0.08). GIR needed to maintain euglycemia were determined over the final 20 min of the clamp studies at stable plasma glucose values and were significantly lower in SCNx mice compared to sham controls (27.6 ± 19.5 *vs.* 74.7 ± 21.1 µmol/min/kg, *P* < 0.01, Fig. 5B, C).

In the basal period, endogenous glucose production (EGP), which equals glucose disposal, was not different between sham and SCNx mice (53.6 ± 16.6 *vs.* 65.0 ± 8.6 µmol/min/kg, ns, Fig. 6A). In the hyperinsulinemic-euglycemic period, glucose disposal was increased by 57% in the sham mice compared to the basal period (83.9 ± 23.8 *vs.* 53.6 ± 16.6 µmol/min/kg, *P* < 0.01) and by 27% in the SCNx mice, although this failed to reach statistical significance (82.8 ± 15.9 *vs.* 65.0 ± 8.6 µmol/min/kg, *P* = 0.06). Hyperinsulinemic glucose disposal rate was not significantly different between sham and SCNx mice. In the hyperinsulinemic-euglycemic period, EGP was

Table 1. Body mass and hyperinsulinemic-euglycemic clamp parameters of sham and SCN lesioned (SCNx) mice. FFA, free fatty acids. Data are represented as mean ± SD, $ *P* < 0.05 basal *vs.* hyperinsulinemic-euglycemic clamp period, * *P* < 0.05 *vs.* sham, ** *P* < 0.01 *vs.* sham.

	Sham		SCNx	
	Basal	**Clamp**	**Basal**	**Clamp**
Body mass (g)	24.9 ± 1.2		29.2 ± 1.9**	
Insulin (ng/ml)	0.5 ± 0.3	5.2 ± 1.1$	1.0 ± 0.3**	4.8 ± 1.9$
Glucose (mmol/l)	4.9 ± 0.8	4.7 ± 0.9	6.7 ± 1.2**	6.8 ± 1.2**
FFA (mmol/l)	0.9 ± 0.2	0.6 ± 0.3$	1.2 ± 0.3*	0.8 ± 0.2
Hematocrit (%)	41.6 ± 4.7	38.5 ± 2.3	41.7 ± 2.7	40.5 ± 0.7

A

Glucose concentration

B

Glucose infusion rate

C

**Steady state
glucose infusion rate**

Fig. 5. Hyperinsulinemic-euglycemic clamp analysis of sham (white) and SCN lesioned (SCNx, black) mice. Line graphs represent the plasma glucose levels (A) and glucose infusion rates (GIR, B) during the hyperinsulinemic period of the clamp. Bar graph represents the clamped steady state GIR (C). Data is represented as mean ± SD, ** *P* < 0.01.

decreased by 84% in sham operated mice compared to the basal period (8.8 ± 12.2 *vs.* 53.6 ± 16.6 μmol/min/kg, *P* < 0.01, Fig. 6B), whereas EGP was decreased by only 7% in SCNx mice (60.3 ± 25.8 *vs.* 65.0 ± 8.6 μmol/min/kg, ns). These data indicate that bilateral ablation of the SCN induces severe hepatic insulin resistance.

SCN lesion with collateral hypothalamic damage

SCN lesioned mice with collateral damage to hypothalamic nuclei involved in metabolism were analyzed separately. SCNx mice with additional, but selective unilateral damage to the PVN had modestly increased body mass compared to sham lesioned mice (29.9 ± 3.6 *vs.* 24.9 ± 1.2 g, *P* < 0.01, Fig. 7A), which was the result of increased fat mass (7.9 ± 2.5 *vs.* 1.9 ± 1.0 g, *P* < 0.01), but not lean mass (16.2 ± 1.0 *vs.* 17.2 ± 1.7 g, ns). SCNx mice with bilateral damage to the PVN were considerably heavier than the sham mice (42.5 ± 3.3 *vs.* 24.9 ± 1.2 g, *P* < 0.01), which was the result of increased fat mass (21.3 ± 4.8 *vs.* 1.9 ± 1.0 g, *P* < 0.01), but also coincided with a decrease in lean mass (13.6 ± 2.2 *vs.* 17.2 ± 1.7 g, *P* < 0.01). SCNx mice with collateral damage to both the PVN and the VMH developed extreme obesity compared to sham mice (49.3 ± 5.1 *vs.* 24.9 ± 1.2 g, *P* < 0.01), which was the result of an excessive increase in fat mass (24.7 ± 3.6 *vs.* 1.9 ± 1.0 g, *P* < 0.01), whereas lean mass was not different (16.8 ± 3.3 *vs.* 17.2 ± 1.7 g, ns).

Insulin sensitivity in SCNx mice with collateral damage was determined by hyperinsulinemic-euglycemic clamp analysis. Glucose infusion rates (GIR) needed to maintain euglycemia, as determined over a period of 20 min at stable plasma glucose values, were significantly

A

B
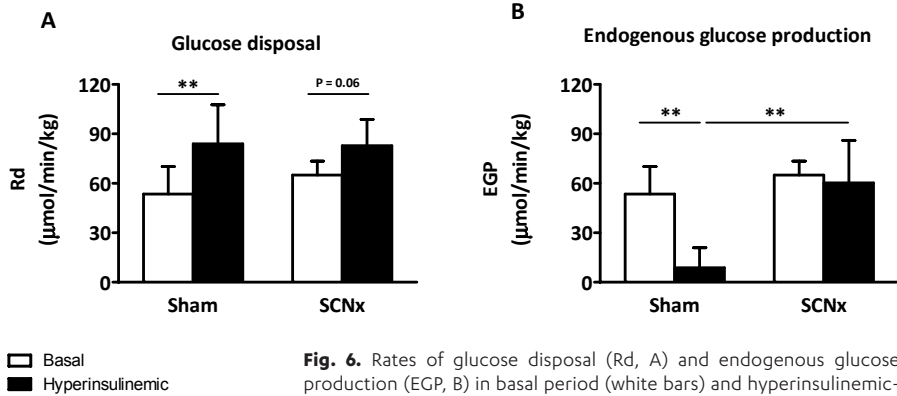
Fig. 6. Rates of glucose disposal (Rd, A) and endogenous glucose production (EGP, B) in basal period (white bars) and hyperinsulinemic-euglycemic clamp period (black bars) of sham and SCN lesioned (SCNx) mice. Data is represented as mean ± SD, ** $P < 0.01$.

A

B
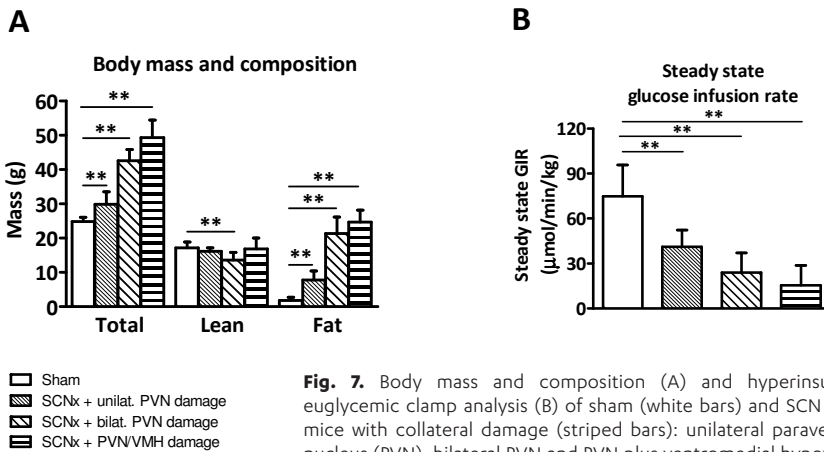
Fig. 7. Body mass and composition (A) and hyperinsulinemic-euglycemic clamp analysis (B) of sham (white bars) and SCN lesioned mice with collateral damage (striped bars): unilateral paraventricular nucleus (PVN), bilateral PVN and PVN plus ventromedial hypothalamus (VMH). Data is represented as mean ± SD, ** $P < 0.01$.

lower in all SCNx mice with collateral damage (SCNx + unilateral PVN damage; 41.3 ± 11.0 µmol/min/kg, SCNx + bilateral PVN damage; 23.9 ± 13.1 µmol/min/kg, SCNx + PVN/VMH damage; 15.4 ± 13.5 µmol/min/kg) compared to sham controls (74.7 ± 21.1 µmol/min/kg, Fig. 7B), suggesting insulin resistance.

DISCUSSION

This study addressed the effects of thermic, bilateral ablation of the SCN on energy metabolism and insulin sensitivity in mice. Since adjacent hypothalamic nuclei, such as PVN and VMH, are involved in energy metabolism, great care was taken to distinguish between SCN lesioned mice and mice with collateral damage to these nuclei. We show that lesioning of the SCN

disrupts the circadian pattern of energy intake, activity and energy expenditure, as expected. However, although selective SCN ablation resulted in only mild overweight compared to sham mice, hepatic insulin sensitivity was severely impaired. Therefore, disturbed SCN function has profound metabolic effects.

Anatomically, the SCN is connected with the VMH and the PVN through the subparaventricular zone of the hypothalamus (25). In mice with collateral damage to the PVN and/or VMH, the obesity and insulin resistance phenotypes were very profound. This is in line with previous data showing that lesions of the PVN (26;27) and VMH (28-31) result in hyperphagia, obesity and obesity-related hyperinsulinemia. Interestingly, unilateral PVN damage in SCN lesioned mice resulted in only mild overweight, comparable to SCN lesion alone. Apparently, PVN damage results in obesity only when the PVN is damaged bilaterally. In light of our data, it is of utmost importance to ascertain correct and exclusive lesioning of the SCN to study the role of the circadian pacemaker in the context of metabolism. In the current study we included 6 mice with exclusive and total SCN lesions, 23 SCN lesioned mice with collateral damage and 17 sham lesioned mice.

The mild increase in weight gain in mice with exclusive SCN lesions compared to sham mice (+17%) is in contrast to a previous finding in rats (10). In rats, lesioning the SCN did not induce an increase in body mass, whereas the effect on body composition was not determined. This discrepancy in body weight gain between the previous study and our study may be due to the use of the obesogenic C57Bl/6J mouse strain in our study, whereas the rat study was performed in Wistar rats. Wistar rats only become obese upon hypercaloric food intake (32). We studied the contribution of the SCN in the circadian regulation of energy metabolism and insulin sensitivity in C57Bl/6J mice, a mouse strain shown to be an excellent model to study development of obesity en insulin resistance (33-35).

Previously, it has been shown that the SCN is involved in the regulation of energy homeostasisin mice (36) and rats (37). In the present study, indirect calorimetry/metabolic cage analysis revealed that ablation of the SCN induced a loss of circadian rhythm in oxygen consumption and physical activity without affecting the 24 h average level of oxygen consumption or activity. This loss of circadian rhythm in homeostasis is in line with previous findings, where SCN lesions eliminated a wide range of rhythms, including leptin (10). Although total food intake over a period of one day and one night was reduced by 26% in SCN lesioned mice, the SCN lesioned mice consumed more during the light part of the day compared to sham mice (46% vs. 32% of total food intake). Recently, it has been shown that mice and rats fed only during the day gained significantly more weight than mice fed only at night (38;39). In another study, the time of intake of a high-fat diet was a determinant of weight gain, adiposity, glucose intolerance, hyperinsulinemia and hyperleptinemia (40). In the aforementioned studies, obesity resulted from a dissociation between the timing of food intake and the intrinsic rhythm of energy expenditure and, thus, animals were eating "against their clock time". In our study, on the other hand, the protocol was essentially different, and animals were not eating at the other part of the cycle, but rather, their circadian system was impaired. Therefore, it remains unclear how the mice with selective SCN lesion developed mild overweight. As it has been shown that the SCN has exerts excitatory effects on thermogenesis

by brown adipose tissue (BAT) (41), the mild weight gain in mice with a selective SCN lesion could be the result of reduced BAT activity.

Indirect calorimetry/metabolic cage analysis further revealed that SCN lesioned mice had lower RER during the day as well as during the night as compared to sham mice. This shows that SCN ablation results in lower relative carbohydrate oxidation rates and, conversely, higher fat oxidation rates compared to sham mice. These data suggest that the oxidative response to food intake is less directed to carbohydrate metabolism when SCN is lesioned, a hallmark for an impaired metabolic flexibility (42). Impaired metabolic flexibility has been associated with impaired insulin sensitivity in humans (43).

We assessed insulin sensitivity by hyperinsulinemic-euglycemic clamp analysis. Compared to the sham operated mice, SCN lesioned mice were hyperglycemic and hyperinsulinemic in the postabsorptive state. Furthermore, at the start of the clamp, the SCNx mice had increased FFA levels compared to sham animals, suggesting a possible removal of inhibitory input from the SCN to the adipose tissue, thereby increasing the basal rate of lipolysis. Increased circulating levels of FFA have been implicated as a possible pathway for developing insulin resistancein obesity (44). Severe hepatic insulin resistance, but not peripheral insulin resistance, was present even though body fat mass was increased only minimally. The SCN is crucial for the circadian control of glucose production and glucose uptake (45-48). Furthermore, there is a direct control of hepatic glucose metabolism resulting from cross communication of the SCN and PVN, further mediated by innervation of the liver (49). It is, therefore, likely that the impaired hepatic insulin sensitivity found in the SCNx groups is, at least in part, a direct result of the disrupted SCN mediated control of glucose and FFA metabolism.

Assessment of insulin sensitivity by hyperinsulinemic-euglycemic clamp technique revealed that all SCNx mice with collateral damage to PVN and/or VMH were very insulin resistant compared to sham mice. Surprisingly, SCNx with or without collateral damage were insulin resistant to a similar extent, even though SCNx mice with bilateral PVN damage and SCNx mice with PVN and VMH damage were much more obese that SCNx mice with unilateral PVN damage or mice with a clean SCN lesion, i.e., the amount of adiposity is not a direct determinant of the insulin resistance. These data further support the conclusion that, independent of obesity, the SCN output is crucial in determining hepatic insulin sensitivity.

We have clamped all mice at their respective basal glucose levels, as it has been shown that alterations in basal fasting glucose levels by itself are sufficient to affect insulin sensitivity (50). As SCN lesioned mice had increased basal glucose levels compared to the sham operated mice, the hyperinsulinemic glucose levels were also higher in the SCNx mice. However, clamping the mice at similar glucose levels, would have resulted in even larger differences in glucose infusion rates between sham and SCNx mice. Therefore, the degree of insulin resistance present in the SCNx mice may even have been underestimated using our clamp protocol.

In conclusion, we demonstrate that exclusive deletion of the SCN induces loss in circadian rhythms in energy metabolism and food intake. Although ablation of the SCN resulted in only mild overweight, SCNx mice were severely insulin resistant in the liver. Great care was taken to distinguish between exclusive SCN lesioned mice from mice that had collateral damage to the PVN and VMH areas, as the latter resulted in severe obesity. It was previously shown that

mice with mutations in clock genes have altered energy homeostasis and glucose metabolism (14;51). Together, the data from the several studies provide solid evidence that the SCN is crucially involved in the maintenance of energy balance and hepatic insulin sensitivity.

ACKNOWLEDGEMENTS

REFERENCE LIST

1. Takahashi, JS, Hong, HK, Ko, CH, McDearmon, EL: The genetics of mammalian circadian order and disorder: implications for physiology and disease. *Nat Rev Genet* 9:764-775, 2008

2. Yamazaki, S, Numano, R, Abe, M, Hida, A, Takahashi, R, Ueda, M, Block, GD, Sakaki, Y, Menaker, M, Tei, H: Resetting central and peripheral circadian oscillators in transgenic rats. *Science* 288:682-685, 2000

3. Davidson, AJ, Yamazaki, S, Arble, DM, Menaker, M, Block, GD: Resetting of central and peripheral circadian oscillators in aged rats. *Neurobiol Aging* 29:471-477, 2008

4. Kalsbeek, A, Buijs, RM: Output pathways of the mammalian suprachiasmatic nucleus: coding circadian time by transmitter selection and specific targeting. *Cell Tissue Res* 309:109-118, 2002

5. Reppert, SM, Weaver, DR: Coordination of circadian timing in mammals. *Nature* 418:935-941, 2002

6. van Cauter, E, Polonsky, KS, Scheen, AJ: Roles of circadian rhythmicity and sleep in human glucose regulation. *Endocr Rev* 18:716-738, 1997

7. Cailotto, C, La Fleur, SE, Van, HC, Wortel, J, Kalsbeek, A, Feenstra, M, Pevet, P, Buijs, RM: The suprachiasmatic nucleus controls the daily variation of plasma glucose via the autonomic output to the liver: are the clock genes involved? *Eur J Neurosci* 22:2531-2540, 2005

8. Weibel, L, Follenius, M, Spiegel, K, Ehrhart, J, Brandenberger, G: Comparative effect of night and daytime sleep on the 24-hour cortisol secretory profile. *Sleep* 18:549-556, 1995

9. Kalra, SP, Bagnasco, M, Otukonyong, EE, Dube, MG, Kalra, PS: Rhythmic, reciprocal ghrelin and leptin signaling: new insight in the development of obesity. *Regul Pept* 111:1-11, 2003

10. Kalsbeek, A, Fliers, E, Romijn, JA, La Fleur, SE, Wortel, J, Bakker, O, Endert, E, Buijs, RM: The suprachiasmatic nucleus generates the diurnal changes in plasma leptin levels. *Endocrinology* 142:2677-2685, 2001

11. Glass, JD, Guinn, J, Kaur, G, Francl, JM: On the intrinsic regulation of neuropeptide Y release in the mammalian suprachiasmatic nucleus circadian clock. *Eur J Neurosci* 31:1117-1126, 2010

12. Foster, RG, Roenneberg, T: Human responses to the geophysical daily, annual and lunar cycles. *Curr Biol* 18:R784-R794, 2008

13. Colwell, CS: Linking neural activity and molecular oscillations in the SCN. *Nat Rev Neurosci* 12:553-569, 2011

14. Turek, FW, Joshu, C, Kohsaka, A, Lin, E, Ivanova, G, McDearmon, E, Laposky, A, Losee-Olson, S, Easton, A, Jensen, DR, Eckel, RH, Takahashi, JS, Bass, J: Obesity and metabolic syndrome in circadian Clock mutant mice. *Science* 308:1043-1045, 2005

15. Nakamura, TJ, Nakamura, W, Yamazaki, S, Kudo, T, Cutler, T, Colwell, CS, Block, GD: Age-related decline in circadian output. *J Neurosci* 31:10201-10205, 2011

16. Swaab, DF, Fliers, E, Partiman, TS: The suprachiasmatic nucleus of the human brain in relation to sex, age and senile dementia. *Brain Res* 342:37-44, 1985

17. Deboer, T, Overeem, S, Visser, NA, Duindam, H, Frolich, M, Lammers, GJ, Meijer, JH: Convergence of circadian and sleep regulatory mechanisms on hypocretin-1. *Neuroscience* 129:727-732, 2004

18. Dörrscheidt, GJ, Beck, L: Advanced methods for evaluating characteristic parameters (T, 7, p) of Circadian Rhythms. *Journal of Mathematical Biology* 2:107-121, 1975

19. De Vogel-van den Bosch, van den Berg, SA, Bijland, S, Voshol, PJ, Havekes, LM, Romijn, HA, Hoeks, J, van, BD, Hesselink, MK, Schrauwen, P, van Dijk, KW: High-fat diets rich in medium- versus long-chain fatty acids induce distinct patterns of tissue specific insulin resistance. *J Nutr Biochem* 22:366-371, 2011

20. van den Berg, SA, Guigas, B, Bijland, S, Ouwens, M, Voshol, PJ, Frants, RR, Havekes, LM, Romijn, JA, van Dijk, KW: High levels of dietary stearate promote adiposity and deteriorate hepatic insulin sensitivity. *Nutr Metab (Lond)* 7:24, 2010

21. van den Berg, SA, Nabben, M, Bijland, S, Voshol, PJ, van Klinken, JB, Havekes, LM, Romijn, JA, Hoeks, J, Hesselink, MK, Schrauwen, P, van Dijk, KW: High levels of whole-body energy expenditure are associated with a lower coupling of skeletal muscle mitochondria in C57Bl/6 mice. *Metabolism* 59:1612-1618, 2010

22. Coomans, CP, Geerling, JJ, Guigas, B, van den Hoek, AM, Parlevliet, ET, Ouwens, DM, Pijl, H, Voshol, PJ, Rensen, PC, Havekes, LM, Romijn, JA: Circulating insulin stimulates fatty acid retention in white adipose tissue via KATP channel activation in the central nervous system only in insulin-sensitive mice. *J Lipid Res* 52:1712-1722, 2011

23. Stienstra, R, Joosten, LA, Koenen, T, van, TB, van Diepen, JA, van den Berg, SA, Rensen, PC, Voshol, PJ, Fantuzzi, G, Hijmans, A, Kersten, S, Muller, M, van den Berg, WB, van, RN, Wabitsch, M, Kullberg, BJ, van der Meer, JW, Kanneganti, T, Tack, CJ, Netea, MG: The inflammasome-mediated caspase-1 activation controls adipocyte differentiation and insulin sensitivity. *Cell Metab* 12:593-605, 2010

24. Coomans, CP, Biermasz, NR, Geerling, JJ, Guigas, B, Rensen, PC, Havekes, LM, Romijn, JA: Stimulatory Effect of Insulin on Glucose Uptake by Muscle Involves the Central Nervous System in Insulin-Sensitive Mice. *Diabetes* 60:3132-3140, 2011

25. Nieuwenhuys R, Voogd J, Huijzen Cv: *The human central nervous system*. Berlin, Springer-Verlag, 2008,

26. Sims, JS, Lorden, JF: Effect of paraventricular nucleus lesions on body weight, food intake and insulin levels. *Behav Brain Res* 22:265-281, 1986

27. Touzani, K, Velley, L: Ibotenic acid lesion of the hypothalamic paraventricular nucleus produces weight gain but modifies neither preference nor aversion for saccharin. *Physiol Behav* 52:673-678, 1992

28. Penicaud, L, Kinebanyan, MF, Ferre, P, Morin, J, Kande, J, Smadja, C, Marfaing-Jallat, P, Picon, L: Development of VMH obesity: in vivo insulin secretion and tissue insulin sensitivity. *Am J Physiol* 257:E255-E260, 1989

29. Grundmann, SJ, Pankey, EA, Cook, MM, Wood, AL, Rollins, BL, King, BM: Combination unilateral amygdaloid and ventromedial hypothalamic lesions: evidence for a feeding pathway. *Am J Physiol Regul Integr Comp Physiol* 288:R702-R707, 2005

30. Kageyama, A, Hirano, T, Kageyama, H, Osaka, T, Namba, Y, Tsuji, M, Adachi, M, Inoue, S: Distinct role of adiposity and insulin resistance in glucose intolerance: studies in ventromedial hypothalamic-lesioned obese rats. *Metabolism* 51:716-723, 2002

31. King, BM, Phelps, GR, Frohman, LA: Hypothalamic obesity in female rats in absence of vagally mediated hyperinsulinemia. *Am J Physiol* 239:E437-E441, 1980

32. Harrold, JA, Widdowson, PS, Clapham, JC, Williams, G: Individual severity of dietary obesity in unselected Wistar rats: relationship with hyperphagia. *Am J Physiol Endocrinol Metab* 279:E340-E347, 2000

33. Gallou-Kabani, C, Vige, A, Gross, MS, Rabes, JP, Boileau, C, Larue-Achagiotis, C, Tome, D, Jais, JP, Junien, C: C57BL/6J and A/J mice fed a high-fat diet delineate components of metabolic syndrome. *Obesity (Silver Spring)* 15:1996-2005, 2007

34. Schreyer, SA, Wilson, DL, LeBoeuf, RC: C57BL/6 mice fed high fat diets as models for diabetes-accelerated atherosclerosis. *Atherosclerosis* 136:17-24, 1998

35. Parekh, PI, Petro, AE, Tiller, JM, Feinglos, MN, Surwit, RS: Reversal of diet-induced obesity and diabetes in C57BL/6J mice. *Metabolism* 47:1089-1096, 1998

36. Phan, TH, Chan, GC, Sindreu, CB, Eckel-Mahan, KL, Storm, DR: The Diurnal Oscillation of MAP (Mitogen-Activated Protein) Kinase and Adenylyl Cyclase Activities in the Hippocampus

Depends on the Suprachiasmatic Nucleus. *J Neurosci* 31:10640-10647, 2011

37. Angeles-Castellanos, M, Salgado-Delgado, R, Rodriguez, K, Buijs, RM, Escobar, C: The suprachiasmatic nucleus participates in food entrainment: a lesion study. *Neuroscience* 165:1115-1126, 2010

38. Arble, DM, Bass, J, Laposky, AD, Vitaterna, MH, Turek, FW: Circadian timing of food intake contributes to weight gain. *Obesity (Silver Spring)* 17:2100-2102, 2009

39. Salgado-Delgado, R, ngeles-Castellanos, M, Saderi, N, Buijs, RM, Escobar, C: Food intake during the normal activity phase prevents obesity and circadian desynchrony in a rat model of night work. *Endocrinology* 151:1019-1029, 2010

40. Bray, MS, Tsai, JY, Villegas-Montoya, C, Boland, BB, Blasier, Z, Egbejimi, O, Kueht, M, Young, ME: Time-of-day-dependent dietary fat consumption influences multiple cardiometabolic syndrome parameters in mice. *Int J Obes (Lond)* 34:1589-1598, 2010

41. Amir, S, Shizgal, P, Rompre, PP: Glutamate injection into the suprachiasmatic nucleus stimulates brown fat thermogenesis in the rat. *Brain Res* 498:140-144, 1989

42. Kelley, DE, He, J, Menshikova, EV, Ritov, VB: Dysfunction of mitochondria in human skeletal muscle in type 2 diabetes. *Diabetes* 51:2944-2950, 2002

43. Corpeleijn, E, Mensink, M, Kooi, ME, Roekaerts, PM, Saris, WH, Blaak, EE: Impaired skeletal muscle substrate oxidation in glucose-intolerant men improves after weight loss. *Obesity (Silver Spring)* 16:1025-1032, 2008

44. Boden, G, Shulman, GI: Free fatty acids in obesity and type 2 diabetes: defining their role in the development of insulin resistance and beta-cell dysfunction. *Eur J Clin Invest* 32 Suppl 3:14-23, 2002

45. Ruiter, M, Buijs, RM, Kalsbeek, A: Hormones and the autonomic nervous system are involved in suprachiasmatic nucleus modulation of glucose homeostasis. *Curr Diabetes Rev* 2:213-226, 2006

46. La Fleur, SE: Daily rhythms in glucose metabolism: suprachiasmatic nucleus output to peripheral tissue. *J Neuroendocrinol* 15:315-322, 2003

47. Arslanian, S, Ohki, Y, Becker, DJ, Drash, AL: Demonstration of a dawn phenomenon in normal adolescents. *Horm Res* 34:27-32, 1990

48. Bolli, GB, De, FP, De, CS, Perriello, G, Ventura, MM, Calcinaro, F, Lolli, C, Campbell, P, Brunetti, P, Gerich, JE: Demonstration of a dawn phenomenon in normal human volunteers. *Diabetes* 33:1150-1153, 1984

49. Kalsbeek, A, La, FS, Van, HC, Buijs, RM: Suprachiasmatic GABAergic inputs to the paraventricular nucleus control plasma glucose concentrations in the rat via sympathetic innervation of the liver. *J Neurosci* 24:7604-7613, 2004

50. Kelley, DE, Mandarino, LJ: Hyperglycemia normalizes insulin-stimulated skeletal muscle glucose oxidation and storage in noninsulin-dependent diabetes mellitus. *J Clin Invest* 86:1999-2007, 1990

51. Rudic, RD, McNamara, P, Curtis, AM, Boston, RC, Panda, S, Hogenesch, JB, Fitzgerald, GA: BMAL1 and CLOCK, two essential components of the circadian clock, are involved in glucose homeostasis. *PLoS Biol* 2:e377, 2004

STIMULATORY EFFECT OF INSULIN ON GLUCOSE UPTAKE BY MUSCLE INVOLVES THE CENTRAL NERVOUS SYSTEM IN INSULIN-SENSITIVE MICE

Claudia P. Coomans
Nienke R. Biermasz
Janine J. Geerling
Bruno Guigas
Patrick C.N. Rensen
Louis M. Havekes
Johannes A. Romijn

4

ABSTRACT

Insulin inhibits endogenous glucose production (EGP) and stimulates glucose uptake in peripheral tissues. Hypothalamic insulin signaling is required for the inhibitory effects of insulin on endogenous glucose production. We examined the contribution of central insulin signaling on circulating insulin-stimulated tissue-specific glucose uptake. Tolbutamide, an inhibitor of ATP-sensitive potassium channels, or vehicle was infused into the lateral ventricle in the basal state and during hyperinsulinemic-euglycemic conditions in postabsorptive, chow fed C57Bl/6J mice and in postabsorptive, diet-induced obese C57Bl/6J mice. Whole body glucose uptake was measured by D-[^{14}C]glucose kinetics and tissue-specific glucose uptake by 2-deoxy-D-[^{3}H] glucose uptake.

During clamp conditions, intracerebroventricular (i.c.v.) administration of tolbutamide impaired the ability of insulin to inhibit EGP by ~20%. In addition, i.c.v. tolbutamide diminished insulin-stimulated glucose uptake in muscle (by ~59%), but not in heart or adipose tissue. In contrast, in diet-induced obese, insulin resistant mice, i.c.v tolbutamide did not affect the effects of insulin during clamp conditions on EGP or glucose uptake by muscle.

In conclusion, insulin stimulates glucose uptake in muscle in part through effects via ATP-sensitive potassium channels in the central nervous system, in analogy with the inhibitory effects of insulin on EGP. High-fat diet-induced obesity abolished the central effects of insulin on liver and muscle. These observations stress the role of central insulin resistance in the pathophysiology of diet-induced insulin resistance.

INTRODUCTION

In response to nutrients, insulin is rapidly released from pancreatic β-cells and decreases plasma glucose levels by inhibiting endogenous glucose production (EGP) and stimulating glucose transport into skeletal muscle, heart and white adipose tissue (WAT). Intake of high-fat diets can lead to insulin resistance, which plays a primary pathophysiological role in the development of T2DM (1;2). Insulin resistance in the liver results in a decreased capacity of insulin to suppress EGP, whereas insulin resistance in peripheral tissues, including muscle, results in reduced insulin-mediated glucose uptake.

In addition to direct effects of insulin on peripheral tissues, insulin acts in the hypothalamus, where it exerts anorexigenic properties by stimulating proopiomelanocortin (POMC)/cocaine and amphetamine regulated transcript (CART) neurons and by inhibiting agouti-related peptide (AgRP)/neuropeptide Y (NPY) neurons (3-5). In fact, hypothalamic insulin signaling appeared necessary for the inhibitory effect of insulin on EGP (6-8). Insulin activates ATP-sensitive potassium channels (K_{ATP} channels) in neurons of the hypothalamus, including POMC/CART- and AgRP/NPY expressing neurons (9;10). Inhibition of these neuronal K_{ATP} channels by intracerebroventricular (i.c.v.) administration of sulfonylurea (either tolbutamide or glibenclamide) impairs the inhibitory effect of insulin on EGP (7). Conversely, activation of hypothalamic K_{ATP} channels enhances insulin-mediated inhibition of EGP (11).

Although the importance of this central action of insulin for the inhibition of EGP is now well established, the role of the central effects of insulin on glucose disposal is still unknown. Therefore, the aim of the present study was to determine the role of the central effect of insulin on tissue-specific insulin-stimulated glucose disposal in mice without and with diet-induced insulin resistance. To this end, we infused tolbutamide, an inhibitor of K_{ATP} channels, into the lateral ventricle and quantified glucose disposal in mice on a regular diet, both in the basal state and during hyperinsulinemic-euglycemic conditions. We show that the central effects of insulin are not only required for inhibition of EGP, but also enhances insulin-mediated glucose uptake in muscle. Furthermore, we show that these central effects of insulin on EGP and tissue-specific uptake of glucose are lost in diet-induced obese mice, stressing the role of central insulin resistance in the pathophysiology of diet-induced insulin resistance.

MATERIALS AND METHODS

Animals

Male C57Bl/6J mice (15 weeks old) were housed in a temperature-controlled room on a 12-hour light-dark cycle. Animals had free access to water and diet (chow or high-fat (45 energy% of fat derived from palm oil; Research Diet Services BV, Wijk bij Duurstede, The Netherlands)). All animal experiments were performed in accordance with the regulations of Dutch law on animal welfare and the institutional ethics committee for animal procedures from the Leiden University Medical Center, Leiden, The Netherlands approved the protocol.

Surgical procedure

For i.c.v. cannula implantation, 15-week-old male mice were anaesthetized with 0.5 mg/kg Medetomidine (Pfizer, Capelle a/d IJssel, The Netherlands), 5 mg/kg Midazolam (Roche, Mijdrecht, The Netherlands) and 0.05 mg/kg Fentanyl (Janssen-Cilag, Tilburg, The Netherlands) and placed in a stereotactic device (TSE systems, Homburg, Germany). A 25 gauge guide cannula was implanted into the left lateral ventricle using the following coordinates from Bregma: 1.0 mm lateral, 0.46 mm posterior and 2.2 mm ventral. The guide cannula was secured to the skull surface with dental cement (GC Europe N.V., Leuven, Belgium) and the anesthesia was antagonized using 2.5 mg/kg Antipamezol (Pfizer, Capelle a/d IJssel, The Netherlands), 0.5 mg/kg Flumazenil (Roche, Mijdrecht, The Netherlands) and 1.2 mg/kg Naloxon (Orpha, Purkersdorf, Austria). After a recovery period of 1 week, cannula placement was verified. Mice that ate >0.3 g in 1 h in response to i.c.v. injection of 5 μg NPY (Bachem, St. Helens, UK) in 1 μl of artificial cerebrospinal fluid (aCSF, Harvard Apparatus, Natick, MA, US) were considered to have the cannula correctly placed and were included in the study (12;13).

Basal and insulin-stimulated glucose metabolism

Postabsorptive (i.e. overnight fasted), body weight-matched male mice were anaesthetized with 6.25 mg/kg Acepromazine (Alfasan, Woerden, The Netherlands), 6.25 mg/kg Midazolam (Roche, Mijdrecht, The Netherlands), and 0.31 mg/kg Fentanyl (Janssen-Cilag, Tilburg, The Netherlands). Tissue-specific glucose uptake was determined, in the basal state and in the hyperinsulinemic-euglycemic state, in separate experiments (Fig. 1). aCSF or the K_{ATP} channel blocker tolbutamide, dissolved in 5% DMSO to a final concentration of 4.8 mM in aCSF, was continuously infused i.c.v. at a rate of 2.5 μl/h using a Harvard infusion pump (7;14). Thirty min after starting the i.c.v. infusion of tolbutamide or vehicle, i.v. infusions were started. In the basal state study, D-[^{14}C]glucose (0.3 μCi/kg/min; Amersham, Little Chalfont, U.K.) was continuously infused for 90 min. In the hyperinsulinemic-euglycemic clamp study, insulin (Actrapid, Novo Nordisk, Denmark) was administered i.v. by primed (4.1 mU), continuous (6.8 mU/h) infusion to attain steady-state insulin levels together with D-[^{14}C]glucose (0.3 μCi/kg/min; Amersham) for 90 min. This infusion rate of insulin was chosen based on previous dose-response studies of hyperinsulinemia, aimed at a five-fold increase in insulin levels which both inhibited EGP and stimulated glucose uptake (15). A variable intravenous infusion of a 12.5% D-glucose solution was used to maintain euglycemia as determined at 10-min intervals via tail bleeding (<3 μl, Accu-chek, Sensor Comfort; Roche Diagnostics, Mannheim, Germany). In a separate experiment, aCSF or the K_{ATP} channel activator diazoxide (dissolved in 5% DMSO, to a final concentration of 2 μg/μl in aCSF) was continuously infused i.c.v. in high-fat fed mice during hyperinsulinemic-euglycemic clamp. To assess basal and insulin-mediated glucose uptake in individual tissues, 2-deoxy-D-[^{3}H]glucose (2-[^{3}H]DG; Amersham) was administered as a bolus (1 μCi) 30 min before the end of both experiments. In the last 20 min of both experiments, blood samples were taken with intervals of 10 min. Subsequently, the mice were sacrificed, perfused with PBS and organs were quickly harvested and snap-frozen in liquid nitrogen.

Plasma analysis

Blood samples were taken from the tail tip into chilled paraoxon-coated capillaries to prevent *ex vivo* lipolysis. The tubes were placed on ice and centrifuged at 4°C. Plasma levels of glucose and free fatty acids (FFA) were determined using commercially available kits and standards according to the instructions of the manufacturer (Instruchemie, Delfzijl, The Netherlands). Plasma insulin levels were measured using a mouse-specific insulin ELISA kit (Crystal Chem Inc., Downers Grove, U.S.). Total plasma ^{14}C-glucose and ^{3}H-glucose were determined in supernatant of 7.5 μl plasma, after protein precipitation using 20% trichloroacetic acid and evaporation to eliminate tritiated water.

Tissue analysis

For determination of tissue 2-[^{3}H]DG uptake, homogenates of brain, heart, skeletal muscle (upper hindlimb) and WAT (epigonadal, visceral and subcutaneous) were boiled, and the supernatants were subjected to an ion-exchange column to separate 2-[^{3}H]DG-6-phosphate (which is trapped within the organ and not phosphorylated) from 2-[^{3}H]DG as described previously (16-18).

Calculations

Turnover rates of glucose (μmol/min/kg) were calculated for the basal state and for the hyperinsulinemic-euglycemic state as the rate of tracer infusion (dpm/min) divided by plasma specific activities of ^{14}C-glucose (dpm/μmol). The ratio was corrected for body weight. EGP was calculated as the difference between the tracer-derived rate of glucose appearance and the glucose infusion rate.

Tissue-specific glucose uptake in brain, muscle and WAT was calculated from tissue 2-[^{3}H]DG content, corrected for plasma specific activity and expressed as micromoles per gram of tissue.

Western blot analysis

Whole hypothalami and skeletal muscles (upper hindlimb) of mice receiving i.c.v. aCSF in basal state and hyperinsulinemic-euglycemic state (n=5) were homogenized by Ultra-Turrax (22.000 rpm; 2x5 sec) in a 6:1 (v/w) ratio of ice-cold buffer containing: 50 mM HEPES (pH 7.6), 50 mM NaF, 50 mM KCl, 5 mM *TSPP (sodium pyrophosphate)*, 1 mM EDTA, 1 mM EGTA, 5 mM β-GP, 1 mM Na3VO4, 1 mM DTT, 1% NP40 and protease inhibitors cocktail (Complete, Roche, Mijdrecht, The Netherlands). Homogenates were centrifuged (13, 200 rpm; 15 min, 4°C) and the protein content of the supernatant was determined using a bicinchoninic acid (BCA) protein assay kit (BCA Protein Assay Kit, Thermo Scientific Pierce Protein Research Products, Rockford, US). Proteins (20-50 μg) were separated by 7-10% SDS-PAGE followed by transfer to a PVDF transfer membrane. Membranes were blocked for 1 h at room temperature in Tris-buffered saline with Tween-20 buffer and 5% non-fat dry milk followed by an overnight incubation with phospho-specific or total antibodies (all from Cell Signaling Technology, Beverly, US). Blots were then incubated with HRP-conjugated secondary antibodies for 1 h at room temperature. Bands were visualized by enhanced chemiluminescence and quantified using Image J (NIH, US).

Statistical analysis

Differences between groups were determined by Mann-Whitney nonparametric tests for two independent samples. The criterion for significance was set at $P < 0.05$. All values shown represent means ± SEM.

RESULTS

I.c.v. tolbutamide administration in post-absorptive, chow fed mice
Plasma parameters and body weight
The design of the infusion studies is shown in Figure 1. In the basal and in the hyperinsulinemic state, body weight, plasma glucose, FFA and insulin levels did not differ between tolbutamide- and vehicle-treated chow fed mice (Table 1). As expected, in the hyperinsulinemic-euglycemic state, insulin levels were five-fold higher and FFA levels were ~50% lower than the values in the basal state, both in the tolbutamide- and vehicle-treated groups. In agreement with the rise in plasma insulin levels, hypothalamic insulin signaling was activated in the hyperinsulinemic-euglycemic state as phosphorylation of PKB on Thr308 (1.2 ± 0.1 *vs.* 1.0 ± 0.1, $P = 0.08$) and its downstream target PRAS40 on Thr246 (1.5 ± 0.1 *vs.* 1.0 ± 0.1, $P < 0.05$) were increased compared to basal state (Fig. 2).
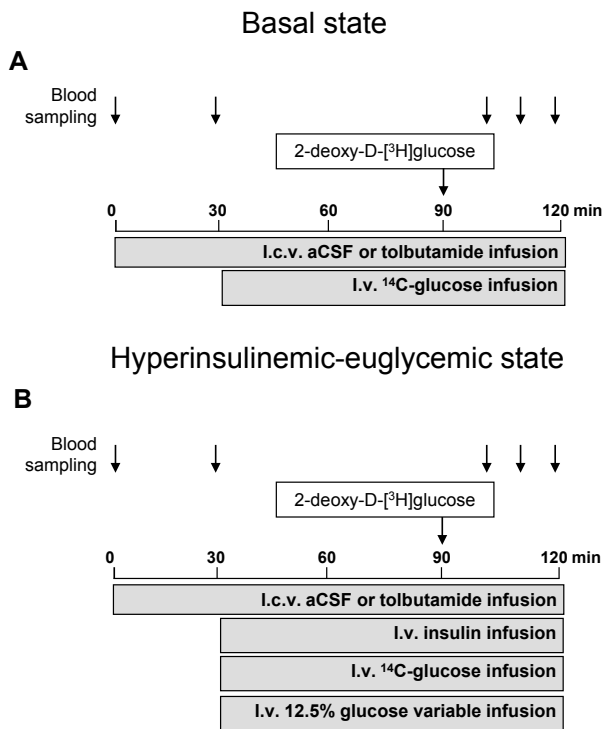
Fig. 1. Schematic representation of the experimental procedures. (A) Basal state. At t=0 min, a continuous i.c.v. infusion of vehicle or tolbutamide was started and maintained throughout the entire experiment. At t=30 min, a primed, continuous i.v. infusion of ^{14}C-glucose was initiated and maintained for the remainder of the experiment. At t=90 min, an i.v. bolus of 2-[^{3}H]DG was administered. At t=0, 100, 110 and 120 min, blood samples were obtained and at t=120 min, the animals were sacrificed and organs harvested. (B) Hyperinsulinemic-euglycemic state. At t=0 min, a continuous i.c.v. infusion of vehicle or tolbutamide was started and maintained throughout the entire experiment. At t=30 min, a hyperinsulinemic-euglycemic clamp was started by primed, continuous infusion of insulin together with ^{14}C-glucose. A variable infusion of 12.5% glucose was used to maintain euglycemia. At t=90 min, an i.v. bolus of 2-[^{3}H]DG was administered. At t=0, 100, 110 and 120 min, blood samples were obtained and at t=120 min, the animals were sacrificed and organs harvested.

Table 1. Plasma parameters of chow fed mice, in basal or hyperinsulinemic-euglycemic state, as measured at the end of the experiments. Throughout the experiments, mice received i.c.v. infusion of vehicle or tolbutamide. Values are means ± SEM for at least 8 mice per group. FFA, free fatty acids. * $P < 0.01$ basal *vs.* hyperinsulinemic state.

	Basal state		Hyperinsulinemic state	
	vehicle	tolbutamide	vehicle	tolbutamide
Body weight (g)	23.5 ± 0.4	23.6 ± 0.4	22.8 ± 0.2	22.8 ± 0.5
Glucose (mmol/l)	5.2 ± 0.2	5.8 ± 0.4	6.2 ± 0.5	6.4 ± 0.5
FFA (mmol/l)	0.6± 0.1	0.6 ± 0.1	0.3 ± 0.1 *	0.3 ± 0.1 *
Insulin (ng/ml)	0.9 ± 0.1	1.0 ± 0.1	5.5 ± 0.4 *	4.9 ± 0.2 *
Hematocrit (%)	44.1 ± 0.7	44.3 ± 1.0	42.2 ± 0.6	42.5 ± 1.1

Glucose infusion rate

In the hyperinsulinemic-euglycemic clamp study, the rate of glucose infusion (GIR) necessary to maintain euglycemia was significantly lower in tolbutamide-treated animals compared to vehicle-treated animals (average GIR 87 ± 6 *vs.* 104 ± 13 µmol/min/kg for the last 20 min of the experiment, $P < 0.05$, Fig. 3A), in the presence of similar glucose levels (average plasma glucose 5.4 ± 0.2 *vs.* 5.6 ± 0.1 mmol/l for the last 20 min of the experiment, ns, Fig. 3B), indicating that i.c.v. tolbutamide decreased insulin sensitivity. The glucose specific activities measured at 10 min intervals in all experiments indicated the presence of steady-state conditions in all groups (Table 2).

Endogenous glucose production and glucose disposal

In the basal state, endogenous glucose production (EGP), which equals glucose disposal, was not different between i.c.v. tolbutamide- and i.c.v vehicle-treated animals (36 ± 4 *vs.* 30 ± 2 µmol/min/kg, respectively, ns, Fig. 4A). In the hyperinsulinemic-euglycemic state, EGP was significantly decreased compared to the basal state (1 ± 1 *vs.* 30 ± 2 µmol/min/kg, respectively, $P < 0.01$). I.c.v. tolbutamide in the hyperinsulinemic state diminished the inhibitory effects of insulin on EGP (12 ± 4 *vs.* 1 ± 1 µmol/min/kg, $P < 0.05$).

Table 2. Specific activity of glucose (dpm/mmol) in the postabsorptive state or in the hyperinsulinemic euglycemic state of chow-fed mice. Throughout the experiment, mice received i.c.v. infusion of aCSF or tolbutamide. Values are means ± SEM for at least 8 mice per group.

	Postabsorptive state		
	100 min	110 min	120 min
vehicle	$11.9 \pm 0.4 \times 10^3$	$11.4 \pm 0.9 \times 10^3$	$11.8 \pm 0.5 \times 10^3$
tolbutamide	$11.0 \pm 1.1 \times 10^3$	$11.3 \pm 0.9 \times 10^3$	$9.4 \pm 1.1 \times 10^3$
	Hyperinsulinemic state		
	100 min	110 min	120 min
vehicle	$4.1 \pm 0.5 \times 10^3$	$4.0 \pm 0.7 \times 10^3$	$4.3 \pm 1.6 \times 10^3$
tolbutamide	$4.1 \pm 0.3 \times 10^3$	$3.8 \pm 0.2 \times 10^3$	$4.2 \pm 0.3 \times 10^3$
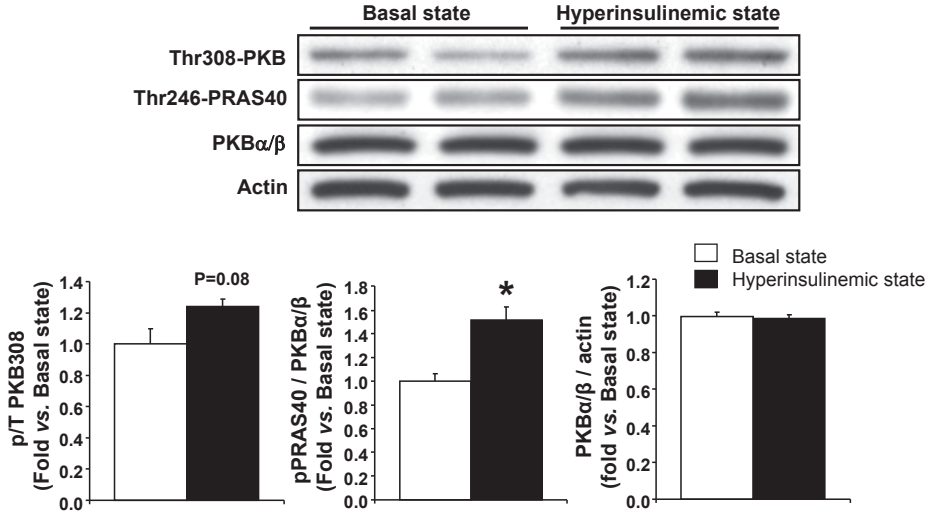
Fig. 2. Phosphorylation state of PKB and PRAS40 in basal state (white bars) or hyperinsulinemic-euglycemic state (black bars) in hypothalamus of chow fed mice. The corresponding quantification of the western blot data was normalized for total protein or actin and expressed as fold change compared to basal state. Values represent means ± SEM for 5 mice per group. * $P < 0.05$ *vs.* vehicle.
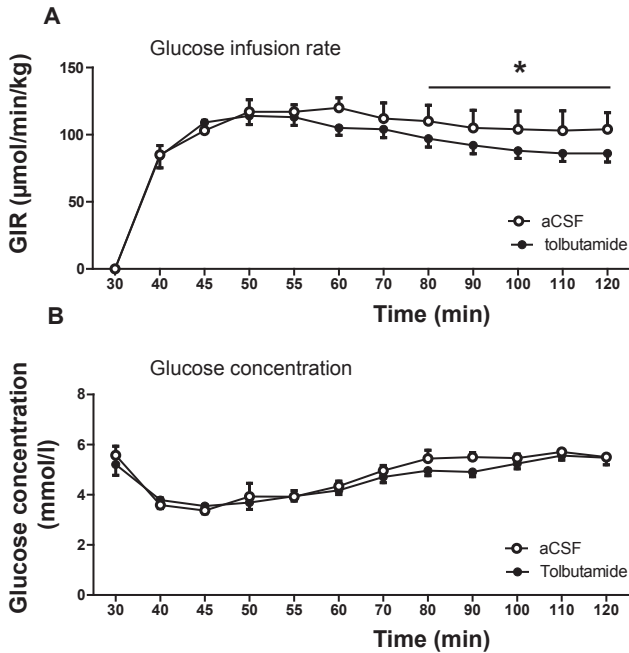
Fig. 3. Glucose infusion rates (GIR, A) and glucose concentrations (B) during hyperinsulinemic-euglycemic clamp in chow fed mice. Throughout the experiment, mice received i.c.v. infusion of vehicle (open circles) or tolbutamide (closed circles). Values represent means ± SEM for at least 8 mice per group. *$P < 0.05$, vehicle *vs.* tolbutamide.

Fig. 4. Rates of endogenous glucose production (EGP, A) and glucose disposal (B) in basal state (white bars) or hyperinsulinemic-euglycemic state (black bars) in chow fed mice. Throughout the experiment, mice received i.c.v. infusion of vehicle or tolbutamide. Values represent means ± SEM for at least 8 mice per group. **$P < 0.01$ basal vs. hyperinsulinemic state, # $P < 0.05$, hyperinsulinemic state: vehicle vs. tolbutamide.

Glucose disposal was increased by ~300% in the hyperinsulinemic-euglycemic state compared to the basal state (120 ± 12 vs. 30 ± 2 µmol/min/kg, respectively, $P < 0.01$, Fig. 4B), whereas i.c.v. tolbutamide in the hyperinsulinemic state tended to reduce glucose disposal (97 ± 3 vs. 120 ± 12 µmol/min/kg, $P = 0.07$).

Tissue-specific glucose uptake

In the basal and hyperinsulinemic-euglycemic states, 2-[^{3}H]DG uptake was measured in brain, muscle (cardiac and skeletal) and WAT (epigonadal, subcutaneous and visceral fat) (Fig. 5). In brain, 2-[^{3}H]DG uptake did not differ between the basal and the hyperinsulinemic states (12 ± 2 vs. 15 ± 4 µmol/g tissue, respectively, ns) and was not affected by i.c.v. tolbutamide (11 ± 1 vs. 14 ± 1 µmol/g tissue for basal and hyperinsulinemic state, respectively, ns). In heart, insulin increased 2-[^{3}H]DG uptake six-fold in the hyperinsulinemic state compared to the rate of uptake measured in the basal state (12 ± 1 vs. 2 ± 1 µmol/g tissue, respectively, $P < 0.05$), but this increase was not affected by i.c.v. tolbutamide. In muscle, insulin increased 2-[^{3}H]DG uptake considerably in the hyperinsulinemic state compared to the basal state (11 ± 3 vs. 1 ± 1 µmol/g tissue, respectively, $P < 0.05$). Remarkably, i.c.v. tolbutamide inhibited the insulin-mediated increase in 2-[^{3}H]DG uptake by muscle by ~59% (5 ± 1 vs. 11± 3 µmol/g tissue, $P < 0.05$). Phosphorylation of PKB on Ser473 (14 ± 1 vs. 14 ± 1, ns) and Thr308 (8 ± 1 vs. 8 ± 1, ns) and its downstream target PRAS40 on Thr246 (14 ± 1 vs. 12 ± 1, ns) were not different between i.c.v. vehicle and i.c.v. tolbutamide infused mice in hyperinsulinemic conditions (Fig. 6). In all fat pads, insulin stimulated 2-[^{3}H]DG uptake in the hyperinsulinemic state compared to the basal state, but this increase was not affected by i.c.v. tolbutamide.
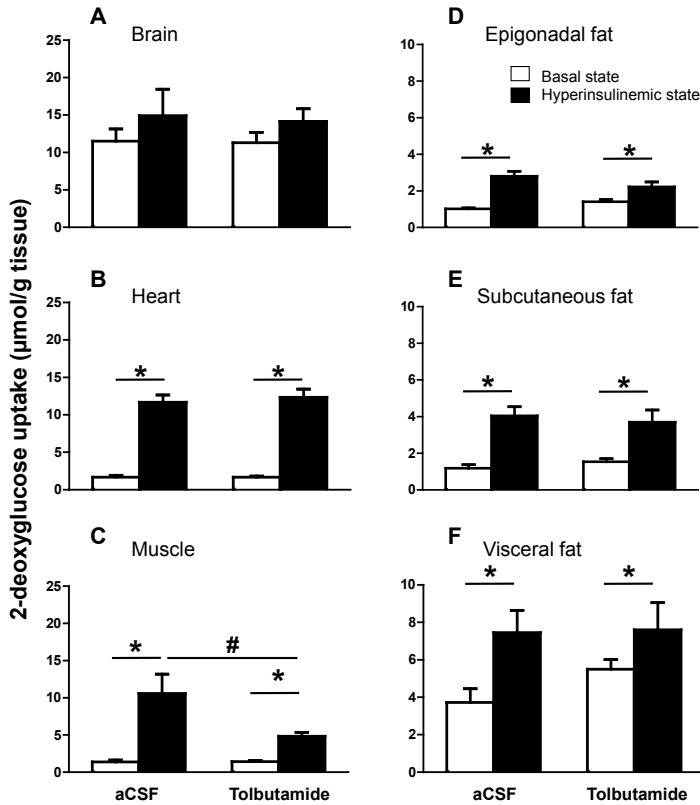
Fig. 5. Tissue-specific glucose uptake in basal state (white bars) or hyperinsulinemic-euglycemic state (black bars) in chow fed mice. Throughout the experiment, mice received i.c.v. infusion of vehicle or tolbutamide. Values represent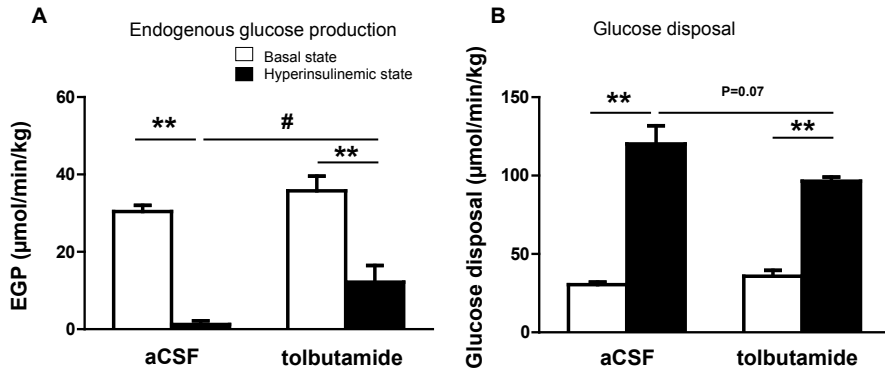 means ± SEM for at least 7 mice per group. *$P < 0.05$ basal *vs.* hyperinsulinemic state, # $P < 0.05$, hyperinsulinemic state: vehicle *vs.* tolbutamide.

Table 3. Plasma parameters of diet-induced obese mice, in basal or hyperinsulinemic-euglycemic state, as measured at the end of the experiments. Throughout the experiments, mice received i.c.v. infusion of vehicle or tolbutamide. Values are means ± SEM for at least 6 mice per group. FFA, free fatty acids. * $P < 0.01$ basal *vs.* hyperinsulinemic state.

	Basal state	Hyperinsulinemic state	
	vehicle	vehicle	tolbutamide
Body weight (g)	36.4 ± 0.8	37.6 ± 1.5	37.4 ± 0.7
Glucose (mmol/l)	5.1 ± 0.4	5.8 ± 0.4	6.2 ± 0.3
FFA (mmol/l)	0.7 ± 0.1	0.3 ± 0.1 *	0.3 ± 0.1 *
Insulin (ng/ml)	1.4 ± 0.4	7.5 ± 0.5 *	7.9 ± 0.6 *
Hematocrit (%)	44.3 ± 0.6	42.2 ± 1.0	42.4 ± 0.8
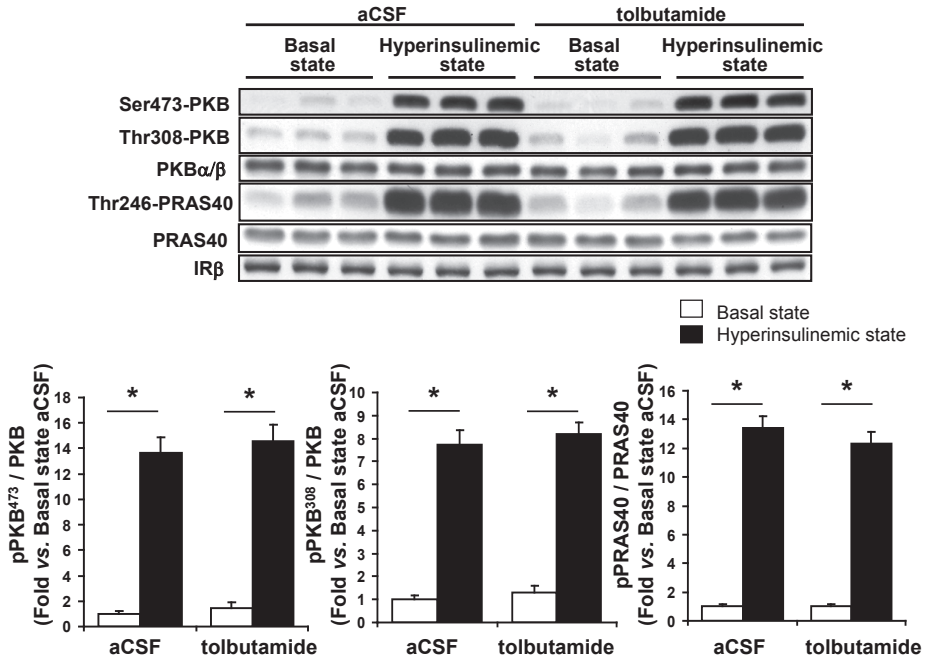
Fig. 6. Phosphorylation state of PKB and PRAS40 in basal state (white bars) or hyperinsulinemic-euglycemic state (black bars) in muscle of chow fed mice receiving i.c.v. infusion of vehicle or tolbutamide. The corresponding quantification of the western blot data was normalized for total protein and expressed as fold change compared to basal state. Values represent means ± SEM for 5 mice per group. * $P < 0.05$ vs. vehicle.

I.c.v. tolbutamide administration in postabsorptive, diet-induced obese mice

Plasma parameters and body weight

Since all parameters in the basal state were not different between i.c.v tolbutamide- and i.c.v. vehicle-treated animals in chow fed conditions, we assessed the effects of i.c.v. tolbutamide in high-fat treated mice only in hyperinsulinemic-euglycemic clamp conditions. Body weight of the diet-induced obese mice was markedly higher compared to chow fed mice ($37 ± 1$ vs. $23 ± 1$ g, respectively, $P < 0.01$, Table 3). Plasma glucose and hematocrit levels were similar in basal and hyperinsulinemic conditions. In the hyperinsulinemic-euglycemic state, insulin levels were five-fold higher compared to the basal state, resulting in a decrease of ~50% in FFA levels. There were no differences observed in body weight, plasma glucose, FFA, insulin and hematocrit levels between i.c.v. tolbutamide- and i.c.v. vehicle-treated animals in the hyperinsulinemic-euglycemic state.

Endogenous glucose production and glucose disposal

The GIR necessary to maintain euglycemia, was not different between tolbutamide- and vehicle-treated animals (Fig. 7). Plasma glucose specific activities obtained during the last 20 min of the experiments indicated the presence of steady-state conditions in all groups (Table 4).
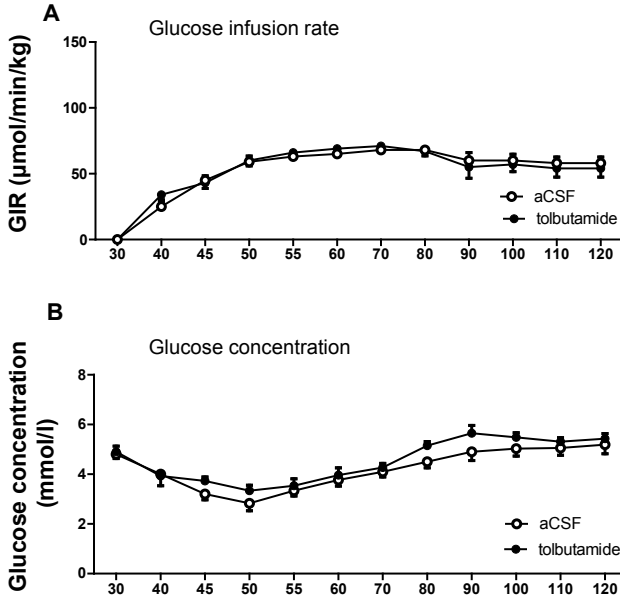
Fig. 7. Glucose infusion rates (GIR, A) and glucose concentrations during a hyperinsulinemic-euglycemic clamp (B) in diet-induced obese mice. Throughout the experiment, mice received i.c.v. infusion of aCSF (open circles) or tolbutamide (closed circles). Values represent mean ± SEM for at least 7 mice per group.
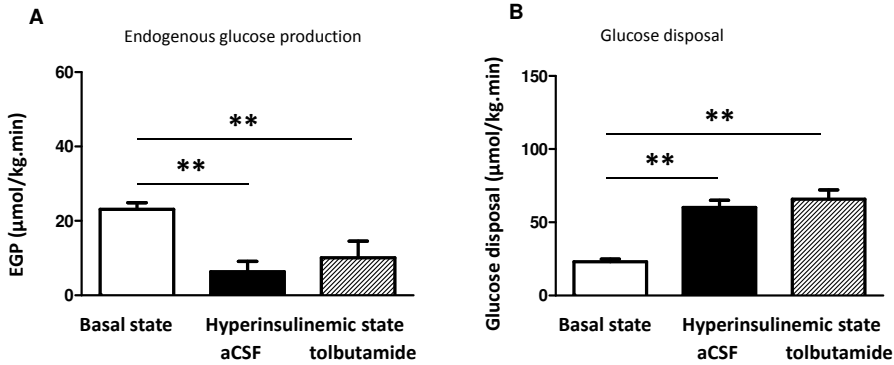
Fig. 8. Rates of endogenous glucose production (EGP, A) and glucose disposal (B) in basal state (white bars) or hyperinsulinemic-euglycemic state (black and hatched bars) in diet-induced obese mice. Throughout the experiment, mice received an i.c.v. infusion of vehicle (white and black bars) or tolbutamide (hatched bars). Values represent means ± SEM for at least 7 mice per group. **$P < 0.01$ basal *vs.* hyperinsulinemic state.

In the hyperinsulinemic-euglycemic state, insulin decreased EGP compared to the basal state by ~74% (6 ± 3 *vs.* 23 ± 2 µmol/min/kg, respectively, $P < 0.01$, Fig. 8A), but surprisingly i.c.v. tolbutamide did not attenuate this effect of insulin in these diet-induced mice (i.c.v. tolbutamide- *vs.* i.c.v. vehicle-treated animals: 10.0 ± 4 *vs.* 6.3 ± 3 µmol/min/kg, ns).

Table 4. Specific activity of glucose (dpm/mmol) in the postabsorptive state or in the hyperinsulinemic euglycemic state of high fat diet-induced obese mice. Throughout the experiment, i.c.v. tolbutamide or aCSF was administered. Values are means ± SEM for at least 8 mice per group.

	Postabsorptive state		
	100 min	110 min	120 min
vehicle	$11.2 \pm 0.9 \times 10^3$	$11.1 \pm 0.7 \times 10^3$	$14.0 \pm 1.0 \times 10^3$
	Hyperinsulinemic state		
	100 min	110 min	120 min
vehicle	$4.0 \pm 0.4 \times 10^3$	$4.3 \pm 0.5 \times 10^3$	$4.3 \pm 0.3 \times 10^3$
tolbutamide	$4.6 \pm 0.4 \times 10^3$	$4.2 \pm 0.3 \times 10^3$	$4.3 \pm 0.2 \times 10^3$

In the hyperinsulinemic-euglycemic state, insulin increased glucose disposal only by ~161% compared to the basal state (60 ± 5 *vs.* 23 ± 2 µmol/min/kg, respectively, $P < 0.01$, Fig. 8B). However, this effect of insulin was not affected by i.c.v. tolbutamide (i.c.v. tolbutamide- *vs.* vehicle-treated animals: 62 ± 6 *vs.* 60 ± 5 µmol/min/kg, ns).

Comparison of the data from this experiment with the previously mentioned chow fed experiments indicated that the obese mice were considerably insulin resistant. Muscle glucose uptake under hyperinsulinemic-euglycemic conditions in high-fat fed mice was significantly lower compared to chow fed mice (7.9 ± 1.1 *vs.* 10.6 ± 2.6 µmol/min/kg, $P < 0.05$). In addition, glucose disposal rate was lower (60.2 ± 4.9 *vs.* 120.1 ± 11.7 µmol/min/kg, $P < 0.05$) and EGP was higher (6.4 ± 2.8 *vs.* 1.2 ± 1.0 µmol/min/kg, $P < 0.05$), indicating both hepatic and peripheral insulin resistance in the diet-induced obese mice.

Tissue-specific glucose uptake

In diet-induced obese mice, we measured tissue-specific 2-[³H]DG uptake in brain, muscle (cardiac and skeletal) and WAT (epigonadal, subcutaneous and visceral fat) in the basal state and in the hyperinsulinemic-euglycemic state (Fig. 9). In muscle, insulin stimulated 2-[³H] DG uptake compared to the basal state (8 ± 1 *vs.* 2 ± 1 µmol/g tissue, respectively, $P < 0.05$). In contrast to chow fed mice, in diet-induced obese mice there was no effect of i.c.v. tolbutamide on insulin-mediated muscle glucose uptake. In accordance with the observation in chow fed mice, insulin increased 2-[³H]DG uptake in the hyperinsulinemic state compared to the basal state in heart and WAT, but not in brain, whereas i.c.v. tolbutamide did not affect 2-[³H]DG uptake in any of these organs.

I.c.v. diazoxide administration in postabsorptive, diet-induced obese mice

In high-fat fed mice we assessed the effects of i.c.v. diazoxide, a K_{ATP} channel activator, on insulin-stimulated muscle glucose uptake (Table 5). There were no differences observed in body weight and plasma glucose between i.c.v. diazoxide and vehicle treated animals. The GIR necessary to maintain euglycemia, glucose disposal and 2-[³H]DG uptake by muscle was not different between i.c.v. diazoxide and vehicle treated animals.
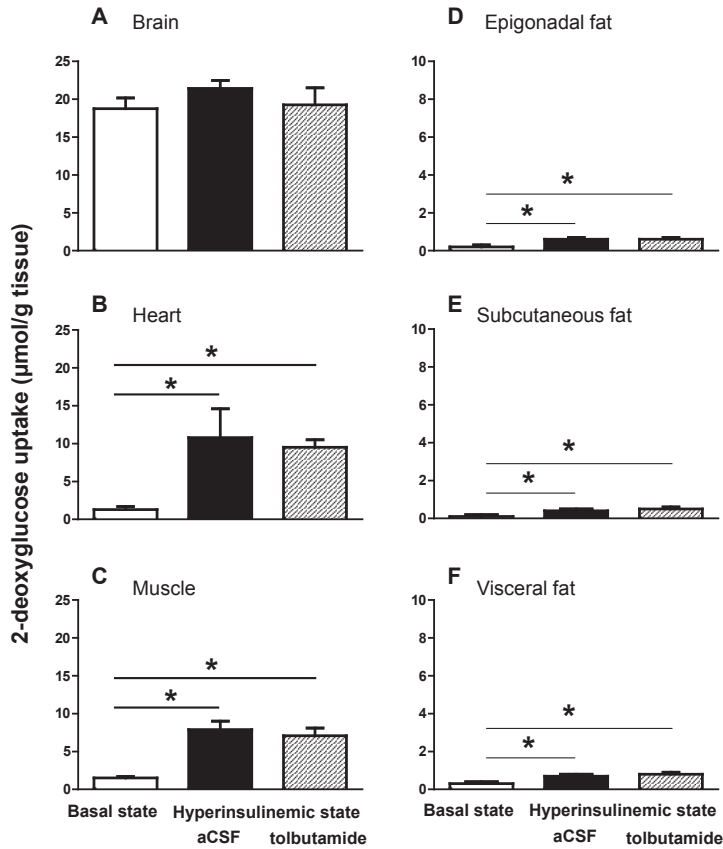
Fig. 9. Tissue-specific glucose uptake in basal state (white bars) or hyperinsulinemic-euglycemic state (black and hatched bars) in diet-induced obese mice. Throughout the experiment, mice received i.c.v. infusion of vehicle (white and black bars) or tolbutamide (hatched bars). Values represent means ± SEM for at least 7 mice per group. *$P < 0.05$ basal *vs*. hyperinsulinemic state.

Table 5. Plasma parameters of high-fat fed mice, in hyperinsulinemic-euglycemic state. Throughout the experiments, mice received i.c.v. infusion of vehicle or diazoxide. Values are means ± SEM for at least 5 mice per group.

	Hyperinsulinemic state	
	vehicle	**diazoxide**
Body weight (g)	31.3 ± 1.7	30.8 ± 0.3
Glucose (mmol/l)	5.6 ± 0.2	5.2 ± 0.4
GIR (µmol/min/kg)	52.4 ± 4.8	54.3 ± 4.6
Glucose disposal (µmol/min/kg)	52.7 ± 4.3	52.1 ± 5.0
Muscle glucose uptake (µmol/g tissue)	7.7 ± 0.7	7.8 ± 0.5

Fig. 10. Phosphorylation state of AMPK in basal state (white bars) or hyperinsulinemic-euglycemic state (black bars) in muscle of chow fed mice receiving i.c.v. infusion of vehicle or tolbutamide. The corresponding quantification of the western blot data was normalized for total protein and expressed as fold change compared to basal state. Values represent means ± SEM for 5 mice per group. * *P* < 0.05 *vs.* vehicle.
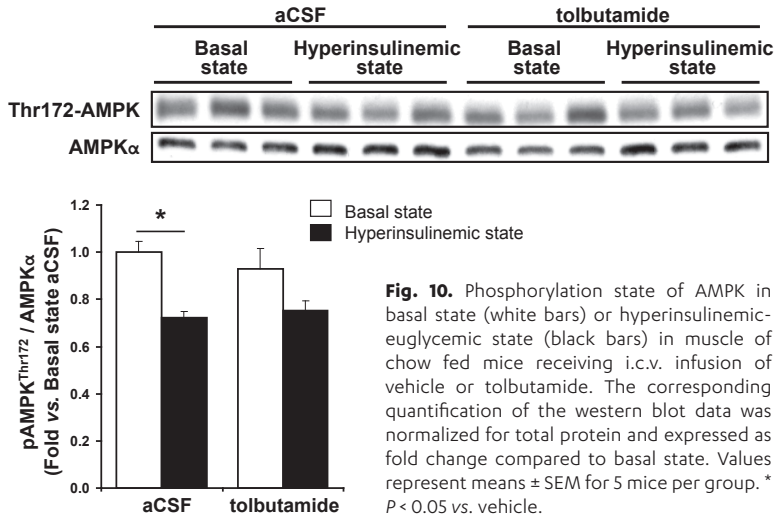
DISCUSSION

This study addressed the effect of central antagonism of insulin signaling on tissue-specific glucose uptake in normal weight and diet-induced obese mice. Inhibition of the central action of insulin by i.c.v. tolbutamide, a K_{ATP} channel blocker, decreased the inhibitory effects of insulin on EGP as well as the insulin-stimulated muscle glucose uptake in chow fed mice. In contrast, in diet-induced obese mice, the effects of insulin on EGP and muscle glucose uptake were not affected by i.c.v. tolbutamide. Collectively, these data indicate that the central effects of insulin are not only required for inhibition of EGP, but also for muscle glucose uptake. In addition, these data indicate that these central effects of insulin on EGP and muscle glucose uptake are absent after 12 weeks of high-fat feeding.

We assessed insulin-mediated effects on EGP and glucose disposal by hyperinsulinemic-euglycemic clamp studies designed to increase plasma insulin concentrations by approximately five-fold above basal levels. This increase resulted in complete inhibition of EGP and a four-fold stimulation of glucose disposal. In complete accordance with the results of Obici *et al*. (7), i.c.v. tolbutamide blunted the effect of hyperinsulinemia on EGP by ~20%. Therefore, this observation confirms that insulin inhibits EGP in part via its action in the CNS. In addition, our results indicate that the central effects of insulin contribute to the stimulatory effects of insulin on muscle glucose uptake, since this effect of insulin was in part inhibited (~59%) by i.c.v. tolbutamide. This inhibition of muscle glucose uptake coincided with a trend in decreased whole body glucose disposal (~20%, *P* = 0.07), which did not reach statistical significance probably due to the limited size of the mouse groups.

The present study indicates that i.c.v. tolbutamide decreased insulin-stimulated muscle glucose uptake in chow fed mice, not by decreasing insulin signaling in skeletal muscle as phosphorylation of PKB and PRAS40 were unaffected by i.c.v. tolbutamide, but, through other, indirect, effects of insulin exerted via the CNS. A role of central insulin signaling in

muscle glucose uptake has been suggested in a previous study on cerebral control of muscle glucose uptake (19). In that study, i.c.v. insulin increased glucose storage in muscle as glycogen. Together with the results obtained in our study, a concept emerges of an insulin-dependent central pathway targeted at skeletal muscle. I.c.v. NPY or AgRP did not stimulate muscle glucose uptake (20). Chronic (7-day) i.c.v. infusion of a-MSH, a POMC derivative, enhanced insulin-stimulated peripheral glucose uptake, although this effect could not be reproduced in an acute setting (21;22). However, i.c.v. infusion of melanotan II, a MC3/4 agonist, enhanced insulin-stimulated muscle glucose uptake (23;24). Therefore, we hypothesize that POMC/CART neurons are potential mediators of the central effect of insulin on muscle glucose uptake.

Previous studies focusing on the role of central K_{ATP} channels in glucose metabolism could not show an effect on glucose disposal (7;11). There are some methodological differences between the studies, including insulin levels and duration of fasting. In previous experiments, we carefully characterized insulin dose-response characteristics on EGP *vs*. glucose disposal in C57Bl/6J mice (14). The data obtained in this dose-finding study indicate that increased insulin levels up to three times the basal levels inhibit EGP, but do not stimulate glucose disposal. Therefore, in the current study we aimed at five-fold increased insulin levels during the clamp as compared to the basal levels, compared to two- to three-fold levels in previous studies (6;11). Using these insulin levels, we were not only capable in reproducing the central effects of insulin on EGP as reported by Obici *et al.*, but in addition to document central effects of insulin on muscle glucose uptake. Therefore, we speculate that the discrepancy in the effects of central K_{ATP} channel modulation on insulin-mediated glucose uptake during hyperinsulinemia between our study and previous studies is explained by the higher insulin levels in our study. Furthermore, Obici *et al*. (7) studied rats fasted for 6 hours and did not find an inhibition of glucose disposal rate by i.c.v. administration of tolbutamide, in contrast to our observations in overnight fasted mice. In a previous study, we documented that 16 h of (overnight) fasting increases muscle insulin sensitivity compared to a shorter duration of fasting (25). Therefore, differences between the duration of fasting may be involved to explain the differential effects of i.c.v. tolbutamide on insulin-stimulated glucose uptake between both studies. Nonetheless, this does not invalidate our conclusions, since the duration of fast was identical in all experiments of our study.

Glucose utilization in skeletal muscle can be stimulated by sympathetic nervous system (SNS) activation and i.c.v. insulin in rats increases SNS activity to the hindlimb (26). Therefore, the observed effect on insulin-mediated glucose uptake in muscle following central K_{ATP} channel inhibition could be the result of reduced insulin-induced activation of the SNS towards muscle. Since the stimulation of muscle glucose uptake by α-adrenergic stimulation involves 5'-AMP-activated protein kinase (AMPK), we measured AMPKα phosphorylation in muscle (27). However, i.c.v. infusion of insulin or K_{ATP} channel inhibition under hyperinsulinemic conditions did not affect activity of AMPK in muscle (Fig. 10). Apparently, the stimulation of muscle glucose uptake by central insulin effects is independent of AMPK activation in muscle. At present, the involvement of autonomic pathways in mediating the central effects of insulin on muscle glucose uptake remains unclear.

Insulin stimulated glucose uptake in heart and WAT. Interestingly, this effect of insulin was greater in visceral fat compared to the other fat compartments, in accordance with previous observations (28-30). The insulin-stimulated glucose uptake by heart and WAT was independent

of central K_{ATP} channel activation, since i.c.v. tolbutamide did not affect tissue-specific glucose uptake in these tissues.

We also assessed the effects of high-fat diet on the central effects of insulin on EGP and tissue-specific glucose uptake. The study was designed for the mice to develop obesity in combination with partial, rather than complete, insulin resistance, and, as a result, effects of central insulin antagonism in these diet-induced obese mice could still be obtained. Indeed, the high-fat diet caused partial insulin resistance, since insulin was still able, although to a lesser extent, to inhibit EGP and stimulate glucose disposal. The high-fat diet abolished the inhibitory effect of i.c.v. tolbutamide on insulin-mediated inhibition of EGP. Furthermore, the inhibitory effect of i.c.v administration of tolbutamide on insulin-stimulated glucose uptake by skeletal muscle was abolished. Our *in vivo* observations in diet-induced obese mice extend the *in vitro* observations by Spanswick *et al.*, showing that physiological levels of insulin activate K_{ATP} channels in glucose responsive neurons of lean, but not of obese rats, suggesting that K_{ATP} channels are already inhibited in the insulin resistant state (10;31-33). Moreover, stimulation of K_{ATP} channels by i.c.v. diazoxide did not improve muscle glucose uptake under hyperinsulinemic-euglycemic clamp conditions in diet-induced obese insulin resistant mice. The absence of effects of i.c.v. tolbutamide in diet-induced obese mice might also involve reduced insulin transport across the blood brain barrier (34). Although the precise mechanism remains to be elucidated, the present study indicates that high-fat diet decreases the central effects of insulin on both EGP and muscle glucose uptake, which may contribute to the pathophysiology of diet-induced insulin resistance. High-fat feeding strongly reduced insulin-stimulated glucose disposal, indicating peripheral insulin resistance. Interestingly, in quantitative terms, insulin-stimulated muscle glucose uptake in chow fed conditions during i.c.v. tolbutamide infusion, was not different from muscle glucose uptake during high-fat conditions (5.2 ± 0.6 *vs*. 7.1 ± 1.0 μmol/g tissue, ns). This remarkable observation indicates that muscle-specific insulin resistance was present for the centrally mediated effects of insulin, rather than for the direct effects of insulin on muscle, at least within the constraints of our high-fat diet mouse model.

Recently, methodological issues have been raised concerning the application of the hyperinsulinemic-euglycemic clamp method in mice (35). To support the validity of our experimental procedures, we documented that we reached steady-state conditions with respect to GIR, plasma glucose concentrations and isotopes, the latter enabling reliable calculations using steady-state comparisons. Another issue that has been raised is that the mice may be subject to serious hemodilution during the clamps. Our data indicate that hemodilation hardly occurred at the end of the clamps in our mice as hematocrit levels remained similar. Furthermore, our clamp procedure was performed in anesthetized mice. However, since all groups received identical sedation, the differences between groups cannot be related to sedation.

Recently, we also documented central effects of insulin on FA uptake (12). Those studies show that i.c.v. tolbutamide administration in hyperinsulinemic-euglycemic clamp conditions, identical to the current conditions, decreases insulin-stimulated retention of FA specifically in WAT. Therefore, the notion emerges that regulation of FA and glucose uptake by modulation of central insulin signaling is tissue-specific. In addition, both

studies indicate that these effects are mediated, at least in part, via K_{ATP} channel activation in the CNS and are absent after high-fat feeding.

We conclude that insulin signaling in the brain not only substantially contributes to the inhibitory effect of insulin on glucose production, but also to the insulin-stimulated glucose uptake by muscle. In diet-induced obese mice, these central effects of insulin on glucose homeostasis are lost. These observations stress the role of central insulin signaling in normal physiological conditions and central insulin resistance in the pathophysiology of diet-induced insulin resistance.

ACKNOWLEDGEMENTS

REFERENCE LIST

1. DeFronzo, RA, Simonson, D, Ferrannini, E: Hepatic and peripheral insulin resistance: a common feature of type 2 (non-insulin-dependent) and type 1 (insulin-dependent) diabetes mellitus. *Diabetologia* 23:313-319, 1982

2. Hollenbeck, CB, Chen, YD, Reaven, GM: A comparison of the relative effects of obesity and non-insulin-dependent diabetes mellitus on in vivo insulin-stimulated glucose utilization. *Diabetes* 33:622-626, 1984

3. Obici, S, Feng, Z, Karkanias, G, Baskin, DG, Rossetti, L: Decreasing hypothalamic insulin receptors causes hyperphagia and insulin resistance in rats. *Nat Neurosci* 5:566-572, 2002

4. Schwartz, MW, Sipols, AJ, Marks, JL, Sanacora, G, White, JD, Scheurink, A, Kahn, SE, Baskin, DG, Woods, SC, Figlewicz, DP: Inhibition of hypothalamic neuropeptide Y gene expression by insulin. *Endocrinology* 130:3608-3616, 1992

5. Schwartz, MW, Woods, SC, Seeley, RJ, Barsh, GS, Baskin, DG, Leibel, RL: Is the energy homeostasis system inherently biased toward weight gain? *Diabetes* 52:232-238, 2003

6. Fisher, SJ, Bruning, JC, Lannon, S, Kahn, CR: Insulin signaling in the central nervous system is critical for the normal sympathoadrenal response to hypoglycemia. *Diabetes* 54:1447-1451, 2005

7. Obici, S, Zhang, BB, Karkanias, G, Rossetti, L: Hypothalamic insulin signaling is required for inhibition of glucose production. *Nat Med* 8:1376-1382, 2002

8. Okamoto, H, Obici, S, Accili, D, Rossetti, L: Restoration of liver insulin signaling in Insr knockout mice fails to normalize hepatic insulin action. *J Clin Invest* 115:1314-1322, 2005

9. Karschin, C, Ecke, C, Ashcroft, FM, Karschin, A: Overlapping distribution of K(ATP) channel-forming Kir6.2 subunit and the sulfonylurea receptor SUR1 in rodent brain. *FEBS Lett* 401:59-64, 1997

10. Spanswick, D, Smith, MA, Mirshamsi, S, Routh, VH, Ashford, ML: Insulin activates ATP-sensitive K+ channels in hypothalamic neurons of lean, but not obese rats. *Nat Neurosci* 3:757-758, 2000

11. Pocai, A, Lam, TK, Gutierrez-Juarez, R, Obici, S, Schwartz, GJ, Bryan, J, guilar-Bryan, L, Rossetti, L: Hypothalamic K(ATP) channels control hepatic glucose production. *Nature* 434:1026-1031, 2005

12. Coomans, CP, Geerling, JJ, Guigas, B, van den Hoek, AM, Parlevliet, ET, Ouwens, DM, Pijl, H, Voshol, PJ, Rensen, PC, Havekes, LM, Romijn, JA: Circulating insulin stimulates fatty acid retention in white adipose tissue via K_{ATP} channel activation in the central nervous system only in insulin-sensitive mice. *J Lipid Res* 2011

13. van den Hoek, AM, Voshol, PJ, Karnekamp, BN, Buijs, RM, Romijn, JA, Havekes, LM, Pijl,

H: Intracerebroventricular neuropeptide Y infusion precludes inhibition of glucose and VLDL production by insulin. *Diabetes* 53:2529-2534, 2004

14. Plum, L: Enhanced PIP3 signaling in POMC neurons causes K_{ATP} channel activation and leads to diet-sensitive obesity. 2006

15. den Boer, MA, Voshol, PJ, Kuipers, F, Romijn, JA, Havekes, LM: Hepatic glucose production is more sensitive to insulin-mediated inhibition than hepatic VLDL-triglyceride production. *Am J Physiol Endocrinol Metab* 291:E1360-E1364, 2006

16. Parlevliet, ET, Schroder-van der Elst JP, Corssmit, EP, Picha, K, O'Neil, K, Stojanovic-Susulic, V, Ort, T, Havekes, LM, Romijn, JA, Pijl, H: CNTO736, a novel glucagon-like peptide-1 receptor agonist, ameliorates insulin resistance and inhibits very low-density lipoprotein production in high-fat-fed mice. *J Pharmacol Exp Ther* 328:240-248, 2009

17. Rossetti, L, Giaccari, A: Relative contribution of glycogen synthesis and glycolysis to insulin-mediated glucose uptake. A dose-response euglycemic clamp study in normal and diabetic rats. *J Clin Invest* 85:1785-1792, 1990

18. van den Hoek, AM, Teusink, B, Voshol, PJ, Havekes, LM, Romijn, JA, Pijl, H: Leptin deficiency per se dictates body composition and insulin action in ob/ob mice. *J Neuroendocrinol* 20:120-127, 2008

19. Perrin, C, Knauf, C, Burcelin, R: Intracerebroventricular infusion of glucose, insulin, and the adenosine monophosphate-activated kinase activator, 5-aminoimidazole-4-carboxamide-1-beta-D-ribofuranoside, controls muscle glycogen synthesis. *Endocrinology* 145:4025-4033, 2004

20. Shiuchi, T, Haque, MS, Okamoto, S, Inoue, T, Kageyama, H, Lee, S, Toda, C, Suzuki, A, Bachman, ES, Kim, YB, Sakurai, T, Yanagisawa, M, Shioda, S, Imoto, K, Minokoshi, Y: Hypothalamic orexin stimulates feeding-associated glucose utilization in skeletal muscle via sympathetic nervous system. *Cell Metab* 10:466-480, 2009

21. Gutierrez-Juarez, R, Obici, S, Rossetti, L: Melanocortin-independent effects of leptin on hepatic glucose fluxes. *J Biol Chem* 279:49704-49715, 2004

22. Obici, S, Feng, Z, Tan, J, Liu, L, Karkanias, G, Rossetti, L: Central melanocortin receptors regulate insulin action. *J Clin Invest* 108:1079-1085, 2001

23. Heijboer, AC, van den Hoek, AM, Pijl, H, Voshol, PJ, Havekes, LM, Romijn, JA, Corssmit, EP: Intracerebroventricular administration of melanotan II increases insulin sensitivity of glucose disposal in mice. *Diabetologia* 48:1621-1626, 2005

24. Toda, C, Shiuchi, T, Lee, S, Yamato-Esaki, M, Fujino, Y, Suzuki, A, Okamoto, S, Minokoshi, Y: Distinct effects of leptin and a melanocortin receptor agonist injected into medial hypothalamic nuclei on glucose uptake in peripheral tissues. *Diabetes* 58:2757-2765, 2009

25. Heijboer, AC: Sixteen hours of fasting differentially affects hepatic and muscle insulin sensitivity in mice. 2005

26. Rahmouni, K, Morgan, DA, Morgan, GM, Liu, X, Sigmund, CD, Mark, AL, Haynes, WG: Hypothalamic PI3K and MAPK differentially mediate regional sympathetic activation to insulin. *J Clin Invest* 114:652-658, 2004

27. Minokoshi, Y, Kim, YB, Peroni, OD, Fryer, LG, Muller, C, Carling, D, Kahn, BB: Leptin stimulates fatty-acid oxidation by activating AMP-activated protein kinase. *Nature* 415:339-343, 2002

28. Clegg, DJ, Brown, LM, Woods, SC, Benoit, SC: Gonadal hormones determine sensitivity to central leptin and insulin. *Diabetes* 55:978-987, 2006

29. Virtanen, KA, Lonnroth, P, Parkkola, R, Peltoniemi, P, Asola, M, Viljanen, T, Tolvanen, T, Knuuti, J, Ronnemaa, T, Huupponen, R, Nuutila, P: Glucose uptake and perfusion in subcutaneous and visceral adipose tissue during insulin stimulation in nonobese and obese humans. *J Clin Endocrinol Metab* 87:3902-3910, 2002

30. Woods, SC, Gotoh, K, Clegg, DJ: Gender differences in the control of energy homeostasis. *Exp Biol Med (Maywood)* 228:1175-1180, 2003

31. Arase, K, Fisler, JS, Shargill, NS, York, DA, Bray, GA: Intracerebroventricular infusions of 3-OHB and insulin in a rat model of dietary obesity. *Am J Physiol* 255:R974-R981, 1988

32. Ono, H, Pocai, A, Wang, Y, Sakoda, H, Asano, T, Backer, JM, Schwartz, GJ, Rossetti, L: Activation of hypothalamic S6 kinase mediates diet-induced hepatic insulin resistance in rats. *J Clin Invest* 118:2959-2968, 2008

33. Woods, SC, D'Alessio, DA, Tso, P, Rushing, PA, Clegg, DJ, Benoit, SC, Gotoh, K, Liu, M, Seeley, RJ: Consumption of a high-fat diet alters the homeostatic regulation of energy balance. *Physiol Behav* 83:573-578, 2004

34. Kaiyala, KJ, Prigeon, RL, Kahn, SE, Woods, SC, Schwartz, MW: Obesity induced by a high-fat diet is associated with reduced brain insulin transport in dogs. *Diabetes* 49:1525-1533, 2000

35. Wasserman, DH, Ayala, JE, McGuinness, OP: Lost in translation. *Diabetes* 58:1947-1950, 2009

THE INSULIN SENSITIZING EFFECT OF TOPIRAMATE INVOLVES K_{ATP} CHANNEL ACTIVATION IN THE CENTRAL NERVOUS SYSTEM

Claudia P. Coomans
Janine J. Geerling
Sjoerd A. A. van den Berg
Hester C. van Diepen
Janny P. Schröder-van der Elst
D. Margriet Ouwens
Hanno Pijl
Patrick C.N. Rensen
Louis M. Havekes
Bruno Guigas
Johannes A. Romijn

5

ABSTRACT

Topiramate is associated with improvement in insulin sensitivity, in addition to its antiepileptic action. However, the mechanism underlying this insulin-sensitizing effect of topiramate is unknown. In the present study, we investigated the insulin-sensitizing effects of topiramate and the underlying mechanism both *in vivo* and *in vitro*.

Male C57Bl/6J mice were fed a run-in high-fat diet for 6 weeks, before receiving topiramate or vehicle mixed in high-fat diet for 6 weeks. In basal and hyperinsulinemic-euglycemic clamp conditions, whole body glucose kinetics was measured using D-[^{14}C]glucose and tissue-specific glucose uptake using 2-deoxy-D-[^{3}H]glucose. In addition, we determined the extent to which these effects of topiramate were mediated through the central nervous system by concomitant infusion of vehicle *vs.* tolbutamide, an inhibitor of ATP-sensitive potassium channels in neurons, into the lateral ventricle. *In vitro*, we examined the direct effects of topiramate on glucose uptake and insulin signaling in C2C12 muscle cells.

Therapeutic concentrations of topiramate (~4 µg/ml) improved insulin sensitivity (glucose infusion rate +58%), which was the result of improved insulin-mediated glucose uptake by heart (+92%), muscle (+116%) and adipose tissue (+586%). Upon infusion of tolbutamide this insulin-sensitizing effect of topiramate was completely abrogated in hyperinsulinemic-euglycemic clamp conditions. Topiramate did not alter glucose uptake or insulin signaling in normal and insulin-resistant C2C12 muscle cells.

Topiramate stimulates insulin-mediated glucose uptake *in vivo* through the central nervous system. These observations illustrate the possibility of pharmacological modulation of peripheral insulin resistance through a target in the central nervous system.

INTRODUCTION

Type 2 diabetes mellitus (T2DM) is a syndrome characterized by impaired insulin secretion in relation to decreased insulin sensitivity. Many drugs have been developed that act on these pathophysiological mechanisms. In recent years, evidence has accumulated that the central nervous system is also involved in the pathophysiology of T2DM. Experimental models have indicated that insulin-mediated effects on different organs are mediated in part through the central nervous system (1-4). Importantly, in insulin resistant conditions these effects of circulating insulin through the central nervous system are lost (1;4). The question arises whether the loss of these effects of insulin, mediated by the central nervous system, are amendable to pharmacological intervention.

Topiramate, a sulfamate-substituted derivative of the monosaccharide D-fructose (5), is used as an antiepileptic drug (6;7). The antiepileptic effects of topiramate are mediated through at least six mechanisms of action within the central nervous system (8-14). Studies in obese, diabetic rats demonstrated that topiramate treatment reduced plasma glucose levels and improved insulin sensitivity independently of weight loss (15;16). However, the mechanism underlying this pharmacological, insulin-sensitizing effect of topiramate is unknown.

We hypothesized that topiramate improves insulin sensitivity not by a direct effect on peripheral organs, but rather through effects within the central nervous system. Therefore, we studied in high-fat fed mice the effects of i.c.v. administered vehicle *vs.* tolbutamide on top of the effects of topiramate on tissue-specific insulin-mediated glucose uptake. Tolbutamide is an inhibitor of ATP-sensitive potassium (K_{ATP}) channels in neurons and i.c.v. administration of tolbutamide blocks the action of circulating insulin in the brain (1;3;4). In addition, we assessed the effects of topiramate in C2C12 muscle cells in order to evaluate the possibility of direct effects of topiramate on insulin signaling and glucose uptake. In this study we show that topiramate improves peripheral insulin sensitivity at least in part by improving insulin sensitivity in the brain.

MATERIALS AND METHODS

Animals

Male C57Bl/6J mice obtained from Charles River Laboratories at an age of 8 weeks were housed in a temperature-controlled room on a 12 h light-dark cycle. From the age of 12 weeks, mice were fed *ad libitum* a run-in high-fat diet for 6 weeks (45 energy% of fat derived from lard; Research Diets Inc, New Brunswick, US), which has previously been shown to induce insulin resistance (17). Subsequently, the animals were randomized according to body weight and fasting plasma glucose levels and were fed *ad libitum* for 6 weeks a high-fat diet containing 3.33% anise (anise cubes, De Ruijter, The Netherlands) with or without 0.12% (w/w) topiramate (Abbott Products GmbH, Hannover, Germany). The mice had free access to water throughout the experiment. Food intake and body weight were measured regularly throughout the experiment. All animal experiments were performed in accordance with the regulations of Dutch law on animal welfare and the institutional ethics committee for animal procedures from the Leiden University Medical Center, Leiden, The Netherlands approved the protocol.

I.c.v. cannula implantation

For i.c.v. cannula implantation, 15-week-old male mice were anaesthetized with 0.5 mg/kg Medetomidine (Pfizer, Capelle a/d IJssel, The Netherlands), 5 mg/kg Midazolam (Roche, Mijdrecht, The Netherlands) and 0.05 mg/kg Fentanyl (Janssen-Cilag, Tilburg, The Netherlands) and placed in a stereotactic device (TSE systems, Homburg, Germany). A 25 gauge guide cannula was implanted into the left lateral ventricle using the following coordinates from Bregma: 1.0 mm lateral, 0.46 mm posterior and 2.2 mm ventral. The guide cannula was secured to the skull surface with dental cement (GC Europe N.V., Leuven, Belgium) and the anesthesia was antagonized using 2.5 mg/kg Antipamezol (Pfizer, Capelle a/d IJssel, The Netherlands), 0.5 mg/kg Flumazenil (Roche, Mijdrecht, The Netherlands) and 1.2 mg/kg Naloxon (Orpha, Purkersdorf, Austria). After a recovery period of 1 week, cannula placement was verified. Mice that ate >0.3 g in 1 h in response to i.c.v. injection of 5 µg NPY (Bachem, St. Helens, UK) in 1 µl of artificial cerebrospinal fluid (aCSF, Harvard Apparatus, Natick, MA, US) were considered to have the cannula correctly placed and were included in the study (1;18).

Hyperinsulinemic-euglycemic clamp studies

Overnight fasted, body weight-matched male mice were anaesthetized with 6.25 mg/kg Acepromazine (Alfasan, Woerden, The Netherlands), 6.25 mg/kg Midazolam (Roche, Mijdrecht, The Netherlands), and 0.31 mg/kg Fentanyl (Janssen-Cilag, Tilburg, The Netherlands). First, basal rates of glucose turnover were determined by administration of a primed continuous intravenous (i.v.) infusion of D-[1-^{14}C]glucose (0.3 µCi/kg/min; Amersham, Little Chalfont, UK) for 60 minutes. Subsequently, insulin (Actrapid, Novo Nordisk, Denmark) was administered i.v. by primed (4.1 mU), continuous (6.8 mU/h) infusion to attain steady-state hyperinsulinemia together with D-[1-^{14}C]glucose (0.3 µCi/kg/min; Amersham, Little Chalfont, UK) for 90 min. A variable i.v. infusion of a 12.5% D-glucose solution was used to maintain euglycemia as determined at 10-min intervals via tail bleeding (<3 µl, Accu-chek, Sensor Comfort; Roche Diagnostics, Mannheim, Germany). To assess insulin-mediated glucose uptake in individual tissues, 2-deoxy-D-[3-^{3}H]glucose (2-[^{3}H]DG; Amersham, Little Chalfont, UK) was administered as a bolus (1 µCi) 30 min before the end of both experiments. In the last 20 min of both experiments, blood samples were taken with intervals of 10 min. Subsequently, the mice were sacrificed and after perfusion, organs were harvested and snap-frozen in liquid nitrogen.

I.c.v. tolbutamide treatment during clamp

As of thirty minutes before the start of the hyperinsulinemic-euglycemic clamp, aCSF or the K_{ATP} channel blocker tolbutamide, dissolved in 5% DMSO to a final concentration of 4.8 mM in aCSF, was continuously infused i.c.v. at a rate of 2.5 µl/h (3;19).

Plasma analysis

Blood samples were taken from the tail tip into chilled paraoxon-coated capillaries to prevent *ex vivo* lipolysis. The tubes were placed on ice and centrifuged at 4°C. Plasma levels of glucose and free fatty acids (FFA) were determined using commercially available kits and standards according to the instructions of the manufacturer (Instruchemie, Delfzijl, The Netherlands) in 96-well plates (Greiner Bio-One, Alphen a/d Rijn, The Netherlands). Plasma insulin levels were

measured using a mouse-specific insulin ELISA kit (Crystal Chem Inc., Downers Grove, U.S.). Total plasma ^{14}C-glucose and ^{3}H-glucose were determined in supernatant of 7.5 µl plasma, after protein precipitation using 20% trichloroacetic acid and evaporation to eliminate tritiated water.

Tissue analysis

For determination of tissue 2-[^{3}H]DG uptake, homogenates of heart, skeletal muscle and adipose tissue were boiled, and the supernatants were subjected to an ion-exchange column (described previously (20-22)) to isolate 2-[^{3}H]DG-6-phosphate, a metabolic end-product of 2-[^{3}H]DG that accumulates in muscle and fat cells.

C2C12 cells

C2C12 skeletal muscle cells were cultured in a humidified atmosphere containing 5% CO_2 in Dulbecco's modified Eagle's Medium (DMEM) containing 25 mM glucose, glutamine and pyruvate (Invitrogen) supplemented with 10% fetal bovine serum (FBS) and 100 units/ml penicillin and 100 µg/ml streptomycin (Invitrogen). For deoxyglucose uptake assay ~15, 000 cells/well were seeded and cultured on 12-well plates (Greiner Bio-One). For Western blot analysis ~25, 000 cells/well were seeded and cultured on 6-well plates (Greiner Bio-One). When reaching confluence, the cells were differentiated into myotubes by replacing the complete growth medium with differentiation medium (same DMEM medium containing antibiotics, but supplemented with 2% horse serum (HS) instead of 10% FBS). The differentiation medium was changed every 48 h. The myotubes were used for experiments at day 7 of differentiation.

Palmitate-induced insulin resistance in C2C12 myotubes

Palmitate-containing medium was prepared to induce insulin resistance in C2C12 myotubes. DMEM basic medium was supplemented with antibiotics and 2% FFA-free bovine serum albumin (BSA). Palmitate was first dissolved in ethanol and then added to medium containing BSA at a final concentration of 0.75 mM. The final medium was sonicated for 5 min and warmed at 55°C for 10 min to allow complex formation between BSA and palmitate. Differentiated myotubes (day 6) were then treated with palmitate for 16 h before performing deoxyglucose uptake assay.

Deoxyglucose uptake assay in C2C12 myotubes

C2C12 myotubes were serum-starved for 4 h before the experiment. After serum starvation, cells were washed once with PBS and once with buffer (50 mM HEPES, 138 mM NaCl, 1.85 mM $CaCl_2$, 1.3 mM $MgSO_4$ and 4.8 mM KCl, pH 7.4) followed by incubation with the same buffer for 45 min at 37 °C in the presence of topiramate (1 or 100 µM) or vehicle. At the end of incubation, cells were challenged with or without 1 µM insulin (Sigma-Aldrich, St. Louis, Missouri, US) for 10 min in the presence of topiramate or vehicle. 2-Deoxy-D-[1-^{14}C] glucose was added to the cells for another 10 min (0.012 µCi/dish). The reaction was ended by washing three times with ice-cold PBS and addition of a lysis buffer containing 1% SDS/0.2 M NaOH. The lysates were transferred into plastic vials, 2 ml of scintillation liquid (Instagel Plus, PerkinElmer, Waltham, Massachusetts, US) was added and radioactivity was measured in a scintillation counter.

Western blot analysis

C2C12 myotubes were serum-starved for 4 h then washed once with PBS and once with 2DG buffer followed by incubation with the same buffer for 45 min at 37°C in the presence of topiramate (1 or 100 μM) or vehicle. At the end of incubation, cells were stimulated with 1 μM insulin. After 20 min, cells were rapidly washed one time with ice-cold PBS and lysed by addition of a buffer containing 12.5% glycerol, 3% SDS and 100 mM TrisPO4, pH 6.8. The cell lysates were then immediately boiled for 5 min and stored at -20°C until use. Protein content was determined using the bicinchoninic acid protein assay (Pierce, Rockford, Illinois, US). Proteins (10 μg) were separated by 10% SDS-PAGE followed by transfer to a PVDF transfer membrane. Membranes were blocked for 1 h at room temperature in Tris Buffer Saline Tween20 (TBST) buffer with 5% non-fat dry milk followed by an overnight incubation with phospho-Ser473-PKB antibody or a mix of PKBα and PKBβ antibodies (all from Cell Signaling Technology, Beverly, US). Blots were then incubated with HRP-conjugated secondary antibodies for 1 h at room temperature. Bands were visualized by enhanced chemiluminescence and quantified using Image J (NIH, US).

Calculations

Turnover rates of glucose (μmol/min/kg) were calculated in basal and hyperinsulinemic conditions as the rate of tracer infusion (dpm/min) divided by plasma specific activity of ^{14}C-glucose (dpm/μmol). The ratio was corrected for body weight. Endogenous glucose production was identical to the glucose appearance rate under basal conditions and calculated as the difference between the tracer-derived rate of glucose appearance and the glucose infusion rate under hyperinsulinemic-euglycemic clamp conditions.

Tissue-specific glucose uptake in heart, skeletal muscle and adipose tissue was calculated from tissue 2-[^{3}H]DG content, corrected for plasma specific activity and expressed as micromoles per gram of tissue.

Statistical analysis

Differences between groups were determined by Mann-Whitney nonparametric tests for two independent samples. The criterion for significance was set at $P < 0.05$. All values shown represent means ± SEM.

RESULTS

In vivo studies

After 6 weeks of run-in high-fat diet, mice were randomized on body weight (26.6 ± 0.5 *vs.* 26.7 ± 0.6 g) and fasting plasma glucose levels (4.2 ± 0.2 *vs.* 4.3 ± 0.2 mmol/l) and received high-fat diet containing topiramate or vehicle during 6 subsequent weeks. After 5 weeks of topiramate treatment, the topiramate concentration in plasma, determined by liquid chromatography tandem mass spectrometry assay as previously described (23), was 3.7 ± 0.2 μg/ml. After 6 weeks of topiramate treatment, the topiramate concentration in the brains of overnight fasted mice was 115 ± 18 ng/g brain tissue.

Effect of topiramate on insulin sensitivity in mice

After 6 weeks of topiramate treatment, insulin sensitivity was assessed using hyperinsulinemic-euglycemic clamp studies. Body weight did not differ between topiramate and vehicle treated mice (table 1). In the basal period of the hyperinsulinemic-euglycemic clamp, endogenous glucose production (EGP), which equals glucose disposal (Rd), was not different between topiramate and vehicle treated animals.

Table 1. Results obtained during the hyperinsulinemic-euglycemic clamp study in vehicle and topiramate treated animals. Data are represented as means ± SEM for at least 7 animals per group. There were no significant differences between any of the parameters.

	Vehicle	Topiramate
Body weight (g)	25.7 ± 0.4	24.9 ± 0.8
Basal hematocrit (%)	40.3 ± 0.2	38.5 ± 0.2
Clamp hematocrit (%)	36.8 ± 0.2	34.9 ± 0.5
Basal insulin (ng/ml)	0.5 ± 0.1	0.5 ± 0.1
Clamp insulin (ng/ml)	5.1 ± 0.4	4.3 ± 0.5
Basal glucose (mmol/l)	4.1 ± 0.1	4.2 ± 0.1
Clamp glucose (mmol/l)	4.5 ± 0.3	4.0 ± 0.2

The glucose infusion rate (GIR) necessary to maintain euglycemia was significantly higher in topiramate treated animals compared to vehicle treated animals (average GIR 84 ± 8 *vs.* 56 ± 4 µmol/min/kg for the last 20 min of the experiment, $P < 0.05$, Fig. 1A and Fig. 2B), in the presence of similar glucose levels (table 1 and Fig. 2A), indicating that topiramate improved insulin sensitivity. The specific activity of ^{14}C-glucose measured at 10 min intervals indicated the presence of steady-state conditions in all groups (table 2).

Table 2. Specific activity of ^{14}C-glucose (dpm/mmol) in the basal period or in the hyperinsulinemic euglycemic period in vehicle and topiramate treated animals. Values are means ± SEM for at least 7 mice per group. There were no significant differences between vehicle *vs.* topiramate treated animals.

	Basal period		Hyperinsulinemic euglycemic period		
	-10 min	0 min	70 min	80 min	90 min
Vehicle	$6.7 ± 0.6 \times 10^3$	$6.2 ± 0.6 \times 10^3$	$6.8 ± 0.4 \times 10^3$	$6.2 ± 0.5 \times 10^3$	$6.3 ± 0.4 \times 10^3$
Topiramate	$6.6 ± 0.5 \times 10^3$	$7.4 ± 0.6 \times 10^3$	$5.3 ± 0.3 \times 10^3$	$5.1 ± 0.2 \times 10^3$	$5.0 ± 0.3 \times 10^3$

In the hyperinsulinemic-euglycemic period, insulin inhibited EGP to the same extent in both groups of mice (92 ± 8 *vs.* 80 ± 7 %, ns, Fig. 1B). Insulin-mediated Rd, however, was increased in the topiramate treated group compared to the vehicle treated group (96 ± 16 *vs.* 47 ± 9 %, respectively, $P < 0.05$, Fig. 1C), indicating that topiramate treatment improved peripheral insulin

sensitivity. Assessment of tissue-specific 2-[³H]DG uptake revealed that topiramate treatment increased insulin-stimulated glucose uptake in heart, skeletal muscle and adipose tissue (gonadal fat pad) (Fig. 1D).
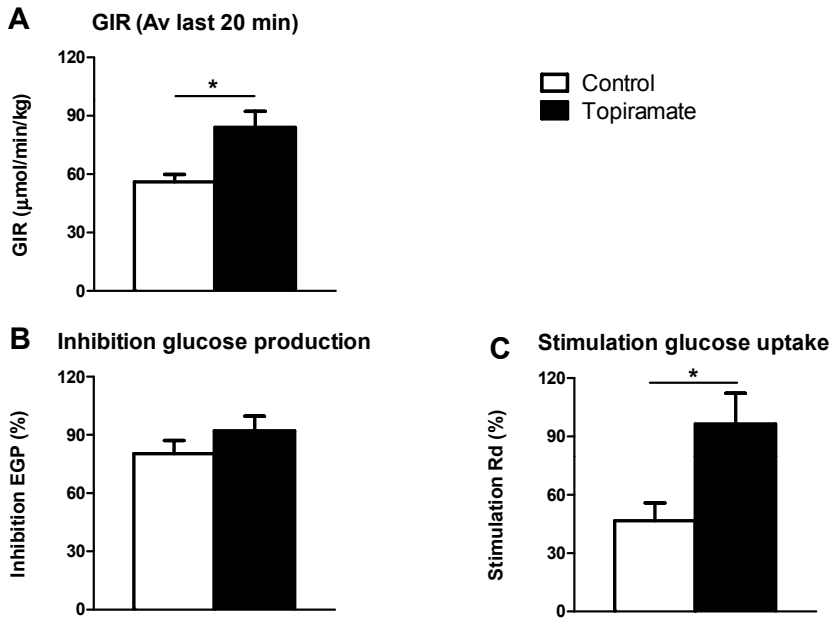
Fig. 1. Glucose infusion rate (GIR, A), endogenous glucose production (EGP, B), glucose disposal (Rd, C) in vehicle treated (white) and topiramate treated (black) animals as measured in hyperinsulinemic-euglycemic clamp studies. Values represent means ± SEM for at least 7 animals per group. *$P < 0.05$ *vs.* vehicle. Av, average.
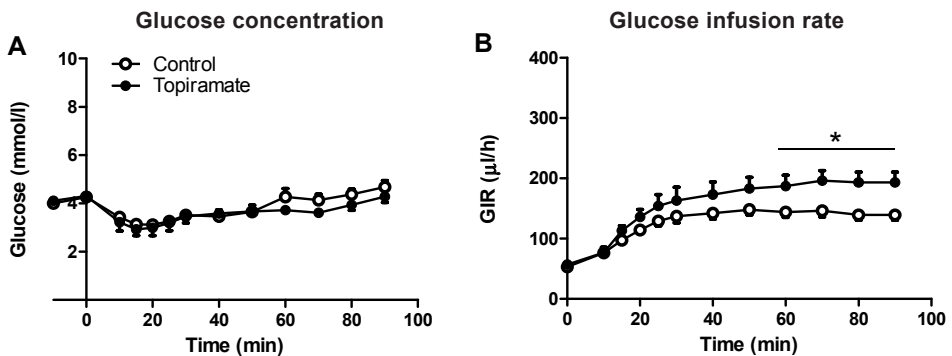
Fig. 2. Glucose concentrations (A) and glucose infusion rates (GIR, B) in vehicle treated (white) and topiramate treated (black) animals as measured in hyperinsulinemic-euglycemic clamp studies. Values represent means ± SEM for 7-10 mice per group. *$P < 0.05$, Topiramate *vs.* control.

Effect of i.c.v. administration of tolbutamide on the effects of topiramate on insulin sensitivity in mice

To determine whether topiramate improved peripheral insulin sensitivity by affecting insulin signaling in the brain, tolbutamide, an inhibitor of ATP-sensitive potassium (K_{ATP}) channels in neurons, or vehicle was infused into the lateral ventricle (i.c.v.) during hyperinsulinemic-euglycemic clamp experiments. In agreement with the first experiment, topiramate treated animals receiving vehicle (aCSF) had higher GIR compared to vehicle treated animals receiving aCSF (average GIR 85 ± 9 *vs.* 55 ± 11 µmol/min/kg for the last 20 min of the experiment, $P < 0.05$, Fig. 3A and Fig. 4B), in the presence of similar glucose levels (table 3 and Fig. 4A). I.c.v. tolbutamide administration in vehicle treated animals did not affect GIR compared to i.c.v. aCSF (66 ± 8 *vs.* 55 ± 11 µmol/min/kg for the last 20 min of the experiment, ns). I.c.v. administration of tolbutamide decreased GIR compared to topiramate treated animals receiving aCSF (average GIR 75 ± 7 *vs.* 85 ± 9 µmol/min/kg for the last 20 min of the experiment, $P < 0.05$), indicating that i.c.v. tolbutamide counteracted, at least in part, the improvement in insulin sensitivity induced

Fig. 3. Glucose infusion rate (GIR, A), endogenous glucose production (EGP, B), glucose disposal (Rd, C) and organ-specific glucose uptake (D) in vehicle treated (white) and topiramate treated animals (black) receiving i.c.v. vehicle (artificial cerebrospinal fluid, aCSF) or tolbutamide. Values represent means ± SEM for at least 7 animals per group. *$P < 0.05$ *vs.* vehicle. Av, average.

by topiramate. The specific activity of ^{14}C-glucose measured at 10 min intervals indicated the presence of steady-state conditions in all groups (table 4). In the basal period as well as in the hyperinsulinemic period, EGP was not different between all groups of mice (Fig. 3B). Insulin-stimulated Rd was again significantly higher in topiramate treated animals compared to vehicle treated animals receiving aCSF (101 ± 15 *vs.* 71 ± 12 %, respectively, *P* < 0.05, Fig. 3C). I.c.v. tolbutamide administration in vehicle treated animals did not affect Rd compared to i.c.v. aCSF (57 ± 16 *vs.* 71 ± 12 µmol/min/kg for the last 20 min of the experiment, ns). However, i.c.v. administration of tolbutamide in topiramate animals diminished the topiramate-improved Rd (81 ± 12 *vs.* 101 ± 15 %, respectively, *P* < 0.05). In accordance, topiramate treated animals had higher 2-[^{3}H]DG uptake in heart, skeletal muscle and adipose tissue compared to vehicle

Table 3. Results of i.c.v. administration of aCSF and tolbutamide obtained from the hyperinsulinemic-euglycemic clamp study in vehicle and topiramate treated animals. Data are represented as means ± SEM for at least 8 animals per group. There were no significant d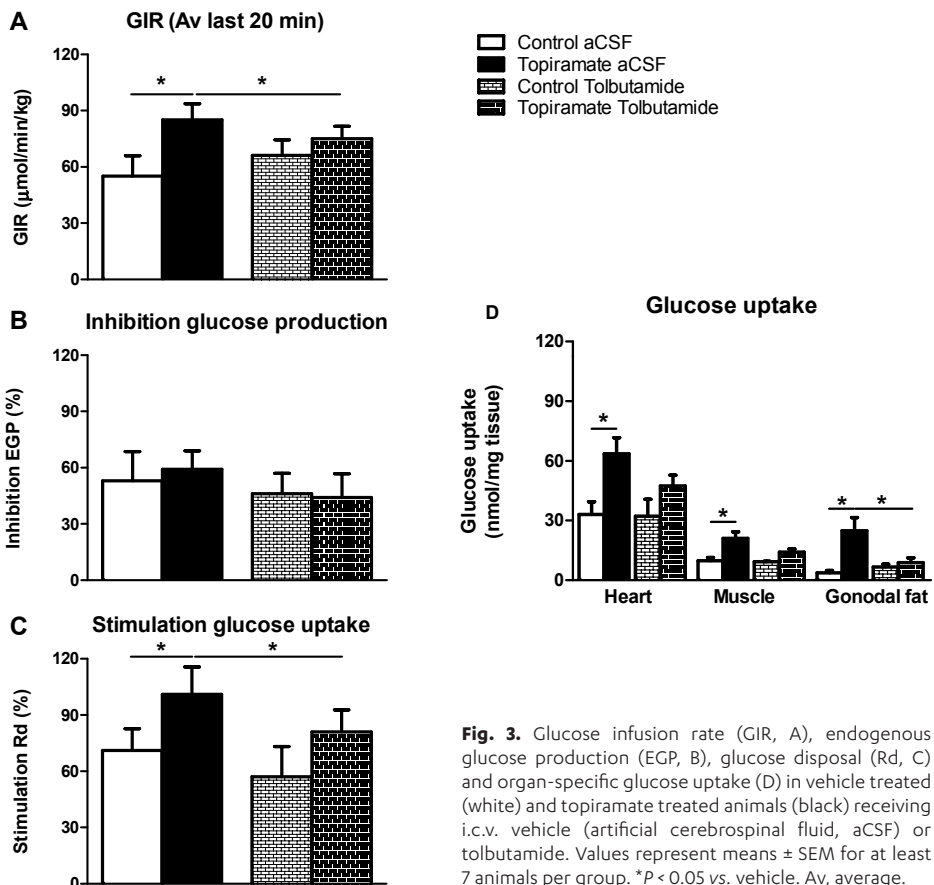ifferences between vehicle *vs.* topiramate treated animals. aCSF, artificial cerebrospinal fluid; FFA, free fatty acids.

	Vehicle		Topiramate	
	aCSF	Tolbutamide	aCSF	Tolbutamide
Body weight (g)	28.6 ± 0.7	28.7 ± 0.7	27.7 ± 0.5	27.8 ± 0.3
Basal hematocrit (%)	40.3 ± 0.2	39.0 ± 0.8	38.5 ± 0.2	37.1 ± 0.3
Clamp hematocrit (%)	36.8 ± 0.2	36.3 ± 0.2	34.9 ± 0.5	34.4 ± 0.4
Basal insulin (ng/ml)	0.6 ± 0.1	0.7 ± 0.1	0.6 ± 0.1	0.6 ± 0.1
Clamp insulin (ng/ml)	4.1 ± 0.4	3.3 ± 0.1	3.4 ± 0.2	3.8 ± 0.4
Basal glucose (mmol/l)	5.0 ± 0.2	5.4 ± 0.3	5.5 ± 0.2	4.9 ± 0.2
Clamp glucose (mmol/l)	5.6 ± 0.3	6.0 ± 0.5	5.8 ± 0.3	5.2 ± 0.3
Basal FFA (mmol/l)	0.7 ± 0.0	0.6 ± 0.1	0.6 ± 0.0	0.7 ± 0.0
Clamp FFA (mmol/l)	0.3 ± 0.0	0.3 ± 0.0	0.3 ± 0.0	0.3 ± 0.0
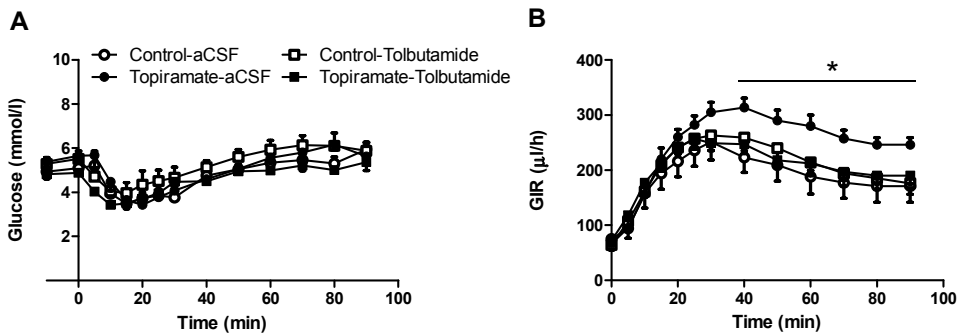
Fig. 4. Glucose concentrations (A) and glucose infusion rates (GIR, B) in vehicle treated (white) and topiramate treated animals (black) receiving i.c.v. vehicle (aCSF) or tolbutamide. Values represent means ± SEM for 7-10 mice per group. **P* < 0.05, Topiramate *vs.* other groups.

treated animals (Fig. 3D). In line with Rd, i.c.v. tolbutamide did not affect 2-[³H]DG uptake compared to i.c.v. aCSF in vehicle treated animals. I.c.v. tolbutamide in topiramate-treated animals abrogated the improvement in insulin-stimulated 2-[³H]DG uptake in heart, skeletal muscle and adipose tissue.

Table 4. Specific activity of ^{14}C-glucose (dpm/mmol) in the basal period or in the hyperinsulinemic euglycemic period in vehicle and topiramate treated animals. Values are means ± SEM for at least 7 mice per group. There were no significant differences between vehicle *vs.* topiramate treated animals.

	Basal period		Hyperinsulinemic euglycemic period		
	-10 min	**0 min**	**70 min**	**80 min**	**90 min**
Vehicle aCSF	$7.2 \pm 1.0 \times 10^3$	$7.7 \pm 0.7 \times 10^3$	$4.3 \pm 0.5 \times 10^3$	$4.4 \pm 0.4 \times 10^3$	$4.4 \pm 0.4 \times 10^3$
Topiramate aCSF	$5.8 \pm 0.5 \times 10^3$	$6.0 \pm 0.5 \times 10^3$	$3.3 \pm 0.2 \times 10^3$	$3.1 \pm 0.2 \times 10^3$	$3.2 \pm 0.3 \times 10^3$
Vehicle Tolbutamide	$6.7 \pm 0.9 \times 10^3$	$6.9 \pm 0.6 \times 10^3$	$3.5 \pm 0.3 \times 10^3$	$3.3 \pm 0.4 \times 10^3$	$3.8 \pm 0.3 \times 10^3$
Topiramate Tolbutamide	$7.9 \pm 1.0 \times 10^3$	$8.0 \pm 0.9 \times 10^3$	$3.9 \pm 0.2 \times 10^3$	$4.4 \pm 0.6 \times 10^3$	$3.9 \pm 0.3 \times 10^3$

In vitro studies

Effect of topiramate on glucose uptake in differentiated myotubes

To exclude that topiramate directly increased glucose uptake at the tissue level, we investigated the direct effects of topiramate on glucose uptake in differentiated C2C12 myotubes (Fig. 5A). Cells were treated with increasing concentrations of topiramate (1 or 100 µM) or vehicle for 45 min and glucose uptake was then measured during the last 20 min, after addition, or not, of 1 µM insulin. Insulin stimulated glucose uptake by about +25% in control condition, i.e. without topiramate. Topiramate did not increase basal or insulin-stimulated glucose uptake (Fig. 5A).

Effect of topiramate on insulin signaling in differentiated myotubes

Western blot analyses were performed to determine whether topiramate affects the insulin signaling pathway in differentiated myotubes by assessing the phosphorylation state of Akt/PKB (Fig. 5B). As expected, insulin increased the phosphorylation state of Akt/PKB on Ser[473] by +583% in control condition. Topiramate did not affect basal or insulin-stimulated phosphorylation of Akt/PKB (Fig. 5B).

Effect of topiramate on glucose uptake in insulin-resistant myotubes

Next, we investigated whether topiramate was able to reverse palmitate-induced insulin resistance in C2C12 myotubes (Fig. 6). After incubation with palmitate for 16 h, C2C12 myotubes were incubated with increasing concentrations of topiramate (1 or 100 µM) for 45 minutes and challenged with or without 1 µM of insulin for 20 min. At maximal concentration of insulin, glucose uptake was increased by +25% in control condition, i.e. without palmitate and topiramate (Fig. 6A). Preincubation with palmitate resulted in a decrease of insulin-stimulated glucose uptake. There was no effect of topiramate on basal or insulin-stimulated glucose uptake (Fig. 6B, C).
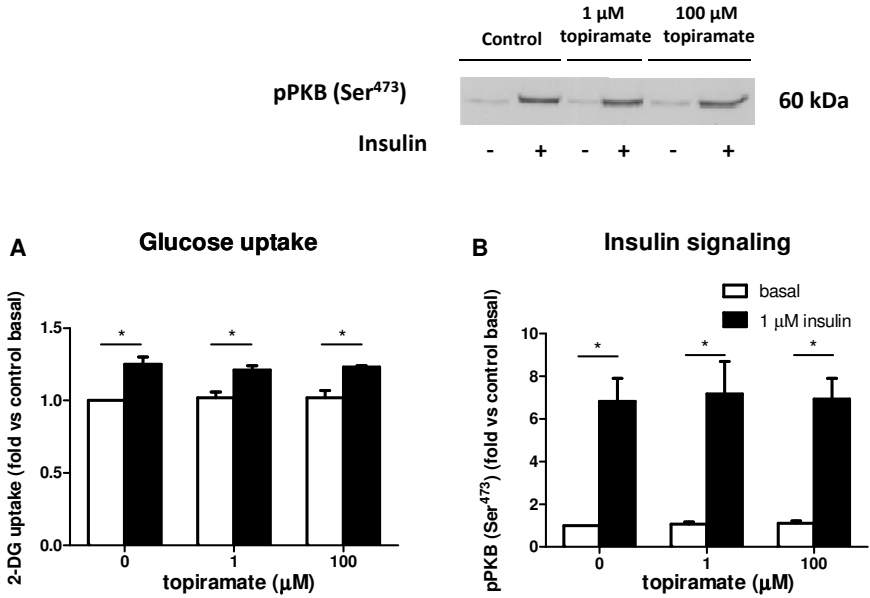
Fig. 5. Glucose uptake (A) and insulin signaling (B) in C2C12 myotubes at basal (white) or insulin-stimulated (black) condition with topiramate (1 or 100 μM) or vehicle. The quantification was normalized for total protein and expressed as fold change compared to vehicle at basal condition. Data are represented as means ± SEM for n=3-4, * $P < 0.05$ *vs.* vehicle.
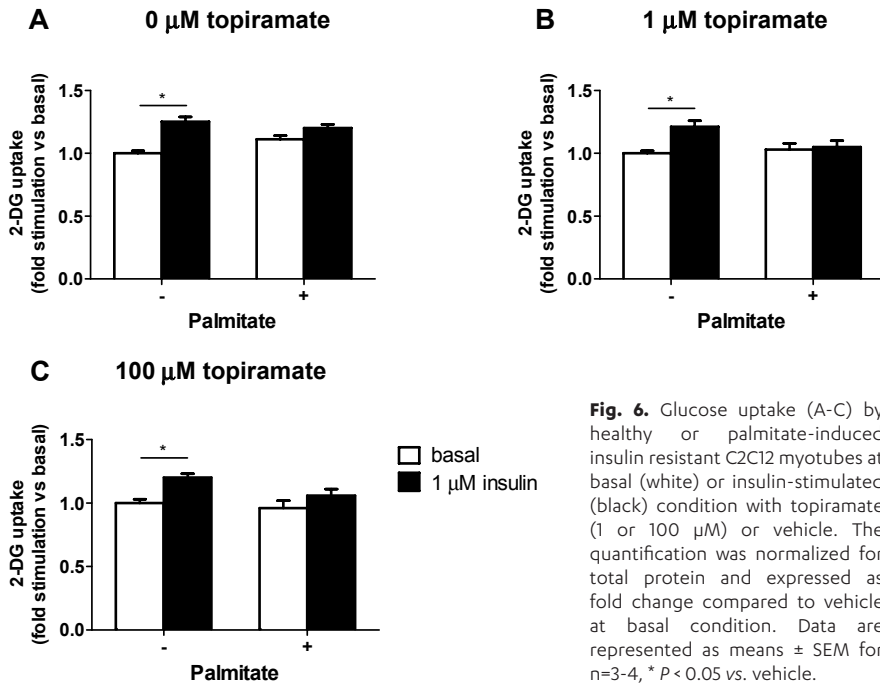
Fig. 6. Glucose uptake (A-C) by healthy or palmitate-induced insulin resistant C2C12 myotubes at basal (white) or insulin-stimulated (black) condition with topiramate (1 or 100 μM) or vehicle. The quantification was normalized for total protein and expressed as fold change compared to vehicle at basal condition. Data are represented as means ± SEM for n=3-4, * $P < 0.05$ *vs.* vehicle.

DISCUSSION

In the present study, topiramate improved insulin sensitivity by increasing glucose uptake by skeletal and cardiac muscle and by adipose tissue in high-fat fed mice. In addition, inhibition of the central action of circulating insulin by i.c.v. administration of tolbutamide, a K_{ATP} channel blocker in neurons, prevented this insulin-sensitizing effect of topiramate. *In vitro*, topiramate had no direct effect on basal or insulin-stimulated glucose uptake. Collectively, these data indicate that topiramate improves peripheral insulin sensitivity indirectly via the brain, rather than directly, in peripheral organs.

The mice were fed a high-fat diet for 6 weeks to reduce insulin sensitivity before topiramate treatment was started, as topiramate exerts its greatest effects in obese, insulin resistent subjects (24). The half-life of topiramate in humans is 21 h, whereas the half-life in rodents is only 1-2 h (25). To obtain stable concentrations of topiramate in plasma of our mice, topiramate was mixed through the diet with addition of 3.33% anise to cover bitter taste. The dose of topiramate used in the present study resulted in concentrations in plasma within the therapeutic range (~4 µg/ml). Hyperinsulinemic-euglycemic clamp analyses revealed that topiramate improved insulin sensitivity, in agreement with previous studies. Those studies indicated that topiramate improved insulin sensitivity independent of weight loss (16;26;27). In the present study, we extend these observations by showing that this insulin-sensitizing effect of topiramate was present in cardiac and skeletal muscle, as well as in adipose tissue. In contrast, topiramate did not improve hepatic insulin sensitivity. This improved insulin sensitivity in muscle and adipose tissue, but not in liver, has previously been associated with enhanced AMPK phosphorylation in muscle but not in liver (26). As α-adrenergic stimulation enhances AMPK phosphorylation, the increased glucose uptake by peripheral organs might be related to increased sympathetic nervous system (SNS) activation (28). Furthermore, the topiramate concentration in plasma correlates with that in cerebral spinal fluid (CSF) (29). Moreover, the effects of topiramate on body weight, body composition and energy metabolism have been associated with altered neuropeptide expression in the hypothalamus (30). Combined with the absence of direct effects of topiramate on insulin sensitivity in muscle cells, we therefore hypothesized that the brain mediated the effects of topiramate on insulin sensitivity.

The indirect effects of circulating insulin, through the central nervous system, on peripheral glucose uptake are blocked by i.c.v. administration of tolbutamide (1;3). Insulin activates ATP-sensitive potassium channels (K_{ATP} channels) in neurons of the hypothalamus (31;32). I.c.v. administration of tolbutamide inhibits activation of these neuronal K_{ATP} channels by insulin (1;3). To test our hypothesis that the central nervous system is involved in the anti-diabetic effects of topiramate by improving insulin signaling in the brain, we administered tolbutamide i.c.v. in topiramate-treated animals during hyperinsulinemic-euglycemic clamp conditions. Interestingly, i.c.v. administration of tolbutamide abolished the improvement of insulin sensitivity by topiramate during clamp conditions. In other words, the insulin-sensitizing effect of topiramate apparently originates from an insulin sensitization effect in the brain. In previous studies, we showed that high-fat feeding results in insulin resistance in the brain (1;4). In the present study, high-fat feeding resulted in similar central insulin resistance as these previous studies, since i.c.v. tolbutamide in vehicle treated animals had no effect on insulin-inhibited

glucose production or insulin-stimulated glucose uptake. I.c.v. tolbutamide in topiramate treated animals abolished the insulin-sensitizing effect of topiramate, suggesting that the brain mediates the effects of topiramate on insulin sensitivity.

Topiramate did not exert any direct effects on basal or insulin-stimulated glucose uptake and insulin signaling in insulin-sensitive or insulin-resistant C2C12 myotubes. Our data are in contrast to a previous study that reported that topiramate increases glucose uptake in cultured insulin-sensitive L6 cells, a rat skeletal muscle cell line, via an AMP-activated protein kinase (AMPK)-mediated pathway (33). Treatment of C2C12 myotubes with topiramate did not increase phosphorylation level of AMPK (Thr172) (data not shown). Stimulation of a rat insulinoma-derived INS-1E cell line with topiramate did not affect glucose-stimulated insulin secretion by these beta cells (data not shown), in line with a previous study (34). Our data support the notion that the effects of topiramate on insulin sensitivity are most likely not the result of direct effects on peripheral organs.

In conclusion, topiramate improves insulin sensitivity in high-fat fed mice by stimulating glucose uptake by skeletal muscle, heart and adipose tissue through effects within the central nervous system. Inhibition of K_{ATP} channel activation in the brain abrogates the insulin-sensitizing effect of topiramate in these mice. These observations indicate that the anti-diabetic effects of topiramate are the result of action in the brain, rather than direct effects of topiramate on peripheral organs. These observations illustrate the possibility of pharmacological treatment of peripheral insulin resistance through targets in the central nervous system.

ACKNOWLEDGEMENTS

REFERENCE LIST

1. Coomans, CP, Geerling, JJ, Guigas, B, van den Hoek, AM, Parlevliet, ET, Ouwens, DM, Pijl, H, Voshol, PJ, Rensen, PC, Havekes, LM, Romijn, JA: Circulating insulin stimulates fatty acid retention in white adipose tissue via K_{ATP} channel activation in the central nervous system only in insulin-sensitive mice. *J Lipid Res* 2011

2. Koch, L, Wunderlich, FT, Seibler, J, Konner, AC, Hampel, B, Irlenbusch, S, Brabant, G, Kahn, CR, Schwenk, F, Bruning, JC: Central insulin action regulates peripheral glucose and fat metabolism in mice. *J Clin Invest* 118:2132-2147, 2008

3. Obici, S, Zhang, BB, Karkanias, G, Rossetti, L: Hypothalamic insulin signaling is required for inhibition of glucose production. *Nat Med* 8:1376-1382, 2002

4. Coomans, CP, Biermasz, NR, Geerling, JJ, Guigas, B, Rensen, PC, Havekes, LM, Romijn, JA: Stimulatory Effect of Insulin on Glucose Uptake by Muscle Involves the Central Nervous System in Insulin-Sensitive Mice. *Diabetes* 2011

5. Shank, RP, Gardocki, JF, Streeter, AJ, Maryanoff, BE: An overview of the preclinical aspects of topiramate: pharmacology, pharmacokinetics, and mechanism of action. *Epilepsia* 41 Suppl 1:S3-S9, 2000

6. Ferrari, A, Tiraferri, I, Neri, L, Sternieri, E: Clinical pharmacology of topiramate in migraine prevention. *Expert Opin Drug Metab Toxicol* 7:1169-1181, 2011

7. McIntyre, RS, Riccardelli, R, Binder, C, Kusumakar, V: Open-label adjunctive topiramate in the treatment of unstable bipolar disorder. *Can J Psychiatry* 50:415-422, 2005

8. White, HS, Brown, SD, Woodhead, JH, Skeen, GA, Wolf, HH: Topiramate modulates GABA-evoked currents in murine cortical neurons by

a nonbenzodiazepine mechanism. *Epilepsia* 41 Suppl 1:S17-S20, 2000

9. White, HS, Brown, SD, Woodhead, JH, Skeen, GA, Wolf, HH: Topiramate enhances GABA-mediated chloride flux and GABA-evoked chloride currents in murine brain neurons and increases seizure threshold. *Epilepsy Res* 28:167-179, 1997

10. Gibbs, JW, III, Sombati, S, DeLorenzo, RJ, Coulter, DA: Cellular actions of topiramate: blockade of kainate-evoked inward currents in cultured hippocampal neurons. *Epilepsia* 41 Suppl 1:S10-S16, 2000

11. Zona, C, Ciotti, MT, Avoli, M: Topiramate attenuates voltage-gated sodium currents in rat cerebellar granule cells. *Neurosci Lett* 231:123-126, 1997

12. Zhang, X, Velumian, AA, Jones, OT, Carlen, PL: Modulation of high-voltage-activated calcium channels in dentate granule cells by topiramate. *Epilepsia* 41 Suppl 1:S52-S60, 2000

13. Herrero, AI, Del, ON, Gonzalez-Escalada, JR, Solis, JM: Two new actions of topiramate: inhibition of depolarizing GABA(A)-mediated responses and activation of a potassium conductance. *Neuropharmacology* 42:210-220, 2002

14. Dodgson, SJ, Shank, RP, Maryanoff, BE: Topiramate as an inhibitor of carbonic anhydrase isoenzymes. *Epilepsia* 41 Suppl 1:S35-S39, 2000

15. Picard, F, Deshaies, Y, Lalonde, J, Samson, P, Richard, D: Topiramate reduces energy and fat gains in lean (Fa/?) and obese (fa/fa) Zucker rats. *Obes Res* 8:656-663, 2000

16. Wilkes, JJ, Nelson, E, Osborne, M, Demarest, KT, Olefsky, JM: Topiramate is an insulin-sensitizing compound in vivo with direct effects on adipocytes in female ZDF rats. *Am J Physiol Endocrinol Metab* 288:E617-E624, 2005

17. van den Berg, SA, Guigas, B, Bijland, S, Ouwens, M, Voshol, PJ, Frants, RR, Havekes, LM, Romijn, JA, van Dijk, KW: High levels of dietary stearate promote adiposity and deteriorate hepatic insulin sensitivity. *Nutr Metab (Lond)* 7:24, 2010

18. van den Hoek, AM, Voshol, PJ, Karnekamp, BN, Buijs, RM, Romijn, JA, Havekes, LM, Pijl, H: Intracerebroventricular neuropeptide Y infusion precludes inhibition of glucose and VLDL production by insulin. *Diabetes* 53:2529-2534, 2004

19. Plum, L, Ma, X, Hampel, B, Balthasar, N, Coppari, R, Munzberg, H, Shanabrough, M, Burdakov, D, Rother, E, Janoschek, R, Alber, J, Belgardt, BF, Koch, L, Seibler, J, Schwenk, F, Fekete, C, Suzuki, A, Mak, TW, Krone, W, Horvath, TL,

Ashcroft, FM, Bruning, JC: Enhanced PIP3 signaling in POMC neurons causes K_{ATP} channel activation and leads to diet-sensitive obesity. *J Clin Invest* 116:1886-1901, 2006

20. Parlevliet, ET, Schroder-van der Elst JP, Corssmit, EP, Picha, K, O'Neil, K, Stojanovic-Susulic, V, Ort, T, Havekes, LM, Romijn, JA, Pijl, H: CNTO736, a novel glucagon-like peptide-1 receptor agonist, ameliorates insulin resistance and inhibits very low-density lipoprotein production in high-fat-fed mice. *J Pharmacol Exp Ther* 328:240-248, 2009

21. Rossetti, L, Giaccari, A: Relative contribution of glycogen synthesis and glycolysis to insulin-mediated glucose uptake. A dose-response euglycemic clamp study in normal and diabetic rats. *J Clin Invest* 85:1785-1792, 1990

22. van den Hoek, AM, Teusink, B, Voshol, PJ, Havekes, LM, Romijn, JA, Pijl, H: Leptin deficiency per se dictates body composition and insulin action in ob/ob mice. *J Neuroendocrinol* 20:120-127, 2008

23. Christensen, J, Hojskov, CS, Poulsen, JH: Liquid chromatography tandem mass spectrometry assay for topiramate analysis in plasma and cerebrospinal fluid: validation and comparison with fluorescence-polarization immunoassay. *Ther Drug Monit* 24:658-664, 2002

24. Astrup, A, Toubro, S: Topiramate: a new potential pharmacological treatment for obesity. *Obes Res* 12 Suppl:167S-173S, 2004

25. Bialer, M, Doose, DR, Murthy, B, Curtin, C, Wang, SS, Twyman, RE, Schwabe, S: Pharmacokinetic interactions of topiramate. *Clin Pharmacokinet* 43:763-780, 2004

26. Wilkes, JJ, Nguyen, MT, Bandyopadhyay, GK, Nelson, E, Olefsky, JM: Topiramate treatment causes skeletal muscle insulin sensitization and increased Acrp30 secretion in high-fat-fed male Wistar rats. *Am J Physiol Endocrinol Metab* 289:E1015-E1022, 2005

27. Stenlof, K, Rossner, S, Vercruysse, F, Kumar, A, Fitchet, M, Sjostrom, L: Topiramate in the treatment of obese subjects with drug-naive type 2 diabetes. *Diabetes Obes Metab* 9:360-368, 2007

28. Minokoshi, Y, Kim, YB, Peroni, OD, Fryer, LG, Muller, C, Carling, D, Kahn, BB: Leptin stimulates fatty-acid oxidation by activating AMP-activated protein kinase. *Nature* 415:339-343, 2002

29. Christensen, J, Hojskov, CS, Dam, M, Poulsen, JH: Plasma concentration of topiramate correlates with cerebrospinal fluid concentration. *Ther Drug Monit* 23:529-535, 2001

30. York, DA, Singer, L, Thomas, S, Bray, GA: Effect of topiramate on body weight and body composition of osborne-mendel rats fed a high-fat diet: alterations in hormones, neuropeptide, and uncoupling-protein mRNAs. *Nutrition* 16:967-975, 2000

31. Karschin, C, Ecke, C, Ashcroft, FM, Karschin, A: Overlapping distribution of K(ATP) channel-forming Kir6.2 subunit and the sulfonylurea receptor SUR1 in rodent brain. *FEBS Lett* 401:59-64, 1997

32. Spanswick, D, Smith, MA, Mirshamsi, S, Routh, VH, Ashford, ML: Insulin activates ATP-sensitive K+ channels in hypothalamic neurons of lean, but not obese rats. *Nat Neurosci* 3:757-758, 2000

33. Ha, E, Yim, SV, Jung, KH, Yoon, SH, Zheng, LT, Kim, MJ, Hong, SJ, Choe, BK, Baik, HH, Chung, JH, Kim, JW: Topiramate stimulates glucose transport through AMP-activated protein kinase-mediated pathway in L6 skeletal muscle cells. *Pharmacogenomics J* 6:327-332, 2006

34. Frigerio, F, Chaffard, G, Berwaer, M, Maechler, P: The antiepileptic drug topiramate preserves metabolism-secretion coupling in insulin secreting cells chronically exposed to the fatty acid oleate. *Biochem Pharmacol* 72:965-973, 2006

CIRCULATING INSULIN STIMULATES FATTY ACID RETENTION IN WHITE ADIPOSE TISSUE VIA K$_{ATP}$ CHANNEL ACTIVATION IN THE CENTRAL NERVOUS SYSTEM ONLY IN INSULIN-SENSITIVE MICE

Claudia P. Coomans
Janine J. Geerling
Bruno Guigas
Anita M. van den Hoek
Edwin T. Parlevliet
D. Margriet Ouwens
Hanno Pijl
Peter J. Voshol
Patrick C. N. Rensen
Louis M. Havekes
Johannes A. Romijn

6

ABSTRACT

Insulin signaling in the central nervous system (CNS) is required for the inhibitory effect of insulin on glucose production. Our aim was to determine whether the CNS is also involved in the stimulatory effect of circulating insulin on the tissue-specific retention of fatty acid (FA) from plasma. In wild-type mice, hyperinsulinemic-euglycemic clamp conditions stimulated the retention of both plasma triglyceride-derived FA and plasma albumin-bound FA in the various white adipose tissues (WAT), but not in other tissues including brown adipose tissue (BAT). Intracerebroventricular (i.c.v.) administration of insulin induced a similar pattern of tissue-specific FA partitioning. This effect of i.c.v. insulin administration was not associated with activation of the insulin signaling pathway in adipose tissue. I.c.v. administration of tolbutamide, a K_{ATP} channel blocker, considerably reduced (during hyperinsulinemic-euglycemic clamp conditions) and even completely blocked (during i.c.v. administration of insulin) WAT-specific retention of FA from plasma. This central effect of insulin was absent in CD36 deficient mice, indicating that CD36 is the predominant FA transporter in insulin-stimulated FA retention by WAT. In diet-induced insulin resistant mice, these stimulating effects of insulin (circulating or i.c.v. administered) on FA retention in WAT were lost. In conclusion, in insulin-sensitive mice, circulating insulin stimulates tissue-specific partitioning of plasma-derived FA in WAT in part through activation of K_{ATP} channels in the CNS. Apparently, circulating insulin stimulates fatty acid uptake in WAT, but not in BAT, directly, and indirectly, through the CNS.

INTRODUCTION

The central nervous system (CNS) is highly sensitive to insulin (1-6). Insulin in the brain is mostly derived from the circulation, and only a modest amount, if any, is produced locally (6;7). Circulating insulin can cross the blood-brain barrier (8;9) and exert metabolic effects in peripheral organs via the CNS. Intracerebroventricular (i.c.v.) administration of insulin decreases food intake, resulting in reduced body weight (3;10;11). In addition, the central action of insulin plays a crucial role in the inhibitory effect of the hormone on hepatic glucose production (4;12).

Recently, a novel regulatory function for the effects of insulin through the CNS with regard to adipose tissue metabolism has been proposed, suggesting that intracellular lipolysis and lipogenesis in WAT is under the neuronal control of central insulin (13;14). Furthermore, it has been shown that central glucose lowers plasma triglyceride (TG) levels by inhibiting the secretion of TG-rich lipoproteins by the liver (15). Taken together, these observations imply an important role of the CNS in general and of central effects of insulin in the CNS in particular in the regulation of whole body TG metabolism.

The aim of the present study was to determine whether circulating insulin affects tissue-specific fatty acid (FA) partitioning from plasma through effects in the CNS. Using a dual tracer method, we report here that circulating insulin stimulates the uptake of TG-derived FA as well as albumin-bound FA specifically in WAT during hyperinsulinemic-euglycemic clamp conditions. Short-term (2.5 h) i.c.v. administration of insulin stimulates the retention of FA in WAT in a similar fashion. This effect, which requires the presence of the long chain FA transporter CD36, was prevented by inhibition of central adenosine triphosphate-dependent potassium (K_{ATP}) channels. Moreover, we show that the increase in FA retention in WAT, induced by hyperinsulinemic-euglycemic clamp conditions, is considerably reduced by inhibition of K_{ATP} channels in the CNS, demonstrating that the well-known effect of circulating insulin on insulin-mediated FA retention in WAT is mediated to a considerable extent by the effects of circulating insulin in the CNS. Finally, we show that these stimulating effects of insulin on FA retention through the CNS in WAT are lost in diet-induced obese mice.

MATERIALS AND METHODS

Animals

Male wild-type (WT) and CD36^{-/-} mice (15 weeks old, both on C57Bl/6J background) were housed in a temperature-controlled room on a 12-hour light-dark cycle and were fed a standard mouse chow diet with free access to water. In the diet-induced obesity experiment, mice were fed *ad libitum* high-fat diet for 12 weeks (45 energy% of fat derived from palm oil; Research Diet Services BV, Wijk bij Duurstede, The Netherlands). All animal experiments were performed in accordance with the regulations of Dutch law on animal welfare and the institutional ethics committee for animal procedures from the Leiden University Medical Center, Leiden, The Netherlands approved the protocol.

Surgical procedure

For i.c.v. cannula implantation, the mice were anaesthetized with 0.5 mg/kg Medetomidine (Pfizer, Capelle a/d IJssel, The Netherlands), 5 mg/kg Midazolam (Roche, Mijdrecht, The Netherlands) and 0.05 mg/kg Fentanyl (Janssen-Cilag, Tilburg, The Netherlands) and placed in a stereotactic device (TSE systems, Homburg, Germany). A 25 gauge guide cannula was implanted into the left lateral ventricle using the following coordinates from Bregma: 1.0 mm lateral, 0.46 mm posterior and 2.2 mm ventral. The guide cannula was secured to the skull surface with dental cement (GC Europe N.V., Leuven, Belgium) and the anesthesia was antagonized using 2.5 mg/kg Antipamezol (Pfizer, Capelle a/d IJssel, The Netherlands), 0.5 mg/kg Flumazenil (Roche, Mijdrecht, The Netherlands) and 1.2 mg/kg Naloxon (Orpha, Purkersdorf, Austria). After a recovery period of 1 week, cannula placement was verified. Mice that ate >0.3 g in 1 h in response to i.c.v. injection of 5 μg neuropeptide Y (NPY, Bachem, St. Helens, UK) in 1 μL of artificial cerebrospinal fluid (aCSF) (Harvard Apparatus, Natick, MA, US) were considered to have the cannula correctly placed and were included in the study (16).

Preparation of radiolabeled emulsion particles

Protein-free VLDL-like triglyceride (TG)-rich emulsion particles were prepared from 100 mg total lipid at a weight ratio of triolein (Sigma, St. Louis, MA, US): egg yolk phosphatidylcholine (Lipoid, Ludwigshafen, Germany): lysophosphatidylcholine (Sigma, St. Louis, MA, US): cholesteryl oleate (Janssen, Beersse, Belgium): cholesterol (Sigma, St. Louis, MA, US) of 70: 22.7: 2.3: 3.0: 2.0 in the presence of 200 μCi of glycerol tri[9, 10(n)-^{3}H]oleate ([^{3}H]TG) (GE Healthcare, Little Chalfont, UK), as previously described (17). Lipids were hydrated in 10 mL of 2.4 M sodium chloride, 10 mM Hepes, 1 mM ethylenediaminetetraacetic acid (EDTA), pH 7.4, and sonicated for 30 min at 10 μm output using a Soniprep 150 (MSE Scientific Instruments, UK) equipped with a water bath for temperature (54°C) maintenance. Subsequently, the emulsion particles were divided into fractions with a different average size by density gradient ultracentrifugation. Intermediate sized (80 nm) [^{3}H]TG-labeled particles were mixed with a trace amount of [^{14}C] oleic acid ([^{14}C]FA) (GE Healthcare, Little Chalfont, UK) complexed with bovine serum albumin (BSA) in a ^{3}H:^{14}C ratio of 3:1.

Tissue-specific TG and FA partitioning

Postabsorptive (mice were fasted for 15 h with food withdrawn at 18:00h the day prior to the study), body weight-matched male mice were anaesthetized with 6.25 mg/kg Acepromazine (Alfasan, Woerden, The Netherlands), 6.25 mg/kg Midazolam (Roche, Mijdrecht, The Netherlands), and 0.31 mg/kg Fentanyl (Janssen-Cilag, Tilburg, The Netherlands). In the hyperinsulinemic-euglycemic clamp studies, insulin (Actrapid, Novo Nordisk, Bagsværd, Denmark) was administered intravenously (i.v.) by primed (4.5 mU), continuous (6.8 mU/h for 2.5 h) infusion to attain steady-state circulating insulin levels of ~ 4 ng/mL (16;18;19). A variable intravenous infusion of a 12.5% D-glucose solution was used to maintain euglycemia as determined at 10-min intervals via tail bleeding (<3 μL, Accu-chek, Sensor Comfort; Roche Diagnostics, Mannheim, Germany). Insulin (0.5 mU/h) (Actrapid, Novo Nordisk, Bagsværd, Denmark) or the K_{ATP} channel blocker tolbutamide (12 nmol/h, (4;20) (Sigma, St. Louis, MA, US) dissolved in aCSF was infused i.c.v. at a constant rate of 2.5 μL/h during the entire experiment

using a Harvard infusion pump. The dose of i.c.v. insulin was ascertained in a dose-finding study, to ensure that plasma insulin and glucose levels did not change. Control animals received 5% DMSO in aCSF. Thirty minutes after the start of the i.c.v. infusions or thirty minutes after the start of the hyperinsulinemic-euglycemic clamp experiments (as indicated), an i.v. infusion of the glycerol tri[³H]oleate-labeled emulsion particles (0.33 nmol/h) together with albumin-bound [¹⁴C]oleic acid (10.22 nmol/h) was started at a rate of 100 µL/h and maintained for 2 h. Blood samples were taken at baseline and 2 h after starting the i.v. infusion. Subsequently, the mice were sacrificed and organs were quickly harvested and snap-frozen in liquid nitrogen.

Plasma analysis

Blood samples were taken from the tail tip into chilled capillaries coated with paraoxon to prevent *ex vivo* lipolysis. The tubes were placed on ice and centrifuged at 4°C. Plasma levels of TG, free fatty acids (FFA) and glucose were determined using commercially available kits and standards according to the instructions of the manufacturer (Instruchemie, Delfzijl, The Netherlands) in 96-wells plates (Greiner Bio-One, Alphen a/d Rijn, The Netherlands). Plasma insulin levels were measured using a mouse-specific insulin ELISA kit (Mercodia AB, Uppsala, Sweden) and plasma leptin levels using a rat/mouse-specific ELISA kit (Millipore, St Charles, USA). Lipids were extracted from plasma according to Bligh and Dyer (21). The lipid fraction was dried under nitrogen, dissolved into chloroform/methanol (5:1 [v/v]) and subjected to *thin layer chromatography (*TLC) (LK5D gel 150; Whatman, US) using hexane: diethylether: acetic acid (83:16:1) [v/v/v]) as mobile phase. Standards for TG and FA were included during the TLC procedure to locate spots of these lipids. Spots were scraped, lipids dissolved in hexane and radioactivity measured (22).

Tissue-specific FA retention analysis

Tissues were dissolved in 5 M potassium hydroxide in 50% (v/v) ethanol. After overnight saponification, protein content was determined in the various organs using a bicinchoninic acid (BCA) protein assay kit (BCA Protein Assay Kit, Thermo Scientific Pierce Protein Research Products, Rockford, US). Retention of radioactivity in the saponified tissues was measured per mg protein and corrected for the corresponding plasma specific activities of [³H]TG and [¹⁴C] FA (23;24).

Western blot analysis

Tissues were homogenized by Ultra-Turrax (22.000 rpm; 2x5 sec) in a 10:1 (v/w) ratio of ice-cold buffer containing: 50 mM 4-(2-hydroxyethyl)-1-piperazineethanesulfonic acid (pH 7.6), 50 mM sodium fluoride, 50 mM potassium chloride, 5 mM *sodium pyrophosphate*, 1 mM EDTA, 1 mM ethylene glycol tetraacetic acid, 5 mM β-glycerophosphate, 1 mM sodium vanadate, 1 mM dithiothreitol, 1% nonyl phenoxypolyethoxylethanol (Tergitol-type NP40) and protease inhibitors cocktail (Complete, Roche, Mijdrecht, The Netherlands). Homogenates were centrifuged (13.200 rpm; 15 min, 4°C) and the protein content of the supernatant was determined using the BCA protein assay kit. Proteins (10-30 µg) were separated by 7-10% SDS-PAGE followed by transfer to a polyvinylidene fluoride transfer membrane. Membranes were blocked for 1 h at room temperature in tris-buffered saline tween-20 buffer with 5% non-fat dry

milk followed by an overnight incubation with phospho-specific or total antibodies (all from Cell Signaling Technology, Beverly, US). Blots were then incubated with horseradish peroxidase-conjugated secondary antibodies for 1 h at room temperature. Bands were visualized by ECL and quantified using Image J (NIH, US).

Statistical analysis

All data are presented as means ± SEM. Most data were analyzed using SPSS. A Kruskall-Wallis test for several independent samples was used, followed by a Mann-Whitney test for independent samples. P-values less than 0.05 were considered statistically significant.

RESULTS

I.v. administration of insulin increases the retention of plasma TG-derived and albumin-bound FA by WAT

To establish to which extent tissue-specific FA uptake from plasma is stimulated by circulating insulin, we compared in various organs the retention of FA derived from both glycerol tri[^{3}H]oleate-labeled VLDL-like emulsion particles and albumin-bound [^{14}C]oleic acid between mice during hyperinsulinemic-euglycemic clamp conditions and mice in basal conditions infused with vehicle (Fig. 1A). During the clamp study, insulin levels were significantly higher as compared to basal conditions (4.4 *vs.* 0.3 ng/mL, $P < 0.01$), whereas average plasma glucose levels remained similar (6.1 *vs.* 5.4 mmol/L, ns). Plasma TG levels were similar (0.3 *vs.* 0.4 mmol/L, ns), whereas plasma free fatty acids (FFA) levels decreased upon insulin administration (0.3 *vs.* 0.7 mmol/L, $P < 0.05$).

As shown in Fig. 1, hyperinsulinemia decreased the retention of plasma TG-derived FA and albumin-bound FA in liver (Fig. 1C), without affecting the retention in brown adipose tissue (Fig. 1B), heart (Fig. 1D) and skeletal muscle (Fig. 1E). Moreover, hyperinsulinemic-euglycemic clamp conditions increased albumin-bound FA retention by 68%, ($P < 0.05$) in visceral fat and TG-derived FA and albumin-bound FA retention by 397% ($P < 0.05$) and 579% ($P < 0.01$), respectively, in subcutaneous fat and by 68% (ns) and 267% ($P < 0.01$), respectively, in epigonadal fat pads (Fig. 1F-H).

I.c.v. administration of insulin increases the retention of plasma TG-derived and albumin-bound FA by WAT

Subsequently, the dual-tracer method was used to determine tissue-specific FA retention after i.c.v. administration of insulin (0.5 mU/h for 2.5 h) (Fig. 2A). Although i.c.v. insulin administration did not alter circulating levels of glucose, TG, FFA, insulin and leptin, it decreased the plasma half-life of [^{3}H]TG by 34% ($P < 0.05$) (Table 1). Central insulin administration did not affect the retention of TG-derived FA and albumin-bound FA in brown adipose tissue, liver, heart and skeletal muscles (Fig. 2B-E). In contrast, i.c.v. insulin administration significantly increased FA retention in the different WAT compartments (Fig. 2F-H): i.c.v. insulin increased the retention of TG-derived FA and albumin-bound FA by 145% ($P = 0.07$) and 71% ($P < 0.05$) in visceral fat, by 72% ($P = 0.06$) and 111% ($P < 0.05$) in subcutaneous fat, and by 58% ($P < 0.05$) and 70% ($P < 0.05$) in epigonadal fat, respectively.
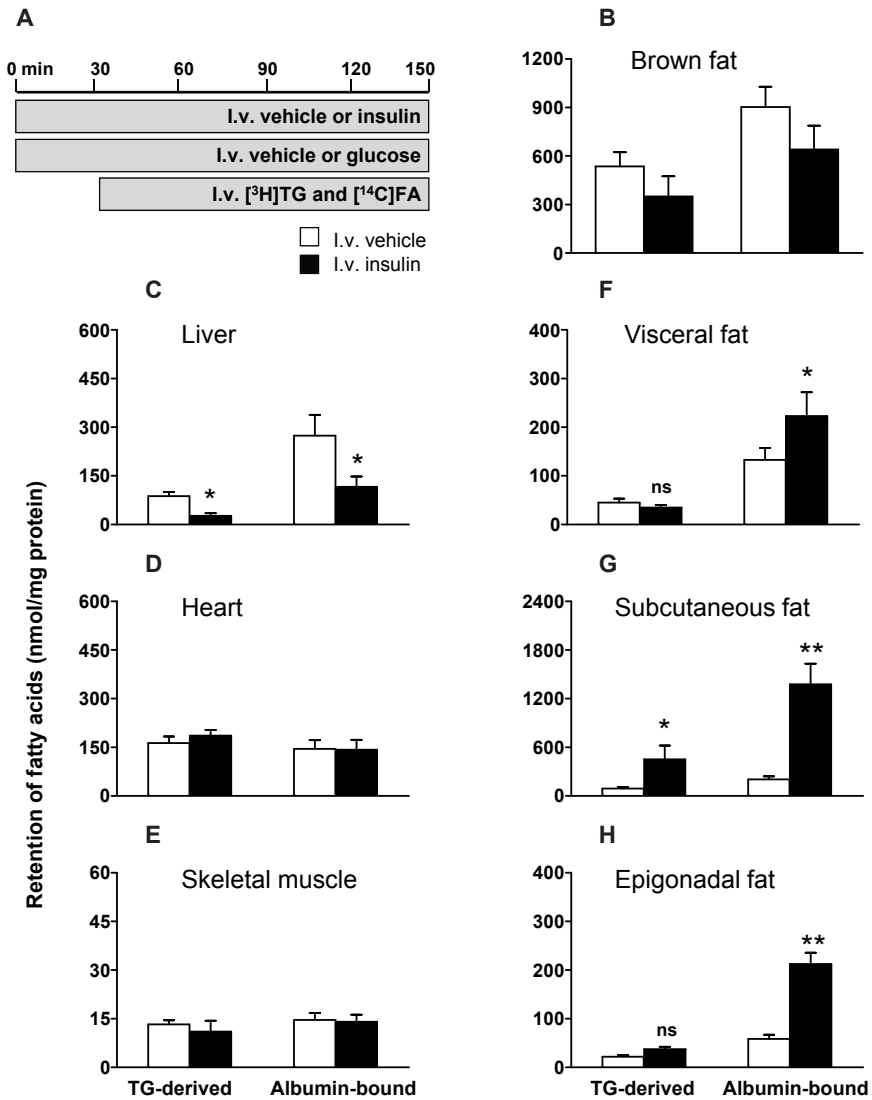
Fig. 1. Circulating insulin stimulates FA retention by WAT, while decreasing FA retention by liver. Postabsorptive, body weight-matched WT mice received continuous i.v. infusion of vehicle (white bars) or insulin/glucose (hyperinsulinemic-euglycemic clamp study, black bars) (A). Infusion of glycerol tri[³H]oleate within VLDL-like emulsion particles and albumin-bound [¹⁴C]oleic acid was started 30 minutes after the start of i.v. infusion of vehicle or glucose/insulin and maintained for 2 h. Subsequently, the mice were sacrificed and the retention of TG-derived FA and albumin-bound FA was determined in brown fat (B), liver (C), heart (D), skeletal muscle (E), visceral fat (F), subcutaneous fat (G) and epigonadal fat (H). Values are means ± SEM for at least 5 mice per group. * $P < 0.05$ *vs*. vehicle, ** $P < 0.01$ *vs*. vehicle.
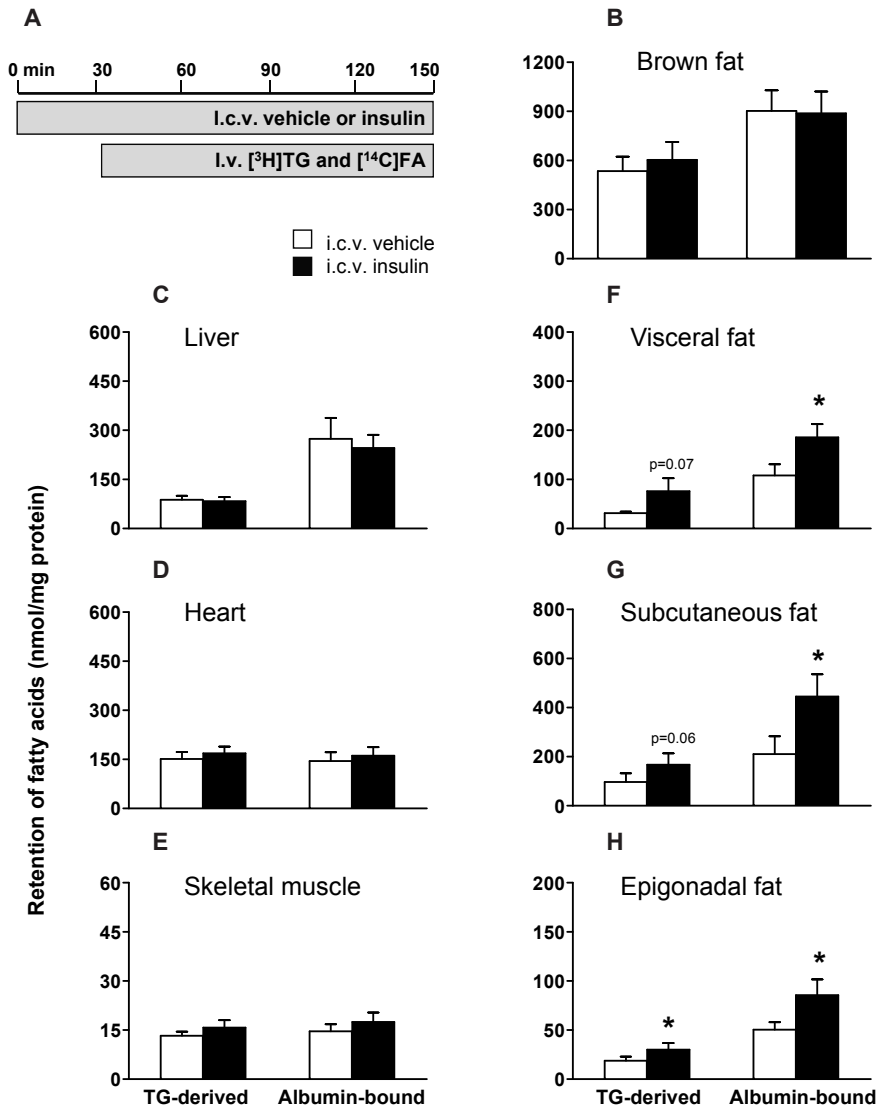
Fig. 2. I.c.v. insulin administration stimulates FA retention by WAT. Postabsorptive, body weight-matched WT mice received continuous i.c.v. infusion of vehicle (white bars) or insulin (black bars, 0.5 mU/h) (A). Thirty minutes after starting the i.c.v. infusion, the mice were infused for 2 h with glycerol tri[^{3}H]oleate within VLDL-like emulsion particles and albumin-bound [^{14}C]oleic acid. Subsequently, the mice were sacrificed and the retention of TG-derived FA and albumin-bound FA was determined in brown fat (B), liver (C), heart (D), skeletal muscle (E), visceral fat (F), subcutaneous fat (G) and epigonadal fat (H). Values are means ± SEM for at least 7 mice per group. * $P < 0.05$ *vs.* vehicle.

Table 1. I.c.v. insulin administration does not affect plasma parameters, except for [³H]TG half-life. Plasma parameters of mice that received i.c.v. infusion of vehicle or insulin obtained at baseline and 2 h after starting an i.v. infusion of glycerol tri[³H]oleate-labeled VLDL-like emulsion particles and albumin-bound [¹⁴C]oleic acid. Values are means ± SEM for at least 9 mice per group. TG, triglycerides; (F)FA, (free) fatty acids. * $P < 0.05$ *vs.* vehicle.

	Baseline		2 hours	
	I.c.v. vehicle	I.c.v. insulin	I.c.v. vehicle	I.c.v. insulin
Glucose (mmol/L)	4.9 ± 0.2	5.5 ± 0.3	4.7 ± 0.2	4.8 ± 0.4
TG (mmol/L)	0.4 ± 0.1	0.3 ± 0.1	0.4 ± 0.1	0.4 ± 0.1
FFA (mmol/L)	0.7 ± 0.1	0.6 ± 0.1	0.7 ± 0.1	0.7 ± 0.1
Insulin (ng/mL)	0.4 ± 0.1	0.4 ± 0.1	0.4 ± 0.1	0.4 ± 0.1
Leptin (ng/mL)	1.0 ± 0.1	1.3 ± 0.4	1.3 ± 0.1	1.4 ± 0.3
Half-life [¹⁴C]FA (min)	-	-	0.6 ± 0.2	0.6 ± 0.1
Half-life [³H]TG (min)	-	-	3.5 ± 0.1	2.3 ± 0.1 *

The effect of i.c.v. insulin administration on FA retention in WAT is independent of modulation of insulin, leptin or cAMP-dependent signaling pathways in WAT

To investigate the molecular mechanism(s) underlying the i.c.v. insulin-induced FA retention in WAT, we studied various signaling pathways involved in the regulation of FA metabolism in both epigonadal and visceral fat. In agreement with the absence of any effect on plasma insulin levels (Table 1), i.c.v. insulin administration did not affect peripheral insulin signaling pathways, as phosphorylation of PKB on Ser473 and Thr308 was not increased in WAT (Fig. 3A-D), nor of FOXO1 on Ser256 (data not shown). In addition, i.c.v. insulin administration did not induce any changes in STAT3 Tyr705 or CREB Ser133 phosphorylation in WAT, indicating that neither leptin nor PKA signaling pathways are modified by i.c.v. insulin administration.

The effect of i.c.v. insulin administration on FA retention by WAT is dependent on the activation of central K$_{ATP}$ channels

Part of the central effects of insulin on the regulation of food intake and hepatic glucose production are dependent on activation of hypothalamic K$_{ATP}$ channels (25). Therefore, we investigated whether the stimulatory effect of i.c.v. insulin administration on FA retention in WAT could be blocked by i.c.v. co-administration of the K$_{ATP}$ channel blocker tolbutamide (Fig. 4A). I.c.v. administration of insulin (0.5 mU/h) did not affect plasma levels of glucose, TG, FFA and insulin, irrespective of co-administration of tolbutamide (12 nmol/h) (Table 2). In accordance with the previous experiments, the plasma half-life of [³H]TG decreased by 29%, ($P < 0.05$) upon i.c.v. insulin administration compared to vehicle. However i.c.v. insulin, administered concurrently with i.c.v. tolbutamide, did not alter plasma TG and FA kinetics. I.c.v. administration of tolbutamide alone did not affect tissue-specific FA partitioning. Comparable to the previous study, FA retention in liver, heart and skeletal muscles was unaltered upon i.c.v. insulin administration and remained unaltered upon co-administration of tolbutamide (Fig. 4B-D).

Table 2. I.c.v. tolbutamide administration does not affect plasma parameters. Plasma parameters of mice that received i.c.v. infusion of vehicle or tolbutamide at baseline or hyperinsulinemic conditions. Values are means ± SEM for at least 6 mice per group. TG, triglycerides; (F)FA, (free) fatty acids. * $P < 0.05$ *vs.* vehicle.

	Baseline				2 hours			
	Vehicle	Insulin	Tolbutamide	Insulin + tolbutamide	Vehicle	Insulin	Tolbutamide	Insulin + tolbutamide
Glucose (mmol/L)	6.4 ± 0.3	6.7 ± 0.1	6.1 ± 0.8	7.0 ± 0.7	5.5 ± 0.3	5.5 ± 0.1	5.6 ± 1.1	5.7 ± 1.6
TG (mmol/L)	0.7 ± 0.1	0.6 ± 0.1	0.7 ± 0.1	0.7 ± 0.1	0.7 ± 0.1	0.7 ± 0.1	0.7 ± 0.1	0.7 ± 0.1
FFA (mmol/L)	1.2 ± 0.1	1.1 ± 0.1	1.0 ± 0.1	1.0 ± 0.1	1.0 ± 0.1	1.0 ± 0.1	1.0 ± 0.1	0.8 ± 0.1
Insulin (ng/mL)	0.3 ± 0.1	0.2 ± 0.1	0.3 ± 0.1	0.3 ± 0.1	0.4 ± 0.1	0.5 ± 0.1	0.4 ± 0.1	0.5 ± 0.1
Half-life [^{14}C]FA (min)	-	-	-	-	0.6 ± 0.1	0.5 ± 0.1	0.6 ± 0.1	0.7 ± 0.1
Half-life [^{3}H]TG (min)	-	-	-	-	2.8 ± 0.5	2.0 ± 0.2*	2.7 ± 0.3	2.8 ± 0.1
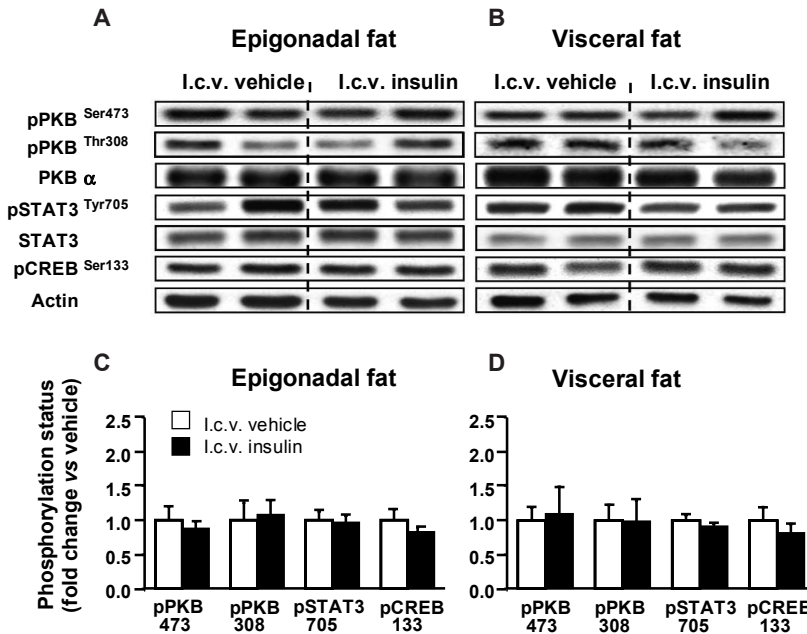
Fig. 3. I.c.v. insulin administration does not affect insulin, leptin and cAMP signaling pathways in WAT. The phosphorylation state of PKB, STAT3 and CREB was analyzed by western blot in both epigonadal fat (A) and visceral fat (B) from mice that received i.c.v. infusion of vehicle or insulin for 2.5 h. The corresponding quantification of the western blot data was normalized for total protein or actin and expressed as fold change compared to vehicle (C-D). Values represent means ± SEM for at least 5 mice per group.
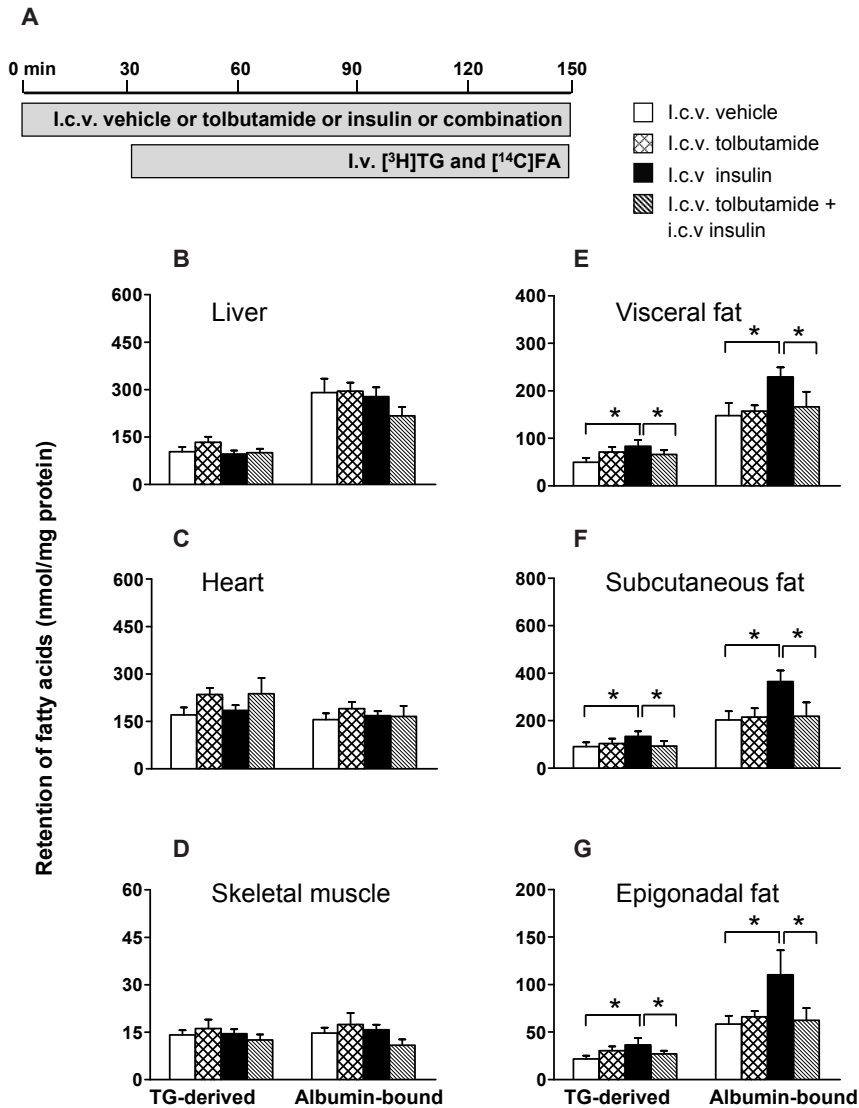
Fig. 4. I.c.v. co-administration of the K_{ATP} channel blocker tolbutamide blocks the stimulation of FA retention in WAT by i.c.v. insulin. Postabsorptive, body weight-matched WT mice received continuous i.c.v. infusion of vehicle (white bars), tolbutamide (cross-hatched bars, 12 nmol/h), insulin (black bars) or insulin in combination with tolbutamide (hatched bars) (A). Thirty minutes after starting the i.c.v. infusion, the mice were infused for 2 h with glycerol tri[3H]oleate within VLDL-like emulsion particles and albumin-bound [14C]oleic acid. Subsequently, the mice were sacrificed and the retention of TG-derived FA and albumin-bound FA was determined in liver (B), heart (C), skeletal muscle (D), visceral fat (E), subcutaneous fat (F) and epigonadal fat (G). Values are means ± SEM for at least 8 mice per group. * $P < 0.05$ *vs.* vehicle.

Interestingly, tolbutamide completely blocked the stimulation of both plasma TG-derived FA and albumin-bound FA retention in WAT induced by i.c.v. insulin administration (Fig. 4E-G).

The effect of circulating insulin on FA retention by WAT is mediated through K_{ATP} channel activation in the CNS

In order to investigate the contribution of the CNS to the effect of circulating insulin on FA retention in WAT, we examined whether i.c.v. administration of the K_{ATP} channel blocker tolbutamide inhibits the insulin-stimulated FA retention in WAT during hyperinsulinemic-euglycemic clamp conditions (Fig. 5A). In steady-state clamp conditions, plasma glucose, TG and insulin concentrations were similar in both groups, as shown in Table 2. Hyperinsulinemia suppressed FFA levels to a similar extent in i.c.v. tolbutamide- and i.c.v. vehicle-infused mice. The glucose infusion rates required to maintain euglycemia, however, were 22% lower in mice that received i.c.v. tolbutamide compared to i.c.v. vehicle ($P < 0.05$). This is consistent with previous findings showing that i.c.v. administration of the K_{ATP} channel blocker tolbutamide impair the inhibition of hepatic glucose production in response to hyperinsulinemia (4;26). The plasma half-life of [³H]TG decreased by 60% ($P < 0.05$) during hyperinsulinemic conditions, but was partly restored by i.c.v. tolbutamide (Table 3). FA retention in liver, heart and skeletal muscles was unaffected by i.c.v. tolbutamide (Fig. 5B-D). Remarkably, i.c.v. tolbutamide considerably decreased the stimulatory effect of circulating insulin during clamp conditions on FA retention in WAT (Fig. 5E-G).

The effect of i.c.v. insulin administration on FA retention in WAT requires the presence of CD36

As CD36 is one of the main long-chain FA transporters and insulin can upregulate translocation and protein expression of CD36 (27;28), we studied to which extent CD36 is involved in the i.c.v. insulin-stimulated FA retention by WAT. Therefore, we investigated the effects of i.c.v. insulin

Table 3. I.c.v. administration of tolbutamide decreases glucose infusion rate during hyperinsulinemic-eugly-cemic clamp conditions. Plasma parameters of mice that received i.c.v. infusion of vehicle or tolbutamide at baseline and during hyperinsulinemic conditions. Values are means ± SEM for at least 9 mice per group. TG, triglycerides; (F)FA, (free) fatty acids; GIR, glucose infusion rate. * $P < 0.05$ vs. vehicle.

	Baseline		Clamp conditions	
	I.c.v. vehicle	I.c.v. tolbutamide	I.c.v. vehicle	I.c.v. tolbutamide
Glucose (mmol/L)	7.3 ± 1.3	7.3 ± 1.0	6.1 ± 0.4	6.7 ± 1.3
TG (mmol/L)	0.4 ± 0.1	0.4 ± 0.1	0.3 ± 0.1	0.3 ± 0.1
FFA (mmol/L)	0.9 ± 0.1	0.8 ± 0.1	0.3 ± 0.1	0.3 ± 0.1
Insulin (ng/mL)	0.3 ± 0.1	0.2 ± 0.1	4.4 ± 1.5	4.1 ± 0.8
GIR (umol/min/kg)	-	-	114 ± 5.7	89 ± 3.2 *
Hematocrit (%)	43 ± 2	42 ± 2	42 ± 2	41 ± 2
Half-life [¹⁴C]FA (min)	-	-	0.5 ± 0.1	0.7 ± 0.1
Half-life [³H]TG (min)	-	-	1.4 ± 0.1	1.7 ± 0.1

Fig. 5. I.c.v. administration of tolbutamide impairs the stimulation of FA retention in WAT induced by hyperinsulinemic-euglycemic clamp conditions. Postabsorptive, body weight-matched mice received continuous i.c.v. infusion of vehicle (black bars) or tolbutamide (12 nmol/h, hatched bars) 30 minutes before the start of hyperinsulinemic-euglycemic clamp study (A). Infusion of glycerol tri[³H]oleate within VLDL-like emulsion particles and albumin-bound [¹⁴C]oleic acid was started 30 minutes after the start of the hyperinsulinemic-euglycemic clamp study and maintained for 2 h. Subsequently, the mice were sacrificed and the retention of TG-derived FA and albumin-bound FA was determined in liver (B), heart (C), skeletal muscle (D), visceral fat (E), subcutaneous fat (F) and epigonadal fat (G). Values are means ± SEM for at least 5 mice per group. * *P* < 0.05 *vs.* vehicle, ** *P* < 0.01 *vs.* vehicle.

on tissue-specific FA retention in CD36^{-/-} *vs.* WT mice (Fig. 6)A. In accordance with previous observations (29), basal plasma TG and FFA levels were increased in CD36^{-/-} mice compared to WT mice by 28% and 26%, respectively ($P < 0.05$), but they remained unaltered, as did circulating glucose and insulin levels, following i.c.v. administration of insulin (data not shown). I.c.v. insulin decreased the half-lives of plasma [³H]TG and [¹⁴C]FA in WT mice, but not in CD36^{-/-} mice (data not shown). Again, we confirmed in WT mice that i.c.v. insulin stimulated the retention of TG-derived FA and albumin-bound FA by 100% ($P < 0.05$) and 107% ($P < 0.05$) in visceral fat, by 53% ($P = 0.09$) and 85% ($P < 0.05$) in subcutaneous fat and by 77% ($P = 0.06$) and 104% ($P < 0.05$) in epigonadal fat pads, respectively. In basal conditions, i.e. i.c.v. administration of vehicle, the retention of both FA by WAT was dramatically decreased in CD36^{-/-} mice compared to wild-type mice (Fig. 6B-D). More importantly, i.c.v. insulin administration did not stimulate FA retention from plasma by WAT in CD36^{-/-} mice. I.c.v. insulin administration did not affect FA retention in other organs of CD36^{-/-} mice, in accordance with the observations made in WT mice (see above). Since i.c.v. insulin administration was unable to stimulate FA retention by WAT in CD36^{-/-} mice, these data suggest that CD36 is the predominant FA transporter mediating i.c.v. insulin-stimulated FA retention by WAT.

The effect of i.c.v. insulin on FA retention in WAT is lost in diet-induced obesity

Subsequently, we examined the effect of i.c.v. insulin administration on FA retention in high-fat fed mice (Fig. 7A). Body weight of the diet-induced obese mice was 40% higher compared to chow fed mice ($P < 0.01$). I.c.v. insulin administration did not alter glucose, TG, FFA and insulin levels (Table 4). In contrast to chow fed mice, i.c.v. administration of insulin did not decrease the plasma half-life of [³H]TG in these diet-induced obese mice. I.c.v. insulin administration did not alter FA retention in liver, heart or skeletal muscles, but surprisingly also not in WAT (Fig. 7B-G).

Table 4. I.c.v. insulin administration in diet-induced obese mice does not affect plasma parameters. Parameters of diet-induced obese mice that received i.c.v. infusion of vehicle or insulin obtained at baseline and 2 h after starting an i.v. infusion of glycerol tri[³H]oleate-labeled VLDL-like emulsion particles and albumin-bound [¹⁴C] oleic acid. Values are means ± SEM for at least 9 mice per group. TG, triglycerides; (F)FA, (free) fatty acids.

	Baseline		2 hours	
	I.c.v. vehicle	**I.c.v. insulin**	**I.c.v. vehicle**	**I.c.v. insulin**
Bodyweight (g)	32.5 ± 0.6	32.0 ± 0.4	32.5 ± 0.6	32.0 ± 0.4
Glucose (mmol/L)	7.7 ± 0.3	7.7 ± 0.2	6.0 ± 0.3	5.6 ± 0.2
TG (mmol/L)	1.0 ± 0.1	0.9 ± 0.1	1.0 ± 0.1	1.0 ± 0.1
FFA (mmol/L)	0.9 ± 0.1	0.8 ± 0.1	0.8 ± 0.1	0.8 ± 0.1
Insulin (ng/mL)	3.8 ± 0.3	4.0 ± 0.4	4.0 ± 0.4	3.8 ± 0.3
Half-life [¹⁴C]FA (min)	-	-	1.1 ± 0.1	1.2 ± 0.1
Half-life [³H]TG (min)	-	-	9.2 ± 1.1	9.4 ± 1.6
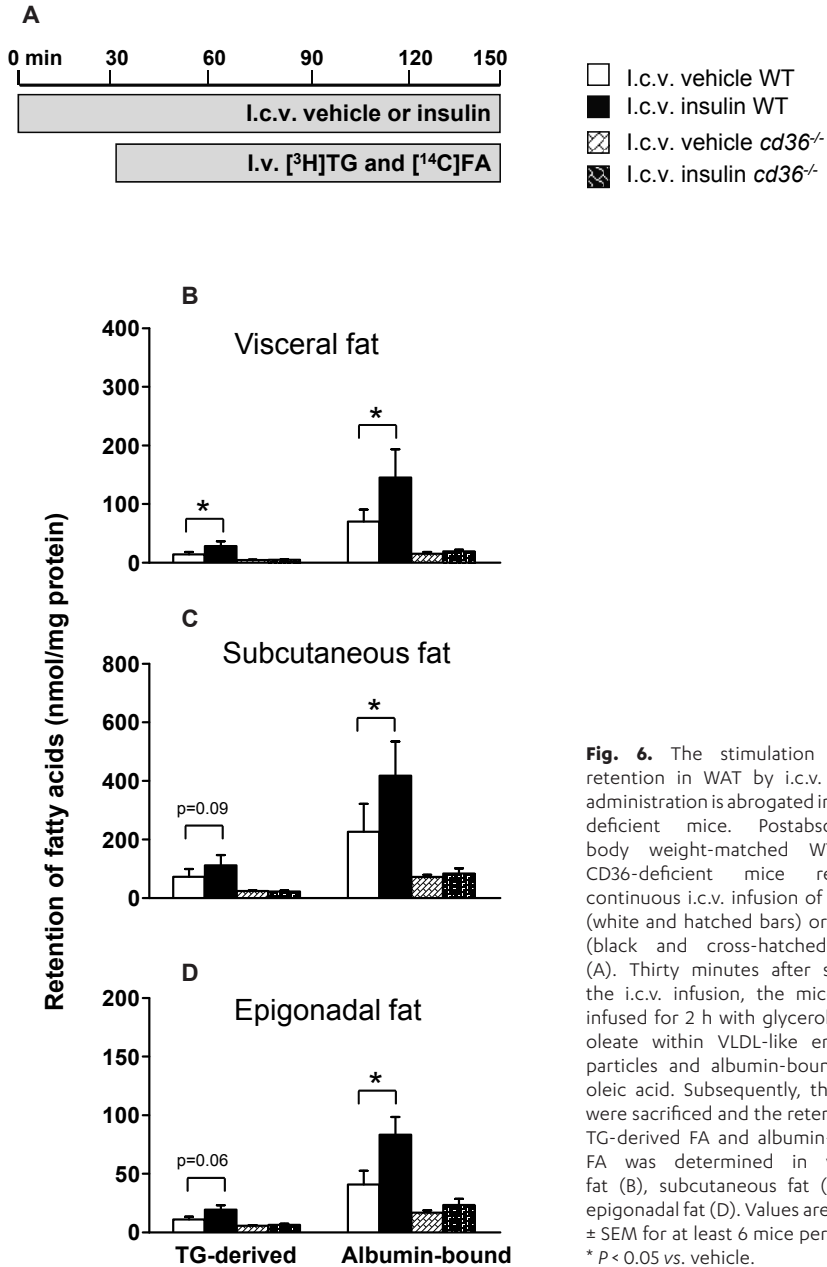
Fig. 6. The stimulation of FA retention in WAT by i.c.v. insulin administration is abrogated in CD36-deficient mice. Postabsorptive, body weight-matched WT and CD36-deficient mice received continuous i.c.v. infusion of vehicle (white and hatched bars) or insulin (black and cross-hatched bars) (A). Thirty minutes after starting the i.c.v. infusion, the mice were infused for 2 h with glycerol tri[^{3}H] oleate within VLDL-like emulsion particles and albumin-bound [^{14}C] oleic acid. Subsequently, the mice were sacrificed and the retention of TG-derived FA and albumin-bound FA was determined in visceral fat (B), subcutaneous fat (C) and epigonadal fat (D). Values are means ± SEM for at least 6 mice per group. * $P < 0.05$ *vs.* vehicle.

Fig. 7. I.c.v. insulin administration in diet-induced obese mice does not stimulate FA retention by WAT. Postabsorptive, body weight-matched WT mice received continuous i.c.v. infusion of vehicle (white bars) or insulin (black bars, 0.5 mU/h) (A). Thirty minutes after starting the i.c.v. infusion, the mice were infused for 2 h with glycerol tri[^{3}H]oleate within VLDL-like emulsion particles and albumin-bound [^{14}C]oleic acid. Subsequently, the mice were sacrificed and the retention of TG-derived FA and albumin-bound FA was determined in liver (B), heart (C), skeletal muscle (D), visceral fat (E), subcutaneous fat (F) and epigonadal fat (G). Values are means ± SEM for at least 9 mice per group.

K$_{ATP}$ channel blockage does not affect circulating insulin-stimulated FA retention by WAT in diet-induced obese mice

Finally, we examined whether i.c.v. administration of the K$_{ATP}$ channel blocker tolbutamide would still inhibit the insulin-stimulated FA retention in WAT during hyperinsulinemic-euglycemic clamp conditions in high-fat fed mice (Fig. 8A). Therefore, we determined FA retention between mice during hyperinsulinemic-euglycemic clamp conditions infused i.c.v. either with tolbutamide or vehicle and mice in basal conditions infused i.c.v. with vehicle. Body weight of the high-fat fed mice was 65% higher compared to chow fed mice (P < 0.01). In steady-state clamp conditions, plasma glucose and TG concentrations were similar between tolbutamide- and vehicle-treated mice, as shown in Table 5. During hyperinsulinemic-euglycemic clamp conditions, circulating insulin levels were fourfold higher in both groups as compared to basal conditions, resulting in a decrease of ~50% in FFA levels. The rate of glucose infusion necessary to maintain euglycemia, was not different between tolbutamide- and vehicle-treated animals. The plasma half-life of [^{3}H]TG was similar in basal conditions as in hyperinsulinemic conditions, irrespective of i.c.v. tolbutamide administration. Similar to chow fed mice, hyperinsulinemia decreased the retention of plasma TG-derived FA and albumin-bound FA in liver, which was unaltered by i.c.v. tolbutamide administration (Fig. 8B). FA retention in liver, heart en skeletal muscles was similar in all groups (Fig. 8B-D). Unlike in chow fed mice, hyperinsulinemia did not stimulate FA retention in WAT and i.c.v. tolbutamide did not decrease FA retention in WAT (Fig. 8E-G).

Table 5. I.c.v. administration of tolbutamide in diet-induced obese mice during hyperinsulinemic-euglycemic clamp conditions does not affect plasma parameters. Parameters of diet-induced obese mice that received i.c.v. infusion of vehicle or tolbutamide at baseline and during basal infusions or hyperinsulinemic conditions. Values are means ± SEM for at least 5 mice per group. TG, triglycerides; (F)FA, (free) fatty acids; GIR, glucose infusion rate.

	Baseline		Basal infusion	Clamp conditions	
	I.c.v. Vehicle	I.c.v. Tolbutamide	I.c.v. Vehicle	I.c.v. Vehicle	I.c.v. Tolbutamide
Body mass (g)	38.6 ± 0.8	38.6 ± 0.4	38.6 ± 0.8	39.6 ± 0.3	38.6 ± 0.4
Glucose (mmol/L)	6.6 ± 0.2	6.0 ± 0.2	5.7 ± 0.2	7.0 ± 0.2	7.5 ± 0.2
TG (mmol/L)	0.8 ± 0.1	0.7 ± 0.1	0.7 ± 0.1	0.7 ± 0.1	0.6 ± 0.1
FFA (mmol/L)	0.9 ± 0.1	0.8 ± 0.1	0.9 ± 0.1	0.5 ± 0.1	0.4 ± 0.1
Insulin (ng/mL)	1.8 ± 0.3	1.4 ± 0.2	2.2 ± 0.3	7.7 ± 0.4	6.9 ± 0.1
GIR (umol/min/kg)	-	-	-	52.4 ± 1.5	53.3 ± 2.7
Hematocrit (%)	44 ± 2	44 ± 1	42 ± 2	41 ± 2	41 ± 2
Half-life [^{14}C]FA (min)	-	-	1.2 ± 0.1	1.5 ± 0.2	1.2 ± 0.1
Half-life [^{3}H]TG (min)	-	-	14.6 ± 1.5	16.1 ± 0.5	17.0 ± 1.2

Fig. 8. I.v. insulin administration in diet-induced obese mice does not stimulate FA retention by WAT. Postabsorptive, body weight-matched mice received continuous i.c.v. infusion of vehicle (white and black bars) or tolbutamide (12 nmol/h, hatched bars) in basal state (i.v. infusion of vehicle; white bars) or hyperinsulinemic-euglycemic state (black and hatched bars) (A). Infusion of glycerol tri[^{3}H]oleate within VLDL-like emulsion particles and albumin-bound [^{14}C]oleic acid was started 30 minutes after initiating the i.v. infusion of vehicle or insulin/glucose, and maintained for 2 h. Subsequently, the mice were sacrificed and the retention of TG-derived FA and albumin-bound FA was determined in liver (B), heart (C), skeletal muscle (D), visceral fat (E), subcutaneous fat (F) and epigonadal fat (G). Values are means ± SEM for at least 5 mice per group. ** $P < 0.01$ *vs.* vehicle.

DISCUSSION

This study addressed the effects of circulating insulin on tissue-specific TG-derived FA and albumin-bound FA retention, and the role of central insulin action in these effects. Circulating insulin, which activated insulin signaling in the brain, stimulated retention of both TG-derived FA and albumin-bound FA in WAT. Centrally administered insulin stimulated retention of both FA sources in a similar manner, but without activating insulin signaling in WAT. Tolbutamide, a K_{ATP} channel blocker, decreased this insulin-stimulated FA partitioning to WAT during peripheral insulin infusion, and even abolished this effect during i.c.v. co-administration with insulin. Taken together, we show that the central effects of circulating insulin contribute on average ~30% to TG-derived FA uptake in WAT and ~66% to albumin-derived FA uptake in WAT to the total effects of circulating insulin during hyperinsulinemic clamp conditions. In contrast, in diet-induced obese mice, centrally administered insulin was unable to stimulate FA retention in WAT. Furthermore, inhibition of central action of i.c.v. administered insulin or circulating insulin by tolbutamide did not affect FA retention in WAT. Collectively, these data indicate that circulating insulin stimulates FA partitioning from plasma to WAT to a considerable extent through indirect effects on central neural pathways and that insulin-stimulated FA partitioning through these central neural pathways is absent in mice with insulin resistance after 12 weeks of high-fat feeding.

First, we determined tissue-specific FA uptake during hyperinsulinemic-euglycemic clamp conditions compared to basal conditions. In agreement with the rise in plasma insulin levels, hypothalamic insulin signaling was activated during hyperinsulinemic-euglycemic clamp conditions as phosphorylation of PKB on Thr308 (1.24 ± 0.05 *vs.* 1.00 ± 0.10, P = 0.08) and its downstream target PRAS40 on Thr246 (1.51 ± 0.11 *vs.* 1.00 ± 0.06, *P* < 0.05) were increased compared to basal conditions (unpublished data). We observed that peripheral as well as i.c.v. insulin administration promotes FA storage specifically in WAT. By employing the dual tracer methods described by Teusink *et al*. (23), we made a distinction between FA derived from plasma TG and FA derived from plasma albumin. Both peripheral and i.c.v. administration of insulin stimulated the retention of both sources of plasma FA in WAT. This insulin-stimulated FA retention by WAT was accompanied by a decreased half-life of TG, reflecting increased turnover of plasma TG. Interestingly, these acute effects of i.c.v. insulin administration on plasma TG and FA fluxes towards WAT, together with recent data showing that brain insulin suppresses intracellular lipolysis and stimulates lipogenesis in adipocytes (14), provide an explanation for the finding that chronic i.c.v. insulin administration increases fat mass (13).

In addition to stimulating FA retention by WAT, peripheral insulin infusion decreased FA storage by the liver. However, i.c.v. administration of insulin or blockage of central K_{ATP} channels did not affect FA retention by the liver. This suggests that the effect of peripheral insulin on liver FA retention is not mediated by the CNS, but, rather, seems to be a direct effect on the liver caused by an associated reduction in the availability of plasma FFA.

Recently, Bartelt *et al*. described the fundamental role of BAT for TG and FA clearance (30). Exposure of mice to cold accelerated TG uptake by BAT, in a lipoprotein lipase (LPL) and CD36-dependent manner. In the current study, we have also determined the effects of insulin on FA retention by BAT. However, peripheral nor central insulin administration increased FA

retention by BAT, indicating that insulin, in contrast to cold exposure, is not a major stimulator of TG and FA uptake by BAT.

The question arises how insulin exerts its indirect effects through the central nervous system on FA uptake in WAT. We used an i.c.v. dose of insulin, ascertained in a dose-finding study, which did not affect plasma insulin and glucose levels. Nonetheless, this i.c.v. dose of insulin stimulated FA uptake by WAT. Therefore, the stimulatory effect of i.c.v. insulin on retention of FA by WAT is not caused by i.c.v. insulin-induced changes in plasma levels of glucose and insulin. We cannot exclude the possibility of other neuroendocrine, insulin-potentiating effects induced by the effects of insulin on the central nervous system, like a decrease in plasma levels of the insulin antagonist epinephrine or corticosterone. Furthermore, it is possible that the indirect effects of insulin through the CNS involve alterations in the activity of the autonomic nerves projecting towards WAT, i.e. in (para)sympathetic activity. In accordance with this concept, we documented in a model of suprarenal fat pads in rats that selective vagotomy (i.e. parasympathetic denervation of the suprarenal fat pads) reduced FA uptake in WAT by 36% during hyperinsulinemic clamp conditions (31). An increase in parasympathetic activity towards WAT might be involved in the indirect effects of circulating insulin through the CNS, although the existence of parasympathetic innervation of other fat compartments is at present uncertain. Alternatively, it might be hypothesized that a change in the activity of the sympathetic activity towards WAT may be involved in the indirect effects of insulin on FA uptake in WAT *in vivo*, as it has been shown that insulin administered in the mediabasal hypothalamus dampens the sympathetic activity (14).

We determined to which extent the stimulatory effects of circulating insulin on FA retention in WAT were mediated through the CNS by i.c.v. administration of tolbutamide. Tolbutamide, which belongs to the sulfonylurea family, inhibits K_{ATP} channels in the hypothalamus when administered i.c.v. (4). Sulfonylureas bind to the K_{ATP} channels on the cell membrane of certain hypothalamic neurons, where they inhibit the hyperpolarizing efflux of potassium (32). Insulin acts in central neurons by opening/activating K_{ATP} channels, and, consequently, i.c.v. administration of tolbutamide blocks central K_{ATP} channel-mediated insulin signaling (4). Our study shows that the rapid stimulatory effect of i.c.v. insulin administration on FA uptake in WAT is blocked by i.c.v. co-administration of tolbutamide. This indicates that tissue-specific stimulation of FA uptake by WAT induced by i.c.v. insulin administration is mediated by activation of K_{ATP} channels in the brain. By blocking central insulin signaling by i.c.v. administration of tolbutamide during hyperinsulinemic-euglycemic clamp conditions, we showed that insulin stimulates FA retention in WAT to a considerable extent via action in the CNS.

We also assessed the effects of high-fat diet on the central effects of circulating insulin on FA retention in WAT. The high-fat diet abolished the stimulating effect of i.c.v. administration of insulin on FA retention in WAT. Furthermore, peripheral administered insulin did not result in FA retention in WAT and blocking central insulin signaling by i.c.v. administration of tolbutamide did not affect the FA retention in WAT. The absence of insulin effects on FA retention in these diet-induced obese mice is probably the result of both high-fat-diet induced insulin resistance of WAT and central insulin resistance associated with blunted activation of hypothalamic K_{ATP} channels (25;33-36). This present study indicates that in high-fat fed conditions, FA partitioning is no longer influenced by (central acting) insulin.

The present results showed that insulin stimulates FA retention in WAT to a considerable extent through action in the CNS. Since insulin stimulates FA transport by upregulating and translocating the long chain FA transporter CD36 in isolated skeletal muscles and cardiac myocytes (27;28), we hypothesize that the stimulating effect of centrally acting insulin on FA retention in WAT can be mediated by CD36 translocation. When administered in CD36-deficient mice, i.c.v. insulin was unable to stimulate FA retention in WAT, suggesting a role of this FA transporter in i.c.v. insulin-stimulated FA retention in WAT. Accordingly, AMP-activated protein kinase (AMPK), which can stimulate FA retention by promoting translocation of CD36 from intracellular pool to the plasma membrane (37), was activated in WAT upon i.c.v. insulin administration (Fig. 9). These preliminary data suggest that central insulin action can lead to CD36 translocation following AMPK activation, thereby resulting in FA retention in WAT.

Recent observations have challenged the traditional notion that adipose tissue acquires FA from TG-rich lipoproteins mediated by the LPL system. Shadid *et al*. documented direct uptake of plasma FFA by adipose tissue in humans in the postabsorptive state (38). In accordance, we previously demonstrated considerable uptake of plasma FFA in adipose tissue in both fed and
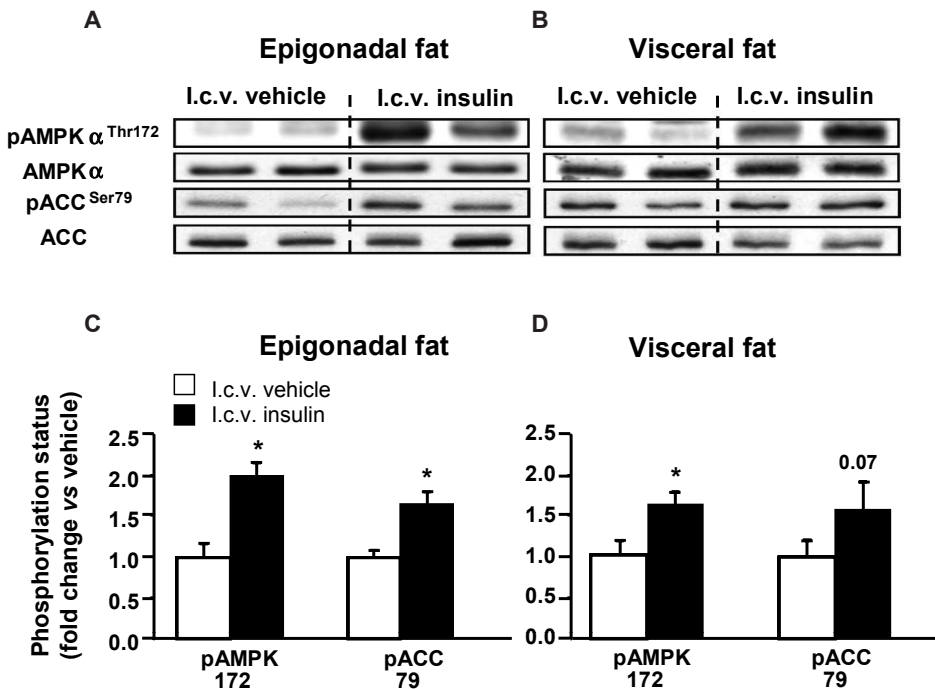
Fig. 9. I.c.v. insulin administration activates AMPK in WAT. The phosphorylation state of AMPK and its downstream target ACC was analyzed by Western blot in both epigonadal fat (A) and visceral fat (B) in mice that received i.c.v. infusion of vehicle or insulin for 2.5 h. The corresponding quantification of the Western blot data was normalized for total protein and expressed as fold change compared to vehicle (C-D). Values represent means ± SEM for at least 5 mice per group. * $P < 0.05$ *vs*. vehicle.

fasted mice (23). In older experiments the uptake of FA in adipose tissue from plasma FFA and plasma TG was assessed by quantification of the uptake as a percentage of the total administered radioactive dose (39). In the present study, we assessed tissue FA uptake from plasma FFA and plasma TG per mg protein after correction for the corresponding plasma specific activities of [^{14}C] FA and [^{3}H]TG. This correction for precursor pool enrichment enabled to assess the absolute rate of FA uptake from the two plasma sources as compared to the assessment of the relative uptake of FA radio-isotopes in relation to the total administered radioactive doses in the older experiments. In addition, there are other methodological differences including labeling procedures of plasma TG, the use of the postabsorptive state *vs.* hyperinsulinemic-euglycemic clamp procedure, that limit a simple comparison of the results of our and those previous experiments.

I.c.v. administration of insulin did not stimulate FA retention by WAT to the same extent as peripherally administered insulin. However, the dose of insulin used in the i.c.v. experiments and the i.v. dose used in the hyperinsulinemic euglycemic clamp experiments cannot easily be compared. The i.c.v. dose of insulin used in the current study was ascertained in a dose-finding study to exclude hormone-sensitive lipase inactivation by i.c.v. insulin (as shown recently by Scherer et al.; (14)). Therefore, the change in FA retention by WAT upon i.c.v. insulin is the result of a net influx of FA, whereas FA retention upon peripheral insulin administration is the result of suppression of lipolysis and FA uptake, explaining the difference in the amount of FA retention by WAT between centrally and peripherally administered insulin.

In conclusion, we show that circulating insulin stimulates tissue-specific FA retention by WAT to a considerable extent by indirect pathways, involving activation of K_{ATP} channels in the brain, which is lost in diet-induced obese mice. These observations highlight a paradigm that circulating hormones can act on target tissues directly, as well as indirectly through the CNS and indicate that such a central pathway is disturbed in insulin resistance of WAT in diet-induced obesity.

ACKNOWLEDGEMENTS

REFERENCE LIST

1.	Banks, WA: The source of cerebral insulin. *Eur J Pharmacol* 490:5-12, 2004

2.	Banks, WA: The blood-brain barrier as a regulatory interface in the gut-brain axes. *Physiol Behav* 89:472-476, 2006

3.	McGowan, MK, Andrews, KM, Grossman, SP: Chronic intrahypothalamic infusions of insulin or insulin antibodies alter body weight and food intake in the rat. *Physiol Behav* 51:753-766, 1992

4.	Obici, S, Zhang, BB, Karkanias, G, Rossetti, L: Hypothalamic insulin signaling is required for inhibition of glucose production. *Nat Med* 8:1376-1382, 2002

5.	Urayama, A, Banks, WA: Starvation and triglycerides reverse the obesity-induced

impairment of insulin transport at the blood-brain barrier. *Endocrinology* 149:3592-3597, 2008

6. Schwartz, MW, Figlewicz, DP, Baskin, DG, Woods, SC, Porte, D, Jr.: Insulin in the brain: a hormonal regulator of energy balance. *Endocr Rev* 13:387-414, 1992

7. Baura, GD, Foster, DM, Porte, D, Jr., Kahn, SE, Bergman, RN, Cobelli, C, Schwartz, MW: Saturable transport of insulin from plasma into the central nervous system of dogs in vivo. A mechanism for regulated insulin delivery to the brain. *J Clin Invest* 92:1824-1830, 1993

8. Schwartz, MW, Sipols, A, Kahn, SE, Lattemann, DF, Taborsky, GJ, Jr., Bergman, RN, Woods, SC, Porte, D, Jr.: Kinetics and specificity of insulin uptake from plasma into cerebrospinal fluid. *Am J Physiol* 259:E378-E383, 1990

9. Margolis, RU, Altszuler, N: Insulin in the cerebrospinal fluid. *Nature* 215:1375-1376, 1967

10. Woods, SC, Lotter, EC, McKay, LD, Porte, D, Jr.: Chronic intracerebroventricular infusion of insulin reduces food intake and body weight of baboons. *Nature* 282:503-505, 1979

11. Porte, D, Jr., Woods, SC: Regulation of food intake and body weight in insulin. *Diabetologia* 20 Suppl:274-280, 1981

12. Konner, AC, Janoschek, R, Plum, L, Jordan, SD, Rother, E, Ma, X, Xu, C, Enriori, P, Hampel, B, Barsh, GS, Kahn, CR, Cowley, MA, Ashcroft, FM, Bruning, JC: Insulin Action in AgRP-Expressing Neurons Is Required for Suppression of Hepatic Glucose Production. *Cell Metab* 5:438-449, 2007

13. Koch, L, Wunderlich, FT, Seibler, J, Konner, AC, Hampel, B, Irlenbusch, S, Brabant, G, Kahn, CR, Schwenk, F, Bruning, JC: Central insulin action regulates peripheral glucose and fat metabolism in mice. *J Clin Invest* 118:2132-2147, 2008

14. Scherer, T, O'Hare, J, ggs-Andrews, K, Schweiger, M, Cheng, B, Lindtner, C, Zielinski, E, Vempati, P, Su, K, Dighe, S, Milsom, T, Puchowicz, M, Scheja, L, Zechner, R, Fisher, SJ, Previs, SF, Buettner, C: Brain insulin controls adipose tissue lipolysis and lipogenesis. *Cell Metab* 13:183-194, 2011

15. Lam, TK, Gutierrez-Juarez, R, Pocai, A, Bhanot, S, Tso, P, Schwartz, GJ, Rossetti, L: Brain glucose metabolism controls the hepatic secretion of triglyceride-rich lipoproteins. *Nat Med* 2007

16. van den Hoek, AM, Voshol, PJ, Karnekamp, BN, Buijs, RM, Romijn, JA, Havekes, LM, Pijl, H: Intracerebroventricular neuropeptide Y infusion precludes inhibition of glucose and VLDL production by insulin. *Diabetes* 53:2529-2534, 2004

17. Rensen, PC, Herijgers, N, Netscher, MH, Meskers, SC, van Eck, M, van Berkel, TJ: Particle size determines the specificity of apolipoprotein E-containing triglyceride-rich emulsions for the LDL receptor versus hepatic remnant receptor in vivo. *J Lipid Res* 38:1070-1084, 1997

18. Heijboer, AC, van den Hoek, AM, Pijl, H, Voshol, PJ, Havekes, LM, Romijn, JA, Corssmit, EP: Intracerebroventricular administration of melanotan II increases insulin sensitivity of glucose disposal in mice. *Diabetologia* 48:1621-1626, 2005

19. Parlevliet, ET, Heijboer, AC, Schroder-van der Elst JP, Havekes, LM, Romijn, JA, Pijl, H, Corssmit, EP: Oxyntomodulin ameliorates glucose intolerance in mice fed a high-fat diet. *Am J Physiol Endocrinol Metab* 294:E142-E147, 2008

20. Plum, L, Ma, X, Hampel, B, Balthasar, N, Coppari, R, Munzberg, H, Shanabrough, M, Burdakov, D, Rother, E, Janoschek, R, Alber, J, Belgardt, BF, Koch, L, Seibler, J, Schwenk, F, Fekete, C, Suzuki, A, Mak, TW, Krone, W, Horvath, TL, Ashcroft, FM, Bruning, JC: Enhanced PIP3 signaling in POMC neurons causes K_{ATP} channel activation and leads to diet-sensitive obesity. *J Clin Invest* 116:1886-1901, 2006

21. Bligh, EG, Dyer, WJ: A rapid method of total lipid extraction and purification. *Can J Biochem Physiol* 37:911-917, 1959

22. Silberkang, M, Havel, CM, Friend, DS, McCarthy, BJ, Watson, JA: Isoprene synthesis in isolated embryonic Drosophila cells. I. Sterol-deficient eukaryotic cells. *J Biol Chem* 258:8503-8511, 1983

23. Teusink, B, Voshol, PJ, Dahlmans, VE, Rensen, PC, Pijl, H, Romijn, JA, Havekes, LM: Contribution of fatty acids released from lipolysis of plasma triglycerides to total plasma fatty acid flux and tissue-specific fatty acid uptake. *Diabetes* 52:614-620, 2003

24. Klieverik, LP, Coomans, CP, Endert, E, Sauerwein, HP, Havekes, LM, Voshol, PJ, Rensen, PC, Romijn, JA, Kalsbeek, A, Fliers, E: Thyroid hormone effects on whole-body energy homeostasis and tissue-specific fatty acid uptake in vivo. *Endocrinology* 150:5639-5648, 2009

25. Spanswick, D, Smith, MA, Mirshamsi, S, Routh, VH, Ashford, ML: Insulin activates ATP-sensitive K+ channels in hypothalamic neurons of lean, but not obese rats. *Nat Neurosci* 3:757-758, 2000

26. Pocai, A, Lam, TK, Gutierrez-Juarez, R, Obici, S, Schwartz, GJ, Bryan, J, guilar-Bryan, L, Rossetti, L: Hypothalamic K(ATP) channels control hepatic glucose production. *Nature* 434:1026-1031, 2005

27. Corpeleijn, E, Pelsers, MM, Soenen, S, Mensink, M, Bouwman, FG, Kooi, ME, Saris, WH, Glatz, JF, Blaak, EE: Insulin acutely upregulates protein expression of the fatty acid transporter CD36 in human skeletal muscle in vivo. *J Physiol Pharmacol* 59:77-83, 2008

28. Chabowski, A, Coort, SL, Calles-Escandon, J, Tandon, NN, Glatz, JF, Luiken, JJ, Bonen, A: Insulin stimulates fatty acid transport by regulating expression of FAT/CD36 but not FABPpm. *Am J Physiol Endocrinol Metab* 287:E781-E789, 2004

29. Goudriaan, JR, Dahlmans, VE, Teusink, B, Ouwens, DM, Febbraio, M, Maassen, JA, Romijn, JA, Havekes, LM, Voshol, PJ: CD36 deficiency increases insulin sensitivity in muscle, but induces insulin resistance in the liver in mice. *J Lipid Res* 44:2270-2277, 2003

30. Bartelt, A, Bruns, OT, Reimer, R, Hohenberg, H, Ittrich, H, Peldschus, K, Kaul, MG, Tromsdorf, UI, Weller, H, Waurisch, C, Eychmuller, A, Gordts, PL, Rinninger, F, Bruegelmann, K, Freund, B, Nielsen, P, Merkel, M, Heeren, J: Brown adipose tissue activity controls triglyceride clearance. *Nat Med* 17:200-205, 2011

31. Kreier, F, Fliers, E, Voshol, PJ, Van Eden, CG, Havekes, LM, Kalsbeek, A, Van Heijningen, CL, Sluiter, AA, Mettenleiter, TC, Romijn, JA, Sauerwein, HP, Buijs, RM: Selective parasympathetic innervation of subcutaneous and intra-abdominal fat--functional implications. *J Clin Invest* 110:1243-1250, 2002

32. van den Top, M, Lyons, DJ, Lee, K, Coderre, E, Renaud, LP, Spanswick, D: Pharmacological and molecular characterization of ATP-sensitive K(+) conductances in CART and NPY/AgRP expressing neurons of the hypothalamic arcuate nucleus. *Neuroscience* 144:815-824, 2007

33. Arase, K, Fisler, JS, Shargill, NS, York, DA, Bray, GA: Intracerebroventricular infusions of 3-OHB and insulin in a rat model of dietary obesity. *Am J Physiol* 255:R974-R981, 1988

34. Woods, SC, D'Alessio, DA, Tso, P, Rushing, PA, Clegg, DJ, Benoit, SC, Gotoh, K, Liu, M, Seeley, RJ: Consumption of a high-fat diet alters the homeostatic regulation of energy balance. *Physiol Behav* 83:573-578, 2004

35. Ono, H, Pocai, A, Wang, Y, Sakoda, H, Asano, T, Backer, JM, Schwartz, GJ, Rossetti, L: Activation of hypothalamic S6 kinase mediates diet-induced hepatic insulin resistance in rats. *J Clin Invest* 118:2959-2968, 2008

36. Clegg, DJ, Gotoh, K, Kemp, C, Wortman, MD, Benoit, SC, Brown, LM, D'Alessio, D, Tso, P, Seeley, RJ, Woods, SC: Consumption of a high-fat diet induces central insulin resistance independent of adiposity. *Physiol Behav* 2011

37. Habets, DD, Coumans, WA, Voshol, PJ, den Boer, MA, Febbraio, M, Bonen, A, Glatz, JF, Luiken, JJ: AMPK-mediated increase in myocardial long-chain fatty acid uptake critically depends on sarcolemmal CD36. *Biochem Biophys Res Commun* 355:204-210, 2007

38. Shadid, S, Koutsari, C, Jensen, MD: Direct free fatty acid uptake into human adipocytes in vivo: relation to body fat distribution. *Diabetes* 56:1369-1375, 2007

39. Bragdon, JH, Gordon, RS, Jr.: Tissue distribution of C14 after the intravenous injection of labeled chylomicrons and unesterified fatty acids in the rat. *J Clin Invest* 37:574-578, 1958

THYROID HORMONE EFFECTS ON WHOLE BODY ENERGY HOMEOSTASIS AND TISSUE-SPECIFIC FATTY ACID UPTAKE *IN VIVO*

Claudia P. Coomans*
Lars P. Klieverik*
Erik Endert
Hans P. Sauerwein
Louis M. Havekes
Peter J. Voshol
Patrick C.N. Rensen
Johannes A. Romijn
Andries Kalsbeek[$]
Eric Fliers[$]

*, [$] *Both authors contributed equally*

ABSTRACT

The effects of thyroid hormone (TH) status on energy metabolism and tissue-specific substrate supply *in vivo* are incompletely understood. To study the effects of TH status on energy metabolism and tissue-specific fatty acid (FA) fluxes, we used metabolic cages as well as ^{14}C-labelled FA and ^{3}H-labeled triglyceride (TG) infusion in rats treated with methimazole and either 0 (hypothyroidism), 1.5 (euthyroidism) or 16.0 (thyrotoxicosis) µg/100g*day of thyroxine for 11 days.

Thyrotoxicosis increased total energy expenditure (TEE) by 38% ($P < 0.05$), resting energy expenditure (REE) by 61% ($P < 0.01$) and food intake by 18% ($P < 0.01$). Hypothyroidism tended to decrease TEE (10%; $P = 0.064$), and REE (12%; $P < 0.05$), but did not affect food intake. TH status did not affect spontaneous physical activity (SPA). Thyrotoxicosis increased fat oxidation ($P < 0.01$), whereas hypothyroidism decreased glucose oxidation ($P < 0.05$). Plasma FA concentration was increased in thyrotoxic, but not in hypothyroid rats. Thyrotoxicosis increased albumin-bound FA uptake in muscle and white adipose tissue (WAT), whereas hypothyroidism had no effect in any tissue studied, suggesting mass-driven albumin-bound FA uptake. During thyrotoxicosis, TG-derived FA uptake was increased in muscle and heart, unaffected in WAT, and decreased in brown adipose tissue. Conversely, during hypothyroidism TG-derived FA uptake was increased in WAT in association with increased lipoprotein lipase activity, but unaffected in oxidative tissues and decreased in liver.

In conclusion, TH status determines EE independently of SPA. The changes in whole body lipid metabolism are accompanied by tissue-specific changes in TG-derived FA uptake in accordance with hyper- and hypometabolic states induced by thyrotoxicosis and hypothyroidism, respectively.

INTRODUCTION

Thyroid hormone (TH) is a primary denominator of energy homeostasis, reflected by the strong association between hyperthyroidism and increased energy expenditure (EE) in man. This is exemplified by the widespread clinical use of calorimetry in addition to the determination of protein bound iodine in diagnosing thyrotoxicosis (1;2) before sensitive thyroxine (T_4) and triiodothyronine (T_3) RIAs became available in the 1970s (3). Whereas modulation of resting EE by thyroid hormone status is well established in humans and rodents, it has been difficult to assess TH effects on total EE (TEE) *in vivo*. In addition, the mechanism of the increased EE induced by THs has remained incompletely understood (4). For example, few studies have addressed how THs influence spontaneous physical activity (SPA) and if changes in SPA may contribute to the alterations in EE associated with thyrotoxicosis and hypothyroidism in freely moving organisms (5;6).

We have previously studied glucose metabolism during thyrotoxicosis in rats and found increased endogenous glucose production and hepatic insulin resistance (7). Furthermore, thyrotoxicosis is associated with major changes in lipid metabolism. Fatty acids (FA) are a preferential fuel source during thyrotoxicosis (8;9), especially during the first days after the induction of thyrotoxicosis (10). These FA are provided to tissues mostly by hydrolysis (*i.e.* lipolysis) of circulating triglyceride (TG)-rich lipoprotein particles by the enzyme lipoprotein lipase (LPL), located in the capillary lumen. In addition, albumin-bound FA are provided to the tissues from the plasma, a process which is independent of LPL. Although there is evidence suggesting that LPL is regulated by TH (11), it is unknown at present how FA fluxes via these two pathways are modulated by TH in metabolically relevant tissues *in vivo*.

The aim of the present study was to examine the effects of thyrotoxicosis and hypothyroidism on whole body energy metabolism and SPA in rats. To delineate how the effects of thyroid status on whole body energy homeostasis are reflected in substrate (*i.e.* lipid) supply on the tissue level *in vivo*, we additionally studied the rates of disappearance and tissue-specific partitioning of both TG-derived and albumin-bound FA. We report effects of thyroid hormone status on TEE, resting energy expenditure (REE), SPA and substrate (*i.e.* glucose and lipid) oxidation, that are paralleled by complex and tissue-specific effects of TH on FA uptake.

MATERIALS AND METHODS

In the first experiment, 3 groups of rats were studied, i.e. hypothyroid (Hypo, n = 7), euthyroid (Eu, n = 7) and thyrotoxic rats (Tox, n = 7). All groups were treated with methimazol (MMI) in drinking water. After 7 days, all groups were implanted with subcutaneous osmotic mini-pumps (day (D) 0), delivering either vehicle (Hypo group), or thyroxine (T_4) at a dose of 1.5 (Eu group) or 16.0 µg/100 g BW*day (Tox group) (7). Rats were subsequently placed in metabolic cages for determining TEE, REE, food intake, respiratory exchange ratio (RER), and fat and glucose oxidation during a 48 h period (D9 and D10).

In the second experiment (D11), hypothyroid (Hypo, n = 9), euthyroid (Eu, n = 8) and thyrotoxic rats (Tox, n = 7) were i.v. infused with albumin-bound ^{14}C-oleate (FA) and VLDL-like

emulsion-incorporated glycerol tri[^{3}H]oleate (TG). This method enables measurement of FA turnover, tissue-specific FA partitioning and differentiation between albumin-bound and TG-derived FA uptake on the tissue level (12).

Animals

Male Wistar rats (Harlan, Horst, the Netherlands) were housed under constant conditions of temperature (21 ± 1°C) and humidity (60 ± 2%) with a 12 h/12 h light/dark (L/D) schedule (lights on 7:00 am). Animals were allowed to adapt for 6 days before the first experimental manipulations. Body weight (BW) was between 320 and 360 g. Food and drinking water was available *ad libitum*. All of the following experiments were conducted with the approval of the Animal Care Committee of the Leiden University Medical Center.

Hormonal treatment; block and replacement

At D0 of the protocol animals were placed in individual cages and treated with methimazole 0.025% (MMI, Sigma, the Netherlands) in drinking water containing 0.3% saccharin. At D7, osmotic minipumps (OMP, Alzet 2ml2, Durect Corp., Cupertino, USA) loaded with L-thyroxine (T$_4$, Sigma, the Netherlands) solved in 6.5 mM NaOH and 50% propylene glycol, were implanted under the dorsal skin during the surgical procedure. OMPs delivered either vehicle (hypothyroid rats), or T$_4$ at a dose of 1.5 µg (replacement dose; euthyroid group) or 16.0 µg (thyrotoxic group) /100 g BW*day, as described previously (7).

Surgery

In all animals an intra-atrial silicone cannula was implanted through the right jugular vein for infusion and sampling (13) during anesthesia (7). The cannula was tunneled to the head subcutaneously, fixed with dental cement to 4 stainless-steel screws inserted into the skull. A mixture of 60% amoxicillin, 20% heparin and 20% saline in polyvinylpyrrolidone (Sigma, the Netherlands) was used to fill the cannula and prevent inflammation and occlusion.

Energy expenditure, fat oxidation, spontaneous physical activity and food intake

At D7, animals were placed into an 8-cage combined, open circuit indirect calorimetry system (LabMaster system, TSE Systems, Bad Homburg, Germany, for the remainder of this manuscript referred to as "metabolic cages"), measuring food and water intake, O$_2$ uptake and CO$_2$ production, as well as SPA. Although the cages including bedding were identical to the cages in which the rats were housed the first 7 days (only the cover of the metabolic cage differs), animals were adapted to this environment before the start of the actual measuring periods (D9 and D10) for approximately 48 h. EE, RER and fat oxidation were calculated from the O$_2$ uptake and CO$_2$ production relative to individual body weights (14). O$_2$ uptake and CO$_2$ production were measured with 10 min intervals. Food and water intake and physical activity were measured continuously. Activity monitoring and detection of animal location was performed with infrared sensor pairs arranged in strips for horizontal (X level) and vertical (Z level) activity, detecting every ambulatory movement. Spontaneous physical activity (SPA or XA), high-frequent activity (XF; equivalent of breathing activity), total activity (XT=XA+XF)

and rearing (Z) were monitored. The infrared sensors for detection of movement allowed continuous recording in both light and dark phases.

Radiolabeled FA infusion

At D11, rats were restrained from access to food from 5h prior to the labelled lipid infusion (i.e. from 9:00 am onwards). Rats were connected to a metal collar attached to polyethylene tubing (for blood-sampling and isotope infusion) which was kept out of reach of the animals by a counterbalanced beam. This allowed all subsequent manipulations to be performed outside the cages without handling the freely moving animals. After obtaining a blood sample for measurement of plasma TH, FA, and TG concentrations (800 μL), rats received a primed (500 μl in 5 min), continuous (500 μl/h) infusion of albumin-bound ^{14}C-oleate (FA) and VLDL-like emulsion-incorporated glycerol tri[^{3}H]oleate (TG) i.v. for 2 h. At the end of the 2 h infusion period we obtained another blood sample (800 μL) for measurement of plasma [^{3}H]-FA and [^{14}C]-FA radioactivity. Rats were sacrificed and striated muscle (M triceps brachii), heart, liver, three white adipose tissue (WAT) depots (gonadal (epididymal), subcutaneous, visceral) and infrascapular brown adipose tissue (BAT) were harvested, snap frozen and stored at -20°C for subsequent analysis.

Preparation of radiolabeled emulsion particles

Protein-free VLDL-like TG-rich emulsion particles were prepared from 100 mg total lipid at a weight ratio of triolein (Sigma, St. Louis, MA, US): egg yolk phosphatidylcholine (Lipoid, Ludwigshafen, Germany): lyso phosphatidylcholine (Sigma, St. Louis, MA, US): cholesteryl oleate (Janssen, Beersse, Belgium): cholesterol (Sigma, St. Louis, MA, US) of 70: 22.7: 2.3: 3.0: 2.0 in the presence of 800 μCi of glycerol tri[9, 10(n)-^{3}H]oleate ([^{3}H]TG) (Amersham, Little Chalfont, UK), as reported previously (15). Lipids were hydrated in 10 mL of 2.4M NaCl, 10 mM Hepes, 1 mM EDTA, pH 7.4, and sonicated for 30 min at 10 μm output using a Soniprep 150 (MSE Scientific Instruments, UK) equipped with a water bath for temperature (54°C) maintenance. The emulsion was separated into fractions with a different average size by density gradient ultracentrifugation. Intermediate (80 nm) [^{3}H]-TG particles were mixed with a trace amount of [^{14}C]-oleic acid (Amersham, Little Chalfont, UK) complexed to bovine serum albumin (BSA).

Tissue uptake analysis

Tissues were dissolved in 5 mol/l KOH in 50% (vol/vol) ethanol. After overnight saponification, protein content was determined in the various organs using BCA kit (BCA Protein Assay Kit, Thermo Scientific). Radioactivity was measured in the saponified organs and corrected for the corresponding protein concentration and plasma specific activities of [^{3}H]-FA and [^{14}C]-FA. Calculations of tissue FA uptake and rate of disappearance were performed as described previously (12).

Analysis of lipoprotein lipase (LPL) and hepatic lipase (HL) activity

Striated muscle, heart, liver and three WAT depots were cut into small pieces and put in 1 mL 2% BSA-containing DMEM medium. Heparin (2 units) was added and samples were incubated at 37°C for 60 minutes. After centrifugation (10 min at 13.000 rpm), the supernatants were

taken and snap-frozen until analysis. Total LPL and HL activity was determined as modified from Zechner et al. (16). In short, the lipolytic activity of tissue supernatant was assessed by determination of [³H]oleate production upon incubation of tissue supernatant with a mix containing an excess of both [³H]triolein, heat-inactivated human plasma as sources of the hydrolase coactivator apoC2 and FA-free BSA as FFA acceptor.

Plasma analysis

Plasma concentrations of the thyroid hormones T_3 and T_4 were determined by an in-house RIA, with inter- and intra-assay CV of 7-8% and 3-4% (T_3), and 3-6 and 2-4% (T_4), respectively. Detection limits for T_3 and T_4 were 0.3 nmol/l and 5 nmol/l, respectively. Plasma TSH concentrations were determined by a chemiluminescent immunoassay (Immulite 2000, Diagnostic Products Corp., Los Angeles, CA), using a rat-specific standard (17). The inter- and intra-assay CV for TSH were less than 4% and 2% at ± 3.5 mU/l, respectively, and the detection limit was 0.2 mU/l. Blood samples were kept in chilled paraoxon-coated Eppendorf tubes to prevent *ex vivo* lipolysis. The tubes were placed on ice and immediately centrifuged at 4°C. Plasma levels of TG and FA were determined using commercially available kits and standards according to the manufacturer's instructions (Instruchemie, Delfzijl, The Netherlands) in 96-wells plates (Greiner Bio-One, Alphen a/d Rijn, The Netherlands). Lipids were extracted from plasma according to Bligh and Dyer (18). The lipid fraction was dried under nitrogen, dissolved into chloroform/methanol (5:1 [vol/vol]) and subjected to TLC (LK5D gel 150; Whatman) using hexane:diethylether:acetic acid (83:16:1) [vol/vol/vol]) as mobile phase. Standards for FA and TG were included during the TLC procedure to locate spots of these lipids. Spots were scraped, lipids dissolved in hexane and radioactivity measured.

Statistics

Both energy homeostasis and FA uptake data were analysed by non-parametric Kruskall-Wallis (KW) test, and a Mann Whitney U *post hoc* test was performed if KW revealed significance to determine which experimental groups differed from each other. Cosinor analysis was performed on the metabolic cage data of individual animals (48 h). Curve fitting was performed using constrained nonlinear regression analysis (SPSS 16.0). Subsequently, only if the significance level (*P* value) of the fitted curve was less than 0.05, data were used to calculate mesor, amplitude and acrophase of the individual curve. Significance was defined at P ≤ 0.05. Data are presented as mean ± SEM.

RESULTS

Effects of thyroid status on energy homeostasis

Body weight and eating behaviour

At the time of starting hormonal (T_4) treatment (osmotic mini-pump implantation; day 0), there were no differences in bodyweight (BW) between groups (Hypo 339 ± 13, Eu 340 ± 5, Tox 345 ± 4 g, ns). At the time of placement in the metabolic cages (day 7), BW was decreased by 13 ± 3 g in thyrotoxic rats, compared with an increase of 2 ± 5 g and 13 ± 9 g in euthyroid and

hypothyroid rats, respectively (Hypo *vs.* Eu ns, Eu *vs.* Tox $P < 0.05$, Hypo *vs.* Tox $P = 0.053$). However, during the whole period in the metabolic cages (day 7-10), BW increased to a similar extent in all groups (Hypo 12 ± 1, Eu 14 ± 3, Tox 12 ± 1 g, ns).

After placement in the metabolic cages animals were allowed to adapt to this new environment for 48 h (day 7-8). Subsequently, we gathered energy homeostasis data for 48 h (day 9-10). During this time period, thyrotoxic rats showed increased cumulative food intake by 18% as compared with euthyroid rats. Hypothyroid rats ate less than euthyroid rats, although this did not reach statistical significance (Hypo 44 ± 2 g, Eu 48 ± 2 g, Tox 57 ± 2 g, Eu vs Tox $P < 0, 01$, Hypo *vs.* Eu $P = 0.128$).

Plasma thyroid hormones

Plasma concentrations of T_3, T_4 and TSH following the 48 h measurement of energy homeostasis are given in Table 1. Plasma T_3 and T_4 concentrations were 163% and 30% higher, respectively, in thyrotoxic rats as compared with euthyroid rats. In hypothyroid rats, plasma T_3 and T_4 concentrations were decreased to 44% and 15%, respectively, of euthyroid levels. Plasma TSH was 12.9 ± 2.2 mU/l in hypothyroid rats, and showed similar values in euthyroid and thyrotoxic rats (0.3 ± 0.1 and 0.2 ± 0.0 mU/l, ns, respectively).

Table 1. Plasma thyroid hormone concentrations after 48 h measurement of energy homeostasis (day 11) in hypothyroid (Hypo), euthyroid (Eu) and thyrotoxic (Tox) rats. * $P < 0.01$ *vs.* Eu.

	Hypo **n = 7**	**Eu** **n = 7**	**Tox** **n = 7**
T_3 (nmol/l)	0.50 ± 0.11 *	1.14 ± 0.07	3.00 ± 0.27 *
T_4 (nmol/l)	20 ± 2 *	136 ± 8	177 ± 8 *
TSH (mU/l)	12.9 ± 2.2 *	0.3 ± 0.1	0.2 ± 0.0

Total EE, physical activity and resting EE

Total EE (TEE) showed a clear diurnal rhythm in all treatment groups, with a rise in the dark (*i.e.* active) period (Fig. 1A). As expected, this was paralleled by a similar rhythm in SPA in all groups (Fig. 1B). There was a marked, 37% increase in mean TEE/kg in thyrotoxic relative to euthyroid rats ($P < 0.05$). This increase persisted when mean TEE was not corrected for BW ($P < 0.05$, data not shown). Hypothyroid rats showed a trend ($P = 0.064$) towards decreased (-10%) mean TEE relative to euthyroid rats. Cosinor analysis revealed similar changes in the mesor of the fitted curves. In addition, there was a decrease in the amplitude of the rhythm in EE by 46% in hypothyroid relative to euthyroid rats ($P < 0.05$) as well as a ~1 h phase-advance of the acrophase relative to euthyroid and thyrotoxic rats ($P < 0.05$). There were no differences in the mean levels of SPA between groups (Kruskall-Wallis, ns). Also mesor, amplitude and acrophase of the fitted curves of SPA exhibited no differences between thyrotoxic, hypothyroid and euthyroid rats (Table 2). Likewise, there were no differences in high-frequency activity (equivalent of breathing; XF), rearing (Z) or total activity (XT) between groups, nor in mesor, amplitude or acrophase of the fitted curves (data not shown).
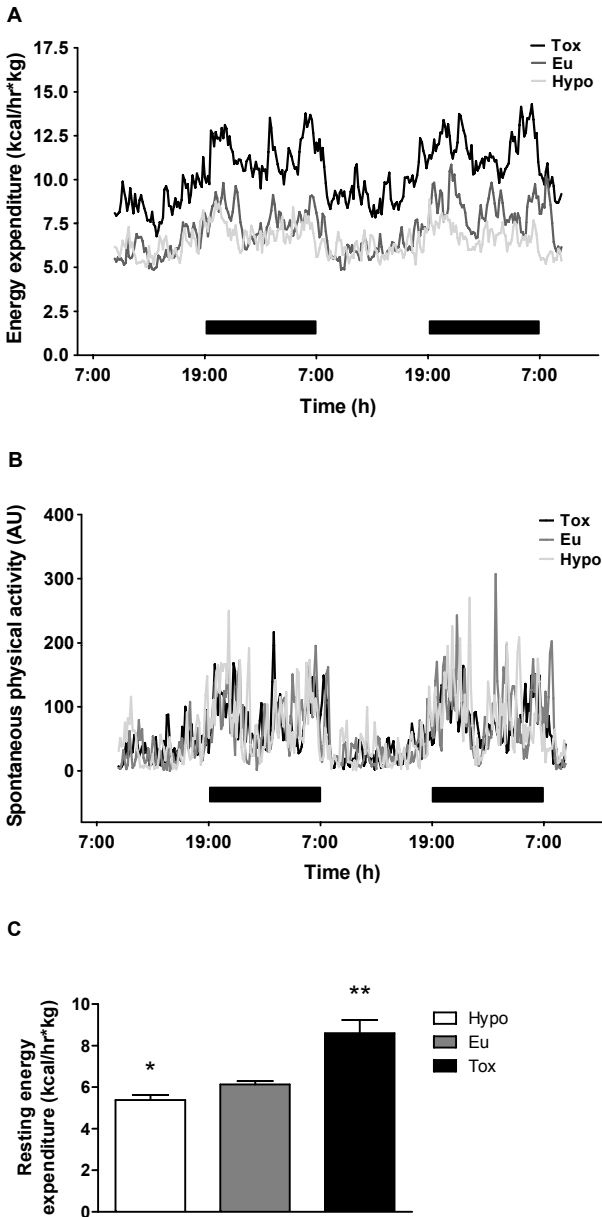
Fig. 1. Forty-eight-hour total energy expenditure (TEE, A) and spontaneous activity (SPA, B) in hypothyroid (Hypo), euthyroid (Eu) and thyrotoxic (Tox) rats entrained to a regular 12/12-h L/D cycle. Horizontal black bars indicate the dark phase of the L/D cycle. Data are mean of 7 animals per group at each time point and the interval between time points was 10 min. Cosinor data and statistical analysis are given in Table 2. Resting energy expenditure (REE, defined as the mean energy expenditure during 10 min intervals of inactivity (see text) in each individual animal, C) in hypothyroid (Hypo), euthyroid (Eu) and thyrotoxic (Tox) rats. Note the increase of REE in Tox *vs.* Eu rats (** $P < 0.01$) that was more pronounced than the decrease of REE in Hypo *vs.* Eu rats (* $P < 0.05$). Data are mean ± SEM of 7 animals per group.

Table 2. Data derived from cosinor curve-fit of all individual animals with statistical analysis. * $P < 0.05$ *vs.* Eu, " $P = 0.073$ *vs.* Eu, ^ $P < 0.05$ *vs.* Tox.

	Energy Expenditure (kcal/h*kg)			
	Mesor	**Amplitude**	**Acrophase (h)**	**n**
Hypo	6.52 ± 0.26 "^	0.64 ± 0.15 *^	23.15 ± 0.16 *^	7
Eu	7.24 ± 0.21	1.19 ± 0.09	00.23 ± 0.18	7
Tox	10.16 ± 0.67 *	1.70 ± 0.32	00.39 ± 0.22	7
	P = 0.001	*P* = 0.009	*P* = 0.015	
	Spontaneous physical activity (AU)			
	Mesor	**Amplitude**	**Acrophase (h)**	**n**
Hypo	63 ± 6	37 ± 8	00.26 ± 0.15	7
Eu	62 ± 5	38 ± 5	01.09 ± 0.35	7
Tox	60 ± 7	33 ± 6	00.13 ± 2.25	7
	P = 0.901	*P* = 0.780	*P* = 0.248	
	Respiratory exchange ratio			
	Mesor	**Amplitude**	**Acrophase (h)**	**n**
Hypo	0.94 ± 0.01 *	0.0123 ± 0.0014 ^	20.44 ± 0.30 *^	7
Eu	0.97 ± 0.01	0.0120 ± 0.0010	22.27 ± 0.24	7
Tox	0.91 ± 0.01*	0.0306 ± 0.0110 *	03.35 ± 2.48	7
	P = 0.014	*P* = 0.032	*P* = 0.018	

In each animal we determined the total number of 10 min intervals in which the activity sensors did not detect any activity (activity units (AU) = 0). Hypothyroid rats tended to spend more time inactive than euthyroid rats (533 ± 72 *vs.* 359 ± 40 min, $P = 0.064$), whereas thyrotoxic rats showed a trend towards less inactivity time compared to euthyroid rats (256 ± 33 min, $P = 0.073$). During these periods of inactivity, mean EE, termed resting EE (REE), was markedly higher in thyrotoxic as compared with euthyroid rats ($P < 0.01$), and lower in hypothyroid rats ($P < 0.05$ *vs.* Eu, Fig. 1C). REE/TEE ratios showed no differences between groups (Hypo 0.83 ± 0.02, Eu 0.85 ± 0.02, Tox 0.82 ± 0.01, KW, ns).

RER and substrate oxidation

Euthyroid rats showed a diurnal rhythm in RER (Fig. 2A), although less evident than the rhythm in TEE and SPA. The nocturnal acrophase fits with a relative increase in glucose oxidation in the dark (*i.e.* feeding) period. Both thyrotoxic and -although to a lesser extent-hypothyroid rats showed a decrease in mean RER levels relative to euthyroid rats (Tox: 94% of Eu levels, $P < 0.01$, Hypo: 96% of Eu levels, $P < 0.05$). In addition, cosinor analysis revealed that the amplitude of the day-night rhythm in RER was markedly increased in thyrotoxic rats (155%, $P < 0.01$). Although the RER phase difference between the euthyroid and thyrotoxic groups did not reach statistical significance ($P = 0.128$), there appeared to be an inverse rhythm in thyrotoxic relative to hypothyroid rats ($P < 0.05$). Hypothyroid animals showed

a RER increase in the early part of the dark period, whereas thyrotoxic rats showed a pronounced trough in RER during the feeding periods at the beginning and end of the dark period. Cosinor analysis confirmed that hypothyroid rats exhibit a decrease ($P = 0.053$) in the mesor of their RER day-night rhythm relative to euthyroid rats, but less pronounced than in thyrotoxic animals ($P < 0.01$). The acrophase of the RER rhythm in hypothyroid animals was ~2 h phase-advanced relative to euthyroid ($P < 0.05$), and almost 7 h relative to thyrotoxic animals ($P < 0.05$).

Substrate oxidation is depicted in Fig. 2B-C. In euthyroid animals, mean levels of glucose oxidation were ~30-fold higher than fat oxidation, in line with *ad libitum* access to carbohydrate-rich chow. Thyrotoxic animals showed no difference in glucose oxidation relative to euthyroid rats, whereas hypothyroid rats showed a mild decrease in mean level of glucose oxidation relative to euthyroid (19%, $P < 0.05$) and thyrotoxic animals (23%, $P < 0.05$, Fig. 2B). Mean levels of fat oxidation were markedly (479%) increased in thyrotoxic relative to euthyroid rats ($P < 0.01$), but there was no difference in fat oxidation between hypothyroid and euthyroid rats (ns, Fig. 2C). Thus, RER showed a decrease in both thyrotoxic and (to a lesser extent) hypothyroid animals relative to euthyroid rats. However, the mechanism of this decrease was different between groups, *i.e.* a decrease of glucose oxidation in hypothyroid animals, and a pronounced increase in fat oxidation in thyrotoxic animals.

Effects of thyroid status on lipid turnover, uptake and partitioning

In order to determine how whole body alterations in fat oxidation induced by thyrotoxicosis and hypothyroidism translated into substrate (*i.e.* FA) uptake at the tissue level, we applied a dual FA-isotope infusion technique that permits differentiation between plasma TG-derived and plasma albumin-bound FA uptake.

Plasma thyroid hormones

Plasma T_3, T_4 and TSH concentrations in thyrotoxic, euthyroid and hypothyroid rats are shown in Table 3.

FA and TG plasma concentrations and rate of disappearance

Plasma FA concentrations were 118% higher in thyrotoxic relative to euthyroid rats ($P < 0.01$). Plasma TG concentrations tended to increase in thyrotoxic ($P = 0.059$) rats, and showed a significant decrease in hypothyroid ($P < 0.05$) compared with euthyroid rats (Table 3).

Rate of disappearance (Rd) of ^{14}C-FA was 59% increased in thyrotoxic relative to euthyroid rats ($P = 0.054$). There were no differences in Rd of ^{3}H-TG between groups (Table 3).

Table 3. Plasma thyroid hormone concentrations before radio-labeled FA infusion (day 11) in hypothyroid (Hypo), euthyroid (Eu) and thyrotoxic (Tox) rats. * P < 0.01 *vs.* Eu.

	Hypo n = 9	Eu n = 8	Tox n = 7
T_3 (nmol/l)	0.41 ± 0.08 *	1.21 ± 0.09	2.78 ± 0.27 *
T_4 (nmol/l)	19 ± 2 *	139 ± 7	187 ± 5 *
TSH (mU/l)	10.9 ± 1.8 *	0.2 ± 0.0	0.2 ± 0.0
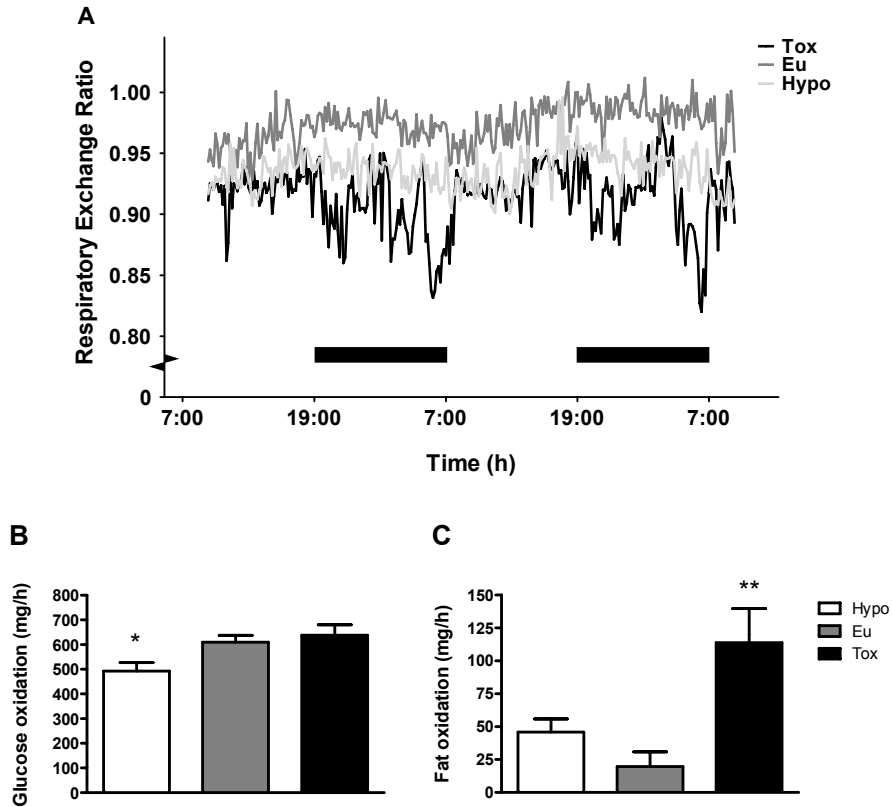
Fig. 2. Forty-eight-hour respiratory exchange ratio (RER, A) in hypothyroid (Hypo), euthyroid (Eu) and thyrotoxic (Tox) rats entrained to a regular 12/12-h L/D cycle. Horizontal black bars indicate the dark phase of the L/D cycle. Data are mean of 7 animals per group at each time point, and the interval between time points was 10 min. Cosinor data and statistical analysis are given in Table 2. Mean 48 h glucose oxidation (B) in hypothyroid (Hypo), euthyroid (Eu) and thyrotoxic (Tox) rats. Note that Hypo rats exhibit decreased glucose oxidation as compared with Eu animals (* $P < 0.05$). Mean 48 h fat oxidation (C) in hypothyroid (Hypo), euthyroid (Eu) and thyrotoxic (Tox) rats. Note that Tox rats exhibit increased fat oxidation as compared with Eu animals (** $P < 0.01$).

Tissue-specific TG-derived FA uptake, lipoprotein lipase, hepatic lipase activity and albumin-bound FA uptake

Thyrotoxicosis induced an increase of TG-derived FA uptake in striated muscle (58%, $P < 0.05$, Fig. 3A), and tended to increase TG-derived FA uptake in heart (78%, $P = 0.059$) relative to euthyroid rats, but did not induce alterations in muscle or heart LPL activity (Fig. 3B). Thyrotoxicosis induced a pronounced decrease in TG-derived FA uptake to 21% of euthyroid levels in BAT ($P < 0.01$). It should be noted that FA uptake was approximately 30-fold higher in BAT as compared to oxidative striated muscle, in line with the high mitochondrial density and high FA oxidative capacity of brown adipocytes. Thyrotoxicosis had no effect on TG-derived FA uptake in any of the WAT depots, although it induced a modest decrease in LPL activity in gonadal WAT (48%, $P < 0.05$). In contrast, hypothyroid rats showed a pronounced increase of

TG-derived FA uptake in gonadal and visceral WAT (184%, $P < 0.01$ and 75%, $P < 0.05$, respectively, Fig. 3A), associated with an increase in LPL activity both in gonadal and visceral WAT (234%, $P < 0.01$ and 306%, $P < 0.05$, respectively, Fig. 3B). In liver, hypothyroid rats showed decreased
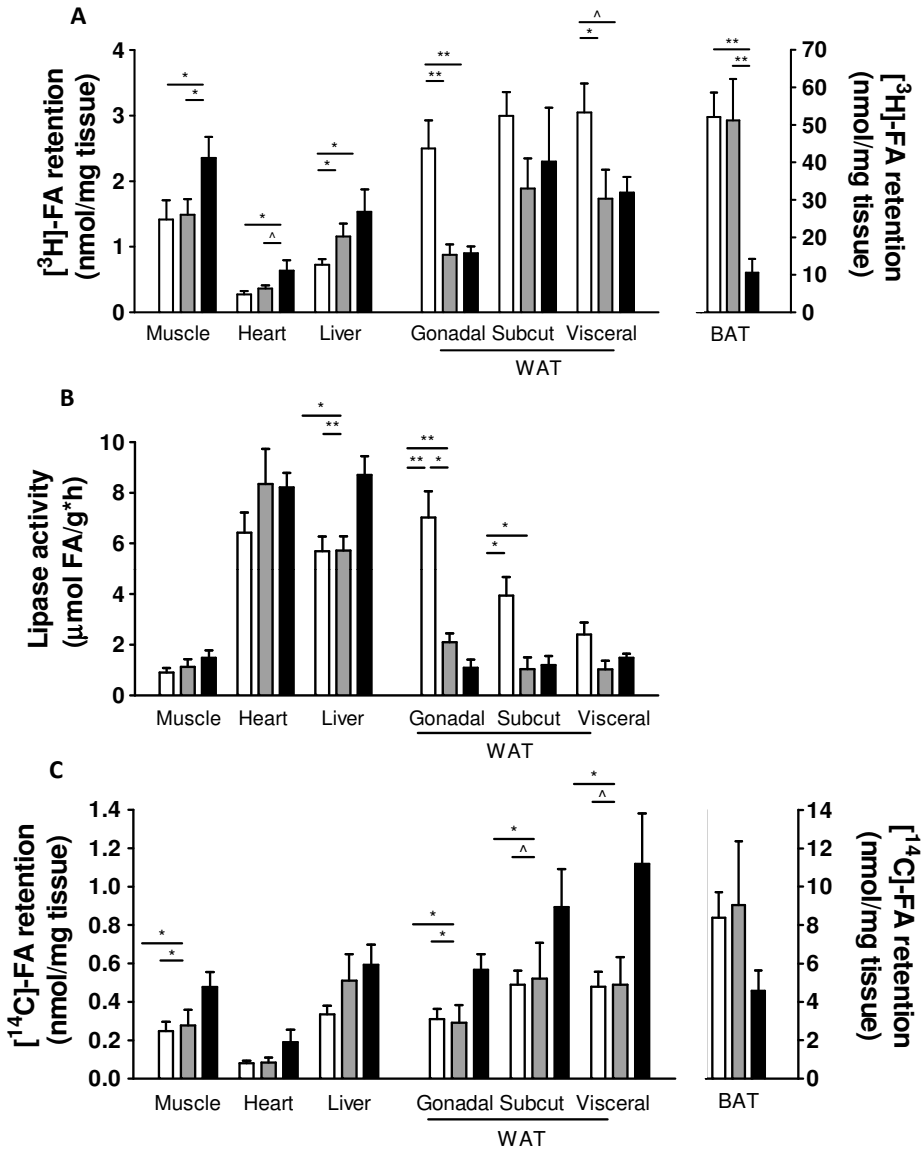
Fig. 3. Triglyceride (TG)-derived fatty acid (FA) uptake (A), lipoprotein lipase activity (B) and albumin-bound FA uptake (C) in striated muscle, heart, liver, three white adipose tissue (WAT) depots (gonadal, subcutaneous, visceral) and brown adipose tissue (BAT) of hypothyroid (Hypo, white bars), euthyroid (Eu, grey bars) and thyrotoxic (Tox, black bars) rats. ^ $0.05 < P < 0.10$, * $P \leq 0.05$, ** $P < 0.01$ vs. Eu.

TG-derived FA uptake relative to euthyroid rats (37%, $P < 0.05$), but no change in HL activity. Conversely, thyrotoxic rats showed no effect on TG-derived FA uptake but an increase in HL activity (52%, $P < 0.01$).

Thyrotoxicosis induced an increase in albumin-bound FA uptake in striated muscle (71%, $P = 0.054$, Fig. 3C), a 97% increase of albumin-bound FA uptake in gonadal WAT ($P < 0.05$), and it similarly tended to increase albumin-bound FA uptake in subcutaneous and visceral WAT (71%, $P = 0.059$ and 129%, $P = 0.059$, respectively). There was no difference in albumin-bound FA uptake between hypothyroid and euthyroid rats in any of the tissues studied.

DISCUSSION

We studied the changes in whole body energy metabolism associated with thyroid hormone status and we delineated how these changes translate into substrate (*i.e.* FA) uptake at the tissue level. Our main findings are that thyrotoxicosis induces a hypermetabolic phenotype (increased TEE, REE, and fat oxidation) as well as increased food intake favouring substrate replenishment. Interestingly, thyrotoxicosis did not increase SPA, indicating that changes in SPA do not contribute to increased TEE. Moreover, hypermetabolism was associated with increased TG-derived FA uptake in most oxidative tissues, whereas TG-derived FA uptake was unaltered in WAT. Conversely, hypothyroidism induced a hypometabolic phenotype with a mild decrease in REE, a trend towards decreased TEE, and a decrease of glucose oxidation. In addition, TG-derived FA uptake was increased in lipid storing WAT, concomitantly with increased LPL activity. However, during hypothyroidism TG-derived FA uptake in oxidative tissues was unaltered. These alterations in TG-derived FA uptake during thyrotoxicosis and hypothyroidism indicate that FA uptake from TG-rich lipoproteins is differentially regulated by thyroid hormones in a tissue-specific manner.

The mechanism of the increase of TEE induced by thyrotoxicosis is incompletely understood. It has been known for many years that REE is highly responsive to thyroid hormones (1). In addition, many thyrotoxic patients show a characteristic resting tremor and self-reported increased physical activity. Conversely, many hypothyroid patients complain of slowness (19). However, there is little experimental evidence indicating that thyroid status modulates locomotor behaviour or SPA, and it is unclear how this relates to the alterations in energy homeostasis induced by hypothyroidism and thyrotoxicosis. This is of particular interest, since accumulating evidence suggests that EE associated with SPA, termed non-exercise activity thermogenesis (NEAT), is an independent (negative) determinant of (development of) obesity in humans and rodents. As thyroid hormone is a principal regulator of energy metabolism, it may also be involved in the regulation of NEAT. The present study shows that although moderate hyperthyroidism increases TEE by 37%, it induces no alterations in SPA. In contrast, resting REE, defined as the energy expended during time periods when no activity was detected, is increased by 61% in thyrotoxic rats. Moreover, hypothyroidism induces a significant 12% decrease of REE, but it does not affect SPA either, and REE/TEE ratios are unaffected by both hypothyroidism and thyrotoxicosis. Together, our data strongly suggest that the increased energy requirements of SPA are not determined by thyroid hormone status

and do not explain increased TEE associated with thyrotoxicosisOur data are in contrast with those of Levine et al. (5) who reported increased SPA during thyrotoxicosis in rats, suggesting that NEAT was a significant component of the increase in TEE. This discrepancy is most likely explained by the pharmacological dose of T_3 used by Levine et al. to induce thyrotoxicosis, resulting in a ~13-fold increase in plasma T_3. In the present study serum T_3 was increased only 2.5-fold, which is within the range of plasma T_3 often found in patients with thyrotoxicosis. Interestingly, this was paralleled by a relatively mild, 30% increase in plasma T_4 concentrations. In thyrotoxic patients, a relative overproduction of T_3 giving rise to increased plasma T_3/T_4 ratios may be observed (20). Deiodinase type 1 (D1), which is mainly expressed in liver and kidney, is positively regulated by T_3 (21). Therefore, D1-mediated T_3 production is thought to be a major source of extra-thyroidal T_3 during hyperthyroidism (22). Indeed, the increased T_3/T_4 ratio in our rat model of thyrotoxicosis is paralleled by an induction of hepatic D1 expression (7), which may underlie the relatively mild increase of plasma T_4 relative to T_3.

Our experimental approach does not allow for measurement of other components of TEE, such as diet-induced thermogenesis (absorption, digestion and metabolism of food) and facultative thermogenesis (energy expended to maintain body temperature during cold exposure in homeothermic species). However, it is reasonable to assume that the 18% increase in 48 h cumulative food intake led to an increase of diet induced thermogenesis in thyrotoxic rats, although this component generally comprises only a minor part (~10-15%) of TEE. Facultative thermogenesis is unlikely to have played a role in our study, as it is generally negligible under thermo-neutral circumstances.

TH is known to play a role in regulating seasonal adaptations in several species, for example reproduction and maintenance of body weight (23;24), but its possible involvement in modulating rhythms of shorter phase, *i.e.* circadian rhythms, has received less attention. This possibility is theoretically supported by thyroid hormone receptor α1 mRNA expression in the region of the main circadian oscillator, *i.e.* the suprachiasmatic nuclei (SCN) (25), although this has not been confirmed at the protein-level (26;27). Previous studies have shown lack of an effect of hypothyroidism on rhythms of locomotor (wheel running) activity (28). Therefore, the subtle effects of hypothyroidism on the acrophase of the daily TEE and RER rhythms we did observe, are most likely occurring downstream of the SCN. Euthyroid rats exhibited a through in RER during the light period, fitting with relatively high fat oxidation during the inactive period when little food is consumed. The shift in acrophase of RER in thyrotoxic rats appears to be mainly due to increased fat oxidation during the nightly feeding periods (data not shown), suggesting that during thyrotoxicosis, high energy demands require mobilization of energy stores on top of the nutrients supplied by increased food intake during the active period.

Lipoprotein lipase (LPL) is the key enzyme regulating tissue-specific FA disposal by hydrolyzing triglycerides (TG) in circulating TG-rich lipoprotein particles. LPL has been proposed as a metabolic "gatekeeper" (29), directing substrate to tissues dependent on the body's metabolic status (30;31). In the present study, we explored TH effects on tissue FA uptake, and we were able to differentiate between TH effects on TG-derived (*i.e.* LPL-dependent) and albumin-bound (*i.e.* LPL-independent) FA uptake on the tissue level. In addition, we measured

tissue-specific LPL activity. In keeping with the observed hypermetabolic state associated with thyrotoxicosis, we found that thyrotoxicosis increases TG-derived FA uptake in major oxidative tissues such as striated muscle and the heart, without affecting TG-derived FA uptake in lipid-storing WAT depots. This increase in TG-derived FA uptake in oxidative tissues was not paralleled by increased local LPL activity. It has been previously reported that the linear relationship between muscle TG-derived FA uptake and LPL activity in euthyroid animals is lost after experimental alterations in thyroid status (32). This may be explained by TH effects on additional determinants of the process of TG-derived FA-uptake. In addition, TH induced stimulation of local blood flow (33;34) may have interfered with FA-uptake, independently of LPL activity.

Conversely, hypothyroidism increased TG-derived FA uptake in WAT. Indeed, earlier studies in rats have also reported increased LPL activity in WAT during hypothyroidism (35) that could be reversed by tri-iodothyronine (T_3) administration (36;37). However, hypothyroidism had no effect on TG-derived FA uptake in oxidative tissues. In the liver, hypothyroidism decreased TG-derived FA uptake but not hepatic lipase (HL) activity, whereas thyrotoxicosis increased HL activity, but not TG-derived FA uptake. Taken together, the present evidence suggests that during thyrotoxicosis, hypermetabolism and increased FA oxidation are facilitated by preferential shuttling of TG-derived FA's to oxidative tissues. Conversely, during hypothyroidism TG-derived FA's are shuttled to lipid storing WAT, away from the liver and oxidative tissues, via increased tissue-specific LPL activity.

Circulating FA that are not incorporated in TG-rich lipoprotein particles are bound to albumin in plasma. We found that thyrotoxicosis increases albumin-bound FA uptake in muscle as well as in the WAT depots, whereas hypothyroidism had no effect on albumin-bound FA uptake in any of the tissues studied. Plasma FA concentration were increased in thyrotoxic, but not in hypothyroid relative to euthyroid animals. This is in line with the notion that tissue uptake of albumin-bound FA is mainly driven by the concentration gradient between the capillary lumen and the intracellular space (30). Interestingly, in contrast to the increase in FA-uptake in oxidative tissues like striated muscle and heart, thyrotoxicosis induced a pronounced decrease of TG-derived FA uptake in BAT. BAT is the main site for adaptive thermogenesis in rodents. During cold exposure, sympathetic stimulation of BAT induces local conversion of T_4 to T_3, thereby generating heat via induction of mitochondrial uncoupling (38). Simultaneously, LPL is markedly induced via a β-adrenergic mechanism, enabling replenishment of the FA used for mitochondrial oxidation (39). During thyrotoxicosis, increased thermogenesis has been proposed to evoke a compensatory decrease in sympathetic tone to BAT (40;41). We now speculate that such a decrease in sympathetic tone may explain the marked decrease in TG-derived FA uptake in the present study, possibly via decreased LPL activity.

In conclusion, our data indicate that FA uptake from TG-rich lipoproteins is regulated by TH in a tissue-specific manner. Thyrotoxicosis increases TG-derived FA uptake in all oxidative tissues except BAT, whereas hypothyroidism increases TG-derived FA uptake in lipid storing WAT via increased LPL activity, and decreases uptake in liver. In contrast, albumin bound FA uptake during hypothyroidism and thyrotoxicosis appears to be merely mass, *i.e.* concentration gradient, driven.

ACKNOWLEDGEMENTS

REFERENCE LIST

1. Baron, DN: Estimation of the basal metabolic rate in the diagnosis of thyroid disease. *Proc R Soc Med* 52:523-525, 1959

2. Luddecke, HF: Basal metabolic rate, protein-bound iodine and radioactive iodine uptake: a comparative study. *Ann Intern Med* 49:305-309, 1958

3. Wiersinga, WM, Chopra, IJ: Radioimmunoassay of thyroxine (T4), 3, 5, 3'-triiodothyronine (T3), 3, 3', 5'-triiodothyronine (reverse T3, rT3), and 3, 3'-diiodothyronine (T2). *Methods Enzymol* 84:272-303, 1982

4. Kim, B: Thyroid hormone as a determinant of energy expenditure and the basal metabolic rate. *Thyroid* 18:141-144, 2008

5. Levine, JA, Nygren, J, Short, KR, Nair, KS: Effect of hyperthyroidism on spontaneous physical activity and energy expenditure in rats. *J Appl Physiol* 94:165-170, 2003

6. Jacobsen, R, Lundsgaard, C, Lorenzen, J, Toubro, S, Perrild, H, Krog-Mikkelsen, I, Astrup, A: Subnormal energy expenditure: a putative causal factor in the weight gain induced by treatment of hyperthyroidism. *Diabetes Obes Metab* 8:220-227, 2006

7. Klieverik, LP, Sauerwein, HP, Ackermans, MT, Boelen, A, Kalsbeek, A, Fliers, E: Effects of thyrotoxicosis and selective hepatic autonomic denervation on hepatic glucose metabolism in rats. *Am J Physiol Endocrinol Metab* 294:E513-E520, 2008

8. Moller, N, Nielsen, S, Nyholm, B, Porksen, N, Alberti, KG, Weeke, J: Glucose turnover, fuel oxidation and forearm substrate exchange in patients with thyrotoxicosis before and after medical treatment. *Clin Endocrinol (Oxf)* 44:453-459, 1996

9. Randin, JP, Scazziga, B, Jequier, E, Felber, JP: Study of glucose and lipid metabolism by continuous indirect calorimetry in Graves' disease: effect of an oral glucose load. *J Clin Endocrinol Metab* 61:1165-1171, 1985

10. Oppenheimer, JH, Schwartz, HL, Lane, JT, Thompson, MP: Functional relationship of thyroid hormone-induced lipogenesis, lipolysis, and thermogenesis in the rat. *J Clin Invest* 87:125-132, 1991

11. Saffari, B, Ong, JM, Kern, PA: Regulation of adipose tissue lipoprotein lipase gene expression by thyroid hormone in rats. *J Lipid Res* 33:241-249, 1992

12. Teusink, B, Voshol, PJ, Dahlmans, VE, Rensen, PC, Pijl, H, Romijn, JA, Havekes, LM: Contribution of fatty acids released from lipolysis of plasma triglycerides to total plasma fatty acid flux and tissue-specific fatty acid uptake. *Diabetes* 52:614-620, 2003

13. Steff ens AB. A method for frequent sampling blood and continuous infusion of fl uids in the rat without disturbing the animal. *Physiol Behav* 4:33-836, 955

14. McLean J.A. and Tobin G. Animal and Human Calorimetry. *Cambridge University Press*:100-112, 1987.

15. Rensen, PC, Herijgers, N, Netscher, MH, Meskers, SC, van Eck, M, van Berkel, TJ: Particle size determines the specificity of apolipoprotein E-containing triglyceride-rich emulsions for the LDL receptor versus hepatic remnant receptor in vivo. *J Lipid Res* 38:1070-1084, 1997

16. Zechner, R: Rapid and simple isolation procedure for lipoprotein lipase from human milk. *Biochim Biophys Acta* 1044:20-25, 1990

17. Kalsbeek, A, Fliers, E, Franke, AN, Wortel, J, Buijs, RM: Functional connections between the suprachiasmatic nucleus and the thyroid gland as revealed by lesioning and viral tracing techniques in the rat. *Endocrinology* 141:3832-3841, 2000

18. Bligh, EG, Dyer, WJ: A rapid method of total lipid extraction and purification. *Can J Biochem Physiol* 37:911-917, 1959

19. Braverman LE and Utiger RD. Introduction to hypothyroidism. The Thyroid, A Fundamental and Clinical Text (9th edition). *Lippincott Williams & Wilkins*:679-700, 2009.

20. Abuid, J, Larsen, PR: Triiodothyronine and thyroxine in hyperthyroidism. Comparison of the acute changes during therapy with

antithyroid agents. *J Clin Invest* 54:201-208, 1974

21. Zavacki, AM, Ying, H, Christoffolete, MA, Aerts, G, So, E, Harney, JW, Cheng, SY, Larsen, PR, Bianco, AC: Type 1 iodothyronine deiodinase is a sensitive marker of peripheral thyroid status in the mouse. *Endocrinology* 146:1568-1575, 2005

22. Bianco, AC, Kim, BW: Deiodinases: implications of the local control of thyroid hormone action. *J Clin Invest* 116:2571-2579, 2006

23. Barrett, P, Ebling, FJ, Schuhler, S, Wilson, D, Ross, AW, Warner, A, Jethwa, P, Boelen, A, Visser, TJ, Ozanne, DM, Archer, ZA, Mercer, JG, Morgan, PJ: Hypothalamic thyroid hormone catabolism acts as a gatekeeper for the seasonal control of body weight and reproduction. *Endocrinology* 148:3608-3617, 2007

24. Yoshimura, T, Yasuo, S, Watanabe, M, Iigo, M, Yamamura, T, Hirunagi, K, Ebihara, S: Light-induced hormone conversion of T4 to T3 regulates photoperiodic response of gonads in birds. *Nature* 426:178-181, 2003

25. Bradley, DJ, Young, WS, III, Weinberger, C: Differential expression of alpha and beta thyroid hormone receptor genes in rat brain and pituitary. *Proc Natl Acad Sci U S A* 86:7250-7254, 1989

26. Alkemade, A, Vuijst, CL, Unmehopa, UA, Bakker, O, Vennstrom, B, Wiersinga, WM, Swaab, DF, Fliers, E: Thyroid hormone receptor expression in the human hypothalamus and anterior pituitary. *J Clin Endocrinol Metab* 90:904-912, 2005

27. Lechan, RM, Qi, Y, Jackson, IM, Mahdavi, V: Identification of thyroid hormone receptor isoforms in thyrotropin-releasing hormone neurons of the hypothalamic paraventricular nucleus. *Endocrinology* 135:92-100, 1994

28. Morin, LP: Propylthiouracil, but not other antithyroid treatments, lengthens hamster circadian period. *Am J Physiol* 255:R1-R5, 1988

29. Greenwood, MR: The relationship of enzyme activity to feeding behavior in rats: lipoprotein lipase as the metabolic gatekeeper. *Int J Obes* 9 Suppl 1:67-70, 1985

30. Frayn, KN, Arner, P, Yki-Jarvinen, H: Fatty acid metabolism in adipose tissue, muscle and liver in health and disease. *Essays Biochem* 42:89-103, 2006

31. Goldberg, IG, Eckel, RH, Abumrad, NA: Regulation of fatty acid uptake into tissues: lipoprotein lipase- and CD36-mediated pathways. *J Lipid Res*, 2008

32. Kaciuba-Uscilko, H, Dudley, GA, Terjung, RL: Influence of thyroid status on skeletal muscle LPL activity and TG uptake. *Am J Physiol* 238:E518-E523, 1980

33. Dimitriadis, G, Mitrou, P, Lambadiari, V, Boutati, E, Maratou, E, Koukkou, E, Panagiotakos, D, Tountas, N, Economopoulos, T, Raptis, SA: Insulin-stimulated rates of glucose uptake in muscle in hyperthyroidism: the importance of blood flow. *J Clin Endocrinol Metab* 93:2413-2415, 2008

34. McAllister, RM, Sansone, JC, Jr., Laughlin, MH: Effects of hyperthyroidism on muscle blood flow during exercise in rats. *Am J Physiol* 268:H330-H335, 1995

35. Gavin, LA, McMahon, F, Moeller, M: Modulation of adipose lipoprotein lipase by thyroid hormone and diabetes. The significance of the low T3 state. *Diabetes* 34:1266-1271, 1985

36. Saffari, B, Ong, JM, Kern, PA: Regulation of adipose tissue lipoprotein lipase gene expression by thyroid hormone in rats. *J Lipid Res* 33:241-249, 1992

37. Gavin, LA, Cavalieri, RR, Moeller, M, McMahon, FA, Castle, JN, Gulli, R: Brain lipoprotein lipase is responsive to nutritional and hormonal modulation. *Metabolism* 36:919-924, 1987

38. Silva, JE: Thermogenic mechanisms and their hormonal regulation. *Physiol Rev* 86:435-464, 2006

39. Carneheim, C, Nedergaard, J, Cannon, B: Beta-adrenergic stimulation of lipoprotein lipase in rat brown adipose tissue during acclimation to cold. *Am J Physiol* 246:E327-E333, 1984

40. Silva, JE: The thermogenic effect of thyroid hormone and its clinical implications. *Ann Intern Med* 139:205-213, 2003

41. Silva, JE. Thermogenesis and the sympathoadrenal system in thyrotoxicosis. The Thyroid, A Fundamental and Clinical Text (9th edition). *Lippincott Wiliiams & Wilkins*:607-620, 2005

GENERAL DISCUSSION
AND FUTURE PERSPECTIVES

8

The prevalence of type 2 diabetes mellitus (T2DM) is rising steadily. The world health organization estimates that by the year 2030 more than 5% of the adult population worldwide is suffering from T2DM, as a consequence of the growing obesity epidemic (1). The development of T2DM is the result of both a deficient insulin secretion by pancreatic ß-cells and insulin resistance, finally resulting in hyperglycemia. In addition to glucose metabolism, fatty acid (FA) metabolism is disturbed in T2DM. Even though the first evidence that the brain is involved in the control of peripheral glucose homeostasis already dates back from 1855, the role of the brain in the regulation of glucose metabolism has since then been virtually overlooked. Only recently it has been shown that insulin as produced by the pancreas in response to a meal, normalizes plasma glucose levels in part via action in the brain (2;3), suggesting that insulin affects peripheral processes in part via action in the brain. The suprachiasmatic nucleus (SCN) located in the anterior hypothalamus of the brain generates 24 h cycles, so called circadian rhythms, and disturbance of the circadian rhythm, for instance by shift work, has been associated with the development of T2DM (4).

The research described in this thesis was performed to elucidate the role of disturbed circadian rhythm in the development of insulin resistance, to ascertain the role of insulin signaling in the brain on peripheral FA and glucose utilization, and to evaluate an experimental therapy with potential brain action in the treatment of T2DM. The major conclusions and implications of our findings and future perspectives will be discussed here.

CIRCADIAN RHYTHM DISTURBANCES AND INSULIN RESISTANCE

The rotation of the earth around its axis imparts light-dark cycles of 24 h and by developing an endogenous circadian (*circa*-about and *dies*-day) clock, animals and plants ensured that physiological processes are carried out at the appropriate time of day (5). Many hormones involved in metabolism, such as insulin (6), glucagon (7), adiponectin (8), corticosterone (9), leptin and ghrelin (10) exhibit circadian oscillation. In addition, the circadian clock regulates metabolism and energy homeostasis in liver and other peripheral tissues, by mediating the expression and/or activity of metabolic enzymes and transport systems involved in cholesterol metabolism, amino acid regulation, drug and toxin metabolism, citric acid cycle and glycogen and glucose metabolism (6;11;12). The rhythmic expression and activity of metabolic pathways is mainly the result of coordinated expression of clock genes (*Clock*, *Bmal1*, *Per1*, *Per2*, *Per3*, *Cry1* and *Cry2*) in liver and adipose tissue (13-15). Although each cell in the body harbors its own endogenous clock system, the central circadian clock in mammals that coordinates the peripheral clocks is located in the suprachiasmatic nucleus (SCN) of the anterior hypothalamus in the brain (16). The SCN clock is composed of multiple, single-cell oscillators, which generate coordinated circadian outputs that regulate rhythms when synchronized (17). Since the SCN oscillation is not exactly 24 h, the circadian pacemaker must be entrained to the external light-dark cycle to prevent drifting out of phase. Light, as perceived by the retina and transmitted to the SCN via the retinohypothalamic tract, is the most potent synchronizer for the SCN (16;18). The SCN transmits its rhythmic signal to

the peripheral oscillators via hormones and the autonomic nervous system (19-21), thereby influencing nearly all aspects of physiology and behavior, including sleep-wake cycles, cardiovascular activity, endocrine system, body temperature, renal activity, physiology of the gastrointestinal tract and hepatic metabolism (16;22). Complete ablation of the SCN abolishes circadian rhythmicity in the periphery as it leads to a loss of synchrony among individual cells and dampening of the rhythm at the population level (23;24). As a result, SCN lesioned (SCNx) rats do not show a circadian rhythm in, for example, glucose plasma levels and glucose uptake (6) or leptin regulation (25).

In **chapter 2** we disrupted circadian rhythmicity by constant light exposure, which resulted in decreased (~50%) SCN output. The relatively mild decrease in SCN rhythm amplitude completely abolished peripheral circadian rhythms in energy metabolism and insulin sensitivity. Determining the oscillatory expression of glycoregulatory genes in liver and muscle could shed more light into how the decrease in SCN output results in complete loss of rhythmicity in peripheral processes. Disruption of circadian rhythm by constant light had an immediate effect on SCN output as well as on energy metabolism. As a result of increased food intake and decreased energy expenditure, constant light exposure stimulated body weight gain instantaneously. This suggests that short term alterations in circadian rhythm, for instance caused by (social) jetlag and disrupted sleep in humans, can have immediate effects on homeostasis, thereby contributing to development of secondary metabolic pathophysiology. Indeed, a single night of partial sleep deprivation acutely reduces energy expenditure in healthy men (26) and induces insulin resistance in type 1 diabetic patients (27), as well as in healthy subjects (28). It should be explored whether interventions aimed at optimizing sleep duration can be beneficial for stabilizing glucose levels in patients with diabetes. As disturbances in circadian rhythms in humans are also associated with dyslipidemia and cardiovascular morbidity and mortality (29-31), and mice mutant for certain clock genes develop hyperlipidemia and increased vascular injury (32-34), it will be of interest to elucidate the involvement of the circadian clock in lipid metabolism and to determine the effect of disturbed circadian rhythm in the development of dyslipidemia and atherosclerosis.

In **chapter 3** we investigated the role of the SCN in more detail, by studying the effect of SCN lesions on energy metabolism and insulin sensitivity. Thermic ablation of the SCN (SCNx) completely disrupted the circadian pattern in energy metabolism, resulting in a higher percentage of food intake during the day. In line with previous studies showing that a shift in energy intake from the nocturnal part of the day to the diurnal part of the day results in adiposity (35-37), the SCNx mice showed a mild increase in body weight, due to increased fat mass. Even though the SCNx mice were only marginally overweight, hepatic insulin sensitivity was severely impaired. The hepatic insulin resistance in these SCNx mice could be the result of disrupted SCN mediated control of glucose production, as the SCN has been shown to directly control glucose production by the liver via innervation (38).

Both **chapter 2** and **3** indicate that disturbances in circadian rhythm can contribute to the development of T2DM. The set-up in the two studies was similar: insulin sensitivity was determined by hyperinsulinemic-euglycemic clamp technique in C57Bl/6J male mice five weeks after the intervention, either constant light exposure or ablation of the SCN, was

started. The chow fed control mice from both studies had a similar body weight and also similar insulin sensitivity. The reduced SCN output, induced by constant light exposure, immediately stimulated weight gain by increasing food intake during the subjective day. Later on, the food intake in constant light was decreased and the weight gain induced by the light intervention stabilized. SCN ablation resulted in complete arrhythmia almost immediately, but this was not reflected in an immediate body weight gain. The body weight development did not differ between SCNx and control mice for the first three weeks after the operation, but when the hyperinsulinemic clamp was performed, SCNx mice were slightly, but significantly heavier. Even though the SCNx mice had a similar body weight compared to mice in constant light on a high-fat diet, the SCNx mice were very insulin resistant, whereas the mice in constant light on a high-fat diet had only lost their circadian variation in insulin sensitivity. Therefore, it will be interesting to determine how much input from the SCN is needed to prevent the development of insulin resistance. As it is now established that disturbances in circadian rhythmicity can contribute to the development of obesity and T2DM, patients with mild rhythm disturbances, such as elderly and shift workers, can benefit from prevention and treatment programs to synchronize behavior and endogenous phase.

Patients treated for large pituitary tumors have disturbed sleep duration and quality, and disturbed circadian movement rhythm (39). These patients also have a higher prevalence of metabolic risk factors, such as dyslipidemia and insulin resistance, as compared to the general population, despite optimal replacement therapy of hypopituitarism (40-43). The sleep disorders as well as the metabolic abnormalities in these patients could be the result of damage to the SCN by the initial tumor, as we show in **chapter 3** that lesions of the SCN completely disrupts circadian rhythm and severely impairs hepatic insulin sensitivity. It needs to be established whether normalization of sleeping patterns in these patients (for example by maintaining a regular schedule for going to bed and waking up and engaging in stimulating activities and light exposure immediately after waking up (44)), can also reverse the metabolic abnormalities.

THE ROLE OF INSULIN SIGNALING IN THE BRAIN

Insulin is secreted by pancreatic β-cells after a meal to normalize glucose levels by inhibiting endogenous glucose production (EGP) and stimulating glucose disposal by peripheral tissues. In part, the effects of circulating insulin are mediated by the brain, as neuron-specific insulin receptor knock-out (NIRKO) mice develop mild insulin resistance and elevated plasma insulin levels in association with obesity (45). Consistent with these data, decreased hypothalamic expression of the insulin receptor (IR) elicits insulin resistance in rats (2). A large body of work has addressed the effect of central insulin administration on EGP. For example, central infusion of insulin has been shown to suppress endogenous glucose production (3) and antagonism of insulin signaling in the brain impairs the ability of circulating insulin to suppress EGP (3). However, much less is known on the central regulation and the downstream mechanism by which central insulin affects peripheral glucose disposal and how this is regulated in an insulin resistant model.

In **chapter 4**, we show that insulin-stimulated glucose uptake during hyperinsulinemic clamp conditions is dependent on insulin signaling in the brain. Blocking insulin signaling in the brain by intracerebroventricular (i.c.v.) administration of the ATP-sensitive potassium (K_{ATP}) channel blocker, tolbutamide, inhibited insulin-stimulated glucose uptake by skeletal muscle, but not heart or adipose tissue. Previously, it was shown that i.c.v. administered insulin increases glucose storage in muscle as glycogen (46). Together with the results obtained in **chapter 4**, a concept emerges of an insulin-dependent central pathway targeted at skeletal muscle.

In the brain, K_{ATP} channels with different properties are found in various cell types: glial cells (47) and dorsal vagal (48), hippocampal (49), and hypothalamic neurons, including proopiomelanocortin (POMC)- and agouti-related peptide (AgRP)/neuropeptide Y (NPY)-expressing neurons of the ARC (50;51). In previous studies, it has been shown that K_{ATP} channels are activated downstream of the insulin receptor. I.c.v. administration of K_{ATP} channel blockers abolish the central effects of insulin on EGP and prevent in part the suppression of EGP by circulating insulin (3). Moreover, activation of K_{ATP} channels in the ARC is sufficient to lower blood glucose by inhibition of hepatic glucose production and gluconeogenesis (52;53). K_{ATP} channels are heterooctameric proteins composed of inwardly rectifying K^+ channel subunits (KIR6.1 or KIR6.2) and regulatory sulfonylurea receptor (SUR) subunits (54;55). Interestingly, mice lacking the SUR1 subunit of the SUR1/Kir6.2 K_{ATP} channel show impaired suppression of hepatic gluconeogenesis and EGP by insulin (52). It remains to be determined how the insulin-signaling cascade leads to the activation of K_{ATP} channels. A possible mechanism could be via the regulation of the intracellular ATP/ADP ratio, either by increasing levels of glucose or AMP-activated kinase (AMPK). A reduction of the ATP/ADP ratio results in closure of K_{ATP} channels, consecutive depolarization, and increased neuronal firing, thereby exerting their effects on second-order neurons.

The orexigenic AgRP/NPY neurons and the anorexigenic POMC-neurons both express insulin receptors and are targeted by insulin (45;56). Interestingly, i.c.v. NPY or AgRP do not stimulate muscle glucose uptake from blood (57), whereas acute and chronic i.c.v. infusion of a POMC agonist enhances insulin-stimulated muscle glucose uptake (58-60). Therefore, insulin may signal through POMC, and not AgRP/NPY, to regulate muscle glucose uptake. As glucose utilization in skeletal muscle can be stimulated by sympathetic activity and i.c.v. insulin in rats increases sympathetic activity to the hind limb (24), it will be of interest to determine whether insulin action in POMC neurons regulates sympathetic activity, thereby stimulating glucose uptake by muscle. It will also be of interest to determine whether activation of K_{ATP} channels is sufficient to stimulate glucose uptake by muscle.

Upon neural stimulation, skeletal muscles are stimulated to take up glucose. This uptake of glucose most probably involves the glucose transporter 4 (GLUT4). GLUT4 is a 12-transmembrane protein expressed in muscle and adipose tissues that catalyzes the transport of glucose across the plasma membrane via an ATP-independent, facilitative diffusion mechanism. Upon stimulation, GLUT4 is recruited to the plasma membrane, resulting in 2-10-fold increase in the surface level of GLUT4. The translocation of GLUT4 to the plasma membrane is responsive to hormones such as insulin and by energy-demanding conditions such as exercise and hypoxia. The insulin-stimulated glucose uptake by muscle involves the phosphatidylinositol 3-kinase (PI3K) pathway,

whereas glucose uptake in response to exercise and hypoxia is PI3K-independent, but involves AMPK activation. In **chapter 4**, we show that under hyperinsulinemic conditions glucose uptake by skeletal muscle is stimulated, which coincides with an increase in insulin signaling in muscle. Blocking insulin signaling in the brain by i.c.v. administration of the K_{ATP} channel blocker tolbutamide inhibited insulin-stimulated glucose uptake by muscle. This inhibition of insulin-stimulated glucose uptake occurred independent of a change in insulin signaling in muscle, but also independent of a change in AMPK activation. So, the brain-mediated glucose uptake by muscle does not involve the PI3K pathway or the "alternative pathway" (involving AMPK). Therefore, more research is needed to determine how insulin signaling in the brain can affect insulin-stimulated glucose uptake by muscle.

Insulin not only regulates glucose metabolism, but also stimulates fat storage in adipose tissue. In **chapter 6**, we show that insulin-stimulated uptake of FA by white adipose tissue (WAT) is also in part dependent on central insulin signaling. I.c.v. administration of the K_{ATP} channel blocker tolbutamide abolished the central effects of insulin on FA uptake by WAT and prevented, in part, the circulating insulin-stimulated FA uptake by WAT. By employing the dual tracer methods described previously (61), we made a distinction between FA derived from plasma triglyceride (TG) and FA derived from plasma albumin. Both peripheral and i.c.v. administrered insulin stimulated the retention of both sources of plasma FA in WAT. This insulin-stimulated FA uptake by WAT was accompanied by a decreased half-life of TG, reflecting increased turnover of plasma TG. Interestingly, these acute effects of i.c.v. insulin administration on plasma TG and FA fluxes towards WAT, together with recent data showing that brain insulin suppresses intracellular lipolysis and stimulates lipogenesis in adipocytes (62), provide an explanation for the finding that chronic i.c.v. insulin administration increases fat mass (63). The indirect effect of insulin on fat storage via the brain might involve alterations in the activity of the autonomic nerves projecting towards WAT. Parasympathetic denervation of WAT reduced FA uptake in WAT by 36% during hyperinsulinemic clamp conditions in rats (64), suggesting that an increase in parasympathetic activity towards WAT might be involved in insulin-stimulated fat storage. In **chapter 6** we show that in CD36-deficient mice, i.c.v. insulin was unable to stimulate fat storage, suggesting a role for the long-chain FA transporter CD36 in i.c.v. insulin stimulated FA uptake. Accordingly, AMPK, which can stimulate FA uptake by promoting translocation of CD36 from intracellular pool to the plasma membrane (65), was activated in WAT upon i.c.v. insulin administration. A concept emerges of an insulin-dependent central pathway, leading to parasympathetic innervation of WAT and via CD36 translocation following AMPK activation resulting in FA uptake by WAT. Insulin also affects FA metabolism by acutely decreasing VLDL secretion by the liver (66;67). Therefore it will be interesting to determine whether this effect is also mediated by insulin action in the brain.

Combining data obtained in **chapter 4** and **chapter 6** indicates that circulating insulin affects glucose and FA metabolism in part via action in the brain. These effects via the brain are organ specific: central insulin signaling is involved in glucose uptake by skeletal muscle, but not heart or WAT, and central insulin signaling is involved in FA uptake by WAT, but not heart, muscle, liver or brown adipose tissue (BAT). The contrasting effects of central insulin suggest a branched-pathway model of hypothalamic insulin signaling in which insulin (in POMC

neurons, via sympathetic activity?) stimulates glucose uptake by muscle, whereas insulin (via parasympathetic activity?) promotes FA uptake in WAT. A tentative model of central insulin signaling is depicted in Fig. 1.
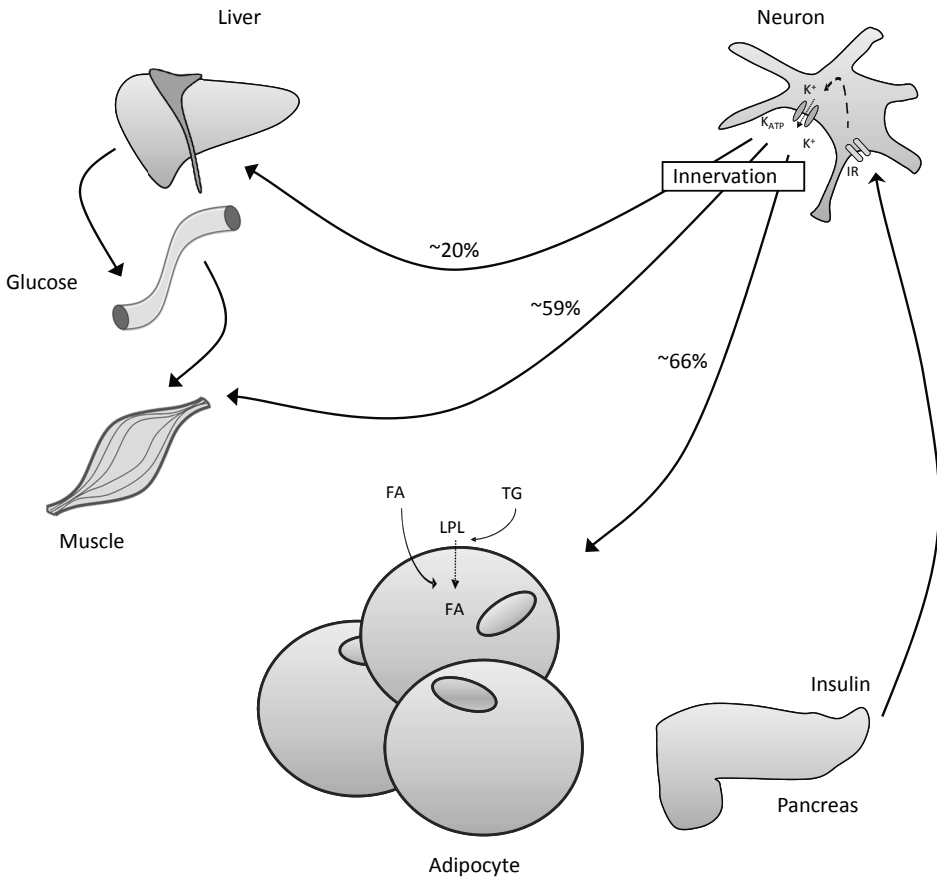
Fig. 1. Tentative model of central insulin signaling. See text for explanation.

The observations in **chapter 4** and **chapter 6** stress the role of central insulin signaling in normal physiological conditions in maintaining glucose and lipid homeostasis. However, high-fat feeding abolished the inhibitory effect of i.c.v. tolbutamide, suggesting central insulin resistance. Our *in vivo* observations in diet-induced obese mice extend *in vitro* observations, showing that insulin activates K_{ATP} channels in glucose responsive neurons of lean, but not of obese rats, suggesting that K_{ATP} channels are already inhibited in the insulin resistant state (68-71). The ability of the brain to sense peripheral inputs and maintain metabolic homeostasis is impaired upon increased caloric intake, thereby contributing to the pathophysiology of obesity

and T2DM. New therapeutic interventions restoring brain insulin action in the hypothalamus of obese individuals could improve peripheral insulin sensitivity and plasma glucose levels.

It is now shown that circulating insulin affects peripheral processes, such as glucose and FA metabolism, in part via action in the brain. The fact that part of insulin's effects are controlled by the brain could reflect a similar situation for other hormones, for instance thyroid hormones (TH). Thyroid hormones (TH) are crucial regulators of metabolism. In **chapter 7** we show that TH status determines energy expenditure and tissue-specific changes in TG-derived FA uptake. TH status also affects glucose homeostasis: endogenous glucose production is increased upon high TH levels and reduced upon decreased TH levels (72-75). Recently it has been shown that TH administration directly in the brain mimics the effect of peripheral TH on glucose metabolism (76;77) and that both peripheral as well as central effects of TH on glucose production depend on sympathetic projections to the liver (77;78). This suggests that TH may affect glucose production in part via action in the brain. At this stage, however, it is unknown how these results reflect the human situation and whether hypothalamic bioavailability of TH is altered in diabetic patients.

PHARMACOLOGIOCAL INTERVENTION IN THE BRAIN

The question arises whether the loss of insulin's actions in the brain induced by high-fat feeding are amendable to pharmacological intervention. In **chapter 5** we studied the effects of topiramate on insulin sensitivity as assessed by hyperinsulinemic-euglycemic clamp analysis. Topiramate, a sulfamate-substituted derivative of the monosaccharide D-fructose (79), is a broad-spectrum antiepileptic drug with potentially additional neurotherapeutic applications such as bipolar disorder and migraine (80;81). Its precise mechanism of action is unknown, although the antiepileptic effects of topiramate are mediated through at least six mechanisms of action within the central nervous system: (i) enhancement of GABA-ergic activity (82;83), (ii) inhibition of kainite/AMPA receptors (84), (iii) inhibition of voltage-dependent sodium channels (85), (iv) inhibition of high-voltage-activated calcium channels (86), (v) increase in potassium conductance (87) and (vi) inhibition of carbonic anhydrase (88). Besides its antiepileptic action, topiramate usage is associated with decreases in body weight. The reduction in body weight by topiramate treatment has been shown in epileptic patients as well as in obese, non-epileptic, persons (89-91). Although loss of appetite resulting in reduced caloric intake can account for initial reductions in body weight, other mechanisms might be involved in the long-term effects of topiramate on weight, as weight loss continued after caloric intake returned to baseline levels (91). Even though the half-life of topiramate is lower in rodents than in humans (~1-2 h), several studies have confirmed that topiramate also reduces food intake and body weight in lean as well as in obese mouse and rat models (92;93). Studies in obese, diabetic rats demonstrate that topiramate treatment reduces plasma glucose levels and improves insulin sensitivity independent of weight loss (94;95). In line with this, we document improved insulin sensitivity in our mice in absence of a reduction in body weight. This improvement in insulin sensitivity was present in (cardiac and skeletal) muscle and adipose tissue, but not in liver. As the concentration of topiramate in plasma correlates with that in cerebral spinal fluid (CSF) (96) and topiramate's

effects on body weight, body composition and energy metabolism are associated with altered neuropeptide expression in the hypothalamus (97), whereas topiramate does not have a direct effect on insulin sensitivity in muscle cells, we hypothesized that the brain mediates the insulin sensitizing effects of topiramate. Since tolbutamide inhibits activation of neuronal K_{ATP} channels by insulin in insulin sensitive subjects, tolbutamide was used to demonstrate the involvement of the brain in the insulin sensitizing effect of topiramate. Central administration of tolbutamide in our mice had no effect on insulin sensitivity during hyperinsulinemic-euglycemic clamp, suggesting insulin resistance in the brain induced by high-fat feeding. I.c.v. tolbutamide in topiramate treated mice inhibited the insulin sensitizing effect of topiramate, suggesting that the improved insulin sensitivity by topiramate originates from an insulin sensitizing effect in the brain directed at muscle and adipose tissue but not liver. This improved insulin sensitivity in muscle and adipose tissue, but not in liver, has previously been associated with enhanced AMPK phosphorylation in muscle but not in liver (92). As α-adrenergic stimulation enhances AMPK phosphorylation, the increased glucose uptake by peripheral organs might be related to increased sympathetic nervous system (SNS) activity (98).

Topiramate treatment has some negative side-effects that need to be overcome before it can be widely used in the clinics as an antidiabetic drug. Drowsiness, dizziness, fatigue and nervousness are common side-effects. Furthermore, determination of body composition by dual-energy X-ray absorptiometry in our mice showed a significant reduction in bone mineral density, in line with reports that topiramate treatment in epileptic children and young women results in hypocalcaemia, increased bone turnover and reduced bone mineral density (99;100), suggesting that topiramate has negative long-term effects on bone development. Taken together, topiramate improves insulin resistance by restoring insulin sensitivity in the brain and this feature renders topiramate as an exciting new drug when negative side effects are overcome, to treat diabetes by itself or in combination with classic antidiabetic drugs.

Other drugs that improve insulin sensitivity probably in part via action in the brain are GLP-1 analogues. GLP-1 is a gut hormone, secreted in response to food. GLP-1 has many beneficial actions: it enhances glucose-stimulated insulin secretion, improves blood glucose profiles in type 2 diabetes patients, reduces body weight and food intake and slows gastric emptying. However, the half-life of native GLP-1 is only a few minutes in humans. Therefore, pharmaceutical companies are developing GLP-1 analogues that have the same beneficial qualities, but with a longer half-life. GLP-1 improves insulin sensitivity in part via activation of GLP-1 receptors in the brain (101;102). The neuronal circuits that are activated by peripheral administered GLP-1 (or its analogues) remain to be identified. One mode of action of GLP-1 could be a modulation of the NPY pathway in the hypothalamus, as i.c.v. GLP-1 completely prevents the orexigenic effects of NPY (103). Furthermore, GLP-1 has been reported to reduce NPY neuronal activity (104). Since NPY has been linked to insulin resistance, chronic administration of GLP-1 or any of its analogues may antagonize NPY-induced insulin resistance. GLP-1 can also improve insulin sensitivity by acting in the brainstem. Located in the brainstem, the nucleus of the solitary tract (NTS) receives vagal afferent input from the gastrointestinal tract. GLP-1 (or its analogues) can activate neurons in the NTS via afferent vagal input (105;106). Elucidating the precise molecular events in the brain that underlie the effects of GLP-1 (and its analogues) will lead to new or improved therapeutic agents.

CONCLUDING REMARKS

As the brain is clearly involved in maintaining peripheral homeostasis, experimental therapies with action in the brain should be considered as promising strategies for the treatment of T2DM and T2DM-associated complications. Disruptions in circadian rhythm, resulting in altered output by the SCN, have an immediate effect on energy metabolism and insulin sensitivity. It has become clear that the brain is able to directly sense circulating hormones and nutrients that provide the brain with information regarding the metabolic status of the body. Thyroid hormones affect glucose metabolism, and possible other processes as well, possibly via action in the brain. Insulin's action in glucose and FA metabolism results in part via central mechanisms. High-fat diet induces not only peripheral insulin resistance, but also central insulin resistance, which can contribute to the pathophysiology of T2DM. Restoring insulin sensitivity in the brain, as we have observed with topiramate, may be a promising new target for T2DM therapies or can extend the action of current therapies.

REFERENCE LIST

1. Wild, S, Roglic, G, Green, A, Sicree, R, King, H: Global prevalence of diabetes: estimates for the year 2000 and projections for 2030. *Diabetes Care* 27:1047-1053, 2004

2. Obici, S, Feng, Z, Karkanias, G, Baskin, DG, Rossetti, L: Decreasing hypothalamic insulin receptors causes hyperphagia and insulin resistance in rats. *Nat Neurosci* 5:566-572, 2002

3. Obici, S, Zhang, BB, Karkanias, G, Rossetti, L: Hypothalamic insulin signaling is required for inhibition of glucose production. *Nat Med* 8:1376-1382, 2002

4. Takahashi, JS, Hong, HK, Ko, CH, McDearmon, EL: The genetics of mammalian circadian order and disorder: implications for physiology and disease. *Nat Rev Genet* 9:764-775, 2008

5. Panda, S, Hogenesch, JB, Kay, SA: Circadian rhythms from flies to human. *Nature* 417:329-335, 2002

6. La Fleur, SE, Kalsbeek, A, Wortel, J, Buijs, RM: A suprachiasmatic nucleus generated rhythm in basal glucose concentrations. *J Neuroendocrinol* 11:643-652, 1999

7. Ruiter, M, La Fleur, SE, Van, HC, van, d, V, Kalsbeek, A, Buijs, RM: The daily rhythm in plasma glucagon concentrations in the rat is modulated by the biological clock and by feeding behavior. *Diabetes* 52:1709-1715, 2003

8. Ando, H, Yanagihara, H, Hayashi, Y, Obi, Y, Tsuruoka, S, Takamura, T, Kaneko, S, Fujimura, A: Rhythmic messenger ribonucleic acid expression of clock genes and adipocytokines in mouse visceral adipose tissue. *Endocrinology* 146:5631-5636, 2005

9. De Boer, SF, Van der Gugten, J: Daily variations in plasma noradrenaline, adrenaline and corticosterone concentrations in rats. *Physiol Behav* 40:323-328, 1987

10. Bodosi, B, Gardi, J, Hajdu, I, Szentirmai, E, Obal, F, Jr., Krueger, JM: Rhythms of ghrelin, leptin, and sleep in rats: effects of the normal diurnal cycle, restricted feeding, and sleep deprivation. *Am J Physiol Regul Integr Comp Physiol* 287:R1071-R1079, 2004

11. Davidson, AJ, Castanon-Cervantes, O, Stephan, FK: Daily oscillations in liver function: diurnal vs circadian rhythmicity. *Liver Int* 24:179-186, 2004

12. La Fleur, SE: Daily rhythms in glucose metabolism: suprachiasmatic nucleus output to peripheral tissue. *J Neuroendocrinol* 15:315-322, 2003

13. Froy, O, Chapnik, N, Miskin, R: Long-lived alphaMUPA transgenic mice exhibit pronounced circadian rhythms. *Am J Physiol Endocrinol Metab* 291:E1017-E1024, 2006

14. Lee, C, Etchegaray, JP, Cagampang, FR, Loudon, AS, Reppert, SM: Posttranslational mechanisms regulate the mammalian circadian clock. *Cell* 107:855-867, 2001

15. Zvonic, S, Ptitsyn, AA, Conrad, SA, Scott, LK, Floyd, ZE, Kilroy, G, Wu, X, Goh, BC, Mynatt, RL, Gimble, JM: Characterization of peripheral circadian clocks in adipose tissues. *Diabetes* 55:962-970, 2006

16. Reppert, SM, Weaver, DR: Coordination of circadian timing in mammals. *Nature* 418:935-941, 2002

17. Herzog, ED, Takahashi, JS, Block, GD: Clock controls circadian period in isolated suprachiasmatic nucleus neurons. *Nat Neurosci* 1:708-713, 1998

18. Quintero, JE, Kuhlman, SJ, McMahon, DG: The biological clock nucleus: a multiphasic oscillator network regulated by light. *J Neurosci* 23:8070-8076, 2003

19. Buijs, RM, Hermes, MH, Kalsbeek, A: The suprachiasmatic nucleus-paraventricular nucleus interactions: a bridge to the neuroendocrine and autonomic nervous system. *Prog Brain Res* 119:365-382, 1998

20. Kennaway, DJ, Voultsios, A, Varcoe, TJ, Moyer, RW: Melatonin in mice: rhythms, response to light, adrenergic stimulation, and metabolism. *Am J Physiol Regul Integr Comp Physiol* 282:R358-R365, 2002

21. Nagai, K, Nagai, N, Shimizu, K, Chun, S, Nakagawa, H, Niijima, A: SCN output drives the autonomic nervous system: with special reference to the autonomic function related to the regulation of glucose metabolism. *Prog Brain Res* 111:253-272, 1996

22. Panda, S, Hogenesch, JB, Kay, SA: Circadian rhythms from flies to human. *Nature* 417:329-335, 2002

23. Welsh, DK, Yoo, SH, Liu, AC, Takahashi, JS, Kay, SA: Bioluminescence imaging of individual fibroblasts reveals persistent, independently phased circadian rhythms of clock gene expression. *Curr Biol* 14:2289-2295, 2004

24. Yoo, SH, Yamazaki, S, Lowrey, PL, Shimomura, K, Ko, CH, Buhr, ED, Siepka, SM, Hong, HK, Oh, WJ, Yoo, OJ, Menaker, M, Takahashi, JS: PERIOD2::LUCIFERASE real-time reporting of circadian dynamics reveals persistent circadian oscillations in mouse peripheral tissues. *Proc Natl Acad Sci U S A* 101:5339-5346, 2004

25. Kalsbeek, A, Fliers, E, Romijn, JA, La Fleur, SE, Wortel, J, Bakker, O, Endert, E, Buijs, RM: The suprachiasmatic nucleus generates the diurnal changes in plasma leptin levels. *Endocrinology* 142:2677-2685, 2001

26. Benedict, C, Hallschmid, M, Lassen, A, Mahnke, C, Schultes, B, Schioth, HB, Born, J, Lange, T: Acute sleep deprivation reduces energy expenditure in healthy men. *Am J Clin Nutr* 93:1229-1236, 2011

27. Donga, E, van, DM, van Dijk, JG, Biermasz, NR, Lammers, GJ, van, KK, Hoogma, RP, Corssmit, EP, Romijn, JA: Partial sleep restriction decreases insulin sensitivity in type 1 diabetes. *Diabetes Care* 33:1573-1577, 2010

28. Donga, E, van, DM, van Dijk, JG, Biermasz, NR, Lammers, GJ, van Kralingen, KW, Corssmit, EP, Romijn, JA: A single night of partial sleep deprivation induces insulin resistance in multiple metabolic pathways in healthy subjects. *J Clin Endocrinol Metab* 95:2963-2968, 2010

29. Karlsson, B, Knutsson, A, Lindahl, B: Is there an association between shift work and having a metabolic syndrome? Results from a population based study of 27, 485 people. *Occup Environ Med* 58:747-752, 2001

30. Dochi, M, Suwazono, Y, Sakata, K, Okubo, Y, Oishi, M, Tanaka, K, Kobayashi, E, Nogawa, K: Shift work is a risk factor for increased total cholesterol level: a 14-year prospective cohort study in 6886 male workers. *Occup Environ Med* 66:592-597, 2009

31. Buijs, RM, Scheer, FA, Kreier, F, Yi, C, Bos, N, Goncharuk, VD, Kalsbeek, A: Organization of circadian functions: interaction with the body. *Prog Brain Res* 153:341-360, 2006

32. Anea, CB, Zhang, M, Stepp, DW, Simkins, GB, Reed, G, Fulton, DJ, Rudic, RD: Vascular disease in mice with a dysfunctional circadian clock. *Circulation* 119:1510-1517, 2009

33. Rudic, RD, McNamara, P, Curtis, AM, Boston, RC, Panda, S, Hogenesch, JB, Fitzgerald, GA: BMAL1 and CLOCK, two essential components of the circadian clock, are involved in glucose homeostasis. *PLoS Biol* 2:e377, 2004

34. Turek, FW, Joshu, C, Kohsaka, A, Lin, E, Ivanova, G, McDearmon, E, Laposky, A, Losee-Olson, S, Easton, A, Jensen, DR, Eckel, RH, Takahashi, JS, Bass, J: Obesity and metabolic syndrome in circadian Clock mutant mice. *Science* 308:1043-1045, 2005

35. Arble, DM, Bass, J, Laposky, AD, Vitaterna, MH, Turek, FW: Circadian timing of food intake contributes to weight gain. *Obesity (Silver Spring)* 17:2100-2102, 2009

36. Bray, MS, Tsai, JY, Villegas-Montoya, C, Boland, BB, Blasier, Z, Egbejimi, O, Kueht, M, Young, ME: Time-of-day-dependent dietary fat consumption influences multiple cardiometabolic syndrome parameters in mice. *Int J Obes (Lond)* 34:1589-1598, 2010

37. Salgado-Delgado, R, ngeles-Castellanos, M, Saderi, N, Buijs, RM, Escobar, C: Food intake during the normal activity phase prevents obesity and circadian desynchrony in a rat model of night work. *Endocrinology* 151:1019-1029, 2010

38. Kalsbeek, A, La, FS, Van, HC, Buijs, RM: Suprachiasmatic GABAergic inputs to the

paraventricular nucleus control plasma glucose concentrations in the rat via sympathetic innervation of the liver. *J Neurosci* 24:7604-7613, 2004

39. Biermasz, NR, Joustra, SD, Donga, E, Pereira, AM, van, DN, van, DM, van der Klaauw, AA, Corssmit, EP, Lammers, GJ, van Kralingen, KW, van Dijk, JG, Romijn, JA: Patients previously treated for nonfunctioning pituitary macroadenomas have disturbed sleep characteristics, circadian movement rhythm, and subjective sleep quality. *J Clin Endocrinol Metab* 96:1524-1532, 2011

40. Biermasz, NR, van, DH, Roelfsema, F: Direct postoperative and follow-up results of transsphenoidal surgery in 19 acromegalic patients pretreated with octreotide compared to those in untreated matched controls. *J Clin Endocrinol Metab* 84:3551-3555, 1999

41. McColm, JR, Stenson, BJ, Biermasz, N, McIntosh, N: Measurement of interleukin 10 in bronchoalveolar lavage from preterm ventilated infants. *Arch Dis Child Fetal Neonatal Ed* 82:F156-F159, 2000

42. Biermasz, NR, van, DH, Roelfsema, F: Long-term follow-up results of postoperative radiotherapy in 36 patients with acromegaly. *J Clin Endocrinol Metab* 85:2476-2482, 2000

43. Biermasz, NR, Dulken, HV, Roelfsema, F: Postoperative radiotherapy in acromegaly is effective in reducing GH concentration to safe levels. *Clin Endocrinol (Oxf)* 53:321-327, 2000

44. Manber, R, Bootzin, RR, Acebo, C, Carskadon, MA: The effects of regularizing sleep-wake schedules on daytime sleepiness. *Sleep* 19:432-441, 1996

45. Bruning, JC, Gautam, D, Burks, DJ, Gillette, J, Schubert, M, Orban, PC, Klein, R, Krone, W, Muller-Wieland, D, Kahn, CR: Role of brain insulin receptor in control of body weight and reproduction. *Science* 289:2122-2125, 2000

46. Perrin, C, Knauf, C, Burcelin, R: Intracerebroventricular infusion of glucose, insulin, and the adenosine monophosphate-activated kinase activator, 5-aminoimidazole-4-carboxamide-1-beta-D-ribofuranoside, controls muscle glycogen synthesis. *Endocrinology* 145:4025-4033, 2004

47. Zawar, C, Plant, TD, Schirra, C, Konnerth, A, Neumcke, B: Cell-type specific expression of ATP-sensitive potassium channels in the rat hippocampus. *J Physiol* 514 (Pt 2):327-341, 1999

48. Trapp, S, Ballanyi, K: K$_{ATP}$ channel mediation of anoxia-induced outward current in rat dorsal vagal neurons in vitro. *J Physiol* 487 (Pt 1):37-50, 1995

49. Fujimura, N, Tanaka, E, Yamamoto, S, Shigemori, M, Higashi, H: Contribution of ATP-sensitive potassium channels to hypoxic hyperpolarization in rat hippocampal CA1 neurons in vitro. *J Neurophysiol* 77:378-385, 1997

50. Dunn-Meynell, AA, Rawson, NE, Levin, BE: Distribution and phenotype of neurons containing the ATP-sensitive K+ channel in rat brain. *Brain Res* 814:41-54, 1998

51. Ibrahim, N, Bosch, MA, Smart, JL, Qiu, J, Rubinstein, M, Ronnekleiv, OK, Low, MJ, Kelly, MJ: Hypothalamic proopiomelanocortin neurons are glucose responsive and express K(ATP) channels. *Endocrinology* 144:1331-1340, 2003

52. Pocai, A, Lam, TK, Gutierrez-Juarez, R, Obici, S, Schwartz, GJ, Bryan, J, guilar-Bryan, L, Rossetti, L: Hypothalamic K(ATP) channels control hepatic glucose production. *Nature* 434:1026-1031, 2005

53. Kishore, P, Boucai, L, Zhang, K, Li, W, Koppaka, S, Kehlenbrink, S, Schiwek, A, Esterson, YB, Mehta, D, Bursheh, S, Su, Y, Gutierrez-Juarez, R, Muzumdar, R, Schwartz, GJ, Hawkins, M: Activation of K$_{ATP}$ channels suppresses glucose production in humans. *J Clin Invest* 2011

54. Inagaki, N, Gonoi, T, Clement, JP, Wang, CZ, Aguilar-Bryan, L, Bryan, J, Seino, S: A family of sulfonylurea receptors determines the pharmacological properties of ATP-sensitive K+ channels. *Neuron* 16:1011-1017, 1996

55. Inagaki, N, Gonoi, T, Clement, JP, Namba, N, Inazawa, J, Gonzalez, G, Aguilar-Bryan, L, Seino, S, Bryan, J: Reconstitution of IKATP: an inward rectifier subunit plus the sulfonylurea receptor. *Science* 270:1166-1170, 1995

56. van Houten, M, Posner, BI, Kopriwa, BM, Brawer, JR: Insulin-binding sites in the rat brain: in vivo localization to the circumventricular organs by quantitative radioautography. *Endocrinology* 105:666-673, 1979

57. Shiuchi, T, Haque, MS, Okamoto, S, Inoue, T, Kageyama, H, Lee, S, Toda, C, Suzuki, A, Bachman, ES, Kim, YB, Sakurai, T, Yanagisawa, M, Shioda, S, Imoto, K, Minokoshi, Y: Hypothalamic orexin stimulates feeding-associated glucose utilization in skeletal muscle via sympathetic nervous system. *Cell Metab* 10:466-480, 2009

58. Obici, S, Feng, Z, Tan, J, Liu, L, Karkanias, G, Rossetti, L: Central melanocortin receptors regulate insulin action. *J Clin Invest* 108:1079-1085, 2001

59. Heijboer, AC, van den Hoek, AM, Pijl, H, Voshol, PJ, Havekes, LM, Romijn, JA, Corssmit, EP: Intracerebroventricular administration

of melanotan II increases insulin sensitivity of glucose disposal in mice. *Diabetologia* 48:1621-1626, 2005

60. Toda, C, Shiuchi, T, Lee, S, Yamato-Esaki, M, Fujino, Y, Suzuki, A, Okamoto, S, Minokoshi, Y: Distinct effects of leptin and a melanocortin receptor agonist injected into medial hypothalamic nuclei on glucose uptake in peripheral tissues. *Diabetes* 58:2757-2765, 2009

61. Teusink, B, Voshol, PJ, Dahlmans, VE, Rensen, PC, Pijl, H, Romijn, JA, Havekes, LM: Contribution of fatty acids released from lipolysis of plasma triglycerides to total plasma fatty acid flux and tissue-specific fatty acid uptake. *Diabetes* 52:614-620, 2003

62. Scherer, T, O'Hare, J, ggs-Andrews, K, Schweiger, M, Cheng, B, Lindtner, C, Zielinski, E, Vempati, P, Su, K, Dighe, S, Milsom, T, Puchowicz, M, Scheja, L, Zechner, R, Fisher, SJ, Previs, SF, Buettner, C: Brain insulin controls adipose tissue lipolysis and lipogenesis. *Cell Metab* 13:183-194, 2011

63. Koch, L, Wunderlich, FT, Seibler, J, Konner, AC, Hampel, B, Irlenbusch, S, Brabant, G, Kahn, CR, Schwenk, F, Bruning, JC: Central insulin action regulates peripheral glucose and fat metabolism in mice. *J Clin Invest* 118:2132-2147, 2008

64. Kreier, F, Fliers, E, Voshol, PJ, Van Eden, CG, Havekes, LM, Kalsbeek, A, Van Heijningen, CL, Sluiter, AA, Mettenleiter, TC, Romijn, JA, Sauerwein, HP, Buijs, RM: Selective parasympathetic innervation of subcutaneous and intra-abdominal fat--functional implications. *J Clin Invest* 110:1243-1250, 2002

65. Habets, DD, Coumans, WA, Voshol, PJ, den Boer, MA, Febbraio, M, Bonen, A, Glatz, JF, Luiken, JJ: AMPK-mediated increase in myocardial long-chain fatty acid uptake critically depends on sarcolemmal CD36. *Biochem Biophys Res Commun* 355:204-210, 2007

66. Sparks, JD, Sparks, CE: Insulin regulation of triacylglycerol-rich lipoprotein synthesis and secretion. *Biochim Biophys Acta* 1215:9-32, 1994

67. Ginsberg, HN, Zhang, YL, Hernandez-Ono, A: Metabolic syndrome: focus on dyslipidemia. *Obesity (Silver Spring)* 14 Suppl 1:41S-49S, 2006

68. Arase, K, Fisler, JS, Shargill, NS, York, DA, Bray, GA: Intracerebroventricular infusions of 3-OHB and insulin in a rat model of dietary obesity. *Am J Physiol* 255:R974-R981, 1988

69. Ono, H, Pocai, A, Wang, Y, Sakoda, H, Asano, T, Backer, JM, Schwartz, GJ, Rossetti, L: Activation of hypothalamic S6 kinase mediates diet-induced hepatic insulin resistance in rats. *J Clin Invest* 118:2959-2968, 2008

70. Spanswick, D, Smith, MA, Mirshamsi, S, Routh, VH, Ashford, ML: Insulin activates ATP-sensitive K+ channels in hypothalamic neurons of lean, but not obese rats. *Nat Neurosci* 3:757-758, 2000

71. Woods, SC, D'Alessio, DA, Tso, P, Rushing, PA, Clegg, DJ, Benoit, SC, Gotoh, K, Liu, M, Seeley, RJ: Consumption of a high-fat diet alters the homeostatic regulation of energy balance. *Physiol Behav* 83:573-578, 2004

72. Dimitriadis, GD, Raptis, SA: Thyroid hormone excess and glucose intolerance. *Exp Clin Endocrinol Diabetes* 109 Suppl 2:S225-S239, 2001

73. Raboudi, N, Arem, R, Jones, RH, Chap, Z, Pena, J, Chou, J, Field, JB: Fasting and postabsorptive hepatic glucose and insulin metabolism in hyperthyroidism. *Am J Physiol* 256:E159-E166, 1989

74. Okajima, F, Ui, M: Metabolism of glucose in hyper- and hypo-thyroid rats in vivo. Minor role of endogenous insulin in thyroid-dependent changes in glucose turnover. *Biochem J* 182:577-584, 1979

75. Okajima, F, Ui, M: Metabolism of glucose in hyper- and hypo-thyroid rats in vivo. Glucose-turnover values and futile-cycle activities obtained with ^{14}C- and ^{3}H-labelled glucose. *Biochem J* 182:565-575, 1979

76. Klieverik, LP, Foppen, E, Ackermans, MT, Serlie, MJ, Sauerwein, HP, Scanlan, TS, Grandy, DK, Fliers, E, Kalsbeek, A: Central effects of thyronamines on glucose metabolism in rats. *J Endocrinol* 201:377-386, 2009

77. Klieverik, LP, Janssen, SF, van, RA, Foppen, E, Bisschop, PH, Serlie, MJ, Boelen, A, Ackermans, MT, Sauerwein, HP, Fliers, E, Kalsbeek, A: Thyroid hormone modulates glucose production via a sympathetic pathway from the hypothalamic paraventricular nucleus to the liver. *Proc Natl Acad Sci U S A* 106:5966-5971, 2009

78. Klieverik, LP, Sauerwein, HP, Ackermans, MT, Boelen, A, Kalsbeek, A, Fliers, E: Effects of thyrotoxicosis and selective hepatic autonomic denervation on hepatic glucose metabolism in rats. *Am J Physiol Endocrinol Metab* 294:E513-E520, 2008

79. Shank, RP, Gardocki, JF, Streeter, AJ, Maryanoff, BE: An overview of the preclinical aspects of topiramate: pharmacology, pharmacokinetics, and mechanism of action. *Epilepsia* 41 Suppl 1:S3-S9, 2000

80. Ferrari, A, Tiraferri, I, Neri, L, Sternieri, E: Clinical pharmacology of topiramate in migraine prevention. *Expert Opin Drug Metab Toxicol* 7:1169-1181, 2011

81. McIntyre, RS, Riccardelli, R, Binder, C, Kusumakar, V: Open-label adjunctive topiramate in the treatment of unstable bipolar disorder. *Can J Psychiatry* 50:415-422, 2005

82. White, HS, Brown, SD, Woodhead, JH, Skeen, GA, Wolf, HH: Topiramate modulates GABA-evoked currents in murine cortical neurons by a nonbenzodiazepine mechanism. *Epilepsia* 41 Suppl 1:S17-S20, 2000

83. White, HS, Brown, SD, Woodhead, JH, Skeen, GA, Wolf, HH: Topiramate enhances GABA-mediated chloride flux and GABA-evoked chloride currents in murine brain neurons and increases seizure threshold. *Epilepsy Res* 28:167-179, 1997

84. Gibbs, JW, III, Sombati, S, DeLorenzo, RJ, Coulter, DA: Cellular actions of topiramate: blockade of kainate-evoked inward currents in cultured hippocampal neurons. *Epilepsia* 41 Suppl 1:S10-S16, 2000

85. Zona, C, Ciotti, MT, Avoli, M: Topiramate attenuates voltage-gated sodium currents in rat cerebellar granule cells. *Neurosci Lett* 231:123-126, 1997

86. Zhang, X, Velumian, AA, Jones, OT, Carlen, PL: Modulation of high-voltage-activated calcium channels in dentate granule cells by topiramate. *Epilepsia* 41 Suppl 1:S52-S60, 2000

87. Herrero, AI, Del, ON, Gonzalez-Escalada, JR, Solis, JM: Two new actions of topiramate: inhibition of depolarizing GABA(A)-mediated responses and activation of a potassium conductance. *Neuropharmacology* 42:210-220, 2002

88. Dodgson, SJ, Shank, RP, Maryanoff, BE: Topiramate as an inhibitor of carbonic anhydrase isoenzymes. *Epilepsia* 41 Suppl 1:S35-S39, 2000

89. Eliasson, B, Gudbjornsdottir, S, Cederholm, J, Liang, Y, Vercruysse, F, Smith, U: Weight loss and metabolic effects of topiramate in overweight and obese type 2 diabetic patients: randomized double-blind placebo-controlled trial. *Int J Obes (Lond)* 2007

90. Stenlof, K, Rossner, S, Vercruysse, F, Kumar, A, Fitchet, M, Sjostrom, L: Topiramate in the treatment of obese subjects with drug-naive type 2 diabetes. *Diabetes Obes Metab* 9:360-368, 2007

91. Ben-Menachem, E, Axelsen, M, Johanson, EH, Stagge, A, Smith, U: Predictors of weight loss in adults with topiramate-treated epilepsy. *Obes Res* 11:556-562, 2003

92. Wilkes, JJ, Nguyen, MT, Bandyopadhyay, GK, Nelson, E, Olefsky, JM: Topiramate treatment causes skeletal muscle insulin sensitization and increased Acrp30 secretion in high-fat-fed male Wistar rats. *Am J Physiol Endocrinol Metab* 289:E1015-E1022, 2005

93. Lalonde, J, Samson, P, Poulin, S, Deshaies, Y, Richard, D: Additive effects of leptin and topiramate in reducing fat deposition in lean and obese ob/ob mice. *Physiol Behav* 80:415-420, 2004

94. Picard, F, Deshaies, Y, Lalonde, J, Samson, P, Richard, D: Topiramate reduces energy and fat gains in lean (Fa/?) and obese (fa/fa) Zucker rats. *Obes Res* 8:656-663, 2000

95. Wilkes, JJ, Nelson, E, Osborne, M, Demarest, KT, Olefsky, JM: Topiramate is an insulin-sensitizing compound in vivo with direct effects on adipocytes in female ZDF rats. *Am J Physiol Endocrinol Metab* 288:E617-E624, 2005

96. Christensen, J, Hojskov, CS, Dam, M, Poulsen, JH: Plasma concentration of topiramate correlates with cerebrospinal fluid concentration. *Ther Drug Monit* 23:529-535, 2001

97. York, DA, Singer, L, Thomas, S, Bray, GA: Effect of topiramate on body weight and body composition of osborne-mendel rats fed a high-fat diet: alterations in hormones, neuropeptide, and uncoupling-protein mRNAs. *Nutrition* 16:967-975, 2000

98. Minokoshi, Y, Kim, YB, Peroni, OD, Fryer, LG, Muller, C, Carling, D, Kahn, BB: Leptin stimulates fatty-acid oxidation by activating AMP-activated protein kinase. *Nature* 415:339-343, 2002

99. Heo, K, Rhee, Y, Lee, HW, Lee, SA, Shin, DJ, Kim, WJ, Song, HK, Song, K, Lee, BI: The effect of topiramate monotherapy on bone mineral density and markers of bone and mineral metabolism in premenopausal women with epilepsy. *Epilepsia* 52:1884-1889, 2011

100. Zhang, J, Wang, KX, Wei, Y, Xu, MH, Su, JM, Bao, YG, Zhao, SY: [Effect of topiramate and carbamazepine on bone metabolism in children with epilepsy]. *Zhongguo Dang Dai Er Ke Za Zhi* 12:96-98, 2010

101. Parlevliet, ET, de Leeuw van Weenen JE, Romijn, JA, Pijl, H: GLP-1 treatment reduces endogenous insulin resistance via activation of central GLP-1 receptors in mice fed a high-fat diet. *Am J Physiol Endocrinol Metab* 299:E318-E324, 2010

102. Knauf, C, Cani, PD, Perrin, C, Iglesias, MA, Maury, JF, Bernard, E, Benhamed, F, Gremeaux, T, Drucker, DJ, Kahn, CR, Girard, J, Tanti, JF, Delzenne, NM, Postic, C, Burcelin, R: Brain glucagon-like peptide-1 increases insulin secretion and muscle insulin resistance to

favor hepatic glycogen storage. *J Clin Invest* 115:3554-3563, 2005

103. Turton, MD, O'Shea, D, Gunn, I, Beak, SA, Edwards, CM, Meeran, K, Choi, SJ, Taylor, GM, Heath, MM, Lambert, PD, Wilding, JP, Smith, DM, Ghatei, MA, Herbert, J, Bloom, SR: A role for glucagon-like peptide-1 in the central regulation of feeding. *Nature* 379:69-72, 1996

104. Seo, S, Ju, S, Chung, H, Lee, D, Park, S: Acute effects of glucagon-like peptide-1 on hypothalamic neuropeptide and AMP activated kinase expression in fasted rats. *Endocr J* 55:867-874, 2008

105. Parkinson, JR, Chaudhri, OB, Kuo, YT, Field, BC, Herlihy, AH, Dhillo, WS, Ghatei, MA, Bloom, SR, Bell, JD: Differential patterns of neuronal activation in the brainstem and hypothalamus following peripheral injection of GLP-1, oxyntomodulin and lithium chloride in mice detected by manganese-enhanced magnetic resonance imaging (MEMRI). *Neuroimage* 44:1022-1031, 2009

106. Abbott, CR, Monteiro, M, Small, CJ, Sajedi, A, Smith, KL, Parkinson, JR, Ghatei, MA, Bloom, SR: The inhibitory effects of peripheral administration of peptide YY(3-36) and glucagon-like peptide-1 on food intake are attenuated by ablation of the vagal-brainstem-hypothalamic pathway. *Brain Res* 1044:127-131, 2005

9

SUMMARY

The prevalence of type 2 diabetes mellitus (T2DM) is rising steadily as a consequence of the growing obesity epidemic. The pathophysiology of T2DM comprises of a combination of insulin resistance and impaired insulin secretion by pancreatic ß-cells, finally resulting in hyperglycemia. In addition to disturbed glucose metabolism, T2DM patients have disturbed lipid metabolism, resulting in concomitant dyslipidemia. Accumulating evidence suggests that the brain is a key player in metabolic regulation and maintenance of metabolic homeostasis. The aim of this thesis was to elucidate the role of the brain in the development of insulin resistance.

The first part of this thesis focused on the role of circadian regulation of insulin sensitivity. Disturbances in circadian rhythms are associated with increased incidence of obesity and T2DM. These disturbances in circadian rhythms can be caused by altered environmental cues, including shift work, jet lag, aging, depression and sleep disorders. In **chapter 2** we examined the effects of a disturbed circadian rhythm on energy metabolism and insulin sensitivity by exposing male C57Bl/6J mice on chow or high-fat diet to constant light. *In vivo* electrophysiological recordings of the central circadian pacemaker, the suprachiasmatic nucleus (SCN), showed that constant light exposure immediately reduces the circadian amplitudes of the SCN neuronal activity pattern and rhythm strength. Constant light exposure immediately resulted in body weight gain, even before high-fat diet feeding resulted in weight gain. The circadian pattern in energy metabolism was completely lost after 5 weeks of constant light exposure. Furthermore, constant light exposure neutralized the normal circadian variation in insulin sensitivity of the liver as well as of peripheral tissues. We concluded that constant light exposure reduces SCN rhythm strength and results in a complete absence of rhythm in energy metabolism and insulin sensitivity.

In **chapter 3** we studied the role of the SCN in the circadian regulation of energy homeostasis and insulin sensitivity. In male, chow fed C57Bl/6J mice, the SCN was bilaterally destroyed by thermic ablation. SCN lesions resulted in loss of circadian rhythm as determined by periodogram analysis. The circadian rhythm in energy metabolism was also completely lost, whereas total energy intake or expenditure was not different between sham and SCN lesioned mice. Nonetheless, deletion of the SCN resulted in a small, but significant increase in body weight, which was accounted for by an increase in fat mass. Furthermore, SCN lesions resulted in hyperglycemia, hyperinsulinemia and severe hepatic insulin resistance. We concluded that bilateral lesions of the SCN resulted in mild overweight and in severe hepatic insulin resistance, again suggesting that malfunctioning of the SCN could be involved in the development of T2DM. Apparently, a reduction in SCN output, as studied in **chapter 2**, resulted in loss of circadian variation in insulin sensitivity, whereas a complete loss in SCN function, as studied in **chapter 3**, caused severe insulin resistance.

The second part of this thesis focused on the role of insulin signaling in the brain. Insulin normalizes plasma glucose levels after a meal by inhibiting the endogenous glucose production (EGP) as well as by stimulating glucose uptake in peripheral tissues, and hypothalamic insulin signaling is required for the inhibitory effects of insulin on EGP. In **chapter 4** we examined the role of the brain in insulin-stimulated tissue-specific glucose uptake. Tolbutamide, an inhibitor of ATP-sensitive potassium (K_{ATP}) channels, or vehicle, was infused intracerebroventricular (i.c.v.)

in the basal state and during hyperinsulinemic-euglycemic conditions in male C57Bl/6J mice on chow or on high-fat diet. On chow diet, i.c.v. administration of tolbutamide impaired the ability of insulin to inhibit EGP during hyperinsulinemicclamp conditions. In addition, i.c.v. tolbutamide diminished insulin-stimulated glucose uptake in muscle, but not in heart or adipose tissue. In contrast, in high-fat fed, insulin resistant mice, i.c.v. administration of tolbutamide did not inhibit the effects of insulin during clamp conditions on EGP or glucose uptake by muscle. We concluded that insulin stimulates glucose uptake in muscle in part through effects via K_{ATP} channels in the brain, in analogy with the inhibitory effects of insulin on EGP and that high-fat diet-induced obesity abolished these central effects of circulating insulin on liver and muscle.

Topiramate is associated with improvement in insulin sensitivity, in addition to its antiepileptic action. The mechanisms underlying the insulin sensitizing effects oftopiramate are unknown. However, these effects could be mediated through the brain as the insulin sensitizing effects of topiramate occur independently of weight loss. In **chapter 5** we investigated the role of the brain in the insulin-sensitizing effects of topiramate both *in vivo* and *in vitro*. Male C57Bl/6J mice were fed a high-fat diet for 6 weeks, to induce insulin resistance, before receiving topiramate or vehicle mixed in high-fat diet for 6 weeks. Therapeutic concentrations of topiramate improved insulin sensitivity, which was the result of improved insulin-mediated glucose uptake by heart, muscle and adipose tissue. Upon i.c.v. infusion of tolbutamide, these insulin sensitizing effects of topiramate were completely abrogated in hyperinsulinemic-euglycemic clamp conditions. Topiramate did not alter glucose uptake or insulin signaling in normal and insulin-resistant C2C12 muscle cells. We concluded that topiramate stimulates insulin-mediated glucose uptake *in vivo* through action in the brain.

Insulin is not only involved in glucose metabolism, but also stimulates fat storage in adipose tissue. In **chapter 6**, we examined the role of the brain in the stimulatory effect of circulating insulin on the tissue-specific retention of fatty acids (FA) from plasma. In male, chow fed C57Bl/6J mice, hyperinsulinemic-euglycemic clamp conditions stimulated the retention of both plasma triglyceride (TG)-derived FA and plasma albumin-bound FA in the various white adipose tissues (WAT), but not in other tissues including brown adipose tissue (BAT). I.c.v. administration of insulin induced a similar pattern of tissue-specific FA partitioning. This effect of i.c.v. insulin administration was not associated with activation of the insulin signaling pathways in adipose tissue. I.c.v. administration of tolbutamideconsiderably reduced (during hyperinsulinemic-euglycemic clamp conditions) and even completely blocked (during i.c.v. administration of insulin) WAT-specific retention of FA from plasma. This central effect of insulin was absent in CD36 deficient mice, indicating that CD36 is the predominant FA transporter in insulin-stimulated FA retention by WAT. In high-fat fed, insulin resistant mice, these stimulating effects of insulin (circulating or i.c.v. administered) on FA retention in WAT were lost. We concluded that, in insulin-sensitive mice, circulating insulin stimulates tissue-specific partitioning of plasma-derived FA in WAT in part through activation of K_{ATP} channels in the brain and that high-fat diet obesity abolished these central effects of circulating insulin on WAT.

Thyroid hormones (TH) are crucial regulators of metabolism that exert their effects probably in part via action in the brain. In **chapter 7** we studied the effects of TH status on whole body energy metabolism. Hyperthyroid rats exhibited markedly increased energy expenditure and

fat oxidation without alterations in spontaneous physical activity. Hypothyroid rats showed a mild decrease in energy expenditure and carbohydrate oxidation. In addition, we studied how these alterations in energy metabolism were associated with tissue-specific FA uptake. The hypermetabolic phenotype of hyperthyroidism was characterized by increased uptake of TG-derived FA in oxidative-tissues, but not in WAT. Conversely, during hypothyroidism TG-derived FA uptake was unaltered in oxidative-tissues, but increased in WAT, which was accompanied by an increased activity in lipoprotein lipase activity. We concluded that TH status determines energy expenditure independently of spontaneous physical activity and that the changes in energy metabolism induced by TH status are accompanied by tissue-specific changes in TG-derived FA uptake.

Taken together, the studies in this thesis contribute to the understanding of the role of the brain in insulin sensitivity. We demonstrated that disturbances in circadian rhythm resulting in alterations in SCN output, can contribute to the development of insulin resistance. We have also shown that insulin-stimulated glucose uptake by muscle and insulin-stimulated FA uptake by WAT is in part dependent on insulin action in the brain. These effects of circulating insulin on peripheral organs via the brain are abrogated by high-fat diet. These brain-dependent effects of insulin could reflect a similar situation for other hormones, for instance thyroid hormones. Furthermore, we demonstrated that topiramateimproves insulin resistance by restoring insulin sensitivity in the brain, suggesting that therapeutical targets in the brain may offer challenging new approaches to treat insulin resistance of peripheral organs in T2DM.

SAMENVATTING

Zwaarlijvigheid (obesitas) is het overmatig opslaan van vet in ons lichaam en wordt veroorzaakt door te veel en te calorierijk eten en te weinig bewegen. Inmiddels heeft de incidentie van obesitas epidemische proporties aangenomen. Als consequentie hiervan lijden ook steeds meer mensen aan suikerziekte (diabetes mellitus type 2). In gezonde mensen wordt de bloedsuikerspiegel (glucose spiegel) strikt gereguleerd om enerzijds te voorkomen dat organen beschadigd worden door een te hoge bloedsuikerspiegel (hyperglycemie) en anderzijds om te voorkomen dat de bloedsuikerspiegel te laag wordt (hypoglycemie) waardoor organen die van glucose afhankelijk zijn, zoals de hersenen, niet meer voldoende brandstof hebben. Het hormoon insuline wordt geproduceerd door de β-cellen van de pancreas als reactie op een maaltijd en is een van de belangrijkste spelers in de regulatie van glucose niveaus in het bloed; het remt de productie van glucose door de lever en stimuleert tegelijkertijd de opname van glucose uit het bloed door spier en vetweefsel. Het netto effect is een normalisatie van de glucose niveaus in het bloed. Diabetes wordt gekenmerkt door een verminderde gevoeligheid voor insuline (insuline resistentie) en een te lage insuline productie. In de beginfase van diabetes, als weefsels al minder gevoelig zijn voor de werking van insuline, is de productie van insuline verhoogd om te zorgen dat het effect van insuline gehandhaafd blijft ondanks de resistentie van de weefsels. Als β-cellen echter niet meer in staat zijn om de verhoogde insuline productie vol te houden, zullen de bloed glucose niveaus stijgen. Dit zal, als het onbehandeld blijft, leiden tot velerlei complicaties en mogelijk zelfs de dood. Insuline is niet alleen betrokken bij de glucose stofwisseling (metabolisme), maar ook bij het vet metabolisme. Het stimuleert de opslag van vet in wit vetweefsel en verlaagt de productie van VLDL (een deeltje dat vet uit de lever naar weefsels transporteert) door de lever. Hierdoor hebben diabetes patiënten ook vaak een verstoord vet metabolisme. De laatste jaren is duidelijk geworden dat de hersenen in belangrijke mate bijdragen aan de regulatie van het metabolisme. Zo is bijvoorbeeld aangetoond dat insuline de glucose productie door de lever deels remt via de hersenen. Als insuline niet zijn functie kan uitoefenen in de hersenen, dan is insuline minder effectief in het remmen van de glucose productie. In dit proefschrift hebben we onderzocht hoe de hersenen bijdragen in de ontwikkeling van insuline resistentie.

Hoofdstuk 1 geeft een introductie in glucose en vet metabolisme. Ook wordt besproken hoe insuline en schildklierhormoon het glucose en vet metabolisme beïnvloeden. De hersenen zijn een belangrijke regulator van het metabolisme. De rol van de hersenen in de regulatie van het glucose en vet metabolisme wordt uiteengezet, met nadruk op de werking van insuline en schildklierhormoon in de hersenen. Verder wordt besproken wat diabetes mellitus type 2 is en wat de huidige behandel methodes zijn. Verstoringen in het dag-nacht (circadiaan) ritme, bv door ploegendiensten, zijn geassocieerd met de ontwikkeling van diabetes. De rol van de biologische klok in het circadiaanritme zal uiteengezet worden en verder worden besproken hoe verstoring van het circadiaan ritme tot diabetes kan leiden. Tenslotteworden de algemene hypothese en inhoud van het proefschrift gepresenteerd.

Het eerste deel van dit proefschrift richtte zich op de rol van de biologische klok in insuline gevoeligheid. Verstoringen in het circadiaan ritme kunnen worden veroorzaakt door ploegendienst, jetlag, depressie en slaapstoornissen, maar ook als we ouder worden, is ons

circadiaan ritme verstoord. In **hoofdstuk 2** onderzochten we de effecten van een verstoord circadiaan ritme op energiehuishouding en insuline gevoeligheid in muizen. Om het normale circadiaan ritme te verstoren werden muizen blootgesteld aan continu licht. Continu licht veroorzaakte geen stress bij de muizen, zoals dat bij mensen wel het geval zou zijn. Elektrofysiologische metingen in de hersenen van deze muizen toonden aan dat constante blootstelling aan licht onmiddellijk een verminderde activiteit in neuronen van de centrale klok (de suprachiasmatische nucleus, SCN) veroorzaakte. Verder resulteerde constant licht in een directe gewichtstoename van de muizen, zelfs voordat een hoog-vet dieet resulteerde in gewichtstoename. Muizen zijn nachtdieren; 's nachts zijn ze actiever en eten dan ook meer. Om bloedsuikerspiegel efficiënter te normaliseren, zijn de muizen 's nachts ook gevoeliger voor de werking van insuline dan overdag. Dit circadiaan ritme in energiehuishouding was na 5 weken in continu licht volledig weg: de muizen waren overdag net zo actief als 's nachts, aten gedurende de hele dag en waren overdag net zo gevoelig voor de werking van insuline als 's nachts. We concludeerden dat continue blootstelling aan licht direct leidt tot verminderde activiteit van de SCN, directe gewichtstoename en afwezigheid van circadiaan ritme in energiehuishouding en insuline gevoeligheid.

In **hoofdstuk 3** onderzochten we welke rol de centrale klok, de SCN, heeft in de regulatie van energiehuishouding en insuline gevoeligheid. Om dit te onderzoeken, hebben we in de hersenen de SCN weggebrand aan twee kanten (bilaterale SCN laesie). Als gevolg hiervan was het circadiaan ritme in de energiehuishouding volledig verloren gegaan: de muizen waren de hele dag door actief en aten hierdoor ook de hele dag. Ondanks dat het circadiaan ritme in energiehuishouding afwezig was, was de totale voedselinname en activiteit niet verandert door de SCN laesie. Toch waren de muizen met SCN laesie iets zwaarder dan de controle muizen door een kleine, maar significante toename in vet massa. Bovendien waren de muizen met SCN laesie erg ongevoelig voor insuline in de lever, wat niet verklaard kon worden door de kleine toename in vet massa. We concludeerden dat bilaterale laesies van de SCN leiden tot een kleine toename in lichaamsgewicht en tot ernstige insuline resistentie. **Hoofdstuk 2** en **3** samen suggereerden dat verstoringen, bv door ploegendienst, of defecten van de centrale klok betrokken kunnen zijn bij de ontwikkeling van diabetes.

Het tweede deel van dit proefschrift richtte zich op de rol van de hersenen in het effect van insuline. Insuline normaliseert glucose niveaus na een maaltijd door glucose productie door de lever te remmen en door opname van glucose inspier en vetweefsel te stimuleren. Het effect van insuline op de glucose productie door de lever loopt deels via de hersenen. In **hoofdstuk 4** onderzochten wij de rol van de hersenen in insuline-gestimuleerde opname van glucose. Het effect van insuline in de hersenen kan geblokkeerd worden door tolbutamide (een remmer van ATP-gevoelige kalium (K_{ATP}) kanalen)direct in hersenvloeistof in te spuiten. Inspuiten van tolbutamide in de hersenenvan muizen verminderde het vermogen van insuline om glucose productie door de lever te remmen, zoals al eerder is aangetoond. Daarnaast verminderde tolbutamide de insuline-gestimuleerde opname van glucose door spieren, maar niet door hart-of vetweefsel. In dieet-geïnduceerde, insuline resistente muizen heeft tolbutamide geen invloed op de effecten van insuline op glucose productie door de lever of glucose-opname door spieren. We concludeerden dat insuline de opname van glucose door spieren deels

stimuleert via K_{ATP} kanaal activatie in de hersenen, net als het remmende effect van insuline op de glucose productie door de lever. Verder concludeerden we dat door dieet-geïnduceerde obesitas de effecten van insuline in de hersenen op lever en spieren verloren zijn.

Topiramaat is een geneesmiddel tegen verschillende vormen van epilepsie. Naast zijn anti-epileptische actie, is topiramaat geassocieerd met verbetering van de insuline gevoeligheid. De mechanismen die hieraan ten grondslag liggen zijn onbekend. Aangezien topiramaat de insuline gevoeligheid kan verbeteren onafhankelijk van gewichtsverlies, zou het kunnen zijn dat de hersenen hierin een rol spelen. In **hoofdstuk 5** onderzochten we of topiramaat de insuline gevoeligheid verbeterd via een effect in de hersenen. Hiertoe kregen muizen eerst een hoog-vet dieet te eten om insuline resistentie te ontwikkelen, voordat topiramaat door het dieet werd gemengd. Therapeutische concentraties van topiramaat verbeterde de insuline gevoeligheid, zonder dat het tot gewichtsverlies leidde. De verbeterde insuline gevoeligheid was het resultaat van verhoogde glucose opname door hart, spier en vetweefsel. Door tolbutamide in de hersenen in te spuiten, kon het effect van topiramaat volledig geblokkeerd worden. Op geïsoleerde spiercellen (gezond of insuline resistent) had topiramaat geen invloed op de glucose opname, wat suggereert dat topiramaat geen direct effect heeft op spiercellen, maar dat het werkt via de hersenen. We concludeerden dat topiramaat via de hersenen de insuline gevoeligheid verbeterd door de glucose opname door hart, spier en vetweefsel te stimuleren.

Insuline is niet alleen betrokken bij glucose metabolisme, maar stimuleert ook de opslag van vetzuren in het vetweefsel. In **hoofdstuk 6** onderzochten we de rol van de hersenen in insuline-gestimuleerde vetzuur opslagin vetweefsel. Een verhoging van insuline niveaus in het bloed zorgde voor een toename in vetzuur opslag in wit vetweefsel, maar niet in andere weefsels zoals bruin vetweefsel. De vetzuren waren afkomstig van zowel triglyceriden als albumine-gebonden (vrije) vetzuren. Inspuiten van insuline direct in hersenvloeistof gaf een vergelijkbaar resultaat. Inspuiten van tolbutamide in de hersenen blokkeerde deels het effect van insuline in het bloed op vetzuur opslag, wat suggereert dat insuline de vetzuur opslag in wit vetweefsel deels via de hersenen stimuleert. De vetzuur vervoerder CD36 is hier hoogstwaarschijnlijk bij betrokken, aangezien het effect van insuline in de hersenen op de vetzuur opslagafwezig was in CD36-deficiente muizen. In dieet-geïnduceerde, insuline resistente muizen had insuline via de hersenen geen effect meer op vetzuur opslag in vetweefsel. Wij concludeerden dat in insuline gevoelige muizen, insuline vetzuur opslag in wit vetweefsel deels stimuleert via K_{ATP} kanaal activatie in de hersenen.

Schildklierhormoon is eenbelangrijke regulator van het metabolisme. Het effect van schildklierhormoon loopt waarschijnlijk deels via de hersenen. In **hoofdstuk 7** hebben we het effect van de schildklierhormoon status bestudeerd op de energiehuishouding. Ratten met verhoogde schildklierhormoon spiegels (hyperthyreoïdie) hadden een verhoogd energieverbruik en verhoogde vet verbranding, maar geen verandering in activiteit. Ratten met lage schildklierhormoon spiegels (hypothyreoïdie) hadden een verlaagd energieverbruik en verlaagde glucose verbranding. Vervolgens hebben we bestudeerd hoe deze veranderingen in de energiehuishouding samen gingen met vetzuur opname. Hyperthyreoïdie ging gepaard met vetzuur opslag afkomstig van triglyceriden in spier en hart, maar niet in vetweefsel.

Hypothyreoidie ging gepaard met vetzuur opslag afkomstig van triglyceriden in vetweefsel, maar niet in spier of hart. Een lokale toename in activiteit van het enzym lipoproteïne lipase zorgde ervoor dat vetzuren uit triglyceriden werden vrijgemaakt. Opname van albumine-gebonden vetzuren was niet onderhevig aan weefsel-specifieke regulatie, maar voornamelijk bepaald door de concentratie van vetzuren in het bloed. We concludeerden dat de schildklierhormoon status de energiehuishouding bepaalt en dat dit samen gaat met weefsel-specifieke veranderingen in vetzuur opslag afkomstig van triglyceriden.

In **hoofdstuk 8** worden de resultaten die gevonden zijn in de **hoofdstukken 2, 3, 4, 5, 6** en **7** besproken in de context van de aanwezige literatuur. Verder wordt besproken wat de klinische implicaties zijn van onze bevindingen en wat de mogelijke richtingen zijn voor toekomstig onderzoek.

Samengevat laten de studies in dit proefschrift zien dat de hersenen een belangrijke rol spelen in de ontwikkeling van diabetes. We hebben aangetoond dat verstoringen in het circadiaan ritme kan bijdragen aan de ontwikkeling van insulineresistentie. We hebben ook aangetoond dat het effect van insuline op het glucose en vetzuur metabolisme deels via de hersenen loopt. Het zou kunnen dat andere hormonen, bijvoorbeeld schildklierhormoon, ook deels werkt via de hersenen. Verder hebben we aangetoond dat topiramaat insuline gevoeligheidverbetert door de gevoeligheid voor insuline in de hersenen te verbeteren. Dit suggereert dat herstellen van insuline gevoeligheid in de hersenen een nieuwe therapeutische mogelijkheid zou kunnen zijn voor de behandeling van diabetes mellitus type 2.

DANKWOORD

Eindelijk is het dan zover, mijn promotie onderzoek is volbracht. Vanzelfsprekend was dit proefschrift er niet gekomen zonder de bijdragen van velen. Mensen die een rol hebben gespeeld in de totstandkoming van dit proefschrift wil ik op deze plaats dan ook bedanken.

Prof. Romijn, beste Hans, bedankt voor het vertrouwen in mij en de stimulerende gesprekken die we de afgelopen jaren gevoerd hebben. Je tomeloze enthousiasme voor het onderzoek is inspirerend. Prof. Havekes, beste Louis, bedankt voor je goede zorgen en je bijdrage aan het tot stand komen van mij boekje. Ik zal de teambuilding weekendjes op jouw boerderij in Frankrijk missen. Prof. Rensen, beste Patrick, ik heb ontzettend veel van je geleerd, dank voor al je input. Ik hoop dat we in de toekomst kunnen blijven samenwerken.

Ik had tijdens mijn promotie geen beter lab kunnen wensen met betrekking tot gezelligheid, steun, belangstelling en collegialiteit. In alfabetische volgorde: Agatha, Alberto, Amanda, Anita, Christel, Clemens, Eric, Gabri, Geertje, Guido, Hanna, Henny, Henry, Hermine, Hetty, Illiana, Ineke, Irene, Isabel, Ivo, Jacqueline, Jan v. K, Jan S, Janine, Janna, Janny, Jeroen, José, Karien, Laura, Lianne v. B, Lianne v.d. W, Lihui, Maggy, Maj, Man-Chi, Margriet, Marieke S, Marit, Marleen, Mariëtte, Martiene, Martijn, Mattijs, Mieke, Nancy, Noortje, Padmini, Peter H, Petra, Randa, Rasvan, Sam, Sander, Susan, Thomas, Trea, Vanessa, Vicky en Wen, bedankt voor alle gezelligheid tijdens werk, besprekingen, congressen, pauzes, lunches en labuitjes. Dank gaat ook uit naar mijn kamer/gang genoten Jitske, Judith en Willeke en later An, Bang-Wen, Ermond en Luis voor alle gezelligheid. Sjoerd, je bent onmisbaar geweest in de laatste fase van mijn proefschrift. Ik ben blij en trots dat je mij straks bij wilt staan als paranimf. Silvia, ik mis onze knutseldagen en onze uitjes. Een fijne collega en nu een "verre" vriendin. Edwin, bedankt voor al je hulp en gezelligheid. Wat leuk dat je weer terug bent. Nienke, onze fijne samenwerking is al beloond met een mooie publicatie en ik weet zeker dat er nog meer zullen volgens. Bedankt voor je vertrouwen in mij. Peter V, dank voor je begeleiding in het begin van mijn promotietraject. Je bent een inspirerend persoon en fijne collega. Marieke V, je bent niet lang bij ons geweest, maar je hebt een onuitwisbare indruk achter gelaten bij mij. Janine, wat hebben we samen veel canules geïmplanteerd, niet alleen in Leiden, maar ook in Brussel. Veel succes met het afronden van je proefschrift. Lars, ik heb genoten van onze succesvolle samenwerking. Jimmy, mijn wetenschappelijke basis is als stagiair bij jou gevormd. Je bent een goede leermeester geweest en een fijne collega. Hanno en Ko, bedankt voor alle nuttige input tijdens werkbesprekingen. Chris, wat zou het lab zonder jou moeten en waar zouden mijn experimenten gestrand zijn zonder jou? Geregeld heb ik jou lastig gevallen met bestellingen die er gisteren al hadden moeten zijn, maar gelukkig was jij daar altijd die kalm samen met mij op zoek ging naar een oplossing, dank daarvoor. Mijn studenten Rosa en Samantha, bedankt voor jullie bijdragen. Ik heb veel van jullie geleerd en ik hoop dat jullie met plezier terug kijken op je stage bij mij. Bruno, thank you for the western blots that you performed for my studies and the thorough revision of my manuscripts. Ben en Fred, bedankt voor de liefdevolle verzorging van mijn diertjes en voor alle gezelligheid in de dierstallen van de E0 (jaja, zo lang loop ik hier al rond), op het LGP en later weer op de E0. De secretaresses, Marjanne, Marjolein en Caroline wil ik bedanken voor hun hulp bij diverse administratieve zaken. Dank aan een ieder die de dagelijkse sleur doorbraken en met mij mee gingen voor een lekkere lebkoffie.

Joke en Thijs, onze samenwerking heeft tot twee mooie hoofdstukken in dit proefschrift geleidt. Bedankt voor de succesvolle samenwerking en de stimulerende discussies. Mijn nieuwe collega's bij neurofysiologie wil ik graag bedanken voor hun belangstelling tijdens de allerlaatste fase.

Iedereen die buiten het werk voor gezelligheid heeft gezorgd, bedankt voor alle steun en afleiding. Heel lang was mijn werk een onderwerp waar niet over gesproken kon worden, maar vanaf nu niet meer! Familie en "schoonfamilie" bedankt voor alle interesse en steun. Ik hoop dat nu duidelijk(er) is wat ik de afgelopen jaren heb gedaan. Lieve Romana, wat hebben we altijd een lol samen. Best Friends Forever! Ik vind het heel fijn dat jij mij bij wilt staan als paranimf. Remko, mijn rots in de branding, altijd daar om mijn tirades op te vangen. Wat fijn dat jij er altijd voor me bent, bedankt voor al je liefde en geduld. Ten slotte, wil ik mijn ouders bedanken voor hun onvoorwaardelijke liefde, begrip en steun. Het is gelukt!

Claudia

LIST OF PUBLICATIONS (FULL PAPERS)

<u>Coomans CP</u>, van den Berg SAA, Houben T, van Klinken JB, van den Berg R, Pronk ACM, Havekes LM, Romijn JA, Willems van Dijk K, Biermasz NR, Meijer JH: Additive effects of constant light exposure and diet on circadian rhythms of energy metabolism and insulin sensitivity. *Submitted*

<u>Coomans CP</u>, van den Berg SAA, Lucassen EA, Houben T, Pronk ACM, van der Spek RDC, Kalsbeek A, Biermasz NR, Willems van Dijk K, Romijn JA, Meijer JH: The suprachiasmatic nucleus controls circadian energy metabolism and insulin sensitivity. *Submitted*

<u>Coomans CP</u>, Geerling JJ, van den Berg SAA, van Diepen HC, Schröder-van der Elst JP, Ouwens DM, Pijl H, Rensen PCN, Havekes LM, Guigas B, Romijn JA: The insulin sensitizing effect of topiramate involves K_{ATP} channel activation in the central nervous system. *Submitted*

Parlevliet ET, Schaper F, Schröder-van der Elst JP, <u>Coomans CP</u>, Elling CE, Pijl H:Obinepitide, a novel Y2/Y4 agonist, and TM30339, a novel Y4 agonist, reduce insulin resistance in high-fat-fed C57Bl/6 mice. *Submitted*

<u>Coomans CP</u>, Biermasz NR, Geerling JJ, Guigas B, Rensen PCN, Havekes LM and Romijn JA: The stimulatory effect of insulin on glucose uptake by muscle involves the central nervous system in insulin-sensitive mice. *Diabetes 60(12):3132-3140, 2011*

<u>Coomans CP</u>, Geerling JJ, Guigas B, van den Hoek AM, Parlevliet ET, Ouwens DM, PijlH, VosholPJ, Rensen PCN, Havekes LM and Romijn JA: Circulating insulin stimulates fatty acid retention in white adipose tissue via K_{ATP} channel activation in the central nervous system only in insulin-sensitive mice. *J. Lipid Res. 52(9):1712-1722, 2011*

de Leeuw van Weenen JE, Auvinen HE, Parlevliet ET, <u>Coomans CP</u>, Schröder-van der Elst JP, Meijer OC, Pijl H: Blocking dopamine D2 receptors by haloperidol curtails the beneficial impact of calorie restriction on the metabolic phenotype of C57Bl6 mice. *J. Neuroendocrinology 23(2):158-167, 2011*

Berbée JFP, <u>Coomans CP</u>, Westerterp M, Romijn JA, Havekes LM, Rensen PCN: Apolipoprotein CI enhances the biological response to lipopolysaccharide via the CD14/TLR4 pathway by LPS-binding elements in both Its N- and C-terminal helix. *J. Lipid Res. 51(7):1943-1952, 2010*

<u>Coomans CP</u>, Klieverik LP, Endert E, Sauerwein HP, Havekes LM, Voshol PJ, Rensen PCN, Romijn JA, Kalsbeek A, Fliers E: Thyroid hormone effects on whole-body energy homeostasis and tissue-specific fatty acid uptake *in vivo*. *Endocrinology 150(12); 5639-5648, 2009*

Whitecross KF, Alsop AE, Cluse LA, Wiegmans A, Banks K, <u>Coomans CP</u>, Peart MJ, Newbold A, Lindeman RK, Johnstone RW: Defining the target specificity of ABT-737 and synergistic anti-tumor activities in combination with histone deacetylase inhibitors. *Blood 113(9); 1982-1991, 2009*

CURRICULUM VITAE

Claudia Pascalle Coomans werd geboren op 22 juni 1980 in Rotterdam. In 1996 behaalde zij haar MAVO diploma, in 1998 haar HAVO diploma en in 2000 haar VWO diploma aan het Johannes Calvijn in Rotterdam. In datzelfde jaar begon zij met haar studie Biomedische Wetenschappen aan de Universiteit Leiden. Na het behalen van haar propedeuse in 2001 is zij een half jaar naar het Karolinska Instituut in Stockholm, Zweden geweest voor een uitwisselingsproject voor de studie Biomedische Wetenschappen. Zij behaalde in 2003 haar Bachelor diploma, waarna zij zich voor de masterfase van haar studie Biomedische wetenschappen specialiseerde in de *Research* richting. De eerste van twee stages voerde zij uit bij TNO Kwaliteit van Leven in Leiden onder begeleiding van dr. J. F. P. Berbée en dr. P. C. N. Rensen. Deze stage richtte zich op apolipoproteine C1-afgeleide peptiden als therapie tegen sepsis. Haar tweede stage voerde zij uit bij het Peter MacCallum Cancer Centre in Melbourne, Australië, onder begeleiding van dr. R. W. Johnstone. Tijdens deze stage deed zij onderzoek naar de therapeutische effectiviteit van een Bcl-2/Bcl-X$_L$ antagonist in kanker. Na het behalen van haar Master diploma in 2005, werkte zij bij Prof. dr. G. Wagemaker aan de Erasmus Universiteit in Rotterdam aan *ex vivo* transfectie van hematopoetische stam cellen gebruik makende van magnetische kracht. In november 2006 begon zij haar promotieonderzoek bij de afdeling Endocrinologie en metabole ziekten van het Leids Universitair Medisch Centrum onder begeleiding van Prof. dr. J. A. Romijn en Prof. dr. ir. L. M. Havekes op een Top InstitutePharma project. Het promotieonderzoek, waarvan de resultaten zijn beschreven in dit proefschrift, werd afgerond in november 2011. Vanaf december 2011 is zij aangesteld als postdoc bij de afdeling Moleculaire Cel Biologie, lab Neurofysiologie, in de groep van Prof. dr. J. H. Meijer van het Leids Universitair Medisch Centrum.